Author:
Knights, Alastair W

Title:
Synthesis and Modification of Polyphosphinoboranes and Polyborosiloxanes

Synthesis and Modification of Polyphosphinoboranes and Polyborosiloxanes

Alastair William Knights

A dissertation submitted to the University of Bristol in accordance with the requirements for the degree of Doctor of Philosophy in the School of Chemistry, Faculty of Science

March 2020

Word Count: 43,435

Abstract

This thesis describes synthetic routes to main group element-containing macromolecules through the polymerisation of inorganic monomers, and the modification of preformed polymers. Investigations into the use of polyphosphinoboranes as hydrogels and flame-retardants are also disclosed.

Chapter 1 gives an overview on main group polymers with a focus on strategies to synthesise polyphosphinoboranes, polysiloxanes, and polyborosiloxanes. Applications of these polymers and related species are discussed including the formation of hydrogels featuring p-block elements.

Chapter 2 describes the post-polymerisation modification of poly(phenylphosphinoborane) via UV-light induced hydrophosphination of olefins giving access to P-di(organosubstituted) polymers. The formation of crosslinked gels and water-soluble polymers using this methodology was also studied.

Chapter 3 describes investigations into the dehydropolymerisation of phenylphosphine-borane ($PhH_2P{\cdot}BH_3$) using $CpFe(CO)_2OTf$ and related precatalysts. These studies suggest that the polymerisation takes place via a hybrid mechanism rather than purely chain-growth as was initially reported. The polymerisation of phosphine-boranes using non-metal precatalysts was also investigated.

Chapter 4 is split into two sections. The first describes the synthesis of hydrogels via UV-light induced reaction of polyphosphinoboranes with methacrylate and acrylate capped poly(ethylene glycol), and dimethacrylate crosslinkers. These gels were found to reversibly swell in water. The second describes the use of polyphosphinoboranes as leach-resistant flame-retardant additives for cotton fabric. When fabric impregnated with polyphosphinoborane was exposed to a flame, the material was found to self-extinguish leaving a char material which contained phosphoric acid and boric acid.

Chapter 5 describes the synthesis of borosiloxane molecules and polymers via dehydrocoupling and demethanative condensation routes under mild, metal-free conditions. The reaction of dimethyl phenylboronate with secondary silanes in the presence of tris(pentafluorophenyl)borane results in the formation of polymers featuring alternating boron and siloxane units in the main chain.

Chapter 6 provides a general outlook for the work reported in this thesis along with some potential avenues for future work.

Acknowledgements

First and foremost, I would like to thank Prof. Ian Manners for his guidance and supervision during my PhD. His dedication and enthusiasm for science and research is an inspiration to me. I would also like to thank Deborah O'Hanlon Manners for all of her help, in particular with navigating the many complexities around carrying out research as a visiting student in Victoria. The people who have helped keep our labs running smoothly have been a great asset to the group and I would like to acknowledge Dr George Whittell in Bristol and Dr Liam Macfarlane at UVic for all their efforts on this part.

I have been lucky to work alongside a huge number of talented and skilled researchers who have provided immeasurable help in my own work as well as supplying many happy memories and friendships. There are too many to name everyone but I would like to particularly thank the past and present members of the main group section: Saurabh Chitnis, Marius Arz, Vincent Annibale, Lipeng Wu, Nicola Oldroyd, Diego Resendiz-Lara, Josh Turner, Thomas Horton, Etienne Lapierre, Subrata Kundu, Mitchell Nascimento, and Justin Kröger. I would also like to thank my other N418 lab-mates: Theresa Dellermann, Rebekah Hailes, Becca Musgrave, and Laura Beckett and everyone else in the Manners group.

In addition, to all my other friends who have been there for me over the years – special mention to my housemates at Sans Campari, and to all the other people I've lived with during my PhD; to Poppy, Stu, and James, the original Norfolk massive; to Benno who has convinced me that everything which is good and bad about a chemistry PhD is also there in other subjects; and to Mao whose company in undergrad labs clearly laid the foundations for any success and interest in research. Lastly, I would like to thank my parents, Sarah and Neville, and my sister, Lucie without whom none of this would be possible.

Declaration

I declare that the work in this dissertation was carried out in accordance with the requirements of the University's *Regulations and Code of Practice for Research Degree Programmes* and that it has not been submitted for any other academic award. Except where indicated by specific reference in the text, the work is the candidate's own work. Work done in collaboration with, or with the assistance of, others, is indicated as such. Any views expressed in the dissertation are those of the author.

Alastair Knights

13th January 2020

Table of Contents

List of Figures

List of Schemes

List of Tables

List of abbreviations

Ad	Adamantyl ($C_{10}H_{16}$)
AIBN	Azobisisobutyronitrile
BAr^F_4	$B(C_6H_3(m\text{-}CF_3)_2)_4$
Bn	Benzyl ($C_6H_5CH_2$)
br.	Broad
cat.	Catalyst
CAAC	Cyclic (alkyl)(amino)carbene
cod	1,5-Cyclooctadiene (C_8H_{12})
Cp	Cyclopentadiene (C_5H_5)
Cp*	Pentamethylcyclopentadiene (C_5Me_5)
Cy	Cyclohexyl (C_6H_{11})
d	Doublet
DCM	Dichloromethane
DFT	Density functional theory
Dipp	2,6-diisopropylphenyl
DMPA	2,2-Dimethoxy-2-phenylacetophenone
dppe	1,2-Bis(diphenylphosphino)ethane
DSC	Differential scanning calorimetry
DTBP	Di-*tert*-butylpyridine
eq.	Equivalents
ESI-MS	Electrospray ionisation mass spectrometry
Et	Ethyl (C_2H_5)
Fc	Ferrocenyl ($Fe(C_5H_5)(C_5H_4)$)
FLP	Frustrated Lewis pair
GPC	Gel permeation chromatography

h	Hours
Hex	Hexyl (C_6H_{15})
*i*Pr	*Iso*-propyl (C_3H_7)
IR	Infrared
LCST	Lower critical solution temperature
m	Multiplet
MALDI	Matrix-assisted laser desorption/ionization
Me	Methyl
MEEP	Poly[bis((methoxyethoxy)ethoxyphosphazene)]
Mes	1,3,5-Trimethylbenzene
Min	Minutes
M_n	Number average molar mass
M_w	Weight average molar mass
*n*Bu	*n*-Butyl (C_4H_9)
nPr	*n*-Propyl (C_3H_7)
NHC	N-heterocyclic carbene
NMR	Nuclear magnetic resonance
OTf	Triflate (CF_3SO_3)
RI	Refractive index
PDI	Polydispersity index
PDMS	Polydimethylsiloxane
Ph	Phenyl (C_6H_5)
Piv	Pivalyl (*t*BuC(O))
POCOP	[μ^3-1,3-(OP*t*Bu$_2$)$_2$C$_6$H$_3$]
ppm	Parts per million
PR	Piers-Rubinsztajn
ROP	Ring-opening polymerisation

s (For NMR data)	Singlet
SEM	Scanning electron microscopy
t	Triplet
*t*Bu	*Tert*-butyl (C_4H_9)
TEMPO	(2,2,6,6-Tetramethylpiperidin-1-yl)oxyl
T_g	Glass-transition temperature
TGA	Thermal gravimetric analysis
THF	Tetrahydrofuran
T_m	Melt transition temperature
Tol	Toluene
TOF	Time of flight
UV	Ultraviolet
wt	Weight

Chapter 1

Introduction

1.1 Research objectives

The aim of the research described in this thesis is to develop synthetic routes to novel main group element-containing polymers and soft materials. Formation and modification of polyphosphinoboranes and investigations into potential applications of these macromolecules as hydrogels and flame-retardants have been investigated. A non-metal catalysed demethanative condensation route to borosiloxane polymers has also been explored.

This introductory chapter serves as an overview on main group element-containing polymers with particular focus on strategies to synthesise polyphosphinoboranes, polysiloxanes, and polyborosiloxanes to place work in later thesis chapters in context. The formation of hydrogels featuring main group elements is also introduced. Each chapter contains a detailed introduction associated with the work reported along with further relevant background information.

1.2 Main group polymers

1.2.1 Catalytic formation of main group element-element bonds

The reduction in activation energy for chemical reactions by transition metal catalysts has played a crucial role in the development of synthetic organic chemistry. A myriad of catalytic transformations have been described in the literature with prominent examples including the Nobel prize recognised development of C-C bond formation via olefin polymerisation,[1] metathesis,[2] and palladium catalysed cross-coupling reactions.[3-5] Transition metals have also found applications in the formation of C-E bonds (E = p-block element), in particular in the cases of hydroboration (E = B),[6-10] hydrophosphination (E = P),[11-14] and hydrosilylation (E = Si)[9, 15] processes. In contrast, the development of synthetic protocols for the formation of bonds between main group elements (E-E bonds) has been comparatively slow.

Routes to E-E bonds were initially developed using salt metathesis and reductive coupling. These often require the use of forcing conditions and/or have poor atom efficiencies, generating significant quantities of by-products. One prominent example of a route to E-E bond formation is Würtz coupling. The use of organoelement precursors and sodium as a reducing agent drives the coupling of elements with the concomitant elimination of a halide salt (Scheme 1.1 a). This has been used extensively in the formation of polysilanes; however, reactions are often low yielding and produce polymer with a multimodal mass distribution (Scheme 1.1 b).[16]

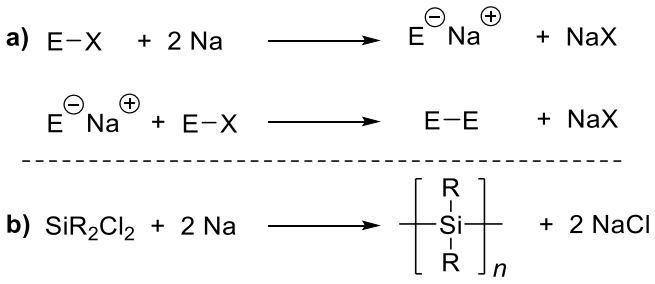

Scheme 1.1 a) General Würtz coupling reaction using sodium; b) formation of polysilanes using Würtz coupling polymerisation.[16]

In the 1980s, the first catalytic example of E-E bond formation was reported. This involved the formation of homonuclear B-B bonds through dehydrocoupling using platinum(II) bromide as a precatalyst giving access to borane clusters (Scheme 1.2 a).[17, 18] Shortly thereafter, examples of Si-Si coupling were reported using a titanium catalyst, facilitating the formation of oligo- and polysilanes (Scheme 1.2 b).[19]

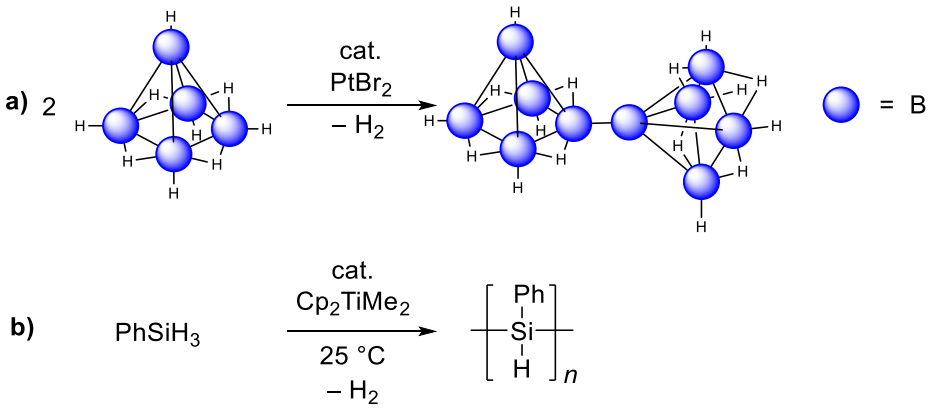

Scheme 1.2 a) Catalytic formation of B-B bonds using $PtBr_2$ yielding borane clusters;[17, 18] b) Formation of polysilanes via catalytic dehydrocoupling of phenylsilane using Cp_2TiMe_2.[19]

The formation of heteronuclear bonds (E-E') between main group elements was first reported in the late 1980s and early 1990s. Transition metal catalysed dehydrocoupling of Si-H and N-H bonds led to

the formation of oligosilazanes (Scheme 1.3 a).[20-22] The formation of Si-P bonds was also achieved using Cp_2TiMe_2 in the dehydrocoupling of silanes with phosphines (Scheme 1.3 b).[23] Since these early reports, a number of examples of metal-catalysed routes for both homo- and heteronuclear bond formation have been developed allowing access to a wide variety of inorganic molecules and materials.[24] The mechanisms of these reactions have also been extensively probed.[25]

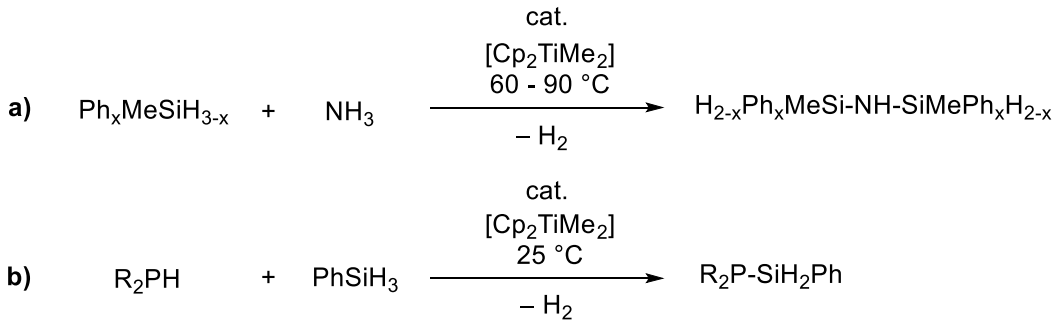

Scheme 1.3 a) Formation of oligosilazanes through dehydrocoupling of silanes and NH_3 catalysed by Cp_2TiMe_2;[20-22] b) Formation of Si-P bonds by catalytic dehydrocoupling of phosphines and silanes.[23]

More recently, there has been significant interest in the use of main group elements to facilitate catalytic transformations typically associated with transition metals.[26-28] Main group species have found usage as catalysts in dehydrocoupling reactions leading to the formation of inorganic element-element bonds.[29] For example, tris(pentafluorophenyl)borane ($B(C_6F_5)_3$) has been utilised as a catalyst for the formation of polyphosphinoboranes $[RR'P\text{-}BH_2]_n$[30] and polysiloxanes $[RR'SiO]_n$[31] (see Sections 1.3 and 1.4) and in the post-polymerisation functionalisation of polysilanes via dehydrocoupling reactions.[32, 33] Reaction of poly(phenylsilane) with *n*PrSH or *p*-tolSH in the presence of catalytic $B(C_6F_5)_3$ resulted in the release of H_2 and formation of a solid copolymer where 15 – 40% Si-S bond formation had taken place (Scheme 1.4).[32]

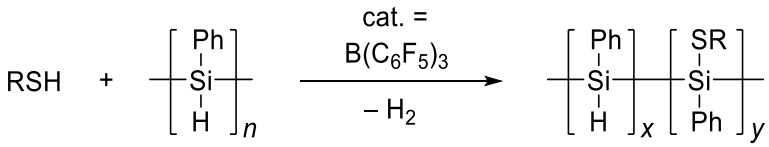

Scheme 1.4 Post-polymerisation modification of poly(phenylsilane) via $B(C_6F_5)_3$ catalysed hetero-dehydrocoupling with thiols.[32]

1.2.2 Main group inorganic polymers

Organic polymers are essential to modern life with applications including, as construction materials, disposable packaging, electronics, and textiles. These plastics have incredible breadth in properties

despite being composed almost entirely from carbon, oxygen and nitrogen. The inclusion of inorganic elements into polymer chains has generated increasing scientific interest due to the potential for accessing macromolecules with unusual physical and chemical properties.[34]

Inorganic polymer research is still an emergent field, in part, owing to the aforementioned difficulties in forming bonds between inorganic p-block elements. A number of techniques that have found extensive utility in the synthesis of organic polymers cannot be easily applied to inorganic systems. Chain-growth methods such addition polymerisation (Scheme 1.5 a)[1, 35] are commonly used protocols for the formation of organic polymers; however, these require unsaturated monomers such as ethylene and styrene. The synthesis of inorganic compounds with multiple element-element bonds is non-trivial and these species are often highly reactive or require large substituents which prohibit polymerisation.[36, 37] Step-growth polymerisations require high purity monomers to achieve high molar mass polymers. This requirement is often challenging for p-block elements due to their propensity to react with air and moisture. Nevertheless, a number of synthetic protocols have emerged giving access to a range of inorganic polymers.[34] Classically, condensation routes (Scheme 1.5 b) have been used in the formation of inorganic polymers such as polysiloxanes $[RR'SiO]_n$, polyphosphazenes $[RR'P{=}N]_n$, and polysilanes $[RR'Si]_n$ which have many fascinating properties such as thermo-oxidative stability and high flexibility at low temperatures. More recently, ring-opening polymerisation (Scheme 1.5 c),[38] and dehydrocoupling polymerisation (Scheme 1.5 d)[39] have been significantly exploited in the synthesis of novel inorganic polymers such as polystannanes, polygermanes, polycarbosilanes, polycarbophosphazenes, polyphosphonates, polyborosiloxanes, polyaminoboranes, polyphosphinoboranes, and hybrid organic/inorganic macromolecules.[34, 40]

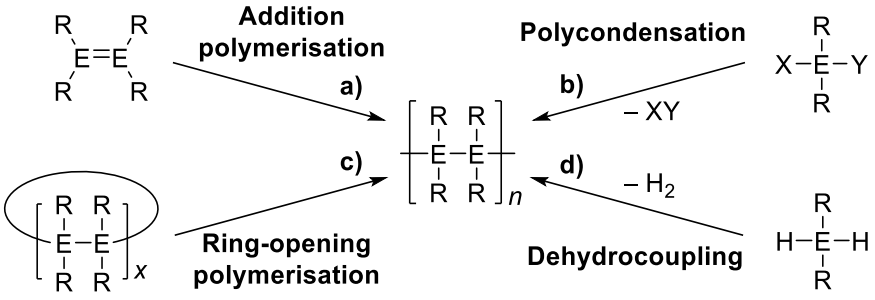

Scheme 1.5 Common polymerisation routes.

1.3 Group 13/15 polymers

1.3.1 Amine– and phosphine-boranes

Amine- and phosphine-borane adducts are classical examples of Lewis base-Lewis acid adducts where a lone pair on nitrogen or phosphorus acts as a two-electron donor to a vacant p-orbital on boron forming a dative bond.[41] For amine-boranes, the electronegativity difference between nitrogen and boron is 1.0 which induces a polarisation in the N-H bond of the adducts. In addition, the N-H hydrogens are protic in nature, whereas, hydrogen atoms attached to boron are hydridic. This characteristic has been exploited in the design of catalysts for the dehydrocoupling of these adducts under mild conditions.

In contrast, the electronegativity difference between phosphorus and boron is low (0.1) making hydrogen release from phosphine-boranes less kinetically favoured than for amine-boranes. Additionally, a single dehydrogenation process would yield the intermediate phosphinoborane $H_2P{=}BH_2$ or aminoborane $H_2N{=}BH_2$. In the 1990s, computational studies suggested that the π-component of bonding in these species are of similar bond strength;[42] however, investigations into the rotational transition states of $H_2B{=}PH_2$ suggests that, unlike for $H_2N{=}BH_2$, there is a significant barrier to pyramidal inversion as the phosphorus atom has a strong tendency to adopt pyramidal geometry. Consequently, the formation of the planar phosphinoborane intermediates in dehydrocoupling processes is less favourable than for amine-boranes and therefore elevated temperatures are often required for the polymerisation of phosphine-boranes.

Amine-boranes have found applications as hydroboration,[43] reducing,[44] and hydrogen transfer agents.[45-48] In particular, ammonia-borane $H_3N{\cdot}BH_3$ has been extensively studied owing to its high hydrogen content (19.6 wt%) making it an excellent candidate for hydrogen storage applications.[49-51] Ammonia borane has also been investigated as a ceramic precursor. Atomic layers of hexagonal boron nitride (*h*-BN) have been prepared from $H_3N{\cdot}BH_3$ using chemical vapour deposition.[52] Single layer *h*-BN is isoelectronic to graphene and has interesting electronic and optical properties leading to a range of applications.[53, 54]

Research into the applications of phosphine-boranes is less well-developed; however, these main group species have found uses in a number of areas including as reducing agents under biological conditions,[55, 56] and as precursors to organophosphorus compounds via modifications, for example,

through hydrophosphination[11, 57-62] and deprotonation, alkylation/coupling reactions.[41, 63] The borane group serves to protect the phosphorus from oxidation and can generally be easily removed via reaction with amines (Scheme 1.6).[64]

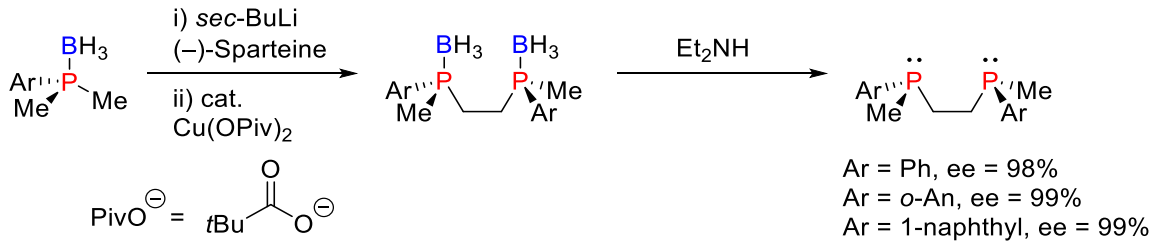

Scheme 1.6 Deprotonation followed by oxidative coupling of $ArMe_2P{\cdot}BH_3$ leading to the formation of chiral bis(phosphine-boranes), and subsequent deprotection using diethylamine.[63]

Polyaminoboranes and polyphosphinoboranes possess main chains consisting of alternating group 13 and 15 atoms. They are isoelectronic to polyolefins which has stimulated fundamental interest in these materials. Amine-boranes can undergo dehydrocoupling thermally in the absence of catalyst at ca. 100 – 150 °C, or at lower temperatures in the presence of a catalyst.[41, 65-67] Of particular note is the use of IrH_2POCOP (POCOP = $[\mu^3$-1,3-$(OPtBu_2)_2C_6H_3]$) which has facilitated the synthesis of a range of polyaminoboranes $[RHN\text{-}BH_2]_n$ (R = H, Me, *n*Bu, $Ph(CH_2)_x$ = 2 – 4)) under mild conditions (Scheme 1.7).[68-70] Several other catalytic systems based on Fe,[71-74] Ru,[75] Rh,[76-78] Co,[79] Ti,[80, 81] and Zr[82] have also been reported.[65-67] The dehydrocoupling of *N*-disubstituted amine-boranes results in the formation of monomeric aminoboranes $R_2N{=}BH_2$ or cyclic species $[R_2N\text{-}BH_2]_x$ rather than polymeric material.[66]

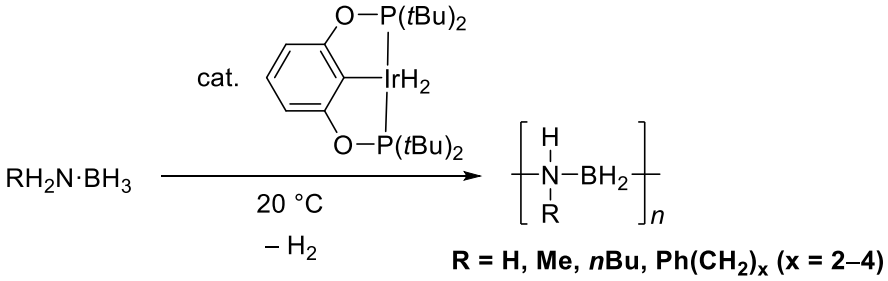

Scheme 1.7 Synthesis of polyaminoboranes via the catalytic dehydrocoupling of $RH_2N{\cdot}BH_3$ in the presence of IrH_2POCOP.[68-70]

1.3.2 Synthesis of phosphine-borane adducts

The first example of a phosphine-borane adduct, phosphine-trichloroborane ($H_3P{\cdot}BCl_3$) was outlined by Besson in 1890.[83] Since this report, two main routes have been established for the synthesis of phosphine-boranes. Most commonly employed is the direct addition of a phosphine to $BH_3{\cdot}L$ (L = THF

or SMe_2) where the more strongly donating phosphine rapidly displaces the labile THF or SMe_2 (Scheme 1.8 a). An alternative preparation that avoids the long-term stability issues of BH_3·THF or the elimination of malodorous by-products, e.g. SMe_2, is by the reduction of chlorophosphines using sodium borohydride (Scheme 1.8 b).[41]

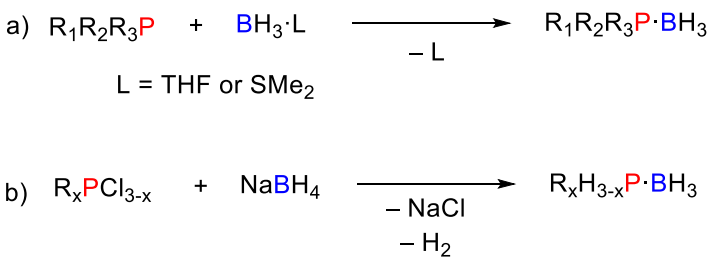

Scheme 1.8 Synthetic routes to phosphine-boranes

1.3.3 Synthesis of polyphosphinoboranes

Polyphosphinoboranes, $[RR'P\text{-}BH_2]_n$ are formally isoelectronic with polyolefins. These polymers were predicted to exhibit high temperature stability and flame-retardancy as early as the 1950s.[41] The synthesis of $[RR'P\text{-}BH_2]_n$ was first reported in the 1950 and 60s period by a thermally induced dehydrocoupling of $PhH_2P{\cdot}BH_3$ in the melt at 150 – 250 °C for 13 h;[84-88] however, these materials were not characterised by modern day techniques such as NMR spectroscopy and where reported, molar masses were low (M_n <2,500). The first example of a high molar mass polyphosphinoborane was reported in 1999, when it was demonstrated that $[Rh(1,5\text{-cod})_2][OTf]$ or $[Rh(\mu\text{-Cl})(1,5\text{-cod})]_2$ (cod = 1,5-cyclooctadiene), could catalyse the dehydropolymerisation of $PhH_2P{\cdot}BH_3$.[89] Since this example, several other routes to polyphosphinoboranes have been reported, in particular, via metal catalysed dehydrocoupling of phosphine-boranes[65] but metal-free routes to polyphosphinoboranes have also been developed.

1.3.3.1 Transition metal-catalysed routes to polyphosphinoboranes

Heating $PhH_2P{\cdot}BH_3$ in toluene in the presence of Rh^I precatalysts $[Rh(1,5\text{-cod})_2][OTf]$ or $[Rh(\mu\text{-Cl})(1,5\text{-cod})]_2$ (0.3 mol%) under reflux for 14 h resulted in the formation of low molar mass $[PhH\text{-}BH_2]_n$ (M_w = 5,600 g mol^{-1}). When solvent free conditions and higher temperatures (130 °C) were employed, in the presence of a Rh^I precatalyst, high molar mass $[PhHP\text{-}BH_2]_n$ was formed (Scheme 1.9, R = Ph). The polymer was isolated as an air and moisture stable solid by precipitation from DCM into hexanes. The $^{31}P\{^1H\}$ NMR spectrum of $[PhHP\text{-}BH_2]_n$ showed a broad singlet at $\delta = -48.9$ ppm, which

splits into a doublet in the ^{1}H coupled spectrum. In the ^{11}B NMR spectrum, a broad resonance was observed at $\delta = -34.7$ ppm and in the ^{1}H NMR spectrum, a broad doublet assigned to the P-H proton, was found at $\delta = 4.25$ ppm alongside a broad multiplet at $\delta = 0.65–2.20$ ppm which corresponded to the BH_2 groups. The M_w was found to be 31,000 g mol^{-1} by static light scattering.[89, 90]

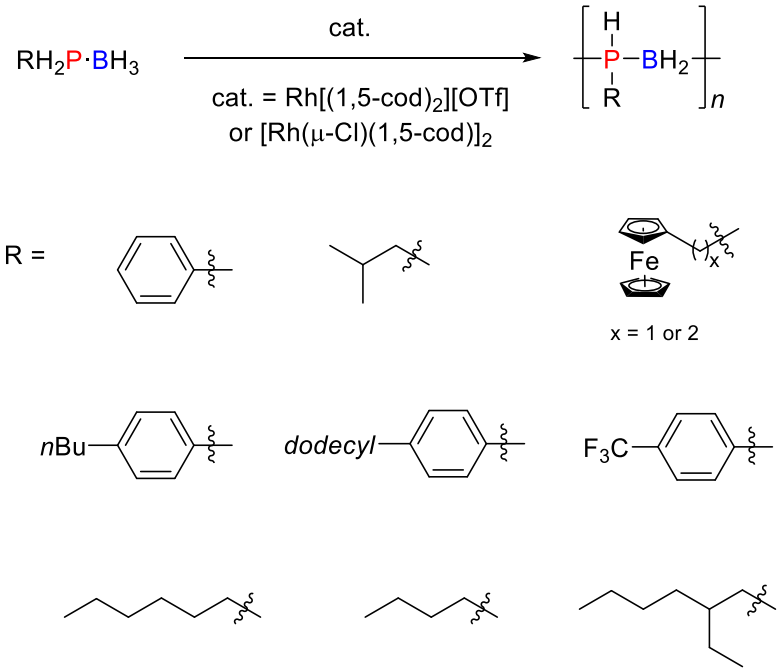

Scheme 1.9 Rh^{I} catalysed dehydrocoupling of P-monosubstituted phosphine-boranes.

$[Rh(\mu\text{-}Cl)(1,5\text{-}cod)]_2$ was subsequently found to be a precatalyst for synthesis of other P-monosubstituted polyphosphinoboranes $[RHP\text{-}BH_2]_n$ (R = *i*Bu, *p*-*n*BuC_6H_4, and *p*-dodecylC_6H_4).[90, 91] These materials were found to have high dispersity and prolonged heating of the polymerisation reaction mixtures yielded insoluble material suggesting the formation of crosslinked and/or very high molar mass material. The dehydrocoupling of more highly activated (*p*-$CF_3C_6H_4$)PH_2·BH_3 allowed a reduction in the reaction temperature to 60 °C yielding polymer with M_w = 56,170 g mol^{-1}.[92] More recently, the substrate scope of this catalyst has been extended to polymerisation of alkyl phosphine-boranes RH_2P·BH_3 (R = *n*Hex, *n*Bu and 2-ethylhexyl) of moderate molar mass (M_w = 3,650 – 19,500 g mol^{-1}) which exhibit very low glass transition temperatures (−58 – −68 °C),[93] and to ferrocenylphosphine-borane adducts (R = Fc or $FcCH_2$, Fc = $Fe(C_5H_5)(C_5H_4)$ giving metal-containing polymer with moderate molar mass when prepared in the melt (M_w = 10,000 – 16,000 g mol^{-1}).

Polymerisation of a quaternised ammonium derivative was also reported, yielding an insoluble ionic polymer $\{[Fe(C_5H_5)\{C_5H_3(CH_2NMe_3)PH(BH_2)\}]I\}_n$ (Scheme 1.9).[94]

The dehydrocoupling of P-disubstituted phosphine-boranes using Rh^I precatalysts has also been investigated yielding dimeric or cyclic species instead of polymer. Heating neat $Ph_2HP{\cdot}BH_3$ in the presence of $[Rh(1,5\text{-cod})_2][OTf]$ or $[Rh(\mu\text{-Cl})(1,5\text{-cod})]_2$ at 90 °C for 14 h resulted in the formation of the linear dimer species $Ph_2HP{\cdot}BH_2\text{-}PPh_2{\cdot}BH_3$ as a white, air-stable, crystalline product (Scheme 1.10).[89] When $Ph_2HP{\cdot}BH_3$ was heated overnight to 120 °C in the presence of a Rh^I precatalyst, a mixture of cyclic trimer $[Ph_2P\text{-}BH_2]_3$ and tetramer $[Ph_2P\text{-}BH_2]_4$ species were formed.[90] Likewise, dehydrocoupling of $(p\text{-}CF_3C_6H_4)_2HP{\cdot}BH_3$ under similar conditions led to formation of either linear dimer, or cyclic trimer and tetramer species.[92]

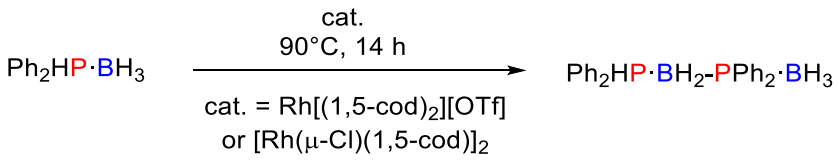

Scheme 1.10 Rh^I catalysed dehydrocoupling of diphenylphosphine-borane.[89]

Early reports on the dehydrocoupling of phosphine-boranes using rhodium precatalysts have inspired the development of other group 9 metal-based catalysts for these polymerisations. $[RhCp^*(PMe_3)Me(ClCH_2Cl)][BAr^F{}_4]$ ($Cp^* = \eta^5\text{-}C_5Me_5$, $Ar^F = 3,5\text{-}(CF_3)_2C_6H_3$) was reported to catalyse the dehydropolymerisation of $PhH_2P{\cdot}BH_3$ in toluene at 100 °C, producing moderate molar mass polymer ($M_n \sim 15{,}000$ g mol^{-1}, polydispersity index (PDI) = $M_w/M_n = 2.2$).[95] The dehydrocoupling of $R_2HP{\cdot}BH_3$ (R = Ph, *t*Bu,) using related precatalysts was found to give linear dimer species $R_2HP{\cdot}BH_2\text{-}PR_2{\cdot}BH_3$.[96, 97] Use of iridium complexes [(POCOP)IrRH] (R = Ph or H) was reported to produce *P*-aryl substituted polyphosphinoboranes $[ArHP\text{-}BH_2]_n$ (Ar = Ph, *p*-Tol, Mes) via dehydrocoupling of the corresponding phosphine-borane (Scheme 1.11).[98] This was proposed to proceed via a two stage mechanism consisting of an initial dehydrogenation process to form a phosphinoborane, $ArHP\text{-}BH_2$ which subsequently undergoes fast chain-growth polymerisation. The evidence for the chain-growth nature was based on the observation of high molar mass material even at low conversion. A similar two-stage pathway has also been postulated for the polymerisation of amine-boranes using $[(POCOP)IrH_2]$.[69]

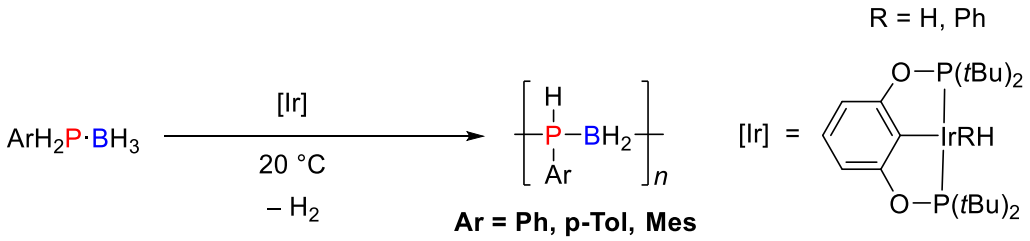

Scheme 1.11 Synthesis of polyphosphinoboranes $[ArHP\text{-}BH_2]_n$ using [(POCOP)IrRH].[98]

In 2015, Manners et al. reported the synthesis of poly(phenylphosphinoborane) via iron-catalysed dehydrocoupling of $PhH_2P{\cdot}BH_3$ in toluene at 100 °C. The molar mass of the polymer was found to be dependent on the $CpFe(CO)_2OTf$ precatalyst loading – increasing the precatalyst loading results in a decrease in the polymer molar mass. This is suggestive of a chain growth mechanism operating.[99] This precatalyst has been shown to be active for the dehydropolymerisation of a number of aryl P-monosubstituted phosphine-boranes $RH_2P{\cdot}BH_3$ in toluene at 100 °C (R = 3,4-$(OCH_2O)C_6H_3$, *p*-$(CF_3O)C_6H_4$, 3,5-$(CF_3)_2C_6H_3$, 2,4,6-$(CH_3)_3C_6H_2$, 2,4,6-*t*$Bu_3C_6H_2$, *p*-BrC_6H_4, *p*-IC_6H_4) giving polymers of (M_n = 12,000 – 209,000 g mol^{-1}, PDI = 1.14 – 2.17),[100, 101] and very recently this has been extended to alkyl substituted phosphine-boranes (R = *t*Bu, 1-Ad, *i*Pr, Cy, *n*Hex, Me), again forming high molar mass polymers (M_n = 18,200 – 57,200 g mol^{-1}, PDI = 1.5 – 3.4) after dehydrocoupling in toluene at 100 °C (Scheme 1.12).[102] As with previous reports on Rh^I precatalysts, attempts to use this catalyst for the dehydrocoupling of P-disubstituted species $Ph_2HP{\cdot}BH_3$ resulted in the formation of linear dimer rather than polymer.[99, 102] Manners and co-workers have also reported the use of $CpM(CO)_2PPh_2BH_3$ (M = Fe, Ru) as precatalysts for the dehydrocoupling of $Ph_2HP{\cdot}BH_3$, again forming the linear dimer in reactions that take place in the melt at 120 °C.[103]

The catalytic dehydrocoupling of phosphine-boranes in toluene at 100 °C using the three-coordinate iron(II) precatalyst [((DippNC(Me))$_2$CH)Fe(CH_2SiMe_3)] (Dipp = 2,6-diisopropylphenyl) was reported by Webster and co-workers in 2017 (Scheme 1.12).[74] This system facilitated the formation of $[RHP\text{-}BH_2]_n$ (R = Ph, Cy); however, while $[PhHP\text{-}BH_2]_n$ was found to be high molar mass (M_n = 55,000 g mol^{-1}, PDI = 1.85), $[CyHP\text{-}BH_2]_n$ was mostly oligomeric in nature (M_n <2,500 g mol^{-1}) with only a minor high molar mass component (<10%). Dehydrocoupling of P-disubstituted analogues resulted in formation of small cyclic or linear dimer products. The dehydrocoupling was shown to be homogeneous

in nature and to not involve radical species based on experiments using TEMPO or iodo(methyl)cyclopropane as radical traps.[74]

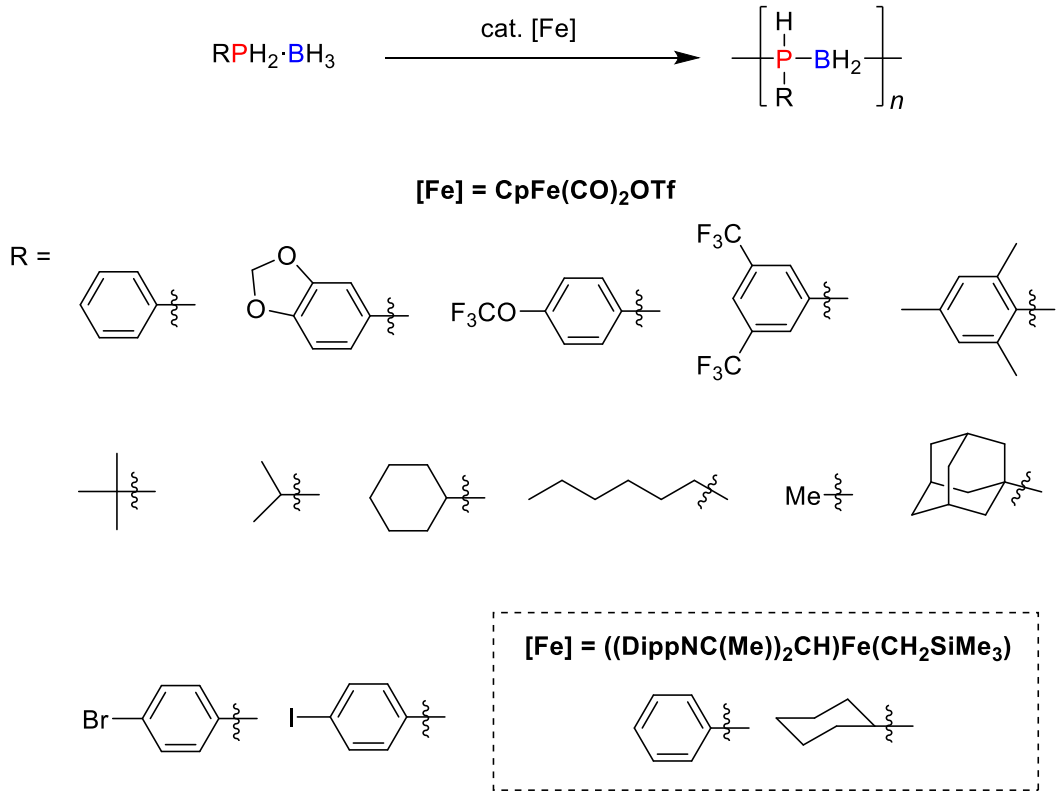

Scheme 1.12 P-monosubstituted polyphosphinoboranes $[RHP\text{-}BH_2]_n$ synthesised using iron precatalysts.

1.3.3.2 Mechanisms of transition metal catalysed phosphine-borane dehydrocoupling

Despite reports on the dehydrocoupling of phosphine-boranes using transition-metal precatalysts, comprehensive mechanistic investigations have proven to be challenging. Nevertheless, a number of informative insights have been reported for different catalysts.

Dehydrocoupling of $Ph_2HP{\cdot}BH_3$ using catalytic amounts of $[Rh(\mu\text{-}Cl)(1,5\text{-}cod)]_2$ showed a colour change from orange to dark red with no evidence of black precipitate forming. Additionally, no induction period was observed and there was an approximately linear relationship between conversion and time. This is suggestive of a homogeneous mechanism operating. Further evidence for this was provided by catalyst poisoning experiments: addition of excess mercury or 0.5 eq. of PPh_3 was found to have no detectable effect on the catalytic activity, nor was filtering a catalytically active solution through a 0.5 µm mesh. Use of preformed rhodium nanoparticles were found to have little catalytic activity suggesting that a heterogeneous pathway is not kinetically competent. This is in stark contrast to the dehydrocoupling of dimethylamine-borane using $[Rh(\mu\text{-}Cl)(1,5\text{-}cod)]_2$ which is believed to

operate through a heterogeneous mechanism.[104] The dehydropolymerisation of P-monosubstituted phosphine-boranes using Rh^I precatalysts is postulated to proceed via a homogeneous step-growth mechanism with very high conversion (>99%) being required for the formation of high molar mass polyphosphinoborane. The requirement of melt conditions and high temperatures in these polymerisation reactions hinders further mechanistic study into this polymerisation and also results in issues with control of molar mass and the formation of branched polymers.

The first detailed study into the mechanism of a Rh-catalysed dehydrocoupling of phosphine-boranes was reported in 2012. Dehydrocoupling of tBu$_2$HP·BH$_3$ in the presence of 5 mol% [Rh(1,5-cod)$_2$][BAr$^F_4$] under melt conditions led to the formation of the linear dimer as the main product after 20 h. A by-product of this reaction was the bis-phosphine-boronium salt [(tBu$_2$HP)$_2$BH$_2$][BH$_4$]. When the reaction was carried out in 1,2-difluorobenzene, the formation of [Rh(PtBu$_2$H)$_2$(η^2-H$_3$BPtBu$_2$BH$_2$PtBu$_2$H)]$^+$ and [Rh(PtBu$_2$H)$_2$(η^6-F$_2$C$_6$H$_4$)]$^+$ were observed. These results suggest that P-B cleavage occurs with substitution of 1,5-cod by phosphine ligands at the Rh centre. Independently synthesised [Rh(PtBu$_2$H)$_2$(η^6-F$_2$C$_6$H$_4$)]$^+$ was also found to be catalytically active and therefore the fragment [Rh(PtBu$_2$H)$_2$]$^+$ was postulated to be the active species.[97]

Further studies were carried out by Weller and co-workers on a related complex ligated by a bidentate phosphine [Rh(η^6-FC$_6$H$_5$)(dppp)][BAr$^F_4$] (dppp = Ph$_2$PCH$_2$CH$_2$CH$_2$PPh$_2$), which is a precatalyst for the dehydrocoupling of R$_2$HP·BH$_3$ (R = Ph, tBu). These studies revealed that when R = Ph, the rate-limiting process for dehydrocoupling involves B-H activation and the turnover-limiting step involves substitution of the oligomeric product by Ph$_2$HP·BH$_3$ at the metal. This results in the formation of a strong chelate complex at the Rh(III) centre [Rh(dppp)H(σ,η-PPh$_2$BH$_3$)(η^1-H$_3$B·Ph$_2$PH)]$^+$ (Scheme 1.13 a). In contrast, no such chelate complex was formed when R = tBu (Scheme 1.13 b) and the dehydrocoupling process was reported to be the turnover-limiting step. It was postulated that the harsh conditions required for complete conversion (90 – 140 °C, melt) may be due to barrier to release of the product from the metal rather than the P-B bond forming step.[96] The effect of the phosphorus substituent was further evaluated by use of electron withdrawing and donating arylphosphine-boranes R$_2$HP·BH$_3$ (R = 4-(CF$_3$) C$_6$H$_4$, 3,5-(CF$_3$)$_2$C$_6$H$_3$,4-(MeO)C$_6$H$_4$). In all cases heating the phosphine-borane in the melt in the presence of catalytic [Rh(η^6-FC$_6$H$_5$)(dppp)][BAr$^F_4$] resulted in the formation of linear dimer

species. Electron withdrawing groups were found to promote dehydrocoupling, although this rate increase was accompanied by competitive P-B bond cleavage to afford phosphine ligated metal species. This was suggested to be due to a weakening of the P-B bond due to the presence of electron withdrawing groups.[105]

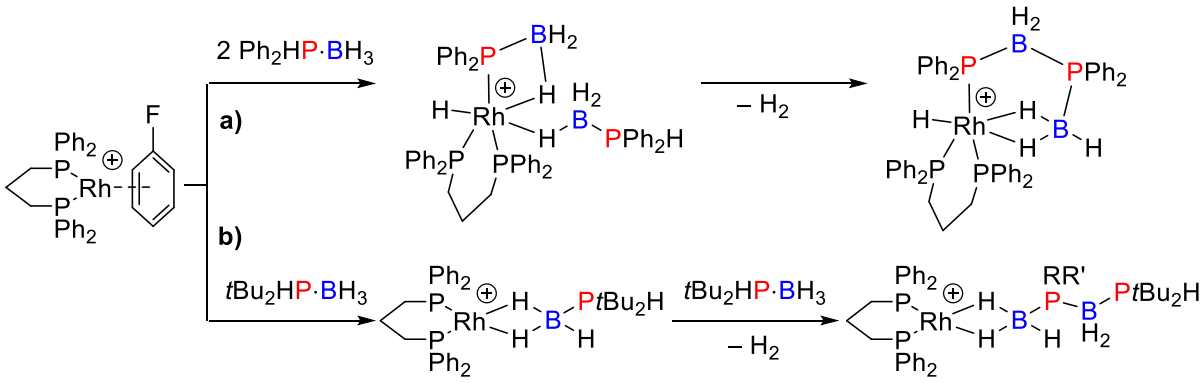

Scheme 1.13 Stoichiometric dehydrocoupling of $R_2HP{\cdot}BH_3$ (R = *t*Bu or Ph) using [Rh(η^6-FC_6H_5)(dppp)][BAr^F_4]. [BAr^F_4] anions omitted for clarity.[96]

Stoichiometric reaction of [Rh(η^6-FC_6H_5)(dppp)][BAr^F_4] with the P-monosubstituted phosphine-borane $CyH_2P{\cdot}BH_3$ resulted in observation of similar intermediates although a mixture of diastereomers were formed as a result of P-H activation at the prochiral phosphorus centre. Subsequent bond P-B bond formation results in the isolation of [Rh(L)(H)(σ,η^2-$PCyH{\cdot}BH_2PCyH{\cdot}BH_3$)][$BAr^F_4$] diastereomers in a 6:1 ratio suggesting that diastereoselectivity is imparted by the metal (Scheme 1.14).[105]

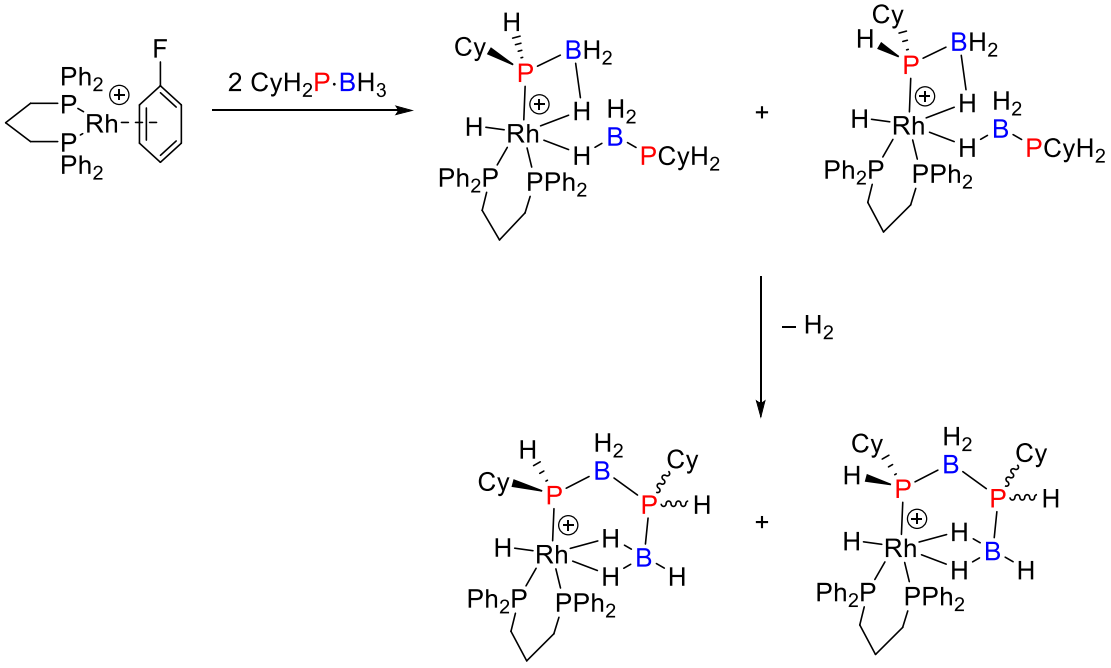

Scheme 1.14 Stoichiometric reaction of [Rh(η^6-FC_6H_5)(dppp)][BAr^F_4] with $CyH_2P{\cdot}BH_3$ resulting in a mixture of [Rh(L)(H)(σ,η^2-$PCyH{\cdot}BH_2PCyH{\cdot}BH_3$)][$BAr^F_4$] diastereomers. [$BAr^F_4$] anions are omitted for clarity.[105]

Combined experimental and computational studies on a related precatalyst [RhCp*(PMe_3)Me($ClCH_2Cl$)][BAr^F_4] have elucidated a likely polymer growth pathway via reversible chain transfer step-growth for $PhH_2P{\cdot}BH_3$. Through the use of P-disubstituted phosphine-boranes $R_2HP{\cdot}BH_3$ (R = Ph, Cy, *t*Bu) as model species, a catalytic cycle to the formation of linear dimer species was postulated, based on labelling and computational studies and the isolation of reaction intermediates (Scheme 1.15). Changing the substituent on phosphorus was found to have a significant effect on the products formed in stoichiometric reactions with [RhCp*(PMe_3)Me($ClCH_2Cl$)][BAr^F_4]. When R = *t*Bu, a base-stabilised phosphinoborane was formed (Scheme 1.15), whereas when R = Ph or Cy, a phosphido-borane was formed.[95]

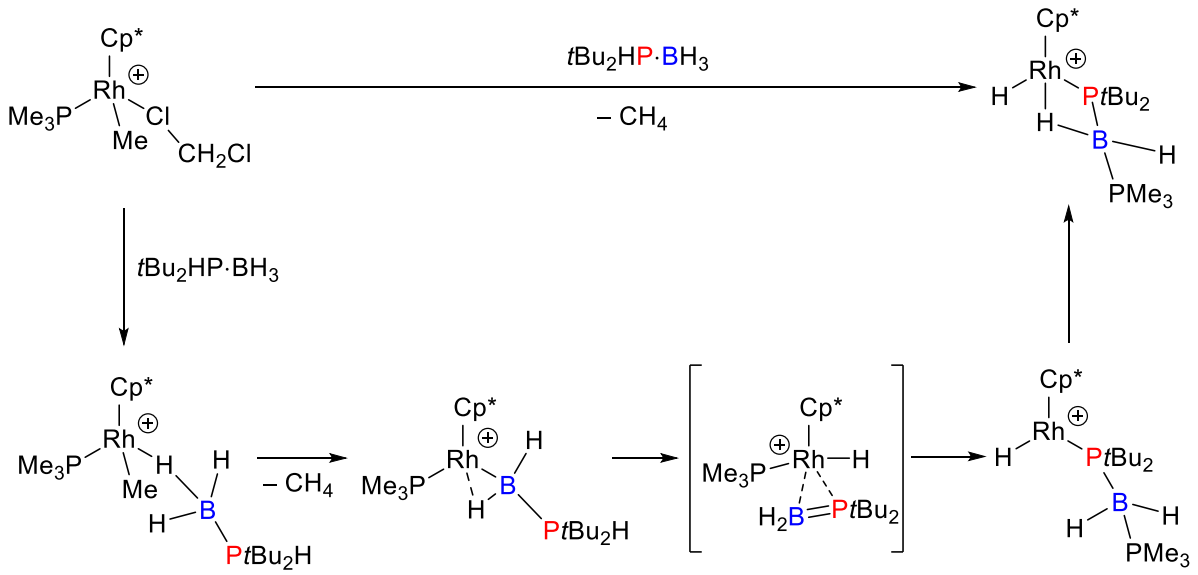

Scheme 1.15 Stoichiometric reaction of [RhCp*(PMe$_3$)Me(ClCH$_2$Cl)][BAr$^F{}_4$] with *t*Bu$_2$HP·BH$_3$. [BAr$^F{}_4$] anions are omitted for clarity.[95]

The report of a solution-based polymerisation of phenylphosphine-borane using CpFe(CO)$_2$OTf as a precatalyst allowed for the exploration of some mechanistic features via a variety of techniques.[99] The polymerisation was shown to be homogeneous by PMe$_3$ poisoning experiment and because use of pre-generated iron nanoparticles were inactive towards polymerisation of PhH$_2$P·BH$_3$. It was reported to operate via a chain growth mechanism based on the observation of high molar mass polymer at low conversion and that an increase in catalyst loading resulted in the formation of lower molar mass polymer. Stoichiometric reaction of CpFe(CO)$_2$OTf and PhH$_2$P·BH$_3$ at room temperature yielded [CpFe(CO)$_2$(PhHPBH$_3$)], a species which was active in dehydropolymerisation. It was postulated that catalysis proceeds via ligand displacement and P-H activation, followed by loss of CO and monomer coordination to the iron centre via a B-H agostic interaction. Computational studies showed this to be slightly endergonic; however, it was reasoned that as the substrate was present in a large excess, that this was a reasonable pathway. Activation of the B-H bond and B-P coupling to generate the growing polymer chain bound to Fe by a B-H σ-bond was postulated to occur and then P-H activation followed by coordination of PhH$_2$P·BH$_3$ with concomitant loss of H$_2$ which then closes the catalytic cycle (Scheme 1.16).

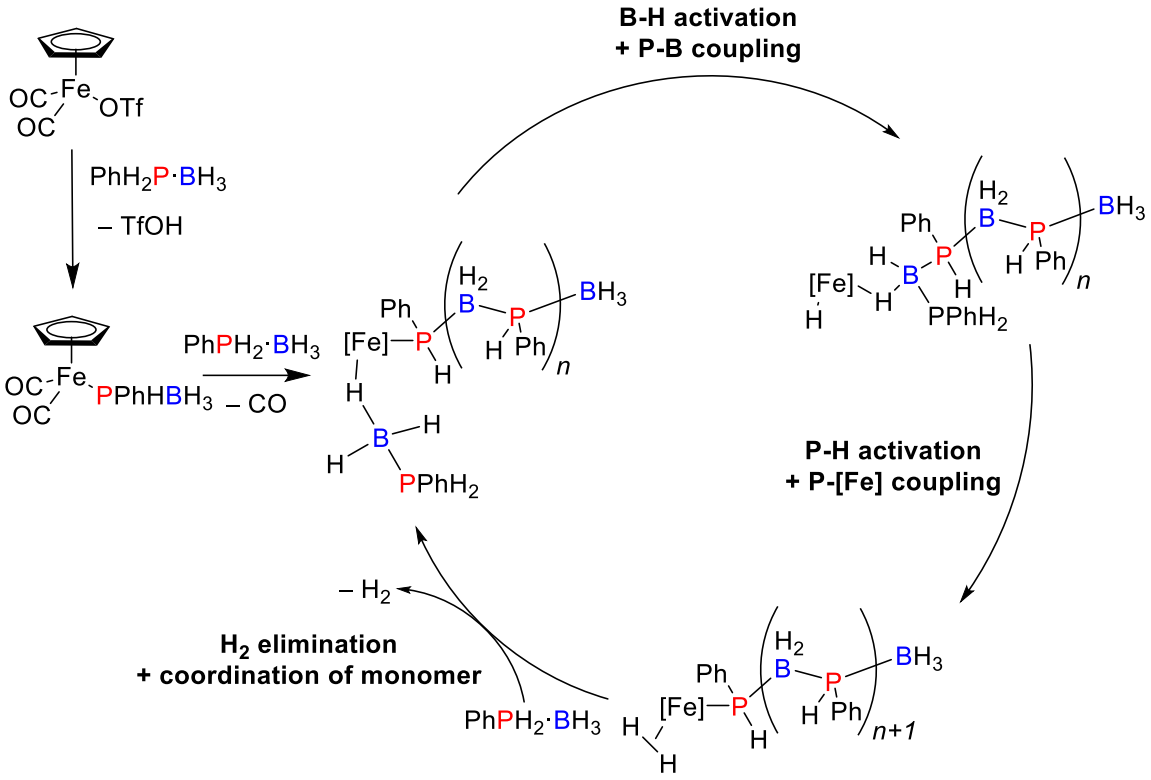

Scheme 1.16 Postulated mechanism for the dehydrocoupling of $PhH_2P{\cdot}BH_3$ using $CpFe(CO)_2OTf$ as a precatalyst.[99]

1.3.3.3 Metal-free routes to polyphosphinoboranes

While yet to achieve the generality of metal-catalysed dehydrocoupling of phosphine-boranes, several metal-free routes to polyphosphinoboranes have been reported. In 2003, Gaumont and co-workers reported the dehydrocoupling of $PhH_2P{\cdot}BH_3$ using $B(C_6F_5)_3$ as a catalyst (0.5 mol%) at 20 °C for 3 d (or 90 °C, 3 h); however, two low molar mass polymer fractions were obtained (M_w = 3,900 g mol^{-1}, PDI = 2.3, M_w = 800 g mol^{-1}, PDI = 1.9) and a number of poorly resolved signals were observed in the ^{31}P NMR spectrum (δ = −52 – −56 ppm) suggesting a mixture of products formed.[30] Dehydrocoupling of $H_3P{\cdot}BH_3$ in the presence of $B(C_6F_5)_3$ (5 mol%) at 70 – 90 °C was also described and reported to form an air- and moisture sensitive oligomeric material (Scheme 1.17).[30]

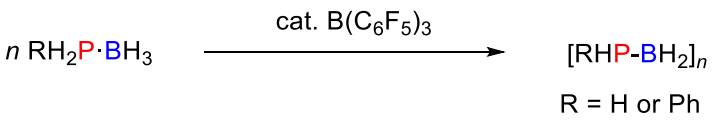

Scheme 1.17 $B(C_6F_5)_3$ catalysed dehydrocoupling of phosphine-boranes.[30]

An alternative addition/head-to-tail polymerisation of transient phosphinoboranes was reported by workers in the Manners and Scheer groups. Thermolysis of amine stabilised phosphinoboranes,

RR'P-BH_2·NMe_3, resulted in the formation of oligo- and polyphosphinoboranes. Heating H_2P-BH_2·NMe_3 in toluene at 80 °C for 20 h gave oligomers of $[H_2P\text{-}BH_2]_n$ which were poorly soluble. Thermolysis of *t*BuHP-BH_2·NMe_3 at 22 – 40 °C resulted in the formation of high molar mass material (Scheme 1.18; M_n = 27,800 – 35,000 g mol^{-1}),[106] and heating MeHP-BH_2·NMe_3 at 50 °C gave material consisting of at least 40 repeat units (identified by ESI-MS).[107] Analogous attempts to form P-disubstituted polymers via thermolysis of Ph_2P-BH_2·NMe_3 resulted in the formation of oligomeric species with a maximum molar mass of 1,200 g mol^{-1} detectable by ESI-MS.[106]

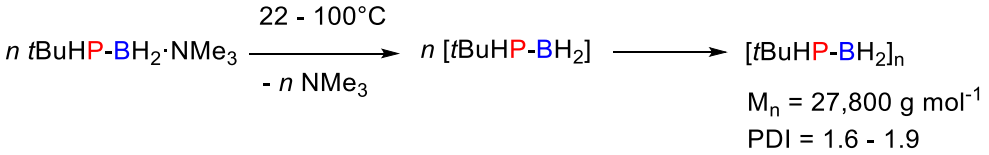

Scheme 1.18 Thermolysis head-to-tail polymerisation route to poly(*tert*-butylphosphinoborane).[106]

Cyclic (alkyl)(amino)carbenes (CAACs) have been recently found to act as a stoichiometric hydrogen acceptor in the dehydrogenation of phosphine-boranes releasing phosphinoborane [RR'P-BH_2] which spontaneously undergoes head-to-tail polymerisation (Scheme 1.19; R = Ph, R' = H, Ph or Et). Reaction of PhH_2P·BH_3 with CAAC^{Me} in THF at 60 °C for 3 h resulted in the formation of high molar mass polymer (M_n = 83,800 g mol^{-1}, PDI = 1.13). Extension to P-disubstituted phosphine-boranes (R = Ph, R' = Ph or Et) resulted in the formation of mostly low molar mass material but around 10% high molar mass material (R' = Ph, M_n = 54,300, PDI = 1.12; R' = Et, M_n = 59,600 g mol^{-1}, PDI = 1.08).[108]

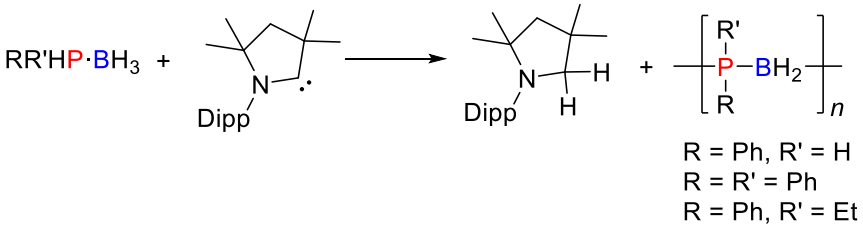

Scheme 1.19 Synthesis of polyphosphinoboranes using CAAC.[108]

1.3.4 Properties and applications of polyphosphinoboranes

With the exception of $[H_2P\text{-}BH_2]_n$,[30] polyphosphinoboranes that have been described in the above sections are generally air- and moisture stable macromolecules. The glass transition temperatures (T_g) of polyphosphinoboranes are highly dependent on phosphorus substituents, varying from −68 to >135 °C. Where comparisons to organic polyolefin analogues have been made, the T_g of the

polyphosphinoborane is generally lower. For example, the T_g of [*i*BuHP-BH_2]$_n$ is 5 °C,[91] whereas for poly(4-methylpent-1-ene) the T_g is 45 – 50 °C.[109] This reduced T_g compared to polyolefin analogues is believed to arise from the P-B bond lengths in polyphosphinoboranes (1.9 – 2.0 Å) being significantly longer than typical C-C bond lengths (1.54 Å). This reduces the steric interactions between polymer side groups and therefore results in a higher degree of torsional flexibility and correspondingly a reduction in T_g.[91]

Polyphosphinoboranes have shown to have applicability as etch-resists for soft lithography.[92, 99, 100] In 2015, a solution of [PhHP-BH_2]$_n$ was drop-cast onto a silicon wafer and a pattern created using a poly(dimethylsiloxane) (PDMS) stamp. After removal of the stamp, the samples were imaged by scanning electron microscopy (SEM) which revealed retention of shape. Hydrophobic surfaces have been formed by spin coating a 5 mg mL^{-1} solution of [RHP-BH_2] (R = *p*-(CF_3O)C_6H_4 and 3,5-(CF_3)$_2C_6H_3$)) onto a glass slide. Advancing water droplet contact angles of 101° and 97° (±2°) were measured for *p*-(CF_3O)C_6H_4 and R = 3,5-(CF_3)$_2C_6H_3$ respectively.[100]

Polyphosphinoboranes have been postulated for a number of other applications including as ceramic precursors to boron phosphide which exhibits interesting semi-conducting properties;[110] as flame-retardants owing to the high phosphorus and boron content of the polymer backbones; as well as in optoelectronics.[111] The formation of gels which reversibly swell in organic solvents has also been reported by extended heating and/or high catalyst loadings during the polymerisation of certain phosphine-boranes.[90, 100] This has been attributed to intramolecular crosslinking during polymerisation; however, there is little control over this crosslinking.

1.4 Polysiloxanes and boron containing analogues

1.4.1 Polysiloxanes: history and properties

Polysiloxanes [RR'SiO]$_n$ are the most intensively studied and commercialised inorganic polymer class. They were first reported at the beginning of the 20th century through the pioneering work of Kipping.[112] In the preparation of tetraphenyl silicon, a species was isolated that was postulated to be a silicoketone or "silicone" (C_6H_5)$_2$Si=O; however, on the basis that this species had little resemblance to benzophenone, it was noted that this could in fact be a polymeric species, an assertion that was later proved to be true.[113]

These polymers possess a number of desirable properties. The strength of the Si-O bond bestows high thermal stability on the polymer and the presence of long Si-O bonds (1.64 Å for PDMS) and irregular bond angles at Si and O (∠ Si-O-Si: 110° and ∠ O-Si-O: 143° for PDMS) results in highly flexible materials with low glass-transition temperatures. These properties have facilitated the use of polysiloxanes in a number of high temperature applications such as in heat transfer agents and high-performance elastomers. The nature of the bonding in polysiloxanes and the typically alkyl side groups result in unusual surface properties such as hydrophobicity giving rise to applications in waterproofing garments and as anti-moulding agents. Siloxane polymers are also highly permeable to gases, transparent, and biocompatible and have found uses in a number of biomedical applications e.g. in contact lenses and artificial skin coatings.[34, 114-116]

1.4.2 Synthesis of polysiloxanes

The vast majority of polysiloxanes synthesised in the ca. 850 kilotonne per year silicone industry are produced from chlorosilanes R_2SiCl_2 (R is most commonly Me) and water through either polycondensation or ROP pathways. Hydrolysis of R_2SiCl_2 gives a mixture of dihydroxy siloxanes which can condense to form polysiloxanes, and cyclic siloxanes which can undergo ROP (Scheme 1.20). The conditions utilised in the hydrolysis of R_2SiCl_2 greatly influences the composition of the products obtained. Basic catalysts and higher temperatures result in high molar mass linear polymers, whereas, acid catalysts produce cyclic molecules or low molar mass oligomers.[115]

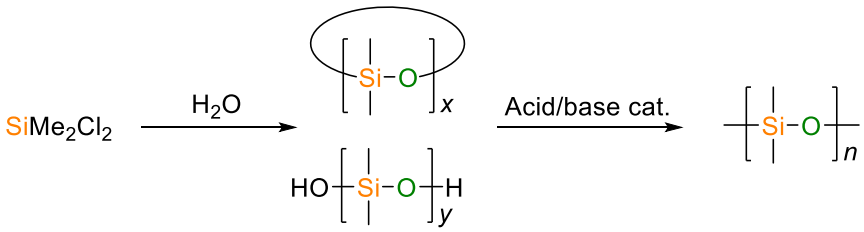

Scheme 1.20 Commercial routes to PDMS.

Cyclic siloxanes can undergo ROP initiated by either anionic or cationic species. Anionic polymerisation can be living in nature through use of initiators such as *n*BuLi. This chain growth polymerisation allows for the formation of high molar mass material with low polydispersity in contrast to polymer produced through step growth polycondensations. The formation of related polycarbosiloxanes has also been reported via ROP of cyclic monomers.[117] While bases such as KOH

and *n*BuLi have often been employed as ROP initiators for the formation of polysiloxanes, NHCs have been shown to be efficient catalysts for ROP of cyclotetra(dimethyl)siloxane (Scheme 1.21).[118] Using primary alcohols for chain termination, polysiloxanes can be formed with controlled molar mass.

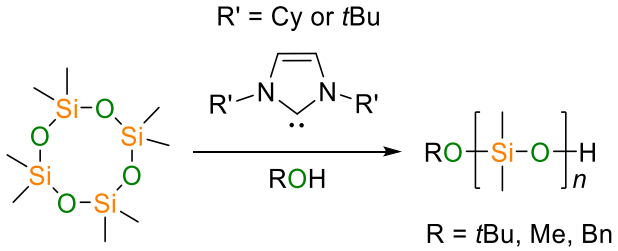

Scheme 1.21 Synthesis of PDMS via ROP of cyclotetrasiloxane.[118]

Despite these well-established routes to polysiloxanes, the majority of commercial silicones consist of a mixture of cyclic and linear polymers with different molar masses. The functional group tolerance of these polymerisations is also limited with incorporation of acidic and basic functionalities a considerable challenge.

One alternative route is through metal-catalysed heterodehydrocoupling of bis(hydrosilanes) with water and diols. 1,4-bis(dimethylsilyl)benzene was found to react with water or diols in the presence of rhodium, platinum, or palladium catalysts, yielding polysiloxane or polysilyl ether products (Scheme 1.22 a).[119, 120] The formation of poly(silarylene-silazenes) was also demonstrated via reaction of 1,4-bis(dimethylsilyl)benzene with ammonia.[121] Transition metal dehydrocoupling has subsequently been extended to the design of a number of stereoregular polysiloxanes (Scheme 1.22 b), and higher order structures.[122-124]

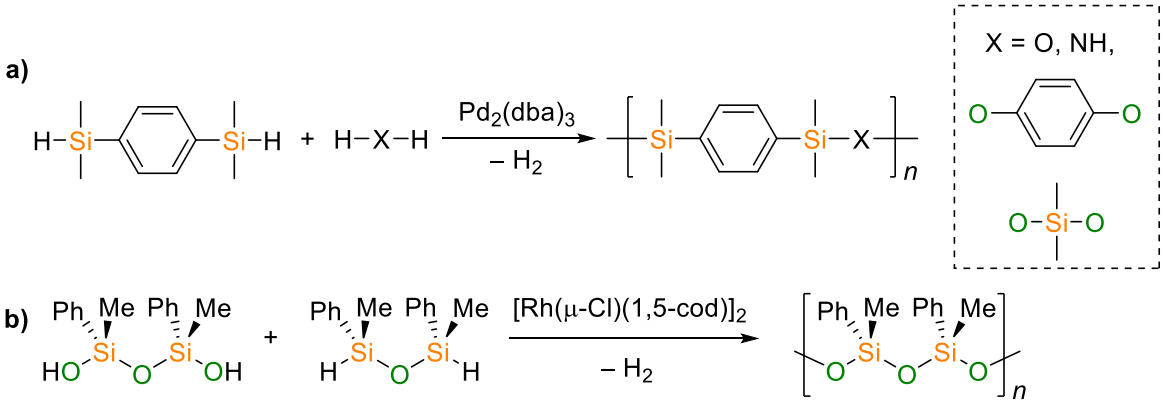

Scheme 1.22 a) Heterodehydrocoupling polymerisation of 1,4-bis(dimethylsilyl)benzene;[119-121] b) Rh^{I} catalysed dehydrocoupling yielding highly syndiotactic polysiloxanes.[122]

1.4.3 Piers-Rubinsztajn (PR) reaction

In the investigations into the reduction of carbonyls using hydrosilanes, Piers and co-workers noted that $B(C_6F_5)_3$ was a competent catalyst for the formation of silyl ethers from the corresponding ketone (Scheme 1.23 I).[125] Subsequent mechanistic investigations invoked the unusual activation of the silane by hydride abstraction rather than activation of the carbonyl as the driving force for this reaction.[126] This seminal finding has heavily influenced the development of main group catalytic chemistry in recent years.[127-132] When excess silane is used in the hydrosilylation of ketones, over reduction of the desired silyl ether was observed resulting in formation of disiloxanes (Scheme 1.23 II).[125]

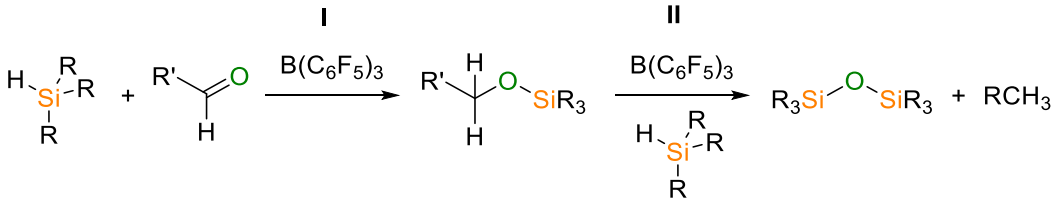

Scheme 1.23 Hydrosilylation of carbonyls in the presence of $B(C_6F_5)_3$ and over reduction to disiloxanes.[125]

While the formation of siloxane is generally undesirable from the organic chemist's perspective, Rubinsztajn and Cella recognised the potential of this methodology for the formation of linear siloxane containing polymers. They reported the heterocondensation process between dihydrosilanes and dialkoxysilanes in the presence of catalytic $B(C_6F_5)_3$ (0.1 mol%) which resulted in the formation of polysiloxanes with elimination of a hydrocarbon as a by-product (Scheme 1.24).[31, 133] This reaction became known as the Piers-Rubinsztajn (PR) reaction.

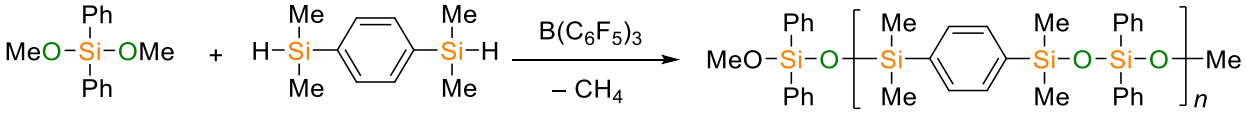

Scheme 1.24 Piers-Rubinsztajn route to polysiloxanes.[31]

1.4.3.1 Mechanism of the PR reaction

The equilibrium between $B(C_6F_5)_3$ and $B(C_6F_5)_3$-carbonyl complexes has been examined in a study of C=O hydrosilylation. The carbonyl complex was found to be favoured by around 10^2;[125] however, the rates of hydrosilylation were inversely proportional to carbonyl concentration, suggesting that formation of $B(C_6F_5)_3$-carbonyl complexes actually inhibit the reaction. It was instead suggested that

$B(C_6F_5)_3$ activates the silane forming a silylium borohydride complex which is the active species in subsequent reduction.

In further studies, the hydrosilylation of imines was investigated.[134] It was found that less basic imines underwent hydrosilylation more readily. This is consistent with activation of the silane being required for the reduction rather than the imine as a less basic imine would be expected to coordinate less strongly to $B(C_6F_5)_3$ and so result in more free borane which can activate the silane.

The mechanism of carbonyl hydrosilylation was investigated thoroughly in the Piers' group using kinetic, competition, isotopic labelling, and crossover experiments. These provided support for silane activation by $B(C_6F_5)_3$, followed by silyl transfer to the carbonyl oxygen and subsequent H^- attack on the carbonyl by a borohydride to afford the resultant silyl ether (Scheme 1.25).[126] More recently, the use of chiral silanes suggested that the hydride transfer takes place enantioselectively with inversion at silicon (Scheme 1.26).[135]

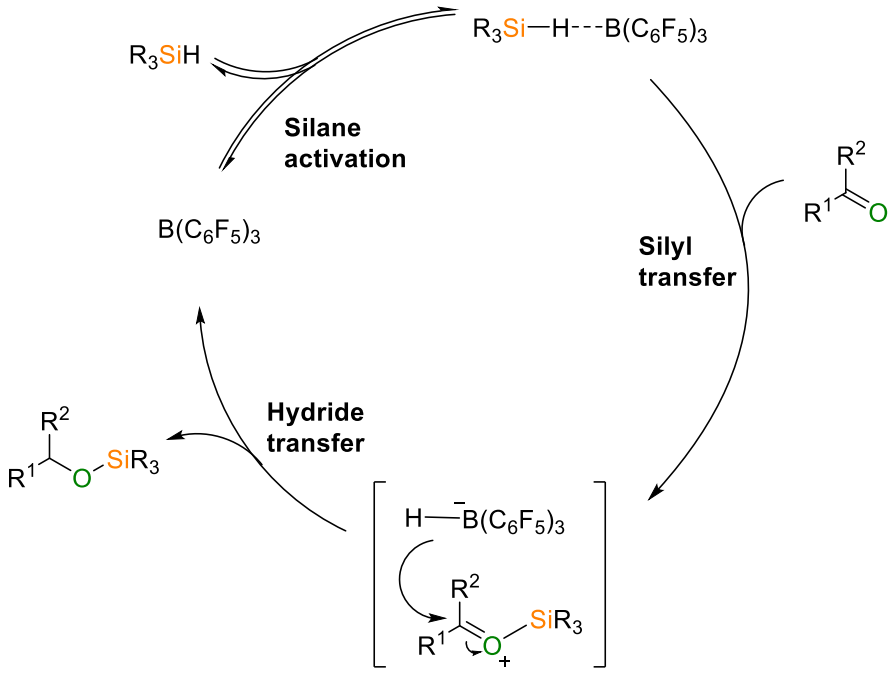

Scheme 1.25 The mechanism of the $B(C_6F_5)_3$ catalysed hydrosilylation of carbonyls resulting in the formation of silyl ethers.[126]

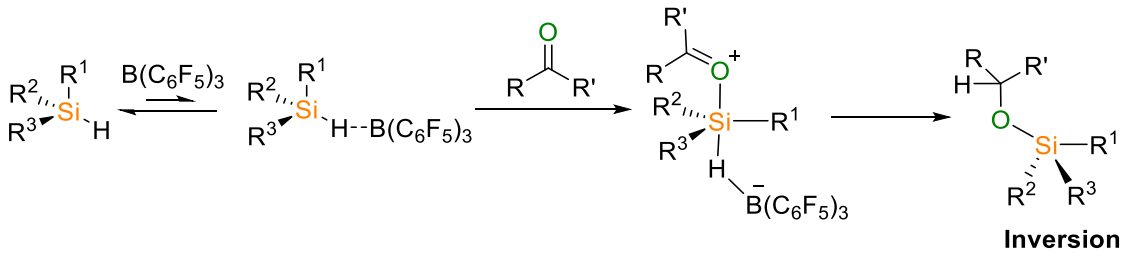

Scheme 1.26 Observed inversion of stereochemistry at silicon during the hydrosilylation of carbonyls catalysed by $B(C_6F_5)_3$.[135]

As previously noted, the extension of this to the coupling of alkoxysilanes and hydrosilanes catalysed by $B(C_6F_5)_3$ is known as the PR reaction. A mechanism for this coupling was proposed where a silane-borane complex is attacked by an alkoxysilane nucleophile,[136] forming a pentacoordinate silyl-H oxonium complex. Substitution then occurs with inversion followed by loss of alkane and siloxane to regenerate free $B(C_6F_5)_3$ (Scheme 1.27 a).

One limitation of the PR reaction is the possibility for metathesis reactions to occur where the hydrosilane is converted to an alkoxysilane which can then itself enter the catalytic cycle to form siloxanes with remaining hydrosilanes. This becomes problematic when the R groups on the hydrosilanes and alkoxysilane are different (Scheme 1.27 b).[137-139] Nevertheless, by careful control of reaction conditions, the PR reaction has become a powerful tool in silicone chemistry, facilitating the formation of diverse polysiloxanes under mild conditions with highly controlled structures e.g. chiral, cyclic, and dendritic polysiloxanes, many of which are inaccessible via classical polymerisation techniques.[140]

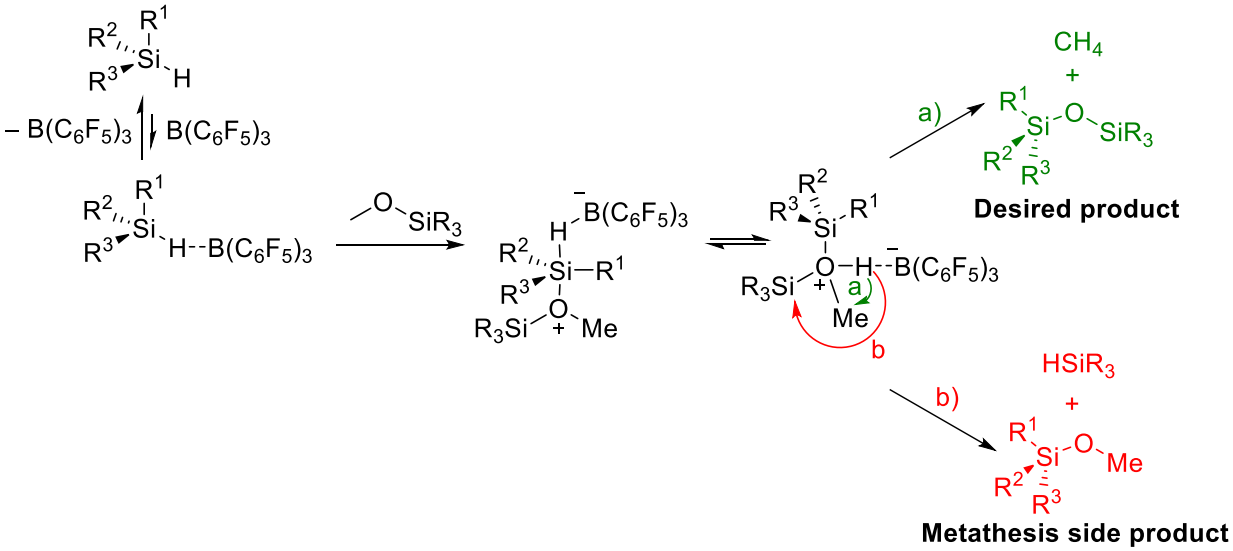

Scheme 1.27 The mechanism of the PR reaction resulting in a) formation of a siloxane bond; b) metathesis reaction generating a silyl ether from the hydrosilanes starting material.[137-139]

1.4.4 Borosiloxanes

Borosiloxanes possess high chemical and thermal stabilities,[141, 142] and have been shown to have promise in applications such as flame retardants,[143] electrolyte additives,[144, 145] ceramic precursors,[146, 147] and chemical sensors for amines[148] and fluoride anions.[149] Owing to the potential applicability of borosiloxanes, research into the formation of Si-O and B-O bonds has been of significant interest. They have been shown to form cyclic and cage structures,[150-153] as well as gels and network polymers.[141, 146, 154-156] There are, however, few examples of well-defined linear polymers consisting of alternating borane and siloxane moieties.[149, 157]

Conventional syntheses of molecular borosiloxanes have involved the reaction of hydroxyborane with silane derivatives[146, 153, 158-161] or the reaction of a silanol with borane derivatives.[162-167] However, these routes, commonly suffer from laborious experimental set up and work up and commonly involve the formation of undesired side products, for example, corrosive HCl. Recently, methods have been developed for the synthesis of borosiloxanes via transition metal catalysed dehydrocoupling; for example, the *O*-borylation of silanols with vinylboronates catalysed by Ru complexes;[168] the photoreaction of bis-boryloxide/boroxine silanes in the presence of water catalysed by Mo, W, and Fe;[169] the Ru-catalysed reaction of hydroboranes with silanes and water;[170] and the Pd-catalysed reaction of silanols with diborons.[171]

1.4.4.1 Synthesis of polyborosiloxanes

In the 1940s, it was found that it was possible to significantly affect the backbone of polysiloxanes through incorporation of boron. Intensive heating of PDMS in the presence of boric acid or boric oxide resulted in formation of crosslinked materials termed "Silly Putty".[172-174] These elastomers have high thermal stability and fascinating viscoelastic properties giving rise to applications including in tectonic modelling, cleaning adhesives, insulating coatings, and in heat resistant materials.[175]

The exact nature of this crosslinking was initially poorly understood and has subsequently been the subject of debate in the literature. Hydrogen bonding through OH groups (Scheme 1.28 a), covalent bonds to the boron centre (Scheme 1.28 b), and dative crosslinking between boronic acids and oxygen atoms on the polysiloxane backbone (Scheme 1.28 c) have all been invoked as possibilities to explain this.[174-176]

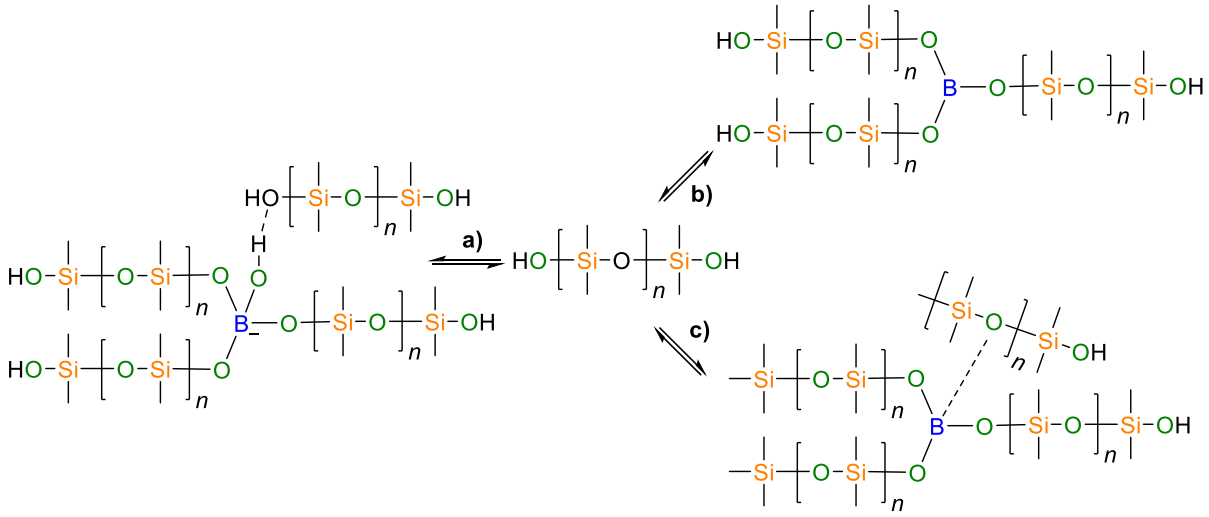

Scheme 1.28 Crosslinking modes proposed for elastomers formed via the condensation of PDMS with boric acid via a) hydrogen bonding through OH groups; b) covalent bonding at the boron centre; c) dative crosslinking between boronic acids and oxygen atoms on the polysiloxane backbone.[176]

While the incorporation of boron into polysiloxanes has been extensively studied, the amount of boron incorporation in the polymer chains is low. The synthesis of materials featuring alternating boron and siloxane units was first reported in 1960 through the condensation reaction between boric acid and R_2SiCl_2 (R = Me,[177] R = Ph).[141] This results in the formation of ill-defined networks and also results in formation of HCl as a by-product (Scheme 1.29). Polyborodiphenylsiloxane was investigated and this polymer was found to exhibit high thermal stability.[141]

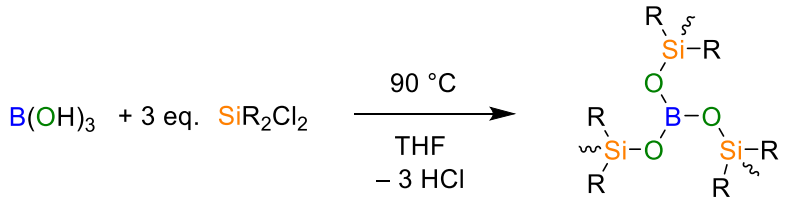

Scheme 1.29 Condensation synthesis of polyborosiloxane resin.[141, 177]

Condensation routes to linear borosiloxanes have also been reported. In 2011, a linear borosiloxane end-capped with phenyl acetylene was reported by Wang and coworkers.[157] This was synthesised by polycondensation of phenylboronic acid with dichlorodiphenylsilane followed by post polymerisation modification of the polymer using in situ generated phenylacetylide (Scheme 1.30). From GPC analysis, the molar mass of this polymer was found to be low and the PDI high (M_w = 5,600 g mol^{-1}, PDI = 2.7). Heating this polymer at elevated temperature (slow heating to 400 °C over 10 h) was found to produce a thermoset which showed weight retention of ca. 90% when heated to 900 °C.

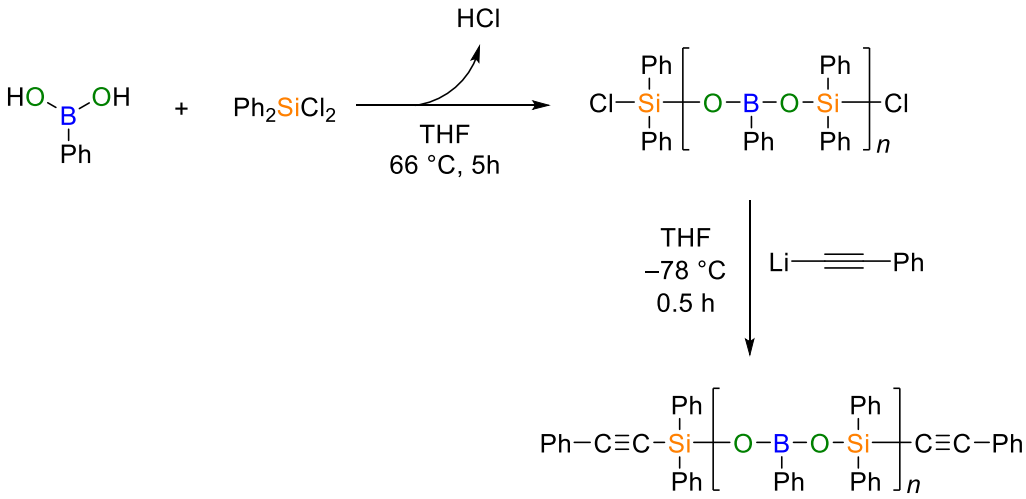

Scheme 1.30 Boron-silicon-acetylene hybrid polymer synthesis.[157]

In 1992, Manners and co-workers took inspiration from the ROP routes to polysiloxanes to attempt to form linear polymers from the ring opening of borosiloxane cycles. Borosiloxane rings of varying size and composition were heated in the presence of K[OSiMe$_3$]; however, while a ring-expansion pathway leading to a mixture of larger cycles was observed, extrusion of boron in the form of phenyl boroxine was also observed and postulated to present a significant thermodynamic barrier to polyborosiloxane formation.[153]

Despite the use of transition metal-catalysed dehydrocoupling as a route to molecular borosiloxanes and to polysiloxanes, there are only very limited reports of the formation of polyborosiloxanes via dehydrocoupling. One example involved the Pd catalysed dehydrocoupling of diphenylsilanediol and mesitylborane at room temperature (Scheme 1.31).[149] A single peak was observed in both the ^{11}B and ^{29}Si NMR spectra, indicating clean formation of the desired polymer. The IR spectrum of this polymer confirmed the formation of Si-O-B linkages with a peak observed at 814 cm^{-1}. The polymer was determined to have an M_n of 42,500 g mol^{-1} and a low PDI of 1.2. A significant limitation of this methodology was the need to generate the mesitylborane in situ due to its inherent instability.

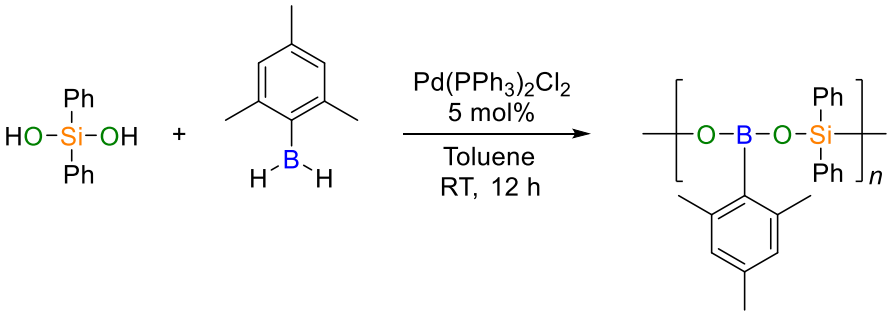

Scheme 1.31 Reaction of diphenylsilanediol and in situ generated mesitylborane to form polyborosiloxane.[149]

Non-metal catalysed formation of borosiloxanes has been reported taking inspiration from the Piers-Rubinsztajn reaction. In 2014, Rubinsztajn reported the synthesis of polyborosiloxane resins from dehydrocarbonative coupling of trimethyl borate and diphenylsilane (Scheme 1.32). The presence of B-O-Si linkages in the insoluble network was determined by IR spectroscopy. The presence of multiple peaks in the ^{29}Si NMR spectrum of this resin with chemicals shifts in the range −38 to −47 ppm suggests that a side metathesis reaction commonly invoked in PR reactions was observed leading to the formation of siloxane linkages within the resin.[154]

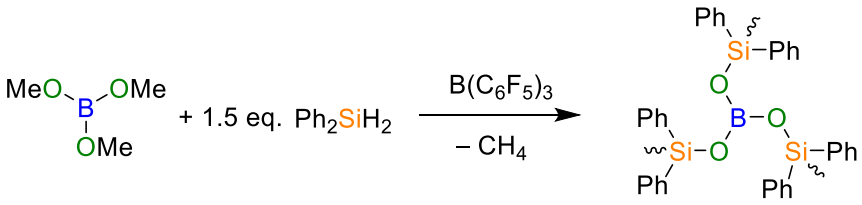

Scheme 1.32 Piers-Rubinsztajn route to borosiloxane resins.[154]

The preparation of a linear polysiloxane/borosiloxane copolymer from reaction of dimethoxydimethylsilane, 1,1,3,3-tetramethyldisiloxane and a substoichiometric amount of

phenylboronic acid in the presence of $B(C_6F_5)_3$ was recently claimed in a patent (Scheme 1.33);[178] however, the product was minimally characterised and so the degree of boron incorporation into the polymer is unclear.

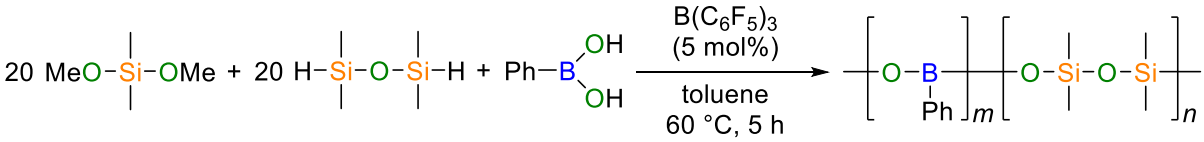

Scheme 1.33 Reaction of dimethoxydimethylsilane, 1,1,3,3-tetramethyldisiloxane, and phenylboronic acid in the presence of $B(C_6F_5)_3$.[178]

1.5 Synthesis of hydrogels from main group polymers

1.5.1 Main group polymer hydrogels

Polymer gels are semi-solid systems consisting of three-dimensional crosslinked polymer networks capable of absorbing large amounts of solvent in their swollen state. These materials are known as hydrogels if the solvent is water,[179] and can be classified as either physical or chemical gels: physical gels are formed when secondary forces, for example H-bonding, ionic, or hydrophobic forces are responsible for formation of a physical network; and chemical gels result when covalent linkages are formed between polymer chains. Physical hydrogels, in particular, are often designed to form under physiological conditions and can be dissolved by changes in, for example, pH and temperature; whereas chemical hydrogels tend to be more robust when formed.[180] Due to their high water content, the properties of hydrogels closely resemble those of biological tissues resulting in excellent biocompatibility.[179] Since the first report on hydrogels and their use as soft contact lenses in 1960,[181] these materials have found uses in a wide variety of biomedical applications, including controlled drug delivery[182] and tissue engineering.[183, 184]

The vast majority of hydrogels that have been hitherto reported are derived from organic polymers, for example, poly(ethylene glycol)[185, 186] and poly(vinyl alcohol),[187] or natural polymers such as chitosan.[188] The incorporation of inorganic elements into hydrogels has generated growth interest as their presence can lead to an improvement in material properties and the incorporation of interesting functionality such as redox responses, high thermal stability, and thermoresponsive swelling behaviour.[189, 190]

1.5.2 Polysiloxane hydrogels

One such method of forming hydrogels featuring main group domains is an inorganic sol-gel polymerisation. This process involves the reaction of metal-containing species to form a metal oxide in the form of an inorganic network under mild conditions (low temperature, mild pH, water solvent).[190] Silicon alkoxides are the most commonly used molecular precursor for the formation of hydrogels through the sol-gel process. The formation of the network is driven by two reactions: hydrolysis and condensation. First the hydrolysis of alkoxysilyl groups gives silanol moieties (Scheme 1.34 a) which can undergo condensation reactions to yield Si-O-Si linkages (Scheme 1.34 b) and c). Because of the tetravalence of the silicon, linkages can form to a number of different partners giving a three-dimensional network. This process has allowed for the formation of inorganic network structures and a variety of hybrid materials with interesting properties. The presence of inorganic elements confers mechanical strength and thermal stability to the material while the organic moieties allows for specific chemical and/or biological functionality. The incorporation of organic and biological entities has resulted in biomedical applications as sensors,[191] the encapsulation of cells[192] and enzymes,[193] bone repair,[194] and tissue engineering,[195-197] as well as a number of non-biological applications.[198]

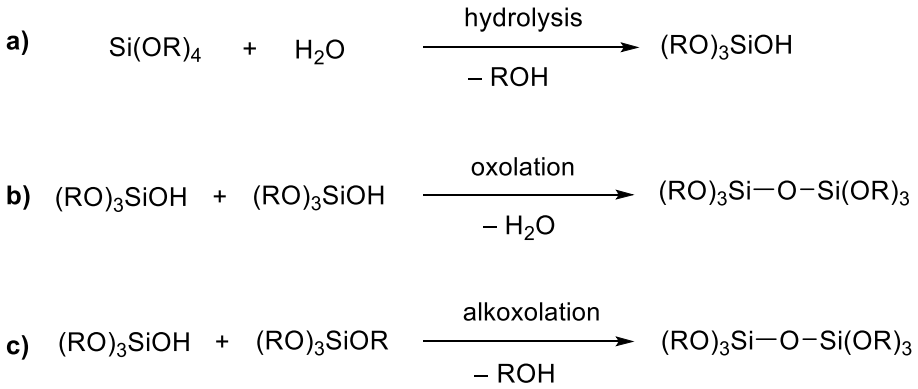

Scheme 1.34 The sol-gel process a) Hydrolysis of a silicon alkoxide resulting in silanol formation; b) condensation of a silanol via oxolation with concomitant loss of H_2O; (c) condensation of a silanol via alkoxolation with concomitant loss of alcohol.[190]

While there have been significant advances in the development of hydrogels incorporating inorganic elements, examples of hydrogels featuring networks made up of inorganic polymer chains linked together are still extremely scarce and mostly confined to polyphosphazenes and polysiloxanes. Polysiloxane gels have found a number of applications in the fields of biocompatible devices such as contact lenses and drug delivery systems.[199-201] PDMS possesses a number of properties that make it

well suited to these applications, including chemical and thermal stability, optical transparency, high flexibility, and nontoxicity and biocompatibility although this has required the development of techniques to overcome its inherent hydrophobicity,[202] for example, through synthesis of copolymers containing hydrophilic polymer blocks such as PEG.[203]

1.5.3 Polyphosphazene hydrogels

Polyphosphazene gels have been investigated and were found to have interesting properties as well as high biocompatibility.[204] For example, the crosslinking of poly[bis((methoxyethoxy)ethoxyphosphazene)] (MEEP) using gamma or UV irradiation produces a gel with a lower critical solution temperature (LCST) in water (Scheme 1.35). While at room temperature, the gel will swell in water, heating this material to above the LCST of 65 °C, resulted in water extrusion.[205-207] Water extrusion above the LCST is due to hydrophobic interactions between alkyl units dominating over the hydrophilic effects of the oxygen atoms in the MEEP side chains. At lower temperatures, the hydrophilic interactions are more significant. Replacement of the alkyl terminal group with a hydrophilic amino unit gives a polymer which does not display a LCST.[204] More recently, polyphosphazenes hydrogels have been developed as injectable materials for biomedical applications.[208-211]

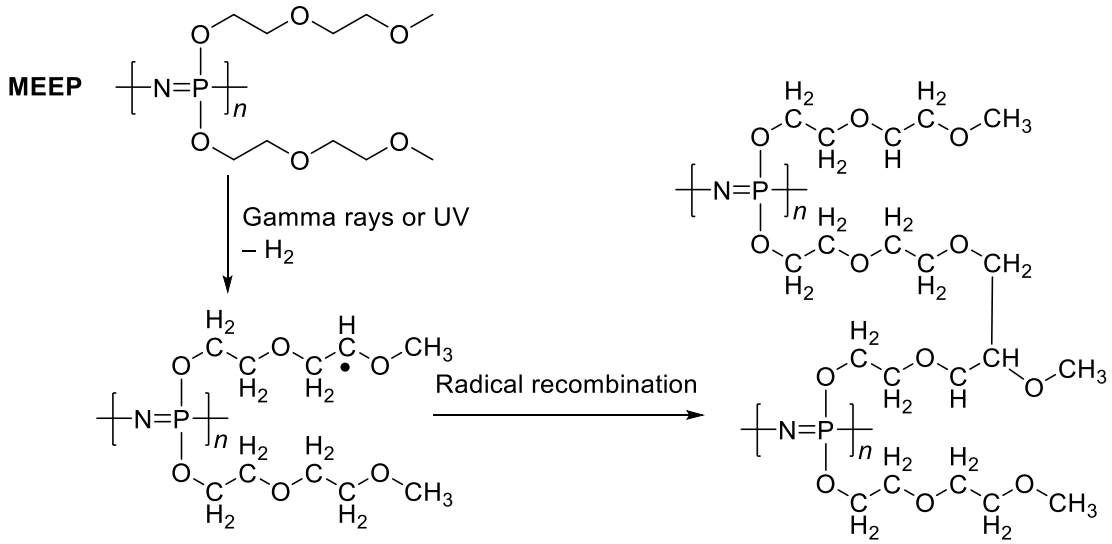

Scheme 1.35 Crosslinking of poly[bis((methoxyethoxy)ethoxyphosphazene)] using gamma rays or UV irradiation.[206]

1.6 Thesis summary and acknowledgement of collaborators

This thesis compiles the results of work on the synthesis and reactivity of main group element-containing polymers with a particular focus on the forming novel polyphosphinoborane materials and borosiloxane polymers. The thesis is composed of four results chapters, each of which has been written in the form of stand alone research papers. The contents of each chapter are as follows:

- **Chapter 2** describes the post-polymerisation modification of poly(phenylphosphinoborane) via hydrophosphination of olefins to form P-di(organosubstituted) polymers $[PhRP\text{-}BH_2]_n$.

This chapter has been reproduced from Knights, A. W., Chitnis, S. C., Manners, I. *Chem. Sci.*, **2019**, 10, 7281–7289.

Collaborators: Dr Saurabh S. Chitnis performed some initial hydrophosphination reactions of 1-octene using poly(phenylphosphinoborane) alongside some preliminary studies on the synthesis of crosslinked poly(phenylphosphinoborane).

- **Chapter 3** describes investigations into the iron-catalysed dehydropolymerisation of phenylphosphine-borane and the synthesis of polyphosphinoboranes using non-metal precatalysts.

Collaborators: Dr Diego A. Resendiz-Lara assisted in the synthesis and characterisation of poly(phenylphosphinoborane) and poly(*tert*-butylphosphinoborane) using triflic acid as a precatalyst.

- **Chapter 4** is split into two sections. The first describes the synthesis of polyphosphinoborane-based hydrogels; and the second describes the use of polyphosphinoboranes as flame-retardant additives.

Collaborators: Justin J. Kröger synthesised and performed swelling experiments on hydrogels **4.3a** – **c** and **4.3e** – **g**.

- **Chapter 5** describes the synthesis and characterisation of borosiloxane molecules and polymers via dehydrocoupling and demethanative condensation routes.

Collaborators: Thomas A. R. Horton performed initial synthesis **5.2a**, **5.2b**, and **5.3a** and carried out kinetic studies on the reaction between **5.5** and Et_3SiH during his Master's research project. Dr Marius I. Arz provided additional scientific insight.

1.7 References

1. Eisch, J. J., *Organometallics* **2012,** *31,* 4917-4932.
2. Grubbs, R. H., *Angew. Chem. Int. Ed.* **2006,** *45,* 3760-3765.
3. Beletskaya, I. P.; Cheprakov, A. V., *Chem. Rev.* **2000,** *100,* 3009-3066.
4. Miyaura, N.; Suzuki, A., *Chem. Rev.* **1995,** *95,* 2457-2483.
5. https://www.nobelprize.org/prizes/lists/all-nobel-prizes-in-chemistry.
6. Shegavi, M. L.; Bose, S. K., *Catal. Sci. Technol.* **2019,** *9,* 3307-3336.
7. Ros, A.; Fernández, R.; Lassaletta, J. M., *Chem. Soc. Rev.* **2014,** *43,* 3229-3243.
8. Hartwig, J. F., *Chem. Soc. Rev.* **2011,** *40,* 1992-1992.
9. Hartwig, J. F., *Acc. Chem. Res.* **2012,** *45,* 864-873.
10. Mkhalid, I. A. I.; Barnard, J. H.; Marder, T. B.; Murphy, J. M.; Hartwig, J. F., *Chem. Rev.* **2010,** *110,* 890-931.
11. Delacroix, O.; Gaumont, A. C., *Curr. Org. Chem.* **2005,** *9,* 1851-1882.
12. Koshti, V.; Gaikwad, S.; Chikkali, S. H., *Coord. Chem. Rev.* **2014,** *265,* 52-73.
13. Bange, C. A.; Waterman, R., *Chem. Eur. J.* **2016,** *22,* 12598-12605.
14. Rosenberg, L., *ACS Catal.* **2013,** *3,* 2845-2855.
15. Troegel, D.; Stohrer, J., *Coord. Chem. Rev.* **2011,** *255,* 1440-1459.
16. Miller, R. D.; Michl, J., *Chem. Rev.* **1989,** *89,* 1359-1410.
17. Corcoran, E. W.; Sneddon, L. G., *J. Am. Chem. Soc.* **1984,** *106,* 7793-7800.
18. Corcoran, E. W.; Sneddon, L. G., *J. Am. Chem. Soc.* **1985,** *107,* 7446-7450.
19. Aitken, C.; Harrod, J. F.; Samuel, E., *J. Organomet. Chem.* **1985,** *279,* C11-C13.
20. Biran, C.; Blum, Y. D.; Glaser, R.; Tse, D. S.; Youngdahl, K. A.; Laine, R. M., *J. Mol. Catal.* **1988,** *48,* 183-197.
21. Blum, Y.; Laine, R. M., *Organometallics* **1986,** *5,* 2081-2086.
22. He, J.; Liu, H. Q.; Harrod, J. F.; Hynes, R., *Organometallics* **1994,** *13,* 336-343.
23. Shu, R.; Hao, L.; Harrod, J. F.; Woo, H.-G.; Samuel, E., *J. Am. Chem. Soc.* **1998,** *120,* 12988-12989.
24. Leitao, E. M.; Jurca, T.; Manners, I., *Nat. Chem.* **2013,** *5,* 817-829.
25. Waterman, R., *Chem. Soc. Rev.* **2013,** *42,* 5629-5641.
26. Power, P. P., *Nature* **2010,** *463,* 171-177.
27. Melen, R. L., *Science* **2019,** *363,* 479-484.
28. Hill, M. S.; Liptrot, D. J.; Weetman, C., *Chem. Soc. Rev.* **2016,** *45,* 972-988.
29. Melen, R. L., *Chem. Soc. Rev.* **2016,** *45,* 775-788.
30. Denis, J.-M.; Forintos, H.; Szelke, H.; Toupet, L.; Pham, T.-N.; Madec, P.-J.; Gaumont, A.-C., *Chem. Commun.* **2003,** 54-55.
31. Rubinsztajn, S.; Cella, J. A., *Macromolecules* **2005,** *38,* 1061-1063.
32. Lee, P. T. K.; Skjel, M. K.; Rosenberg, L., *Organometallics* **2013,** *32,* 1575-1578.
33. Lee, P. T. K.; Rosenberg, L., *Dalton Trans.* **2017,** *46,* 8818-8826.
34. Priegert, A. M.; Rawe, B. W.; Serin, S. C.; Gates, D. P., *Chem. Soc. Rev.* **2016,** *45,* 922-53.
35. Braun, D., *Int. J. Polym. Sci.* **2009,** *2009,* 893234.
36. Power, P. P., *Chem. Rev.* **1999,** *99,* 3463-3504.
37. Rivard, E.; Power, P. P., *Inorg. Chem.* **2007,** *46,* 10047-10064.
38. Nuyken, O.; Pask, S. D., *Polymers* **2013,** *5,* 361-403.
39. Clark, T. J.; Lee, K.; Manners, I., *Chem. Eur. J.* **2006,** *12,* 8634-48.
40. Jäkle, F.; Vidal, F., *Angew. Chem. Int. Ed.* **2019,** *58,* 5846-5870.
41. Staubitz, A.; Robertson, A. P. M.; Sloan, M. E.; Manners, I., *Chem. Rev.* **2010,** *110,* 4023-4078.
42. Power, P. P., *Angew. Chem. Int. Ed.* **1990,** *29,* 449-460.
43. Hutchins, R. O.; Learn, K.; Nazer, B.; Pytlewski, D.; Pelter, A., *Org. Prep. Proced. Int.* **1984,** *16,* 335-372.
44. Sanyal, U.; Jagirdar, B. R., *Inorg. Chem.* **2012,** *51,* 13023-13033.
45. Robertson, A. P. M.; Leitao, E. M.; Manners, I., *J. Am. Chem. Soc.* **2011,** *133,* 19322-19325.
46. Sloan, M. E.; Staubitz, A.; Lee, K.; Manners, I., *Eur. J. Org. Chem.* **2011,** *2011,* 672-675.

47. Jiang, Y.; Blacque, O.; Fox, T.; Frech, C. M.; Berke, H., *Organometallics* **2009,** *28,* 5493-5504.
48. Staubitz, A.; Robertson, A. P. M.; Manners, I., *Chem. Rev.* **2010,** *110,* 4079-124.
49. Bluhm, M. E.; Bradley, M. G.; Butterick, R.; Kusari, U.; Sneddon, L. G., *J. Am. Chem. Soc.* **2006,** *128,* 7748-7749.
50. Stephens, F. H.; Pons, V.; Tom Baker, R., *Dalton Trans.* **2007,** 2613-2626.
51. Peng, B.; Chen, J., *Energy Environ. Sci.* **2008,** *1,* 479-483.
52. Whittell, G. R.; Manners, I., *Angew. Chem. Int. Ed.* **2011,** *50,* 10288-10289.
53. Kubota, Y.; Watanabe, K.; Tsuda, O.; Taniguchi, T., *Science* **2007,** *317,* 932-934.
54. Golberg, D.; Bando, Y.; Huang, Y.; Terao, T.; Mitome, M.; Tang, C.; Zhi, C., *ACS Nano* **2010,** *4,* 2979-2993.
55. Almasieh, M.; Lieven, C. J.; Levin, L. A.; Di Polo, A., *J. Neurochem.* **2011,** *118,* 1075-1086.
56. Seidler, E. A.; Lieven, C. J.; Thompson, A. F.; Levin, L. A., *ACS Chem. Neurosci.* **2010,** *1,* 95-103.
57. Bourumeau, K.; Gaumont, A.-C.; Denis, J.-M., *Tetrahedron Lett.* **1997,** *38,* 1923-1926.
58. Bourumeau, K.; Gaumont, A.-C.; Denis, J.-M., *J. Organomet. Chem.* **1997,** *529,* 205-213.
59. Gaumont, A.-C.; Brown, J. M.; Hursthouse, M. B.; Coles, S. J., *Chem. Commun.* **1999,** 63-64.
60. Mimeau, D.; Delacroix, O.; Gaumont, A.-C., *Chem. Commun.* **2003,** 2928-2929.
61. Mimeau, D.; Gaumont, A.-C., *J. Org. Chem.* **2003,** *68,* 7016-7022.
62. Pican, S.; Gaumont, A.-C., *Chem. Commun.* **2005,** 2393-2395.
63. Muci, A. R.; Campos, K. R.; Evans, D. A., *J. Am. Chem. Soc.* **1995,** *117,* 9075-9076.
64. Brunel, J. M.; Faure, B.; Maffei, M., *Coord. Chem. Rev.* **1998,** *178-180,* 665-698.
65. Han, D.; Anke, F.; Trose, M.; Beweries, T., *Coord. Chem. Rev.* **2019,** *380,* 260-286.
66. Staubitz, A.; Hoffmann, J.; Gliese, P., Group 13–Group 15 Element Bonds Replacing Carbon–Carbon Bonds in Main Group Polyolefin Analogs. In *Smart Inorganic Polymers*, Hey-Hawkins, E.; Hissler, M., Eds. Wiley-VCH: Weinheim, Germany, 2019; pp 17-39.
67. Colebatch, A. L.; Weller, A. S., *Chem. Eur. J.* **2019,** *25,* 1379-1390.
68. Staubitz, A.; Presa Soto, A.; Manners, I., *Angew. Chem. Int. Ed.* **2008,** *47,* 6212-6215.
69. Staubitz, A.; Sloan, M. E.; Robertson, A. P. M.; Friedrich, A.; Schneider, S.; Gates, P. J.; Günne, J. S. a. d.; Manners, I., *J. Am. Chem. Soc.* **2010,** *132,* 13332-13345.
70. Resendiz-Lara, D. A.; Whittell, G. R.; Leitao, E. M.; Manners, I., *Macromolecules* **2019,** *52,* 7052-7064.
71. Vance, J. R.; Robertson, A. P. M.; Lee, K.; Manners, I., *Chem. Eur. J.* **2011,** *17,* 4099-4103.
72. Vance, J. R.; Schäfer, A.; Robertson, A. P. M.; Lee, K.; Turner, J.; Whittell, G. R.; Manners, I., *J. Am. Chem. Soc.* **2014,** *136,* 3048-3064.
73. Anke, F.; Han, D.; Klahn, M.; Spannenberg, A.; Beweries, T., *Dalton Trans.* **2017,** *46,* 6843-6847.
74. Coles, N. T.; Mahon, M. F.; Webster, R. L., *Organometallics* **2017,** *36,* 2262-2268.
75. Marziale, A. N.; Friedrich, A.; Klopsch, I.; Drees, M.; Celinski, V. R.; Schmedt auf der Günne, J.; Schneider, S., *J. Am. Chem. Soc.* **2013,** *135,* 13342-13355.
76. Adams, G. M.; Ryan, D. E.; Beattie, N. A.; McKay, A. I.; Lloyd-Jones, G. C.; Weller, A. S., *ACS Catal.* **2019,** *9,* 3657-3666.
77. Colebatch, A. L.; Hawkey Gilder, B. W.; Whittell, G. R.; Oldroyd, N. L.; Manners, I.; Weller, A. S., *Chem. Eur. J.* **2018,** *24,* 5450-5455.
78. Johnson, H. C.; Robertson, A. P. M.; Chaplin, A. B.; Sewell, L. J.; Thompson, A. L.; Haddow, M. F.; Manners, I.; Weller, A. S., *J. Am. Chem. Soc.* **2011,** *133,* 11076-11079.
79. Boyd, T. M.; Andrea, K. A.; Baston, K.; Johnson, A.; Ryan, D. E.; Weller, A., *Chem. Commun.* **2020,** *56,* 482-485.
80. Jurca, T.; Dellermann, T.; Stubbs, N. E.; Resendiz-Lara, D. A.; Whittell, G. R.; Manners, I., *Chem. Sci.* **2018,** *9,* 3360-3366.
81. LaPierre, E. A.; Patrick, B. O.; Manners, I., *J. Am. Chem. Soc.* **2019,** *141,* 20009-20015.
82. Metters, O. J.; Flynn, S. R.; Dowds, C. K.; Sparkes, H. A.; Manners, I.; Wass, D. F., *ACS Catal.* **2016,** 6601-6611.
83. Besson, A., *C. R. Acad. Sci.* **1890,** *110,* 516.

84. Burg, A. B., *J. Inorg. Nucl. Chem.* **1959,** *11*, 258.
85. Burg, A. B.; Wagner, R. I., *J. Am. Chem. Soc.* **1953,** *75*, 3872-3877.
86. Burg, A. B.; Wagner, R. I., Phosphinoborine compounds and their preparation. Patent, U. S. 3071553, 1963.
87. Burg, A. B.; Wagner, R. I., Phosphinoborine compounds and their preparation. Patent, U. S. 2948689, 1960.
88. Korshak, V. V.; Zamyatina, V. A.; Solomatina, A. I.; Fedin, E. I.; Petrovskii, P. V., *J. Organomet. Chem.* **1969,** *17*, 201-212.
89. Dorn, H.; Singh, R. A.; Massey, J. A.; Lough, A. J.; Manners, I., *Angew. Chem. Int. Ed.* **1999,** *38*, 3321-3323.
90. Dorn, H.; Singh, R. A.; Massey, J. A.; Nelson, J. M.; Jaska, C. A.; Lough, A. J.; Manners, I., *J. Am. Chem. Soc.* **2000,** *122*, 6669-6678.
91. Dorn, H.; Rodezno, J. M.; Brunnhöfer, B.; Rivard, E.; Massey, J. A.; Manners, I., *Macromolecules* **2003,** *36*, 291-297.
92. Clark, T. J.; Rodezno, J. M.; Clendenning, S. B.; Aouba, S.; Brodersen, P. M.; Lough, A. J.; Ruda, H. E.; Manners, I., *Chem. Eur. J.* **2005,** *11*, 4526-4534.
93. Cavaye, H.; Clegg, F.; Gould, P. J.; Ladyman, M. K.; Temple, T.; Dossi, E., *Macromolecules* **2017,** *50*, 9239-9248.
94. Pandey, S.; Lönnecke, P.; Hey-Hawkins, E., *Eur. J. Inorg. Chem.* **2014,** 2456-2465.
95. Hooper, T. N.; Weller, A. S.; Beattie, N. A.; Macgregor, S. A., *Chem. Sci.* **2016,** *7*, 2414-2426.
96. Huertos, M. A.; Weller, A. S., *Chem. Sci.* **2013,** *4*, 1881-1888.
97. Huertos, M. A.; Weller, A. S., *Chem. Commun.* **2012,** *48*, 7185-7185.
98. Paul, U. S. D.; Braunschweig, H.; Radius, U., *Chem. Commun.* **2016,** *52*, 8573-8576.
99. Schäfer, A.; Jurca, T.; Turner, J.; Vance, J. R.; Lee, K.; Du, V. A.; Haddow, M. F.; Whittell, G. R.; Manners, I., *Angew. Chem. Int. Ed.* **2015,** *54*, 4836-41.
100. Turner, J. R.; Resendiz-Lara, D. A.; Jurca, T.; Schäfer, A.; Vance, J. R.; Beckett, L.; Whittell, G. R.; Musgrave, R. A.; Sparkes, H. A.; Manners, I., *Macromol. Chem. Phys.* **2017,** *218*, 1700120.
101. Arz, M. I.; Knights, A. W.; Manners, I., *Macromol. Rapid Commun.* **2019,** 1900468.
102. Resendiz-Lara, D.; Annibale, V. T.; Knights, A. W.; Chitnis, S. S.; Manners, I., *Manuscript submitted* **2020**.
103. Lee, K.; Clark, T. J.; Lough, A. J.; Manners, I., *Dalton Trans.* **2008,** *26*, 2732-2740.
104. Jaska, C. A.; Manners, I., *J. Am. Chem. Soc.* **2004,** *126*, 1334-1335.
105. Hooper, T. N.; Huertos, M. A.; Jurca, T.; Pike, S. D.; Weller, A. S.; Manners, I., *Inorg. Chem.* **2014,** *53*, 3716-3729.
106. Marquardt, C.; Jurca, T.; Schwan, K.-C.; Stauber, A.; Virovets, A. V.; Whittell, G. R.; Manners, I.; Scheer, M., *Angew. Chem. Int. Ed.* **2015,** *54*, 13782-13786.
107. Stauber, A.; Jurca, T.; Marquardt, C.; Fleischmann, M.; Seidl, M.; Whittell, G. R.; Manners, I.; Scheer, M., *Eur. J. Inorg. Chem.* **2016,** 2684-2687.
108. Oldroyd, N. L.; Chitnis, S. S.; Annibale, V. T.; Arz, M. I.; Sparkes, H. A.; Manners, I., *Nat. Commun.* **2019,** *10*, 1370.
109. Rastogi, S.; Höhne, G. W. H.; Keller, A., *Macromolecules* **1999,** *32*, 8897-8909.
110. Kumashiro, Y., *J. Mater. Res.* **1990,** *5*, 2933-2947.
111. Jacquemin, D., *J. Phys. Chem. A* **2004,** *108*, 500-506.
112. Thomas, N. R., *Silicon* **2010,** *2*, 187-193.
113. Kipping, F. S.; Lloyd, L. L., *J. Chem. Soc.* **1901,** *79*, 449-459.
114. Mark, J. E.; Allcock, H. R.; West, R., *Inorganic Polymers*. Second Edition ed.; Oxford University Press: New York, 2005.
115. Mark, J. E.; Schaefer, D. W.; Gui, L., *The Polysiloxanes*. Oxford University Press: New York, 2015.
116. Abe, Y.; Gunji, T., *Prog. Polym. Sci.* **2004,** *29*, 149-182.
117. Lohmeijer, B. G. G.; Dubois, G.; Leibfarth, F.; Pratt, R. C.; Nederberg, F.; Nelson, A.; Waymouth, R. M.; Wade, C.; Hedrick, J. L., *Org. Lett.* **2006,** *8*, 4683-6.
118. Rodriguez, M.; Marrot, S.; Kato, T.; Stérin, S.; Fleury, E.; Baceiredo, A., *J. Organomet. Chem.* **2007,** *692*, 705-708.

119. Li, Y.; Kawakami, Y., *Macromolecules* **1999,** *32,* 3540-3542.
120. Li, Y.; Kawakami, Y., *Macromolecules* **1999,** *32,* 8768-8773.
121. Li, Y.; Kawakami, Y., *Macromolecules* **1999,** *32,* 6871-6873.
122. Oishi, M.; Moon, J.-Y.; Janvikul, W.; Kawakami, Y., *Polym. Int.* **2001,** *50,* 135-143.
123. Li, Y.; Seino, M.; Kawakami, Y., *Macromolecules* **2000,** *33,* 5311-5314.
124. Kawakami, Y.; Li, Y.; Liu, Y.; Seino, M.; Pakjamsai, C.; Oishi, M.; Cho, Y. H.; Imae, I., *Macromol. Res.* **2004,** *12,* 156-171.
125. Parks, D. J.; Piers, W. E., *J. Am. Chem. Soc.* **1996,** *118,* 9440-9441.
126. Parks, D. J.; Blackwell, J. M.; Piers, W. E., *J. Org. Chem.* **2000,** *65,* 3090-3098.
127. Piers, W. E., The Chemistry of Perfluoraryl boranes. In *Adv. Organomet. Chem.*, West, R.; Hill, A., Eds. Elsevier Academic Press: San Diego, 2005; Vol. 52, pp 1-76.
128. Lawson, J. R.; Melen, R. L., *Inorg. Chem.* **2017,** *56,* 8627-8643.
129. Stephan, D. W.; Erker, G., *Angew. Chem. Int. Ed.* **2015,** *54,* 6400-6441.
130. Piers, W. E.; Chivers, T., *Chem. Soc. Rev.* **1997,** *26,* 345-354.
131. Piers, W. E.; Marwitz, A. J. V.; Mercier, L. G., *Inorg. Chem.* **2011,** *50,* 12252-12262.
132. Oestreich, M.; Hermeke, J.; Mohr, J., *Chem. Soc. Rev.* **2015,** *44,* 2202-2220.
133. Cella, S; Rubinsztajn, J. A., Silicone condensation reaction. Patent, U. S. 7064173, 2006.
134. Blackwell, J. M.; Sonmor, E. R.; Scoccitti, T.; Piers, W. E., *Org. Lett.* **2000,** *2,* 3921-3923.
135. Rendler, S.; Oestreich, M., *Angew. Chem. Int. Ed.* **2008,** *47,* 5997-6000.
136. Chojnowski, J.; Rubinsztajn, S.; Cella, J. A.; Fortuniak, W.; Cypryk, M.; Kurjata, J.; Kaźmierski, K., *Organometallics* **2005,** *24,* 6077-6084.
137. Chojnowski, J.; Rubinsztajn, S.; Fortuniak, W.; Kurjata, J., *J. Inorg. Organomet. Polym.* **2007,** *17,* 173-187.
138. Chojnowski, J.; Fortuniak, W.; Kurjata, J.; Rubinsztajn, S.; Cella, J. A., *Macromolecules* **2006,** *39,* 3802-3807.
139. Chojnowski, J.; Rubinsztajn, S.; Fortuniak, W.; Kurjata, J., *Macromolecules* **2008,** *41,* 7352-7358.
140. Brook, M. A., *Chem. Eur. J.* **2018,** *24,* 8458-8469.
141. Yajima, S.; Hayashi, J.; Okamura, K., *Nature* **1977,** *266,* 521-522.
142. Borisov, S. N.; Voronkov, M. G.; Lukevits, E. Y., *Organosilicon Heteropolymers and Heterocompounds*. Plenum Press: New York, 1970.
143. Lu, S.-Y.; Hamerton, I., *Prog. Polym. Sci.* **2002,** *27,* 1661-1712.
144. Li, J.; Xing, L.; Zhang, R.; Chen, M.; Wang, Z.; Xu, M.; Li, W., *J. Power Sources* **2015,** *285,* 360-366.
145. Han, Y.-K.; Yoo, J.; Yim, T., *Electrochim. Acta* **2016,** *215,* 455-465.
146. Schiavon, M. A.; Armelin, N. A.; Yoshida, I. V. P., *Mater. Chem. Phys.* **2008,** *112,* 1047-1054.
147. Bai, H. W.; Wen, G.; Huang, X. X.; Han, Z. X.; Zhong, B.; Hu, Z. X.; Zhang, X. D., *J. Eur. Ceram. Soc.* **2011,** *31,* 931-940.
148. Liu, W.; Pink, M.; Lee, D., *J. Am. Chem. Soc.* **2009,** *131,* 8703-8707.
149. Puneet, P.; Vedarajan, R.; Matsumi, N., *ACS Sensors* **2016,** *1,* 1198-1202.
150. Neville, L. A.; Spalding, T. R.; Ferguson, G., *Angew. Chem. Int. Ed.* **2000,** *39,* 3598-3601.
151. Beckett, M. A.; Hibbs, D. E.; Hursthouse, M. B.; Malik, K. M. A.; Owen, P.; Varma, K. S., *J. Organomet. Chem.* **2000,** *595,* 241-247.
152. O'Dowd, A. T.; Spalding, T. R.; Ferguson, G.; Gallagher, J. F.; Reed, D., *J. Chem. Soc., Chem. Commun.* **1993,** 1816-1817.
153. Foucher, D. A.; Lough, A. J.; Manners, I., *Inorg. Chem.* **1992,** *31,* 3034-3043.
154. Rubinsztajn, S., *J. Inorg. Organomet. Polym.* **2014,** *24,* 1092-1095.
155. Wang, Q.; Fu, L.; Hu, X.; Zhang, Z.; Xie, Z., *J. Appl. Polym. Sci.* **2006,** *99,* 719-724.
156. Sorarù, G. D.; Dallabona, N.; Gervais, C.; Babonneau, F., *Chem. Mater.* **1999,** *11,* 910-919.
157. Cheng, R.; Zhou, Q.; Ni, L.; Chen, Y.; Wang, J., *J. Appl. Polym. Sci.* **2011,** *119,* 47-52.
158. Hong, F. E.; Eigenbrot, C. W.; Fehlner, T. P., *J. Am. Chem. Soc.* **1989,** *111,* 949-956.
159. Mingotaud, A.-F.; Héroguez, V.; Soum, A., *J. Organomet. Chem.* **1998,** *560,* 109-115.
160. Beckett, M. A.; Rugen-Hankey, M. P.; Sukumar Varma, K., *Polyhedron* **2003,** *22,* 3333-3337.
161. Makarova, E. A.; Shimizu, S.; Matsuda, A.; Luk'yanets, E. A.; Kobayashi, N., *Chem. Commun.* **2008,** 2109-2111.

162. Gridina, V. F.; Klebanskii, A. L.; Dorofeyenko, L. P.; Krupnova, L. Y., *Polym. Sci. (USSR)* **1968,** *9*, 2196-2202.
163. Metcalfe, R. A.; Kreller, D. I.; Tian, J.; Kim, H.; Taylor, N. J.; Corrigan, J. F.; Collins, S., *Organometallics* **2002,** *21*, 1719-1726.
164. Thieme, K.; Bourke, S. C.; Zheng, J.; MacLachlan, M. J.; Zamanian, F.; Lough, A. J.; Manners, I., *Can. J. Chem.* **2002,** *80*, 1469-1480.
165. Zhao, Z.; Cammidge, A. N.; Cook, M. J., *Chem. Commun.* **2009,** 7530-7532.
166. Kijima, I.; Yamamoto, T.; Abe, Y., *Bull. Chem. Soc. Jpn.* **1971,** *44*, 3193-3194.
167. Fujdala, K. L.; Oliver, A. G.; Hollander, F. J.; Tilley, T. D., *Inorg. Chem.* **2003,** *42*, 1140-1150.
168. Marciniec, B.; Walkowiak, J., *Chem. Commun.* **2008,** 2695-2697.
169. Ito, M.; Itazaki, M.; Nakazawa, H., *J. Am. Chem. Soc.* **2014,** *136*, 6183-6186.
170. Chatterjee, B.; Gunanathan, C., *Chem. Commun.* **2017,** *53*, 2515-2518.
171. Yoshimura, A.; Yoshinaga, M.; Yamashita, H.; Igarashi, M.; Shimada, S.; Sato, K., *Chem. Commun.* **2017,** *53*, 5822-5825.
172. Mcgregor, R. R; Warrick, E. L., Treating dimethyl silicone polymer with boric oxide. Patent, U. S. US2431878A, 1943.
173. Wright, J. G. E., Process for making puttylike elastic plastic, siloxane derivative composition containing zinc hydroxide. Patent, U. S. 2541851A, 1944.
174. Zinchenko, G. A.; Mileshkevich, V. P.; Kozlova, N. V., *Polym. Sci. (USSR)* **1981,** *23*, 1421-1429.
175. Liu, Z.; Picken, S. J.; Besseling, N. A. M., *Macromolecules* **2014,** *47*, 4531-4537.
176. Foran, G. Y.; Harris, K. J.; Brook, M. A.; Macphail, B.; Goward, G. R., *Macromolecules* **2019,** *52*, 1055-1064.
177. Vale, R. L., *J. Chem. Soc.* **1960,** 2252-2257.
178. Li, M.; Ge, T.; Ding, H.; Lai, G. Patent, C. 107312175A, 2017.
179. Buwalda, S. J.; Boere, K. W. M.; Dijkstra, P. J.; Feijen, J.; Vermonden, T.; Hennink, W. E., *J. Control. Release* **2014,** *190*, 254-273.
180. Hennink, W. E.; van Nostrum, C. F., *Adv. Drug Deliv. Rev.* **2012,** *64*, 223-236.
181. Wichterle, O.; Lím, D., *Nature* **1960,** *185*, 117-118.
182. Hoare, T. R.; Kohane, D. S., *Polymer* **2008,** *49*, 1993-2007.
183. Caló, E.; Khutoryanskiy, V. V., *Eur. Polym. J.* **2015,** *65*, 252-267.
184. Peppas, N. A.; Hilt, J. Z.; Khademhosseini, A.; Langer, R., *Adv. Mater.* **2006,** *18*, 1345-1360.
185. Bakaic, E.; Smeets, N. M. B.; Hoare, T., *RSC Adv.* **2015,** *5*, 35469-35486.
186. Lin, C.-C., *RSC Adv.* **2015,** *5*, 39844-39853.
187. Kumar, A.; Han, S. S., *Int. J. Polym. Mater.* **2017,** *66*, 159-182.
188. Ahmadi, F.; Oveisi, Z.; Samani, S. M.; Amoozgar, Z., *Res. Pharm. Sci.* **2015,** *10*, 1-16.
189. Hempenius, M. A.; Cirmi, C.; Savio, F. L.; Song, J.; Vancso, G. J., *Macromol. Rapid Commun.* **2010,** *31*, 772-783.
190. Montheil, T.; Echalier, C.; Martinez, J.; Subra, G.; Mehdi, A., *J. Mater. Chem. B* **2018,** *6*, 3434-3448.
191. Shchipunov, Y. A.; Khlebnikov, O. N., *Colloid J.* **2011,** *73*, 418-429.
192. Shchipunov, Y. A.; Karpenko, T. y. Y.; Bakunina, I. Y.; Burtseva, Y. V.; Zvyagintseva, T. y. N., *J. Biochem. Bioph. Methods* **2004,** *58*, 25-38.
193. Savage, T. J.; Dunphy, D. R.; Harbaugh, S.; Kelley-Loughnane, N.; Harper, J. C.; Brinker, C. J., *ACS Biomater. Sci. Eng.* **2015,** *1*, 1231-1238.
194. Zhang, J.; Liu, W.; Gauthier, O.; Sourice, S.; Pilet, P.; Rethore, G.; Khairoun, K.; Bouler, J.-M.; Tancret, F.; Weiss, P., *Acta Biomater.* **2016,** *31*, 326-338.
195. Boyer, C.; Figueiredo, L.; Pace, R.; Lesoeur, J.; Rouillon, T.; Visage, C. L.; Tassin, J.-F.; Weiss, P.; Guicheux, J.; Rethore, G., *Acta Biomater.* **2018,** *65*, 112-122.
196. Rederstorff, E.; Rethore, G.; Weiss, P.; Sourice, S.; Beck-Cormier, S.; Mathieu, E.; Maillasson, M.; Jacques, Y.; Colliec-Jouault, S.; Fellah, B. H.; Guicheux, J.; Vinatier, C., *J. Tissue Eng. Regener. Med.* **2017,** *11*, 1152-1164.
197. Viguier, A.; Boyer, C.; Chassenieux, C.; Benyahia, L.; Guicheux, J.; Weiss, P.; Rethore, G.; Nicolai, T., *J. Mater. Sci.: Mater. Med.* **2016,** *27*, 99.

198. Sanchez, C.; Belleville, P.; Popall, M.; Nicole, L., *Chem. Soc. Rev.* **2011,** *40,* 696-753.
199. Quinn, K. J.; Courtney, J. M., *Br. Polym. J.* **1988,** *20,* 25-32.
200. Ren, Z.; Yan, S., *Prog. Mater Sci.* **2016,** *83,* 383-416.
201. Clarson, S. J.; Semlyen, J. A., *Siloxane Polymers*. Prentice Hall: New Jersey, 1993.
202. Abbasi, F.; Mirzadeh, H.; Katbab, A.-A., *Polym. Int.* **2001,** *50,* 1279-1287.
203. Gökaltun, A.; Kang, Y. B.; Yarmush, M. L.; Usta, O. B.; Asatekin, A., *Sci. Rep.* **2019,** *9,* 7377.
204. Allcock, H. R., Water-Soluble Polyphosphazenes and Their Hydrogels. In *Hydrophilic Polymers*, American Chemical Society: Washington DC, 1996; Vol. 248, pp 3-29.
205. Allcock, H. R.; Gebura, M.; Kwon, S.; Neenan, T. X., *Biomaterials* **1988,** *9,* 500-508.
206. Allcock, H. E.; Kwon, S.; Riding, G. H.; Fitzpatrick, R. J.; Bennett, J. L., *Biomaterials* **1988,** *9,* 509-513.
207. Bennett, J. L.; Dembek, A. A.; Allcock, H. R.; Heyen, B. J.; Shriver, D. F., *Chem. Mater.* **1989,** *1,* 14-16.
208. Cho, J.-K.; Park, J. W.; Song, S.-C., *J. Pharm. Sci.* **2012,** *101,* 2382-2391.
209. Potta, T.; Chun, C.; Song, S.-C., *Biomaterials* **2009,** *30,* 6178-6192.
210. Potta, T.; Chun, C.; Song, S.-C., *Biomacromolecules* **2010,** *11,* 1741-1753.
211. Potta, T.; Chun, C.; Song, S.-C., *Biomaterials* **2010,** *31,* 8107-8120.

Chapter 2

Photolytic, radical-mediated hydrophosphination: A convenient post-polymerisation modification route to P-di(organosubstituted) polyphosphinoboranes $[RR'P\text{-}BH_2]_n$

2.1 Abstract

Polymers with a phosphorus-boron main chain have attracted interest as novel inorganic materials with potentially useful properties since the 1950s. Although examples have recently been shown to be accessible via several routes, the materials reported so far have been limited to P-mono(organosubstituted) materials, $[RHP\text{-}BH_2]_n$ which contain P-H groups. Here we report a general route for the post-polymerisation modification of such polyphosphinoboranes giving access to a large range of previously unknown examples featuring P-disubstituted units. Insertion of alkenes, $R'CH{=}CH_2$ into the P-H bonds of poly(phenylphosphinoborane), $[PhHP\text{-}BH_2]_n$ was facilitated by irradiation under UV light in the presence of the photoinitiator 2,2-dimethoxy-2-phenylacetophenone (DMPA) and (2,2,6,6-tetramethylpiperidin-1-yl)oxyl (TEMPO) under benchtop conditions giving high molar mass, air-stable polymers, $[PhR'P\text{-}BH_2]_n$ with controlled functionalisation and tunable material properties. The mechanistic explanation for the favourable effect of the addition of TEMPO was also investigated and was proposed to be a consequence of reversible binding to radical species formed from the photolysis of DMPA. This new methodology was extended to the formation of crosslinked gels and to water-soluble bottlebrush copolymers showcasing applicability to form a wide range of polyphosphinoborane-based soft materials with tunable properties.

2.2 Introduction

Polymers featuring elements other than carbon in the main chain are attracting widespread interest as functional soft materials with an expanding range of applications. These macromolecules possess attributes that complement those of easily processed state of the art organic polymers by introducing additional features such as unusual thermooxidative stability, low temperature elasticity, flame retardancy, tunable optoelectronic properties, and the ability to form ceramic films and fibers on pyrolysis.[1-9]

Polyphosphinoboranes, $[RR'P\text{-}BH_2]_n$ are formally isoelectronic with polyolefins, and have recently emerged as a new class of inorganic polymers,[10, 11] with potential uses as precursors to semiconductor based ceramics, etch-resists, flame-retardant materials, and as piezoelectrics.[12-17] The development of new and improved routes to high molar mass polyphosphinoboranes is therefore an expanding area of research.[18-28] It is now possible to access several derivatives of P-monosubstituted polyphosphinoboranes $[RHP\text{-}BH_2]_n$ where R is an alkyl or aryl substituent via catalytic dehydrogenation using Rh, Ir, or Fe precatalysts, or thermally-induced Lewis base elimination routes (Scheme 2.1 a). In contrast, examples of P-disubstituted polyphosphinoboranes (i.e. $[RR'P\text{-}BH_2]_n$, R and R' ≠ H) are extremely scarce. Early work in the 1950s and 1960s claimed the formation of polymeric materials via thermally-induced dehydrocoupling of phosphine-borane adducts $R_2HP{\cdot}BH_3$ at ca. 200 °C, often in the presence of additives such as amines, which were suggested to prevent cyclisation.[29-32] However, the products were not unambiguously characterised and, where reported, yields and molar masses were very low. Attempts to apply current catalytic routes towards P-disubstituted polyphosphinoborane targets by dehydrocoupling of secondary phosphine boranes, $RR'HP{\cdot}BH_3$, have been unsuccessful to date, yielding instead dimers, small rings, or oligomeric materials.[11, 18, 20, 22, 33] High molar mass P-disubstituted polyphosphinoboranes would be devoid of P-H bonds and are likely to be the most thermally and environmentally robust and therefore the most realistically useful in applications. Strategies to access these materials are therefore of substantial interest.

Post-polymerisation modification (PPM), for example, by activation of main-chain E-X (X = halogen, H) bonds of inorganic polymers such as polysiloxanes,[34, 35] polyphosphazenes,[36] polysilanes,[37-40] and

polyferrocenylsilanes,[41, 42] is a well-known strategy for functionalising polymers allowing the tuning of diverse physical and chemical properties.[43] Indeed, the broad scope of PPM for polydihalophosphazenes is vital to the applications of polyphosphazene-based materials.[44-46] This methodology has also been used to synthesise bottlebrush polymers[47] and polyphosphazene gels which have interesting elastomeric properties.[44]

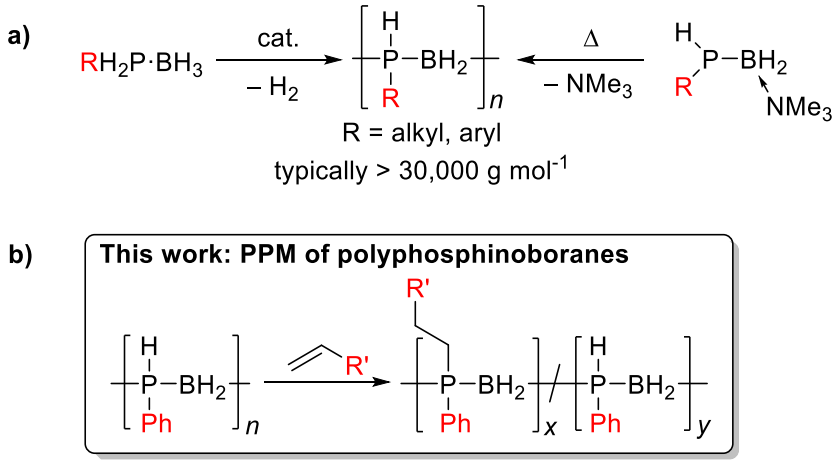

Scheme 2.1 a) Synthesis of high molar mass derivatives of $[RHP\text{-}BH_2]_n$ b) Post-polymerisation modification as a strategy to access high molar mass P-disubstituted derivatives of $[RR'P\text{-}BH_2]_n$.

We envisioned that a PPM approach involving conversion of preformed high molar mass polyphosphinoborane $[RHP\text{-}BH_2]_n$ to the target disubstituted $[RR'P\text{-}BH_2]_n$ polymers would overcome the limitations associated with existing synthetic routes and give access to a more robust and tunable class of P-disubstituted polyphosphinoboranes. Herein, we report conditions under which a broad range of alkenes undergo insertion into the P-H bonds of poly(phenylphosphinoborane) to yield high molar mass derivatives of $[PhR'P\text{-}BH_2]_n$ ($R' \neq H$, Scheme 2.1 b). In addition, we disclose the extension of this hydrophosphination approach to prepare crosslinked elastomers and water-soluble materials based on polyphosphinoborane backbones.

2.3 Results and discussion

2.3.1 Hydrophosphination of 1-octene using $[PhHP\text{-}BH_2]_n$

The hydrophosphination of alkenes with primary and secondary phosphines is a well-studied reaction for which numerous catalytic and radical based protocols have been reported.[48, 49] This addition is analogous to the ubiquitous thiol-ene addition reaction and has recently been exploited for the synthesis of phosphorus-containing network polymers.[50, 51] Interestingly, the insertion of alkenes into P-H bonds

of phosphine-borane adducts (RR'HP·BH_3 R = Ph, R' = Ph or Me) has also been reported by Gaumont and co-workers,[52] providing a model for the putative addition of alkenes to P-monosubstituted poly(phenylphosphinoborane) [PhHP-BH_2]$_n$ (**2.1**).

For all of our investigations, **2.1** was synthesised via previously reported iron-catalysed dehydrocoupling of phenylphosphine-borane ($PhH_2P{\cdot}BH_3$).[18] $PhH_2P{\cdot}BH_3$ was heated to 100 °C in toluene for 20 h in the presence of 1 mol% [$FeCp(CO)_2OTf$], yielding polymer as a pale yellow solid with a molar mass of around 68,000 g mol^{-1} and a PDI of 1.5. The discolouration of this polymer is reported to come from residual iron species remaining despite repeated precipitation from DCM into cold pentane (−78 °C).[25]

Initial studies showed that, unlike for the aforementioned phosphine-borane adducts studied by Gaumont, heating **2.1** (0.2 mmol) with 1-octene (0.2 mmol) in THF (0.5 ml) at 60 °C for 24 h did not result in detectable insertion of the alkene into the P-H bonds of the polymer based on ^{31}P NMR analysis. However, when the reaction mixture was irradiated under UV light for 20 h at 20 °C (Table 2.1, entry 1), a single peak emerged in its ^{31}P NMR spectrum at δ = −23.5 ppm with no apparent $^1J_{PH}$ coupling (cf. δ = −48.9 ppm, $^1J_{PH}$ = 349 Hz for **2.1**). The ^{1}H NMR spectrum of the reaction mixture showed a significant reduction in the intensity of the P-H resonances and emergence of a number of broad peaks in the 0.8 – 1.3 ppm region corresponding to new aliphatic protons. These spectroscopic data are consistent with insertion of 1-octene into the P-H bond of **2.1**. Analogous to Gaumont's work with phosphine-borane adducts,[52] the emergence of a single peak in the ^{31}P NMR spectrum suggests that exclusive anti-Markovnikov addition had taken place within the NMR detection limit. Integration of the resonances in the ^{31}P NMR spectra indicated around 90% conversion to the P-disubstituted species (Figure 2.1) yielding a random copolymer consisting of [Ph(octyl)P-BH_2] and [PhHP-BH_2] units.

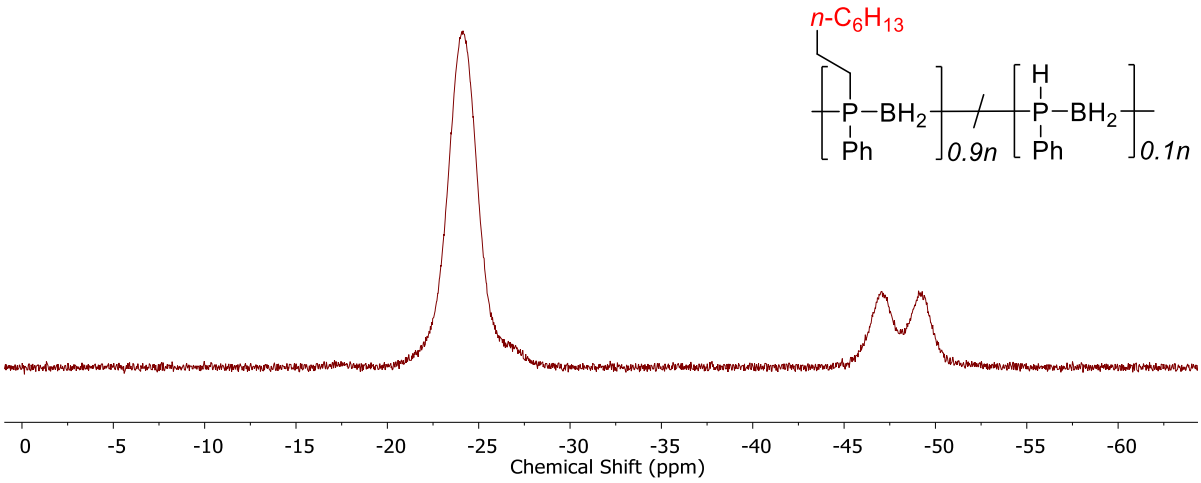

Figure 2.1 ^{31}P NMR spectrum (122MHz, 25 °C, $CDCl_3$) after PPM of **2.1** with 1-octene by UV irradiation for 20 h at 20 °C.

The molar mass of the product was determined by gel permeation chromatography (GPC) using polystyrene standards. A bimodal distribution was observed (M_n = 83,000 g mol^{-1}, PDI = 1.2; and M_n <3,000 g mol^{-1}) with a high molar mass polymer/low molar mass polymer peak ratio of 3:7.[18] We interpret the presence of these two fractions as evidence that growth in molar mass by alkene addition is accompanied by main-chain cleavage (vide infra). We postulate that this chain cleavage is caused by undesired radical induced side reactions such as backbiting and β-scission reactions, processes commonly invoked in the photodegradation of organic polymers.[53] Analysis of the above reaction mixture by NanoSpray electrospray ionisation mass spectrometry (ESI-MS, positive mode, DCM solvent), showed a repeat unit of 234.2 m/z, which corresponds to a successive loss of [Ph(octyl)P-BH_2]. As expected for conversion of 80 – 90%, repeat units of 122.0 m/z corresponding to loss of [PhHP-BH_2] were also observed. The maximum observed m/z was around 3,000, much lower than that observed by GPC; however, this is analogous with previous characterisation of polyphosphinoboranes[18, 25] and polyaminoboranes,[54] and is a noted limitation of ESI-MS for molar mass determination of these polymers.[55] Matrix-assisted laser desorption/ionisation time of flight mass spectrometry (MALDI-TOF MS) was also undertaken in an attempt to overcome the low m/z detection limit of ESI-MS; however, no high molar mass fraction was detected suggesting problems with the ionisation of these materials under MALDI conditions.

A limitation of this methodology is that the hydrophosphination was slow, requiring 20 h to achieve 90% conversion. A variety of different conditions were therefore investigated to optimise this reaction

(Table 2.1). Given the success of UV-promoted hydrophosphination (Table 2.1, entry 1), the introduction of a photoinitiator was investigated: addition of 10 mol% 2,2-dimethoxy-2-phenylacetophenone (DMPA) to the reaction mixture and irradiation under UV light in THF showed a marked increase in reaction rate (90% conversion in 1 h, entry 2). Significantly, the reaction could be scaled up to 2 mmol without loss of activity (entry 3); whereas, for UV irradiation without an initiator, a drastic reduction in reaction rate was observed upon scale up (entry 4). Decreasing the amount of DMPA to 1 mol% led to a slower reaction rate (entry 5) and increasing the amount of DMPA to 30 mol% did not accelerate the reaction further (entry 6). Lowering the reaction temperature to 0 °C also resulted in a lower conversion after 1 h (entry 7). The reaction proceeded equally well in THF or chlorobenzene, and a slight increase in conversion after 0.25 h was observed when using toluene or 1,2-dichlorobenzene (entries 8 – 11). Changing the solvent did not have a significant effect on the molar mass profile of the resulting polymer according to GPC analysis and because of the higher volatility and therefore easier removal of THF from the polymer products, THF was used for all subsequent reactions. Yields and molar masses obtained when reactions are carried out in air were comparable to those obtained using dry and degassed solvents under a nitrogen atmosphere.

As with the case in which no photoinitiator was used, a bimodal molar mass distribution was observed upon analysis of the polymer product of entry 2 by GPC (Figure 2.2). In an effort to minimise any molar mass decline accompanying this reaction, an analogous reaction was attempted using blue light instead of UV light; however, no reaction was observed (SI Table S2.1, entry 1). While the targeted hydrophosphination did not occur under these conditions, use of blue light irradiation together with photocatalyst 9-mesityl-10-methylacridinium perchlorate and diphenyliodinium triflate did result in the desired reaction taking place (25% conversion after 16 h) (SI Table S2.1, entry 2); however, given the sluggish nature of this reaction, this methodology was not pursued further.

TEMPO is well known to reversibly bind to organic radical species leading to its pioneering use in the field of nitroxide-mediated polymerisation (NMP).[56, 57] This reversible binding establishes an activation-deactivation equilibrium which reduces the concentration of active radical species giving a more controlled polymer growth. Given the success of NMP protocols to control radical reactions, we investigated the effect of addition of TEMPO to the hydrophosphination of 1-octene with **2.1**. When

100 mol% of TEMPO was added to an NMR tube containing **2.1** (0.2 mmol), 1-octene (0.2 mmol), DMPA (0.02 mmol) and THF (0.5 mL), no reaction was observed after irradiation for 1 h (Table 2.1, entry 12). However, when instead, 10 mol% of TEMPO was added under otherwise analogous reaction conditions, the conversion after 1 h was comparable to the case where no TEMPO was used (compare entries 13 and 2). Furthermore, upon characterisation of the molar mass of the polymer using GPC, it was now found that significantly more high molar mass material remained (peak ratio 7:3 high molar mass polymer/low molar mass polymer), suggesting that polymer degradation during the course of the reaction was significantly reduced (Figure 2.2). We postulate that the TEMPO acts to reduce the concentration of reactive radicals via reversible binding to the radical species produced from the photoinitiator resulting in a more controlled hydrophosphination without detrimental side reactions that cause chain cleavage. A similar degree of conversion was found when an alternative nitroxide, di-tert-butyl nitroxide, was used in place of TEMPO (entry 14).

We also found that it was possible to carry out the hydrophosphination of 1-octene using **2.1** thermally at 60 °C in THF using 10 mol% AIBN as an initiator. This thermally induced hydrophosphination is significantly slower than the UV mediated version (taking 27 h to reach 90% conversion, Figure S2.1); however, this allowed for convenient monitoring of the reaction by ^{31}P NMR (vide infra).

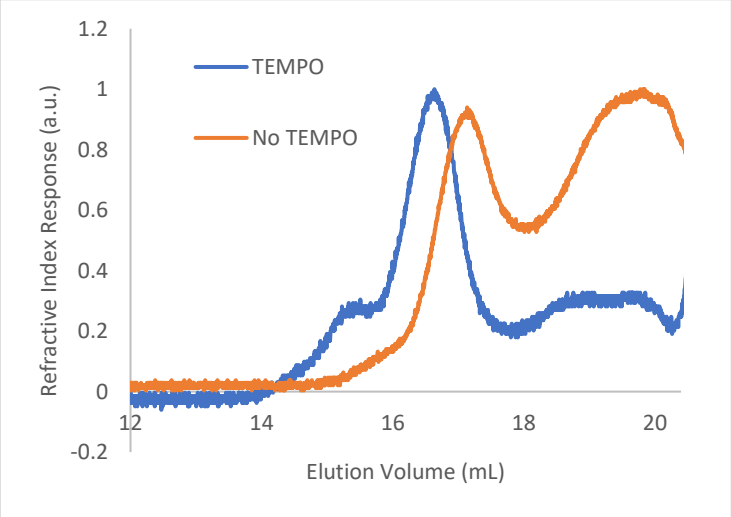

Figure 2.2 GPC chromatograms of the reaction of **2.1** with 1-octene in the presence of DMPA (10 mol%) with and without the addition of TEMPO (10 mol%).

Table 2.1 Effect of reaction conditions on the hydrophosphination reaction of 1-octene with **2.1**.

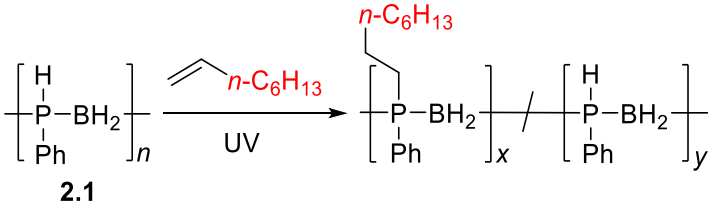

2.1

Entry[a]	Additives	Solvent	Time	Conversion (%)[b]
1	None	THF	20 h	90
2	DMPA (10 mol%)	THF	1 h	90
3[c]	DMPA (10 mol%)	THF	1 h	91
4[c]	None	THF	24 h	35
5	DMPA (1 mol%)	THF	1 h	62
6	DMPA (30 mol%)	THF	1 h	90
7[d]	DMPA (10 mol%)	THF	1 h	65
8	DMPA (10 mol%)	THF	0.25 h	75
9	DMPA (10 mol%)	Chlorobenzene	0.25 h	69
10	DMPA (10 mol%)	Toluene	0.25 h	87
11	DMPA (10 mol%)	1,2-Dichlorobenzene	0.25 h	86
12	DMPA (10 mol%) TEMPO (100 mol%)	THF	1 h	0
13	DMPA (10 mol%) TEMPO (10 mol%)	THF	1 h	90
14	DMPA (10 mol%) Di-tert-butyl nitroxide (10 mol%)	THF	1 h	88

[a]All reactions were carried out with 0.2 mmol of **2.1** and one equivalent of 1-octene in a borosilicate NMR tube in 0.5 mL solvent and irradiated under UV light at 20 °C unless stated otherwise. UV irradiation was carried out using a 125 W medium-pressure mercury lamp; [b]Determined by ^{31}P NMR integrations, conversion = (x / (x + y)) × 100; [c]2 mmol of $[PhHP\text{-}BH_2]_n$, one equivalent of 1-octene and 5 mL THF; [d]Reaction carried out at 0 °C.

2.3.2 Mechanistic studies

We propose that the reaction of poly(phenylphosphinoborane) and 1-octene in the presence of 10 mol% DMPA and irradiation under UV light takes place via a radical chain reaction in which a radical initiator (In$^{\cdot}$) forms from the photolysis of DMPA (Scheme 2.2A), and subsequently abstracts a hydrogen atom from phosphorus on the polymer chain (Scheme 2.2B). This then adds to the alkene in an anti-Markovnikov fashion to give the most stable secondary radical based on the alkyl chain (Scheme 2.2C). To continue the radical chain reaction, a hydrogen is abstracted from another position on the polymer chain (Scheme 2.2D). This is analogous to the mechanism reported by Gaumont and co-workers for the microwave irradiation induced hydrophosphination of alkenes using secondary phosphine-boranes.[52] Introduction of TEMPO into this system has an interesting effect: UV irradiation of **2.1** (0.2 mmol), 1-octene (0.2 mmol), DMPA (0.02 mmol) and THF (0.5 mL) at 20 °C, shows 75% conversion from **2.1** to the P-disubstituted polymer after just 10 minutes (determined by ^{31}P NMR spectroscopy of the crude reaction mixture). However, in contrast, when 10 mol% TEMPO was present in an analogous reaction mixture, there was minimal conversion to the P-disubstituted polymer after 10 minutes of UV irradiation (Figure S2.2). Nevertheless, analysis by ^{31}P NMR spectroscopy of both reactions after 1 h of irradiation shows comparable degrees of conversion of around 90% (Figure S2.3). This suggests that the addition of TEMPO causes an induction period for the hydrophosphination reaction. We also explored an analogous thermal reaction using AIBN and TEMPO wherein an NMR tube were charged with **2.1** (0.1 mmol), 1-octene (0.1 mmol), AIBN (0.01 mmol), TEMPO (0.01 mmol) and THF (0.5 mL) and was placed in an oil bath at 60 °C. The reaction was monitored by ^{31}P NMR spectroscopy. A clear induction period was observed, with no detectable conversion by ^{31}P NMR spectroscopy after 1 h but around 10 % conversion after 2 h, with continually increasing conversion thereafter (Figure 2.3). We postulate that the induction periods that we observe are caused by reversible reaction of TEMPO with the radical species produced from the photodegradation of DMPA under UV light (Scheme 2.2E) or by thermal degradation of AIBN. The adducts formed could then break down initiating the hydrophosphination reaction. The formation of the 2-cyanopropyl-TEMPO adduct (Figure 2.4A) has been reported previously from the heating of a solution of AIBN and TEMPO in toluene,[58] and so it is plausible that we are also forming this species prior to any reaction with the polymer. We also attempted

to isolate an adduct between DMPA and TEMPO. The photodegradation of DMPA has been reported to yield several products,[59] a number of which could conceivably react with TEMPO complicating any investigation. Nevertheless, analysis of the crude reaction mixture after the irradiation of equimolar amounts of DMPA with TEMPO in THF by ESI-MS showed signals that correspond to 2,2,6,6-tetramethylpiperidin-1-yl benzoate fragments (Figure 2.4B), as well as hydrogenated TEMPO supporting our hypothesis that an adduct forms between TEMPO and radicals derived from DMPA (Figure S2.4).

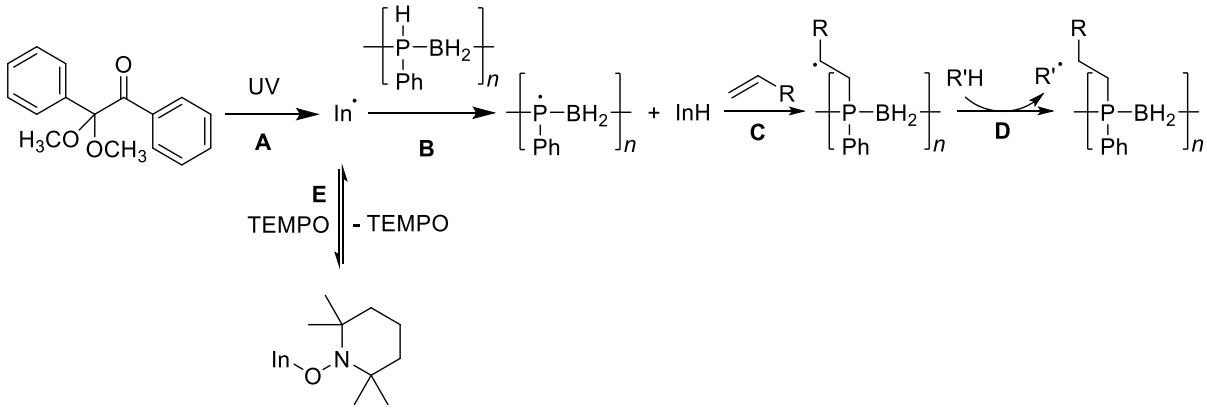

Scheme 2.2 Proposed reaction mechanism for the UV- induced hydrophosphination of alkenes using 1 in the presence of DMPA (and the effect of addition of TEMPO to the reaction mixture).

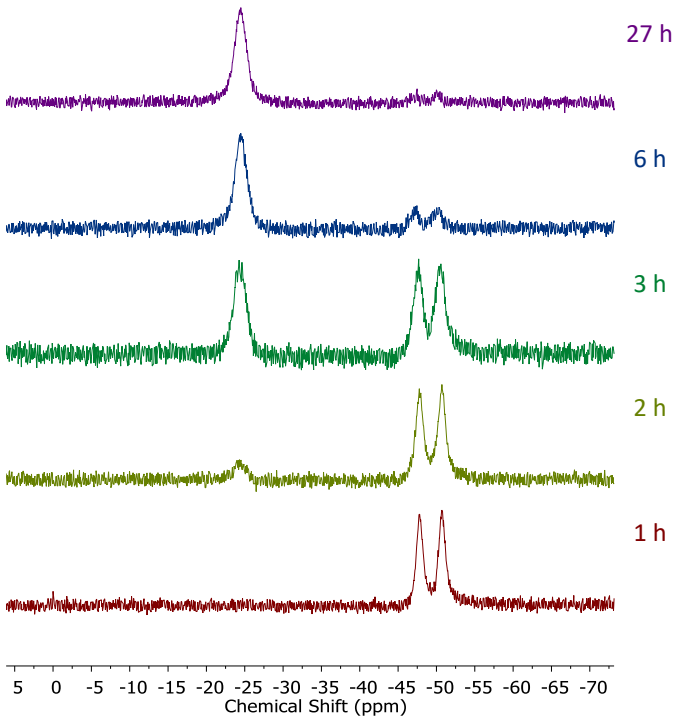

Figure 2.3 ^{31}P NMR (122 MHz, in situ in THF) spectra showing the progress of the hydrophosphination reaction between 1-octene and **2.1** in the presence of AIBN and TEMPO at 60 °C.

Since these proposed adducts closely resemble alkoxyamine compounds that are commonly used as initiators in NMP,[60] we sought to determine if alkoxyamines could facilitate the reaction of 1-octene with **2.1**. Heating an NMR tube charged with **2.1** (0.1 mmol), 1-octene (0.1 mmol), toluene (0.5 mL) and 0.01 mmol of the commercially available N-tert-butyl-N-(2-methyl-1-phenylpropyl)-O-(1-phenylethyl)hydroxylamine (Figure 2.4C) to 100 °C, resulted in the desired hydrophosphination reaction taking place, albeit much more slowly than using our photoinitiated system (Figure S2.5). Significantly when this alkoxyamine was used, no induction period was observed supporting our assertion that adduct formation is involved in the first step of the photoinitiated hydrophosphination in the presence of DMPA and TEMPO.

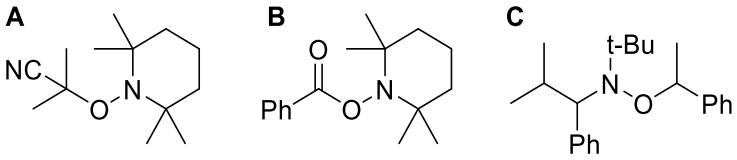

Figure 2.4 Chemical structures of nitroxide adducts A) formed by the reaction of AIBN and TEMPO B) formed by the reaction of DMPA and TEMPO C) a commercially available and commonly used NMP initiator.

In nitroxide mediated polymerisations, it is generally accepted that the nitroxide is able to reversibly bind to the growing polymer chain and this mediates the reaction resulting in a controlled polymer growth. In order to test whether TEMPO is binding to phosphorus based radicals on the polyphosphinoborane main chain, **2.1** (0.2 mmol) was irradiated with DMPA (0.2 mmol) and TEMPO (0.2 mmol) in THF (0.5 mL) at 20 °C. Analysis of the crude reaction mixture by ^{31}P NMR spectroscopy after 4 h, showed the emergence of a very minor signal with a chemical shift of ca. 115 ppm which we tentatively assign to the polymer bound to TEMPO (Figure S2.6) due to the similarity in chemical shift to the recently reported Ph_2POTEMP (^{31}P: δ 110.8 ppm);[61] however, no evidence of binding of TEMPO to the polymer chain could be observed by mass spectrometry. Addition of 1-octene and continued irradiation resulted in the disappearance of this signal at 115 ppm and the emergence of the signal at −23.5 ppm which corresponds to the hydrophosphination of 1-octene by **2.1** (Figure S2.7).

2.3.3 Large scale syntheses and properties of P-disubstituted polyphosphinoboranes

Following the success of this new hydrophosphination methodology, we targeted the isolation of a series of polymers to investigate the difference in their physical properties. To this end we targeted

various degrees of substitution of poly(phenylphosphinoborane) using 1-octene by varying the reaction stoichiometry (0.1 eq. 1-octene – polymer **2.2a**, 0.6 eq. – polymer **2.2b**, 1 eq. – polymer **2.2c**, and 2 eq. – polymer **2.2d**) (Scheme 2.3). We also targeted other alkenes: allylbenzene (1 eq. – polymer **2.3**), allyl pentafluorobenzene (1 eq. – polymer **2.4**), and 1H,1H,2H-perfluorohexene (1 eq. – polymer **2.5**). The synthesis of these polymers followed the same procedure, **2.1** (2 mmol), DMPA (0.2 mmol), TEMPO (0.2 mmol), and alkene were added to a vial and dissolved in THF (5 mL). The reaction mixture was irradiated under UV light for 2 h at 20 °C for **2.2a** – **c** and **2.3 – 2.5**. For polymer **2.2d**, the reaction mixture was irradiated for 24 h at 20 °C. The polymers were isolated by precipitation from THF into H_2O/isopropanol (1:1 v/v) at −20 °C (polymers **2.2b**, **2.2c**, **2.2d**, and **2.5**) or from DCM into pentane at −78 °C (polymer **2.2a**, **2.3**, and **2.4**) and then dried under vacuum at 40 °C for at least 48 h. The polymers were isolated as light-yellow solids except for **2.2c** and **2.2d** which were pale yellow-brown gums. The discolouration for these polymers likely originates from small amounts of residual iron species from the polymerisation of phenylphosphine-borane using [$FeCp(CO)_2OTf$]. The ^{11}B NMR spectra of the resultant polymers showed little change from that of the parent poly(phenylphosphinoborane) (a broad singlet at around −34 ppm). ^{31}P NMR chemical shifts of these isolated polymers were found at around −24 ppm. As expected, a singlet was observed in the ^{1}H-coupled ^{31}P NMR spectra alongside a doublet at δ = −48.9 ppm corresponding to [PhHP-BH_2] units in all polymers except **2.2d**. From the ^{31}P NMR spectra, the degree of conversion to the P-disubstituted polymer could be calculated. When 1 eq. alkene was used, conversions of between 72 and 82% were observed (Table 2.2, polymers **2.2c**, **2.3**, **2.4**, and **2.5**). Different degrees of substitution could be obtained by varying the reaction stoichiometry (compare polymers **2.2a** – **d**). To obtain the fully P-disubstituted polymer **2.2d**, a greatly extended reaction time and two equivalents of 1-octene were required. We postulate that this is due to reactive sites becoming less accessible as conversion approaches 100%. The successful incorporation of the alkene was confirmed by ESI-MS and for each polymer, fragments corresponding to [PhRP-BH_2] repeat units could be detected. The molar masses of these polymers were determined by GPC relative to polystyrene standards and were found to range from M_n = 81,000 to 130,000 g mol^{-1}. No change in the ^{31}P NMR spectra or GPC chromatograms were detected after the solid polymers were exposed to air for 6 months, indicating that these polymers are air-stable. These polymers also appear to be water-stable as addition

of a few drops of water to a THF solution of these polymers (5 mg in 1 mL THF) and leaving open to air for 24 h at 20 °C also resulted in no change in the NMR spectra or GPC chromatograms.

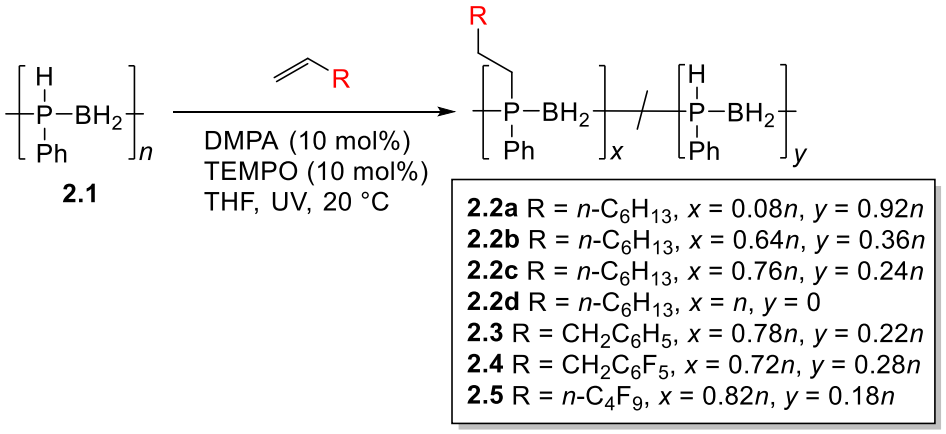

Scheme 2.3 Reaction conditions for the hydrophosphination of alkenes with **2.1**.

The thermal properties of functionalised polyphosphinoboranes polymers **2.2 – 2.5** were investigated by thermogravimetric analysis (TGA, N_2 atmosphere, heating rate 10 °C min^{-1}) and differential scanning calorimetry (DSC, heating rate 10 °C min^{-1}) (Table 2.2). Thermal stability was quantified by comparing $T_{5\%}$: the temperature at which the polymer loses 5% of its original mass. P-disubstituted polymers were found to have slightly higher $T_{5\%}$ values than **2.1** except for **2.2a** and **2.5** which were marginally lower. The thermal stability of the octyl substituted polymers increased up to around 60% insertion (Table 2.2, compare data for polymers **2.1** and **2.2b**), but little further increase was observed with additional alkene insertion (polymers **2.2c** and **2.2d**). The onset of mass loss has been attributed to thermally induced H_2-loss leading to further polymer degradation pathways.[13] These results suggest that the presence of an octyl group at every other repeat unit is sufficient to suppress the inter-chain P-H/B-H interaction required for H_2 elimination. However, higher degrees of insertion presumably enhance P-B backbone fission due to steric pressure and the concomitant molar mass decline is likely to reduce the thermal stability of the polymer. It has also been postulated that thermally induced crosslinking is important for thermal stability of polyphosphinoboranes. As the number of P-disubstituted units increases, this would become increasingly difficult as there are both fewer sites available for crosslinking and a higher steric bulk reducing favourable interactions between polymer chains.

Reflecting the random addition of 1-octene along the polymer backbone, only one glass transition temperature (T_g) was observed for **2.2 – 2.5** (Table 2.2) The T_g values for **2.2a** – **d** are lower than that of

2.1, which is ascribed to the presence of long alkyl side chains that increase the polymer free volume and therefore reduce T_g. Consistently, the T_g values for **2.2a – d** also show an inverse relationship with the extent of alkene insertion as expected for greater incorporation of a long alkyl chain. Polymers **2.2c** and **2.2d** have glass transition temperatures significantly below room temperature and are gums whereas the other polymers are glassy solids. Polymers **2.3 – 2.5** have T_g values that are higher than for **2.1**, which we tentatively ascribe to greater interactions between the fluorinated and/or aryl groups in the polymer side chains increasing the rigidity of the polymer.

Table 2.2 Properties of functionalised polymers.

Polymer	Percentage insertion (%)[a]	M_n (g mol^{-1})	$T_{5\%}$ (°C)[b]	Ceramic Yield (%)[c]	T_g (°C)
2.1[d]	0	68,000	180	46	38
2.2a	8	130,000[e]	160	51	30
2.2b	64	130,000	208	27	15
2.2c	76	81,000	197	20	9
2.2d	100	112,000	216	6	4
2.3	78	104,000	194	19	50
2.4	72	130,000	210	34	67
2.5	82	92,000	175	8	43

[a]Determined by integration of ^{31}P NMR spectra, Conversion = (x / (x + y)) × 100; [b]Temperature at 5% mass loss; [c]Ceramic yields were measured at 600 °C after the sample mass was stable; [d]Ref. 16; [e]A significant higher molecular weight shoulder was observed in the GPC chromatogram of **2.2a**.

2.3.4 Synthesis of crosslinked poly(phenylphosphinoborane)

Following the success of the insertion of alkenes into P-H bonds of **2.1**, we sought to extend this methodology to other polyphosphinoborane-based soft materials. We found that when **2.1** is irradiated with 0.1 eq. of 1-octene, a significant shoulder is detected to the high molar mass polymer fraction (Figure S2.12). We assign this to competitive polymer cross-linking (by P-P or P-B bond formation) at low degrees of substitution. This hypothesis is supported by irradiation of **2.1** with 10 mol% DMPA in the absence of alkene, which yielded material with very high molar mass (>400,000 g mol^{-1}, Figure S2.63). Further irradiation under these conditions results in the formation of insoluble material

suggesting a higher degree of cross-linking. In an attempt to achieve a more controlled cross-linking, the potential of hydrophosphination of dienes was investigated. To this end, a solution containing **2.1**, 1,5-hexadiene (15 mol%), DMPA (10 mol%), and TEMPO (10 mol%) was irradiated in THF at 20 °C for 24 h. A soft, pale yellow solid was obtained, which showed reversible organogel behaviour upon exposure to excess THF or vacuum (Figure 2.5). This material was purified by repeated extraction with THF until the washings were colourless. Drying of this material under vacuum yields a pale-yellow brittle solid. This material undergoes reversible organogel swelling behaviour: if left in THF for 48 h, the material swells to 210% of its original mass; and subsequent application of vacuum reverts the gel back to its brittle phase. No glass transition temperature was found when the material was analysed by DSC. The ceramic yield of this crosslinked poly(phenylphosphinoborane) was found to be 54%, slightly higher than for non-crosslinked polyphosphinoboranes. These properties are promising for further utility of crosslinked polyphosphinoboranes and the use of different polymer precursor and crosslinking agents should yield gels with markedly different properties.

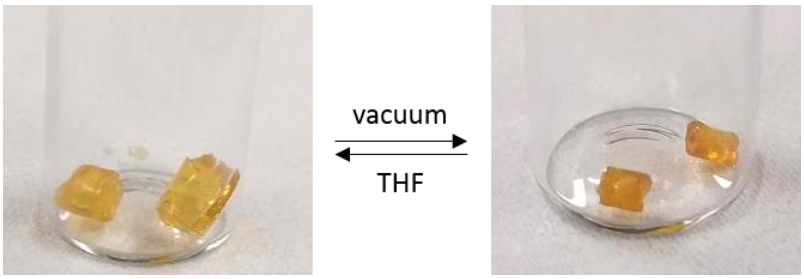

Figure 2.5 Left: soft yellow gel obtained after soaking 1,5-hexadiene-crosslinked **2.1** in THF for 48 h. Right: brittle solid obtained upon exposure of the crosslinked material to dynamic vacuum at ambient temperature for 24 h.

2.3.5 Synthesis and characterisation of a water-soluble bottlebrush polyphosphinoborane

We explored the formation of a polyphosphinoborane bottlebrush polymer via the grafting-to reaction of **2.1** with two eq. of poly(ethylene glycol) (PEG) methyl ether methacrylate in the presence of DMPA (10 mol%) and TEMPO (10 mol%) in THF (Scheme 2.4). After UV irradiation for 2h and subsequent removal of THF from the resultant solution and redissolution in $CDCl_3$, a grafting density of 58% was determined by integration of the ^{31}P NMR spectrum. This is in the range typically found for grafting-to approaches to bottlebrush polymer formation (grafting densities <60% for grafting-to approaches).[62] **2.6** was found to be water-soluble (the first water-soluble polymer with a polyphosphinoborane backbone) and no significant change in the chemical shifts of the ^{31}P NMR peaks was observed whether

$CDCl_3$ or D_2O was used as the solvent indicating that the polymer is water stable, although significant broadening of the signals is observed when D_2O is the solvent (compare Figure S2.72 and Figure S2.73). To remove excess PEG methyl ether methacrylate, dialysis was performed using dialysis tubing in water (molecular weight cut-off: 12,000 – 14,000 g mol^{-1}). The successful removal of the PEG methyl ether methacrylate was confirmed by comparison of the dynamic light scattering trace for **2.6** and for PEG methyl ether methacrylate (Figure S2.75 and Figure S2.76).

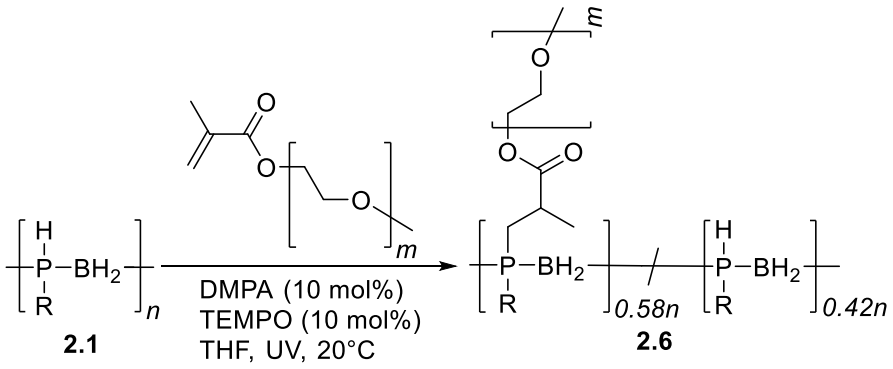

Scheme 2.4 The synthesis of bottlebrush polymer **2.6** by reaction of **2.1** with poly(ethylene glycol) methyl ether methacrylate (M_n = 950 g mol^{-1}).

After purification, **2.6** was determined to have a M_n of 156,000 g mol^{-1} and a PDI of 1.3 by GPC analysis in THF. The thermal properties of this polymer were investigated by DSC and TGA. No T_g was detected by DSC analysis; however, a T_m at 40 °C was observed for the PEG side chains. The $T_{5\%}$ was found to be 301 °C, significantly higher than for other linear polyphosphinoboranes. This suggests that the presence of the long PEG chains imparts significant additional thermal stability, and this bodes well for future research into applications of this interesting class of polyphosphinoborane polymers.

2.4 Conclusions

We have achieved the synthesis of P-di(organosubstituted) polyphosphinoboranes using a mild, scalable, photoinitiated process for inserting olefins into the P-H bonds of preformed P-monosubstituted derivatives under benchtop conditions. The use of DMPA and TEMPO and UV irradiation serves to minimise molar mass decline during the course of this hydrophosphination reaction and facilitated the formation of random copolymers with controlled functionalisation as well as fully P-disubstituted derivatives. Investigations into the mechanistic reason behind the favourable effect of TEMPO addition suggested that reversible binding of TEMPO to radical species formed during the reaction could be

preventing deleterious side reactions from occurring which lead to polymer degradation. The material properties of the new high molar mass polymers are tunable by the choice of alkene employed. We also describe the synthesis of the first controllably crosslinked polyphosphinoborane, a material that exhibits organogel behaviour, and the synthesis of a water-soluble bottlebrush polymer featuring a polyphosphinoborane backbone. The results described offer promise for unlocking new applications for polyphosphinoboranes and relevant work in the area is currently underway in our group.

2.5 Supporting information

2.5.1 Materials

Anhydrous, deuterated solvents were purchased from Sigma Aldrich, and stored over activated molecular sieves (4 Å). $PhH_2P{\cdot}BH_3$,[63] $CpFe(CO)_2OTf$,[64] and $[PhHP\text{-}BH_2]_n$[18] were synthesised via literature procedures. All other commercially available compounds were used without further purification.

Photoirradiation experiments under ultraviolet (UV) light were carried out with Pyrex-glass filtered emission from a 125 W medium pressure mercury lamp. The emission lines of the mercury lamp are: 577-579, 546, 436, 408-405, 366-365, 334, 313, 302, 297, 289, 270, 265, 254 nm. Experiments under blue light were performed using a 3 W lamp, emissions 450 – 495 nm.

NMR spectra were recorded using Oxford Jeol ECS 400 MHz, Bruker Nano 400 MHz, Bruker Avance III HD 500 MHz Cryo, or Varian VNMR 500 MHz spectrometers. ^{1}H and ^{13}C NMR spectra were reference to residual signals of the solvent ($CDCl_3$: ^{1}H: $\delta = 7.24$, ^{13}C: $\delta = 77.0$; C_6D_5H: ^{1}H: $\delta = 7.20$, ^{13}C: $\delta = 128.0$). ^{11}B, ^{19}F, and ^{31}P NMR spectra were referenced to external standards (^{11}B: $BF_3{\cdot}OEt_2$ ($\delta = 0.0$); ^{19}F: $CFCl_3$ ($\delta = 0.0$); ^{31}P: 85% H_3PO_4 (aq.) ($\delta = 0.0$)). Chemical shifts (δ) are given in parts per million (ppm) and coupling constants (J) are given in Hertz (Hz), rounded to the nearest 0.5 Hz.

Electrospray ionisation (ESI) mass spectra were recorded using a Waters Synapt G2S spectrometer by NanoSpray Ionisation. Solutions (40 μL) of approximately 1 mg mL^{-1} were loaded into the sample tray, and aliquots of 3 μL were introduced into the spectrometer using a spray voltage of 1.5 kV. Positive and negative ion spectra were recorded at a rate of one scan per second and summed to produce the final spectra. MALDI-TOF MS was performed using a Bruker Ultraflextreme running in reflector mode. Samples were prepared using a trans-2-(3-(4-tert-butylphenyl)-2-methyl-2-propenylidene)

malononitrile matrix (20 mg mL^{-1} in THF) which was mixed with the polymer sample (2 mg mL^{-1} in THF), in a 10:1 (v/v) ratio. Approximately 1 μL of the mixed solution was deposited onto a MALDI-TOF MS sample plate and allowed to dry in air prior to analysis.

Gel permeation chromatography (GPC) was performed on a Malvern RI max Gel Permeation Chromatograph, equipped with an automatic sampler, pump, injector, and inline degasser. The columns (2 × T5000) were contained within an oven (35 °C) and consisted of styrene/divinyl benzene gels. Sample elution was detected by means of a differential refractometer. THF (Fisher) containing 0.1 %w/w [nBu$_4$N][Br] was used as the eluent at a flow rate of 1 mL min^{-1}. Samples were dissolved in THF (2 mg mL^{-1}) and filtered with a Ministart SRP15 filter (poly(tetrafluoroethylene) membrane of 0.45 μm pore size) before analysis. The calibration was conducted using monodisperse polystyrene standards obtained from Aldrich. The lowest and highest molecular weight standards used were 2,300 Da and 994,000 Da respectively.

Differential scanning calorimetry (DSC) thermograms were measured using a Thermal Advantage DSCQ100 coupled to a RCS90 refrigerated cooling system with a heating/cooling rate of 10 °C min^{-1}. DSC samples were placed in hermetic aluminium pans for analysis.

Thermal gravimetric analysis (TGA) was carried out using a Thermal Advantage TGAQ500 with a heating rate of 10 °C min^{-1} under a nitrogen atmosphere. Samples were placed in platinum pans for analysis. DSC and TGA results were analysed using WinUA V4.5A by Thermal Advantage.

Dynamic light scattering (DLS) experiments were carried out using a Malvern Zetasizer Nano S instrument using a He-Ne laser (λ = 632 nm). Samples dissolved in THF (1 mg mL^{-1}) were filtered through a 0.45 μm filter into an optical glass cuvette prior to analysis. The measurements were performed on a Malvern Instruments Zetasizer Nano S using a 5 mW He-Ne laser (633 nm) at 20 °C.

2.5.2 Procedures for the hydrophosphination of poly(phenylphosphinoborane)

2.5.2.1 General NMR scale reaction conditions for Table 1

An NMR tube was charged with poly(phenylphosphinoborane) (**2.1**) (0.2 mmol), 1-octene (0.2 mmol), and solvent (0.5 mL) and any additive specified. The solution was irradiated ca. 3 cm away from a mercury lamp. After the specified amount of time, a ^{31}P NMR spectrum was recorded of the crude reaction mixture and the conversion calculated from the integration of the signals.

2.5.2.2 Attempted hydrophosphination by means of irradiation with blue light

2.1 (49 mg, 0.4 mmol), 1-octene (62.8 μL, 0.4 mmol), diphenyliodonium triflate (86 mg, 0.2 mmol), 9-mesityl-10-methylacridinium perchlorate (0.8 mg, 2 x 10^{-3} mmol), and toluene (2 mL) were added to a Schlenk flask equipped with a magnetic stirrer. The resultant solution was irradiated ca. 3 cm away from a 3 W blue light emitting lamp for 16 h, after which an in situ ^{31}P NMR spectrum was obtained to determine reaction conversion (Table S2.1, entry 2).

The analogous reaction with no diphenyliodonium triflate or 9-mesityl-10-methylacridinium perchlorate present was also attempted (Table S2.1, entry 1). In this case no reaction was observed.

Table S2.1 Hydrophosphination attempts using blue light irradiation.

Entry	Additives	Temperature (°C)	Time	Conversion[a]
1	None	20	16 h	0
2	$[Ph_2I][OTf]$, photocatalyst	20	16 h	25

[a]Determined by ^{31}P NMR integrations, conversion = (x / (x + y)) × 100

2.5.2.3 Hydrophosphination of 1-octene by poly(phenylphosphinoborane) in the presence of AIBN

An NMR tube was charged with **2.1** (0.1 mmol), 1-octene (0.1 mmol), AIBN (0.01 mmol) and THF (0.5 mL). The solution was heated to 60 °C for 27 h and then analysed by ^{31}P NMR spectroscopy.

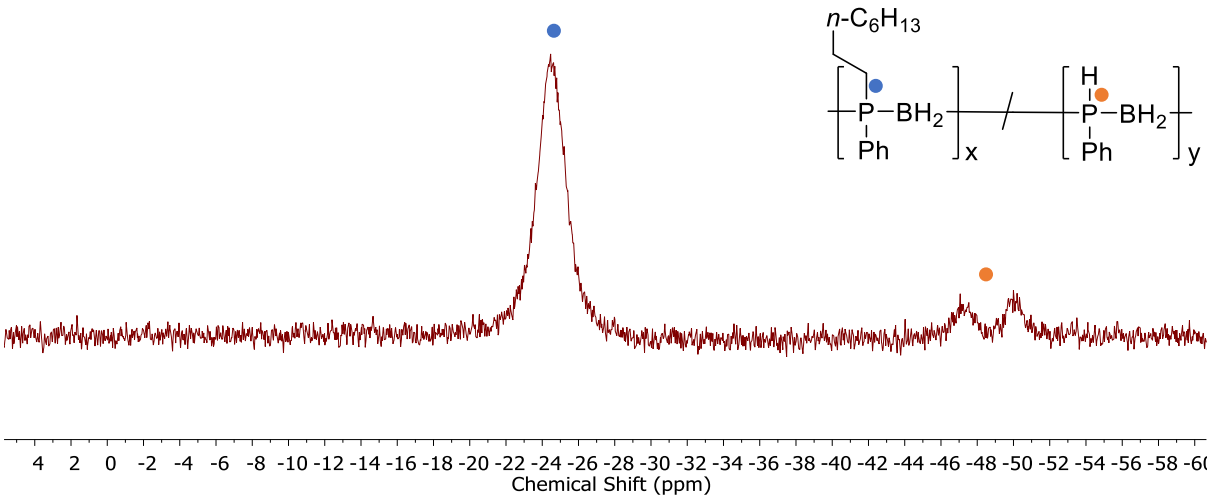

Figure S2.1 In situ ^{31}P NMR spectrum (122MHz) of the hydrophosphination reaction of 1-octene using **2.1** in the presence of AIBN after 27 h.

2.5.3 Investigations into the mechanism of the hydrophosphination of 1-octene using poly(phenylphosphinoborane)

2.5.3.1 Hydrophosphination of 1-octene using poly(phenylphosphinoborane) in the presence of DMPA vs DMPA and TEMPO

Two NMR tubes were charged with **2.1** (0.2 mmol), 1-octene (0.2 mmol), DMPA (0.02 mmol), THF (0.5 mL). To one was added TEMPO (0.02 mmol). The solutions were irradiated ca. 3 cm away from a mercury lamp for 10 min and then analysed by ^{31}P NMR spectroscopy. The samples were then irradiated for a further 50 minutes and analysed again by ^{31}P NMR.

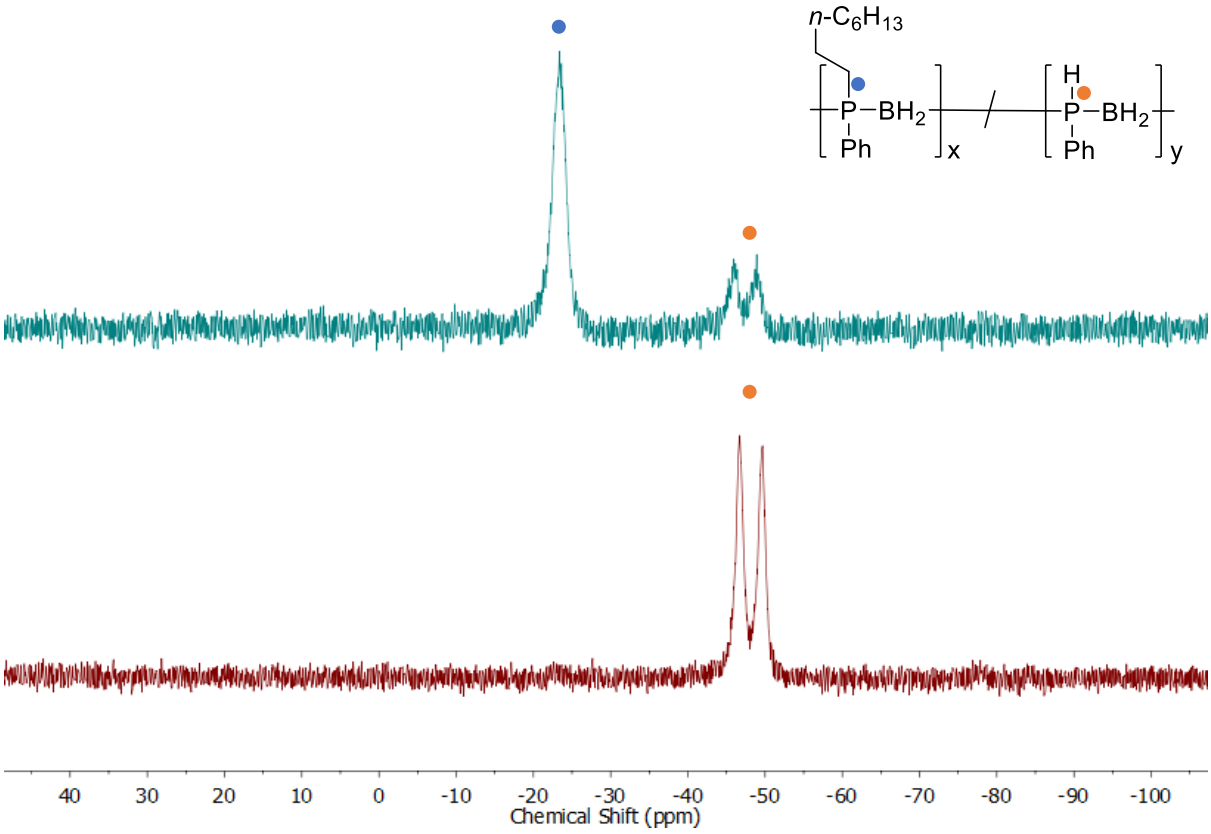

Figure S2.2 In situ ^{31}P NMR spectra (122MHz) taken after 10 min of the hydrophosphination of 1-octene using **2.1** in the presence of DMPA (top) or DMPA and TEMPO (bottom).

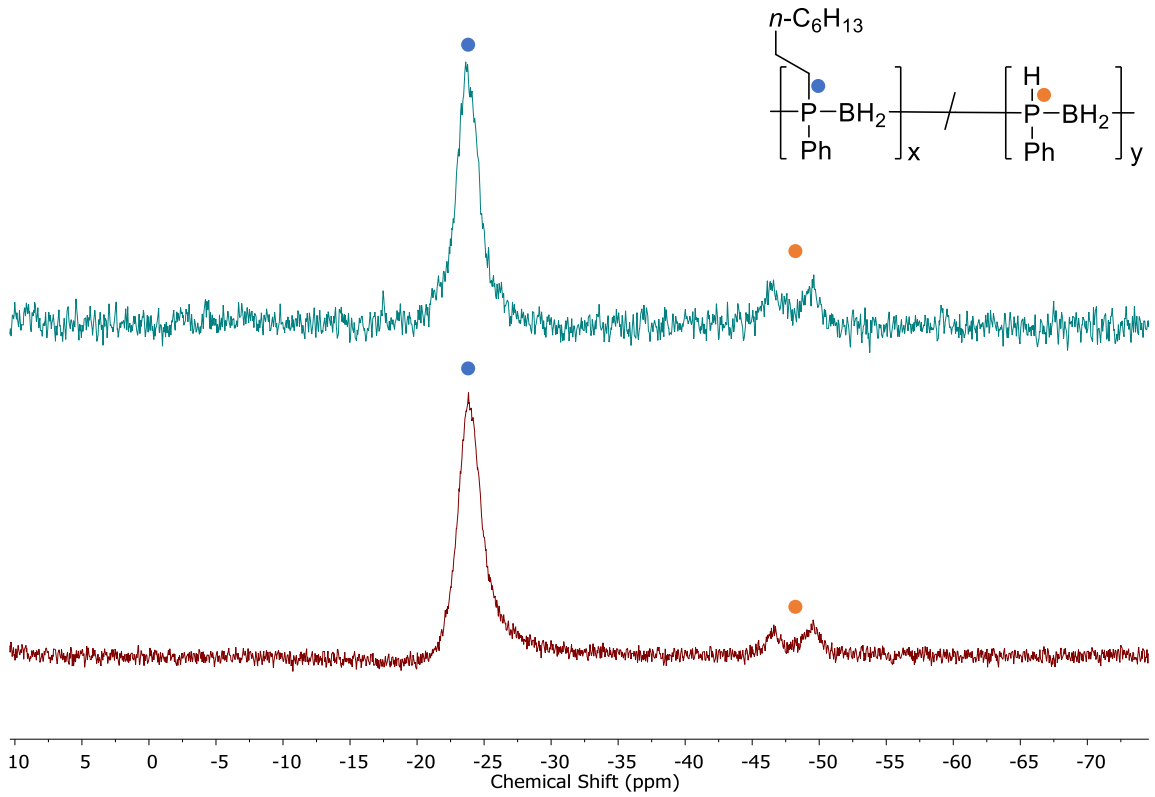

Figure S2.3 In situ ^{31}P NMR spectra (122MHz) taken after 1 h of the hydrophosphination of 1-octene using **2.1** in the presence of DMPA (top) or DMPA and TEMPO (bottom).

2.5.3.2 Mass spectrum after the irradiation of DMPA with TEMPO

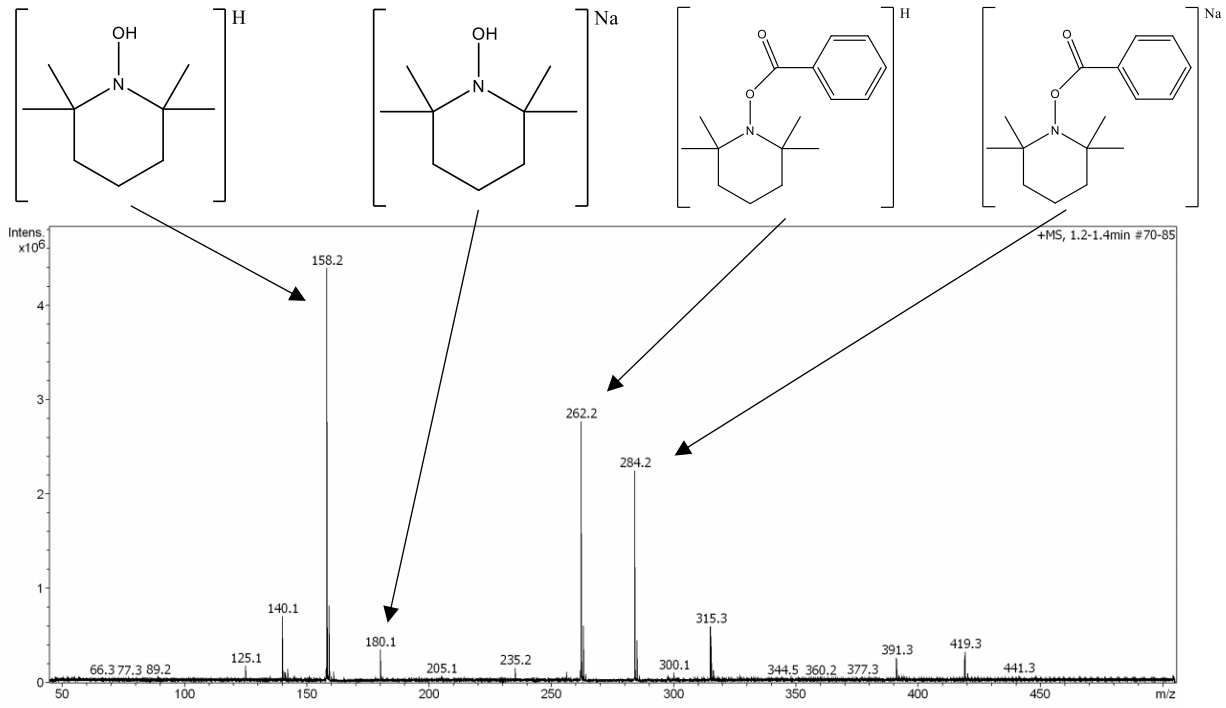

Figure S2.4 ESI-MS (+) of the reaction of DMPA and TEMPO in THF.

2.5.3.3 Hydrophosphination reaction using N-tert-butyl-N-(2-methyl-1-phenylpropyl)-O-(1-phenylethyl)hydroxylamine

An NMR tube was charged with **2.1** (0.1 mmol), 1-octene (0.1 mmol), N-tert-butyl-N-(2-methyl-1-phenylpropyl)-O-(1-phenylethyl)hydroxylamine (0.01 mmol) and toluene (0.5 mL). The solution was heated to 100 °C and monitored by ^{31}P NMR spectroscopy.

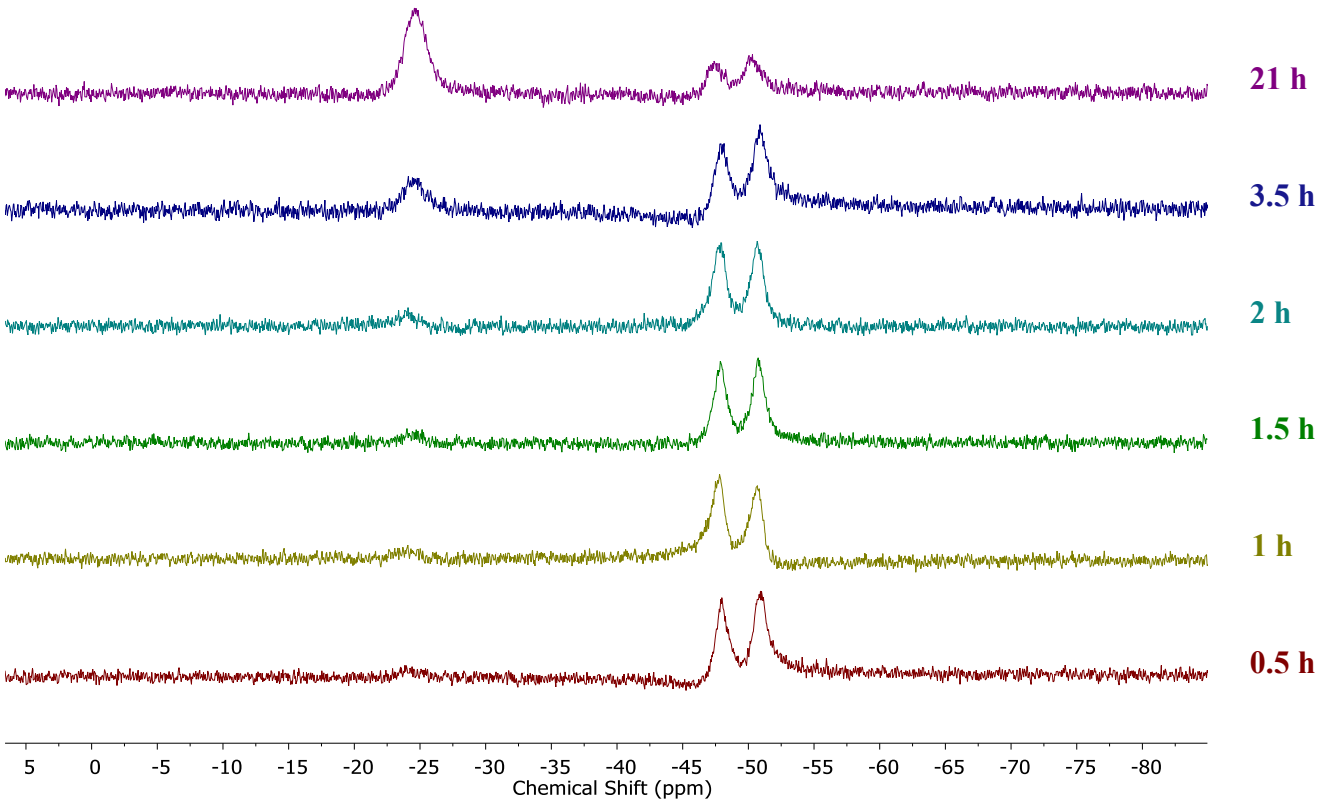

Figure S2.5 In situ ^{31}P NMR spectra of the hydrophosphination of 1-octene using **2.1** in the presence of N-tert-butyl-N-(2-methyl-1-phenylpropyl)-O-(1-phenylethyl)hydroxylamine.

2.5.3.4 Irradiation of poly(phenylphosphinoborane) with DMPA and TEMPO

To an NMR tube was added **2.1** (0.2 mmol), DMPA (0.2 mmol), TEMPO (0.2 mmol) and THF (0.5 mL). This was irradiated at 20 °C for 4 h and then the crude reaction mixture was analysed by ^{31}P NMR spectroscopy (Figure S2.6). Subsequently, 1-octene (0.2 mmol) was added and the mixture irradiated for a further 2 h and then again analysed by ^{31}P NMR (Figure S2.7).

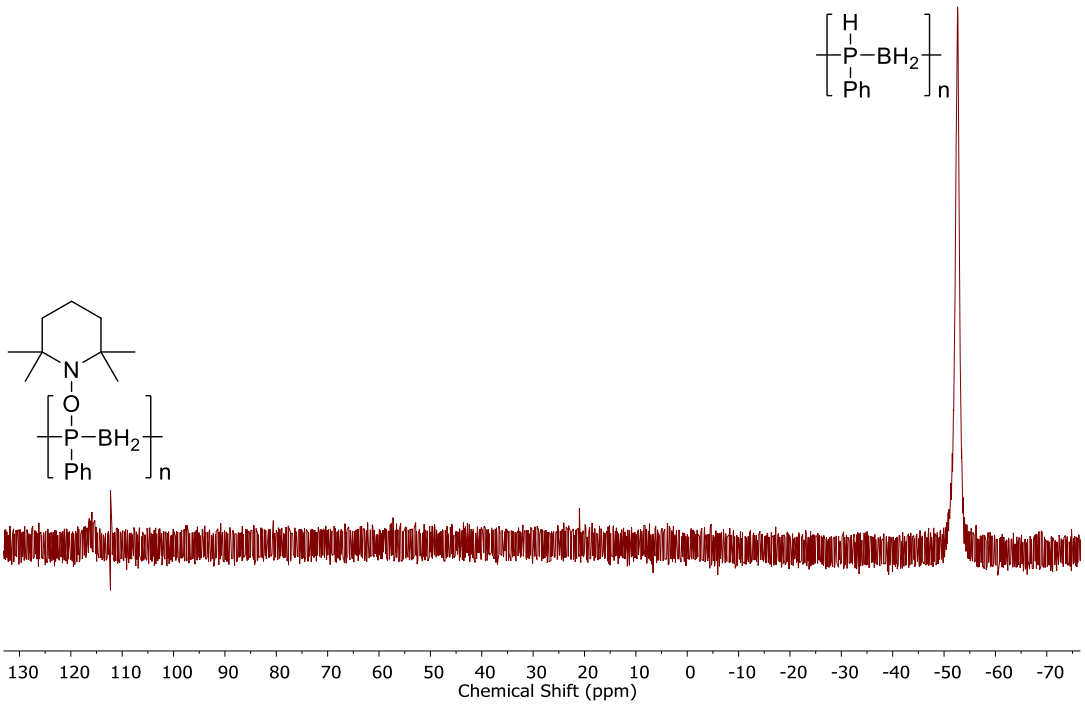

Figure S2.6 In situ $^{31}P\{H\}$ NMR spectra of the reaction between **2.1**, DMPA and TEMPO after 4 h UV irradiation at 20 °C.

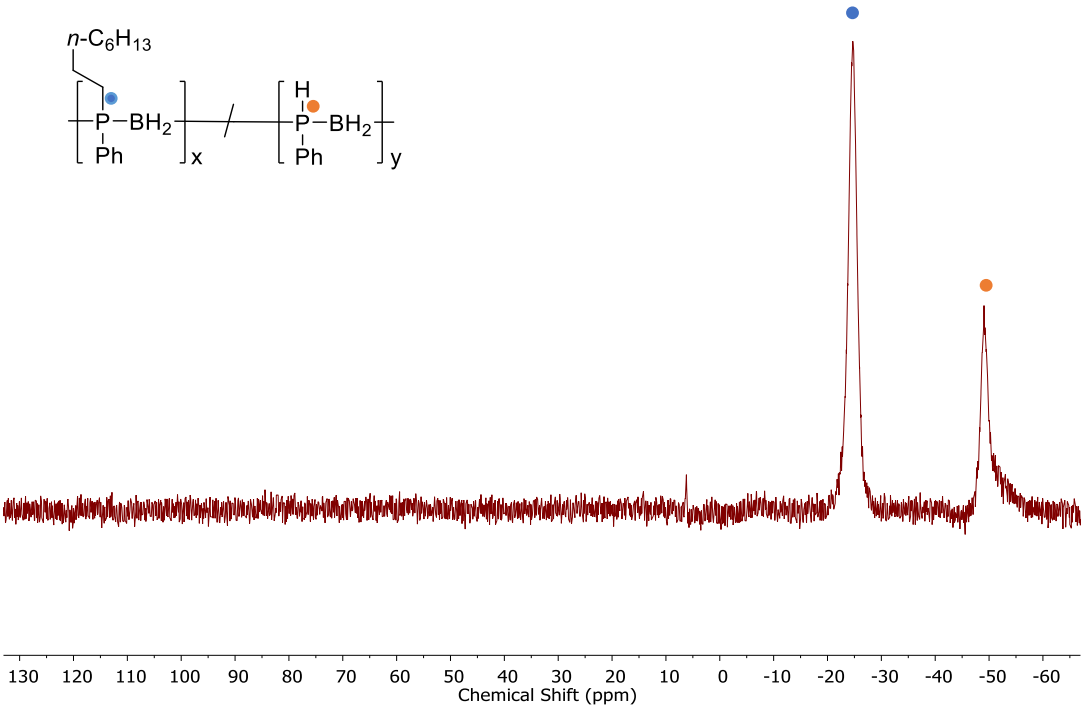

Figure S2.7 In situ $^{31}P\{H\}$ NMR spectra after 1 eq. 1-octene was added to the reaction mixture and it was irradiated for a further 2 h at 20 °C.

2.5.4 Synthesis and characterisation of P-disubstituted polyphosphinoboranes

2.5.4.1 General procedure for isolation of modified polyphosphinoborane derivatives:

2.1 (2 mmol), alkene (various equivalents), (DMPA) (0.2 mmol), TEMPO (0.2 mmol), and THF (5 mL) were added to a 14 mL vial equipped with a magnetic stirrer. The resultant solution was irradiated ca. 3 cm away from a mercury lamp. Volatiles were then removed under vacuum and the resultant solid was purified by precipitation (see specific syntheses for details). The polymer was then dried under vacuum at 40 °C for a minimum of 48 h.

2.5.4.2 Synthesis and characterisation of polymer 2.2a

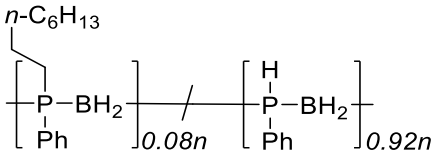

2.1 (244 mg, 2 mmol), 1-octene (31.4 μL, 0.2 mmol), DMPA (51 mg, 0.2 mmol), TEMPO (31 mg, 0.2 mmol), and THF (5 mL) were added to a 14 mL vial equipped with a magnetic stirrer. The resultant solution was irradiated ca. 3 cm away from a mercury lamp for 2 h. Volatiles were then removed under vacuum and the resultant solid was purified by precipitation from DCM into pentane at −78 °C (3 × 25 mL). The polymer was then dried under vacuum at 40 °C for 48 h yielding **2.2a** as an orange solid (conversion: 8%; yield: 159 mg, 61%).

Spectroscopic data:

^{1}H NMR (400 MHz, $CDCl_3$) δ 7.50 – 6.88 (br m, Ar*H*), 4.28 (br d, *J* = 360 Hz), 1.83 – 0.68 (br m, C*H*$_2$, C*H*$_3$, B*H*$_2$).

^{11}B NMR (128 MHz, $CDCl_3$) δ −34.5 (br s).

^{31}P NMR (162 MHz, $CDCl_3$) δ −23.6 (s, 8%, PhR*P*-BH_2), −48.7 (d, *J* = 358 Hz, 92%, PhH*P*-BH_2).

GPC (2 mg mL^{-1}) M_n = 130,000 g mol^{-1}, PDI = 1.9.

$T_{5\%}$ = 160 °C; ceramic yield = 51%; T_g = 30 °C.

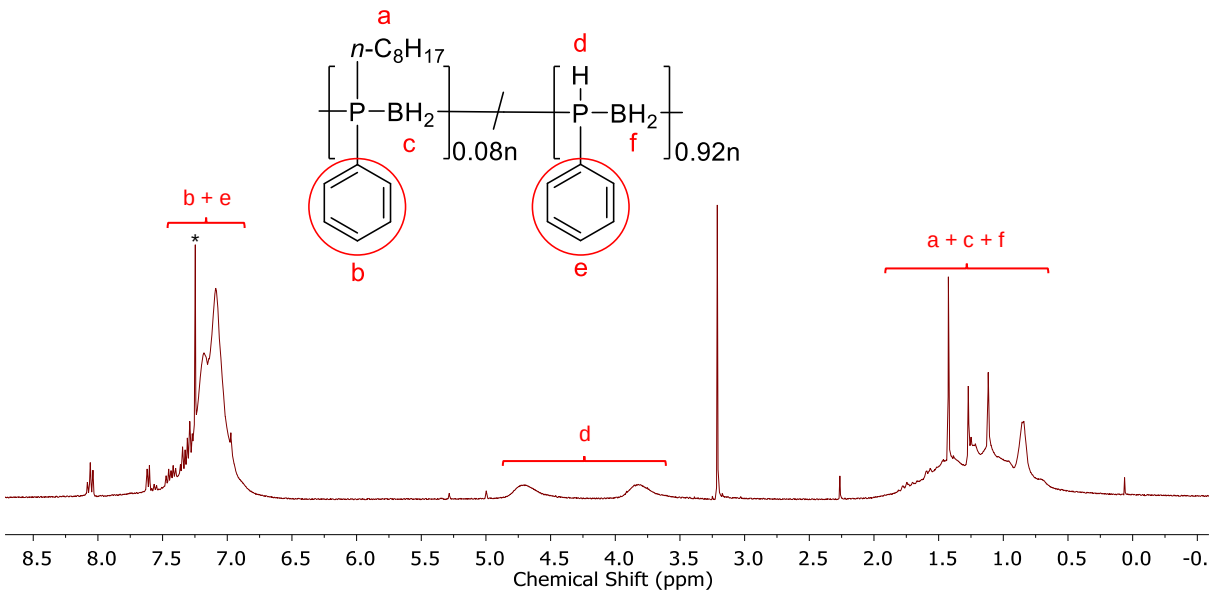

Figure S2.8 ^{1}H NMR spectrum (400 MHz, 25 °C, $CDCl_3$) of **2.2a**. Deuterated chloroform residual signal denoted by *.

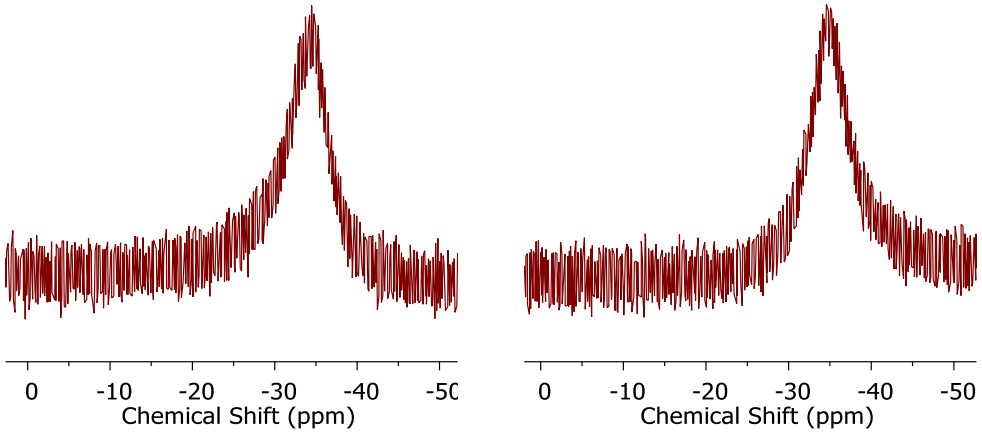

Figure S2.9 ^{11}B (left) and ^{11}B{H} (right) NMR spectra (128 MHz, 25 °C, $CDCl_3$) of **2.2a**.

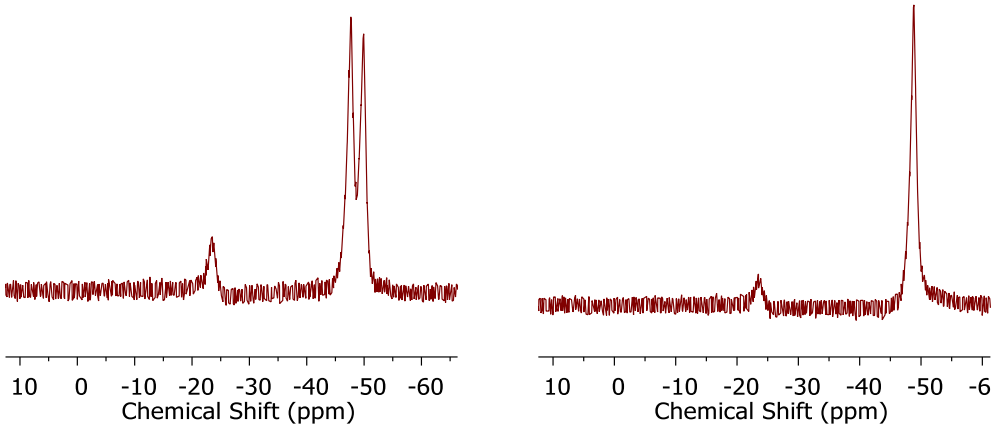

Figure S2.10 ^{31}P (left) and ^{31}P{H} (right) NMR spectra (162 MHz, 25 °C, $CDCl_3$) of **2.2a**.

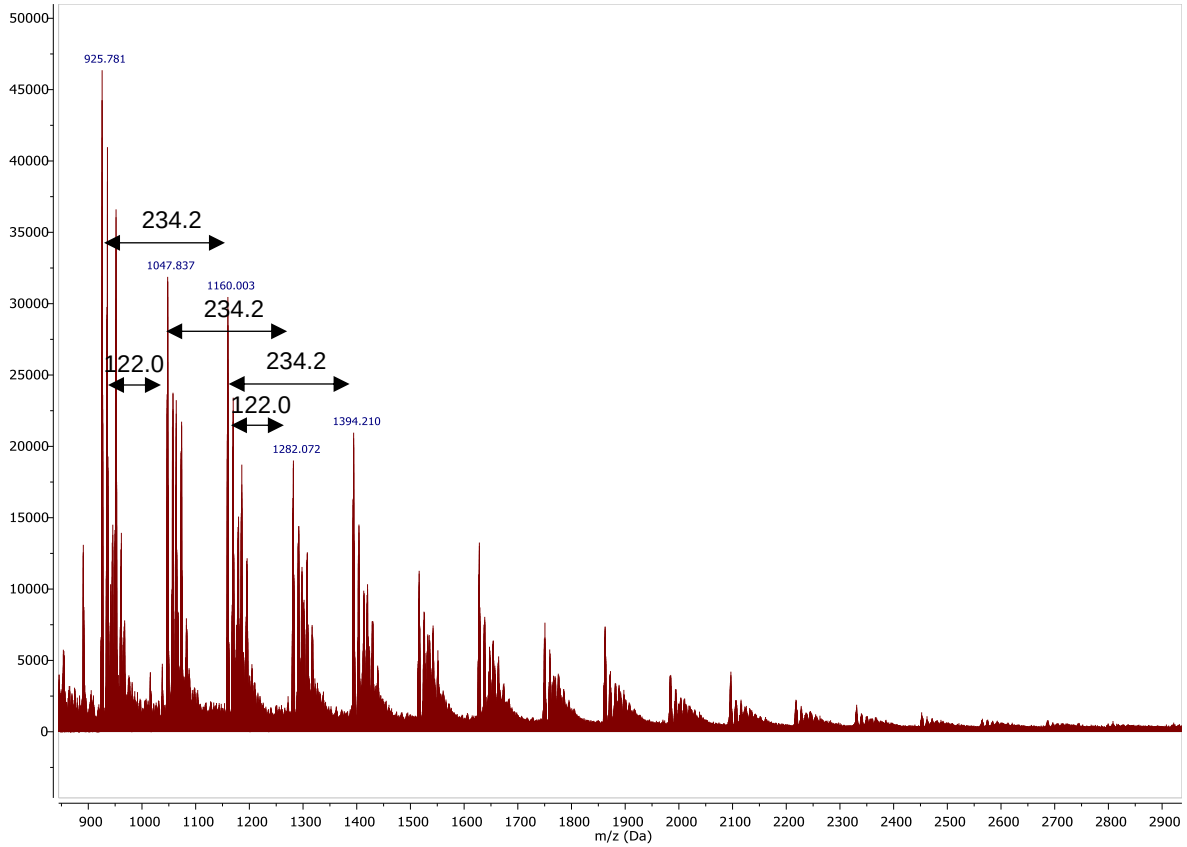

Figure S2.11 ESI-MS (+) of **2.2a** in DCM.

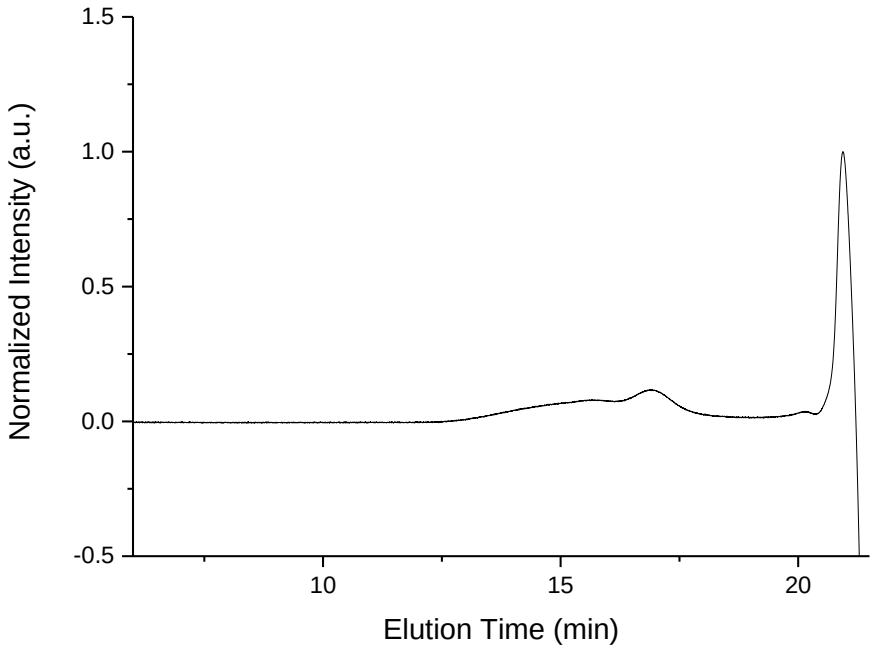

Figure S2.12 GPC chromatogram of **2.2a** (2 mg mL^{-1} in THF, 0.1 w/w % $n$$Bu_4NBr$ in the THF eluent).

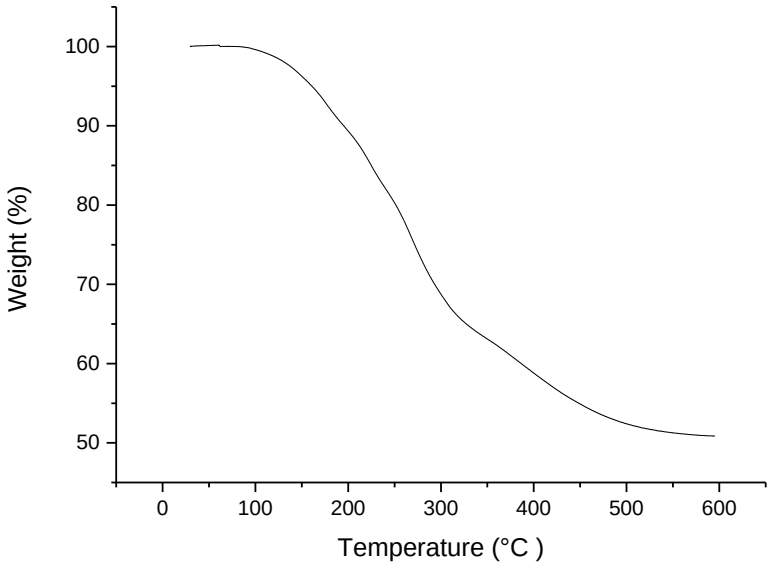

Figure S2.13 TGA thermogram of **2.2a** (heating rate: 10 °C min^{-1}).

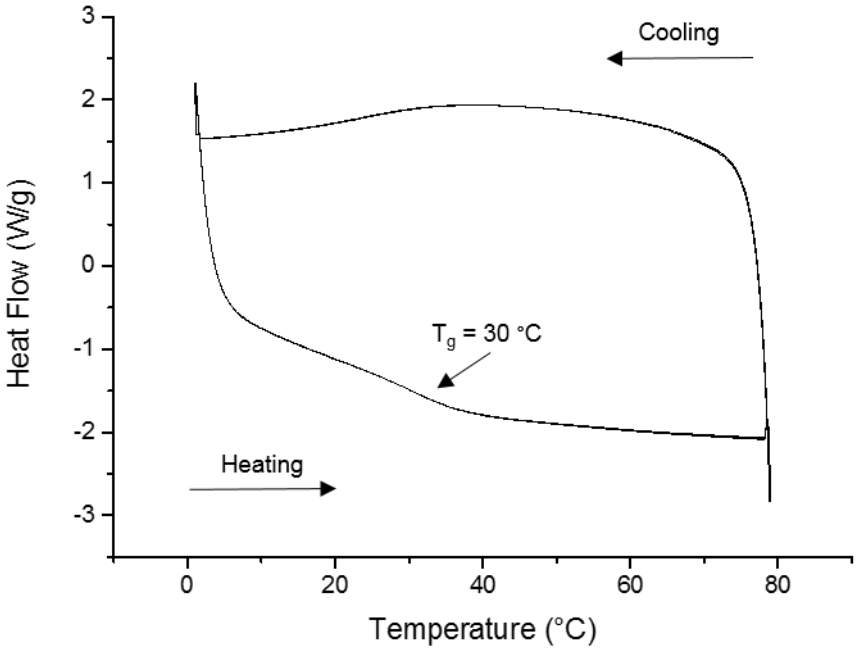

Figure S2.14 DSC thermogram of **2.2a**, first cycle excluded (heating rate: 10 °C min^{-1}).

Figure S2.15 Photograph of isolated **2.2a.**

2.5.4.3 Synthesis and characterisation of polymer 2.2b

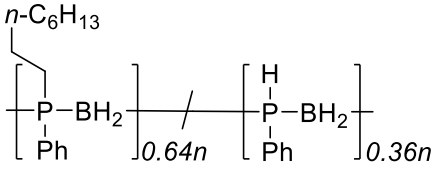

2.1 (244 mg, 2 mmol), 1-octene (157 µL, 1.2 mmol), DMPA (51 mg, 0.2 mmol), TEMPO (31 mg, 0.2 mmol), and THF (5 mL) were added to a 14 mL vial equipped with a magnetic stirrer. The resultant solution was irradiated ca. 3 cm away from a mercury lamp for 2 h. Volatiles were then removed under vacuum and the resultant solid was purified by precipitation from THF into H_2O/isopropanol (1:1 v/v) at −20 °C (3 × 25 mL). The polymer was then dried under vacuum at 40 °C for 48 h yielding **2.2b** as an orange solid (conversion: 64%; yield: 293 mg, 76%).

Spectroscopic data:

^{1}H NMR (400 MHz, $CDCl_3$) δ 7.51 – 6.80 (br m, Ar*H*), 4.12 (br d, *J* = 355 Hz, PhP*H*), 1.75 – 0.58 (br m, CH_2, CH_3, BH_2).

^{11}B NMR (128 MHz, $CDCl_3$) δ −32.7 (br s).

^{31}P NMR (162 MHz, $CDCl_3$) δ −24.0 (s, 64%, PhR*P*-BH_2), −48.1 (d, *J* = 359 Hz, 36%, PhH*P*-BH_2).

GPC (2 mg mL^{-1}) M_n = 130,000 g mol^{-1}, PDI = 1.5.

$T_{5\%}$ = 208 °C; ceramic yield = 27%; T_g = 15 °C.

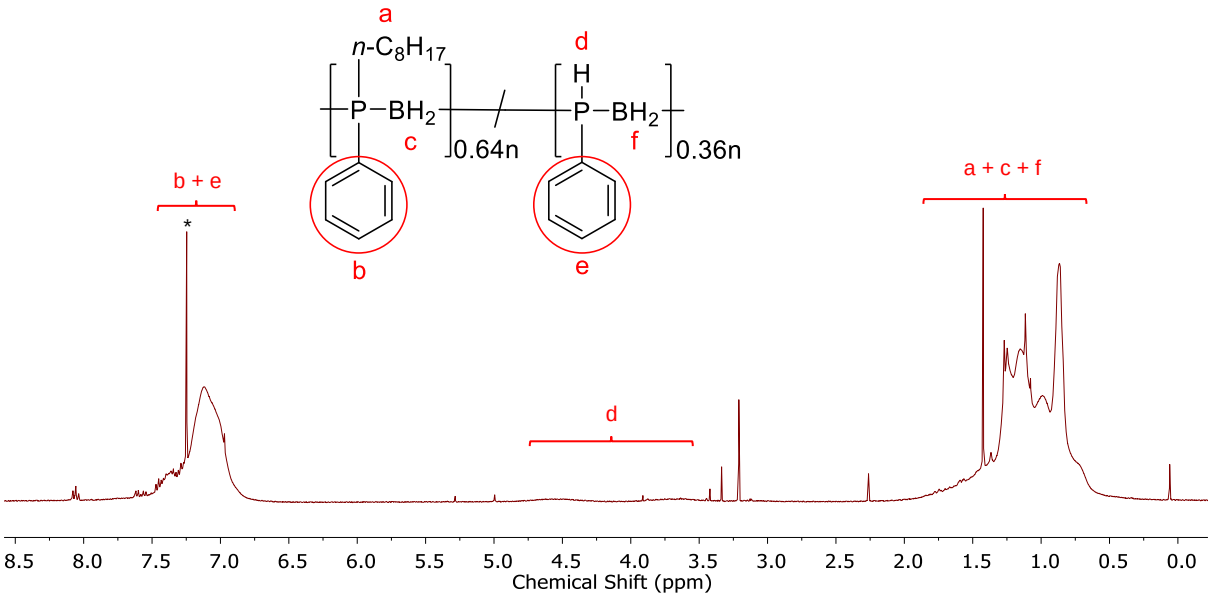

Figure S2.16 ^{1}H NMR spectrum (400 MHz, 25 °C, $CDCl_3$) of **2.2b**. Deuterated chloroform residual signal denoted by *.

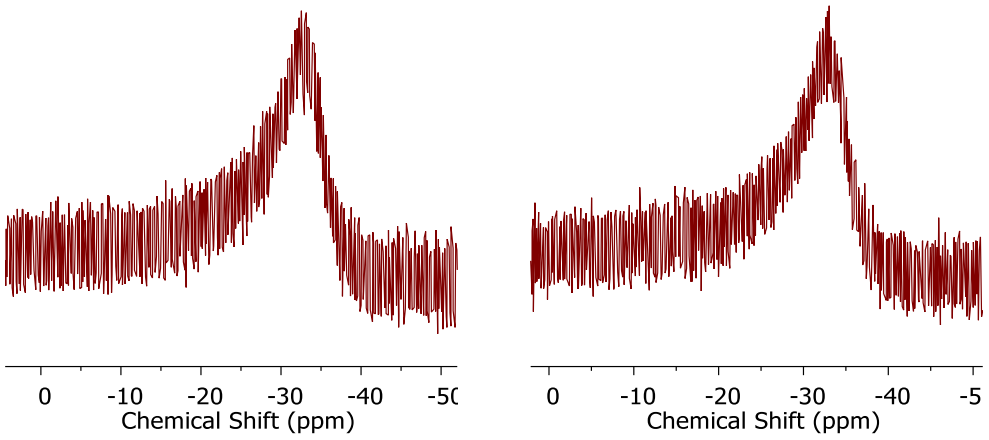

Figure S2.17 ^{11}B (left) and ^{11}B{H} (right) NMR spectra (128 MHz, 25 °C, $CDCl_3$) of **2.2b**.

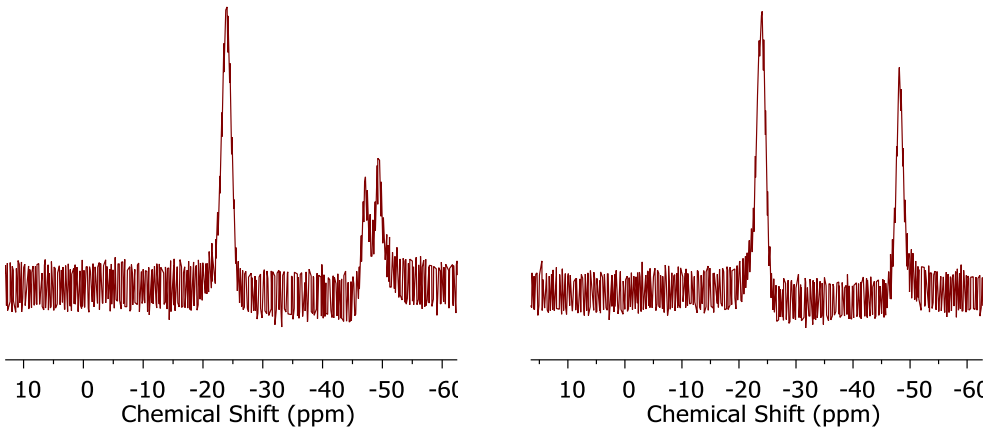

Figure S2.18 ^{31}P (left) and ^{31}P{H} (right) NMR spectra (162 MHz, 25 °C, $CDCl_3$) of **2.2b**.

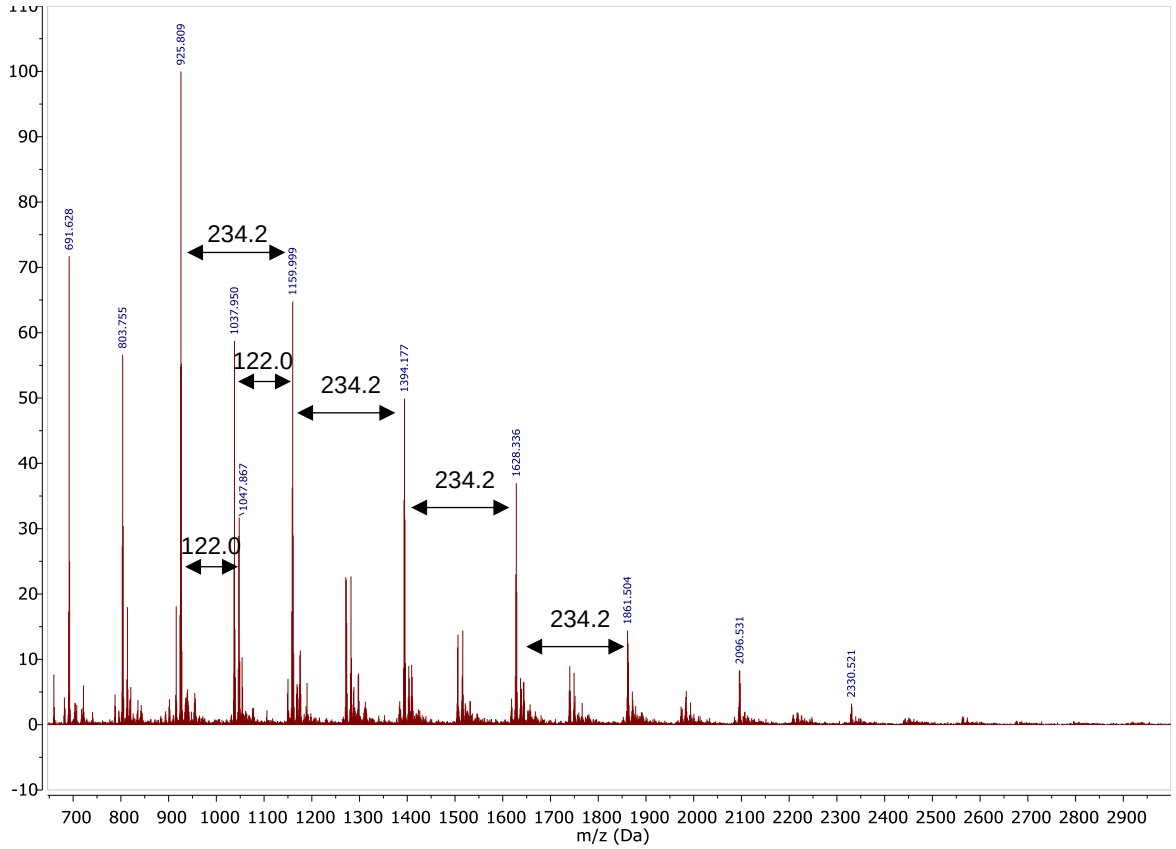

Figure S2.19 ESI-MS (+) spectrum of **2.2b** in DCM.

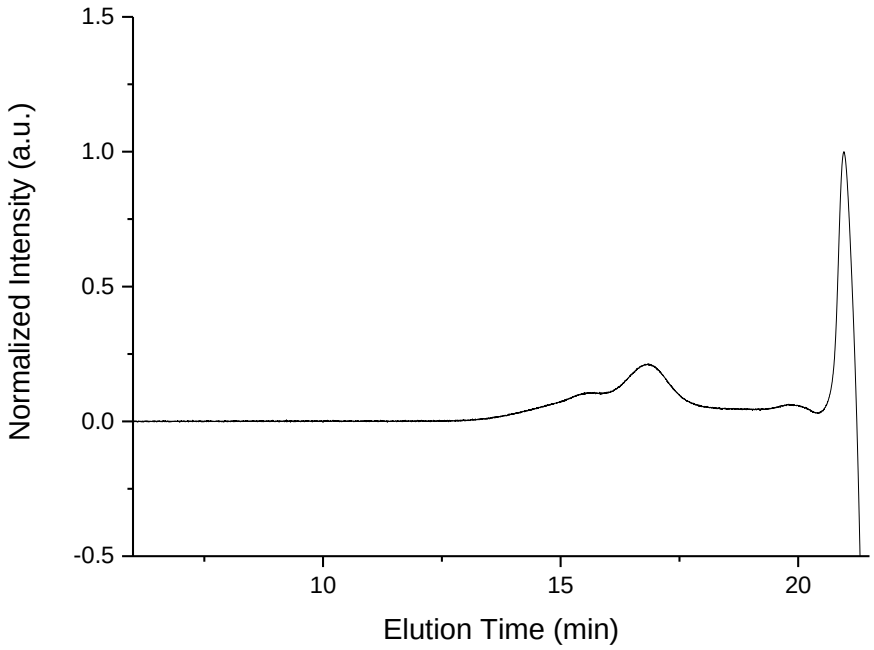

Figure S2.20 GPC chromatogram of **2.2b** (2 mg mL^{-1} in THF, 0.1 w/w % $n$$Bu_4NBr$ in the THF eluent).

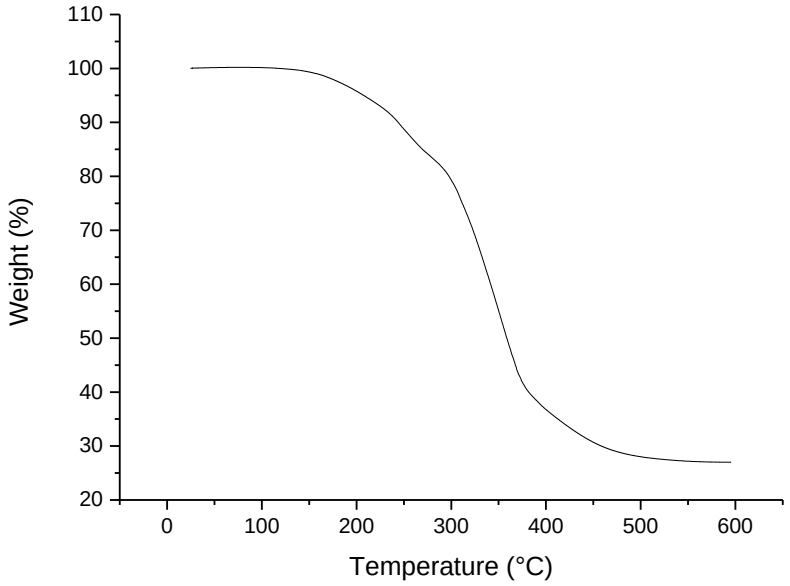

Figure S2.21 TGA thermogram of **2.2b** (heating rate: 10 °C min^{-1}).

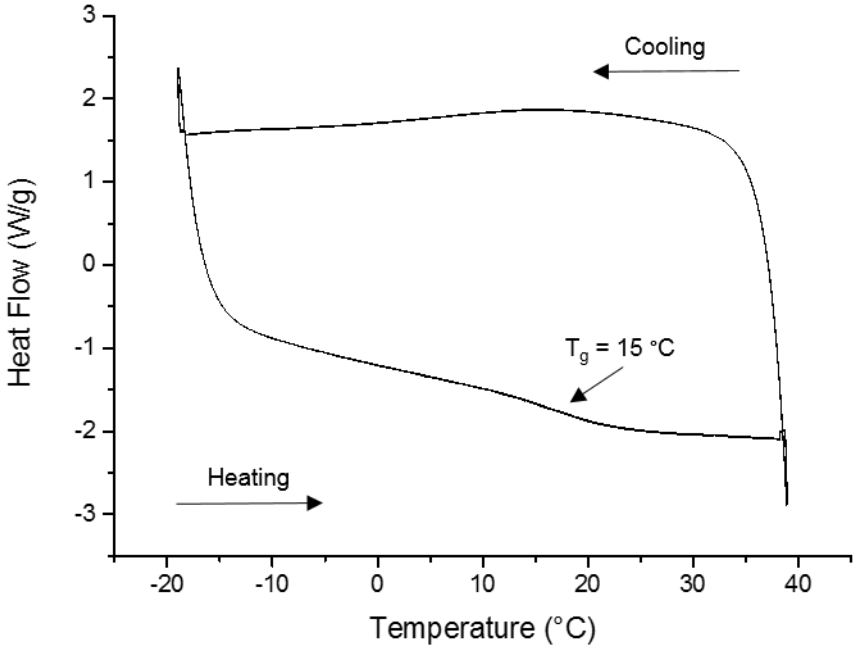

Figure S2.22 DSC thermogram of **2.2b**, first cycle excluded (heating rate: 10 °C min^{-1}).

Figure S2.23 Photograph of isolated **2.2b**.

2.5.4.4 Synthesis and characterisation of polymer 2.2c

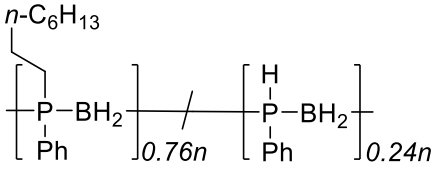

2.1 (244 mg, 2 mmol), 1-octene (159 µL, 2 mmol), DMPA (51 mg, 0.2 mmol), TEMPO (31 mg, 0.2 mmol), and THF (5 mL) were added to a 14 mL vial equipped with a magnetic stirrer. The resultant solution was irradiated ca. 3 cm away from a mercury lamp for 2 h. Volatiles were then removed under vacuum and the resultant solid was purified by precipitation from THF into H_2O/isopropanol (1:1 v/v) at −20 °C (3 × 25 mL). The polymer was then dried under vacuum at 40 °C for 48 h yielding **2.2c** as a gummy orange solid (conversion: 76%; yield: 305 mg, 72 %).

Spectroscopic data:

^{1}H NMR (400 MHz, $CDCl_3$) δ 7.64 – 6.89 (br m, Ar*H*), 4.10 (br d, *J* = 343 Hz, PhP*H*), 2.02 – 0.59 (br m, CH_2, CH_3, BH_2).

^{11}B NMR (128 MHz, $CDCl_3$) δ −32.5 (br s).

^{31}P NMR (162 MHz, $CDCl_3$) δ −24.0 (s, 76%, PhR*P*-BH_2), −48.2 (d, *J* = 356.0 Hz, 24%, PhH*P*-BH_2).

GPC (2 mg mL^{-1}) M_n = 81,000 g mol^{-1}, PDI = 1.2.

$T_{5\%}$ = 197 °C; ceramic yield = 20%; T_g = 9 °C.

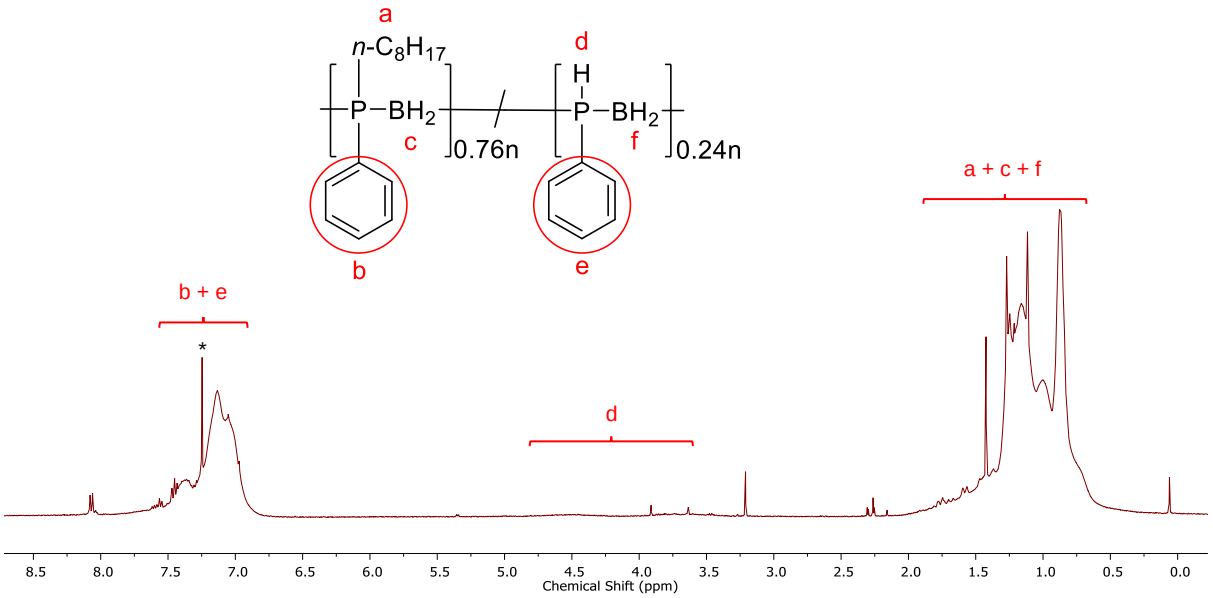

Figure S2.24 ^{1}H NMR spectrum (400 MHz, 25 °C, $CDCl_3$) of **2.2c**. Deuterated chloroform residual signal denoted by *.

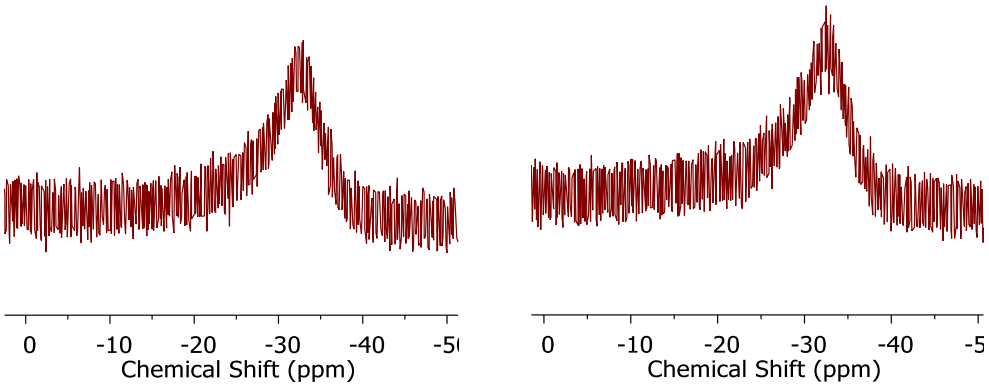

Figure S2.25 ^{11}B (left) and ^{11}B{H} (right) NMR spectra (128 MHz, 25 °C, $CDCl_3$) of **2.2c**.

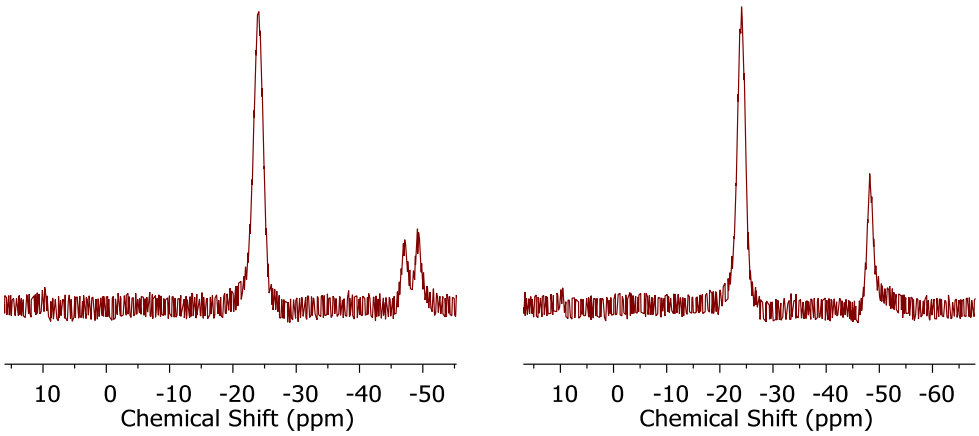

Figure S2.26 ^{31}P (left) and ^{31}P{H} (right) NMR spectra (162 MHz, 25 °C, $CDCl_3$) of **2.2c**.

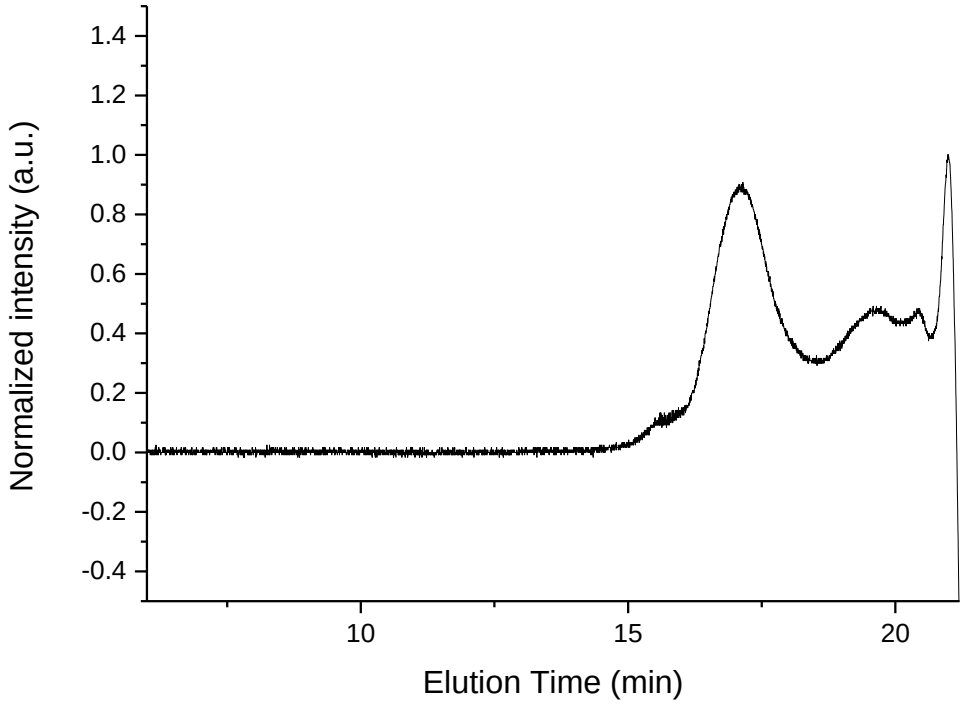

Figure S2.27 GPC chromatogram of **2.2c** (2 mg mL^{-1} in THF, 0.1 w/w % *n*Bu$_4$NBr in the THF eluent).

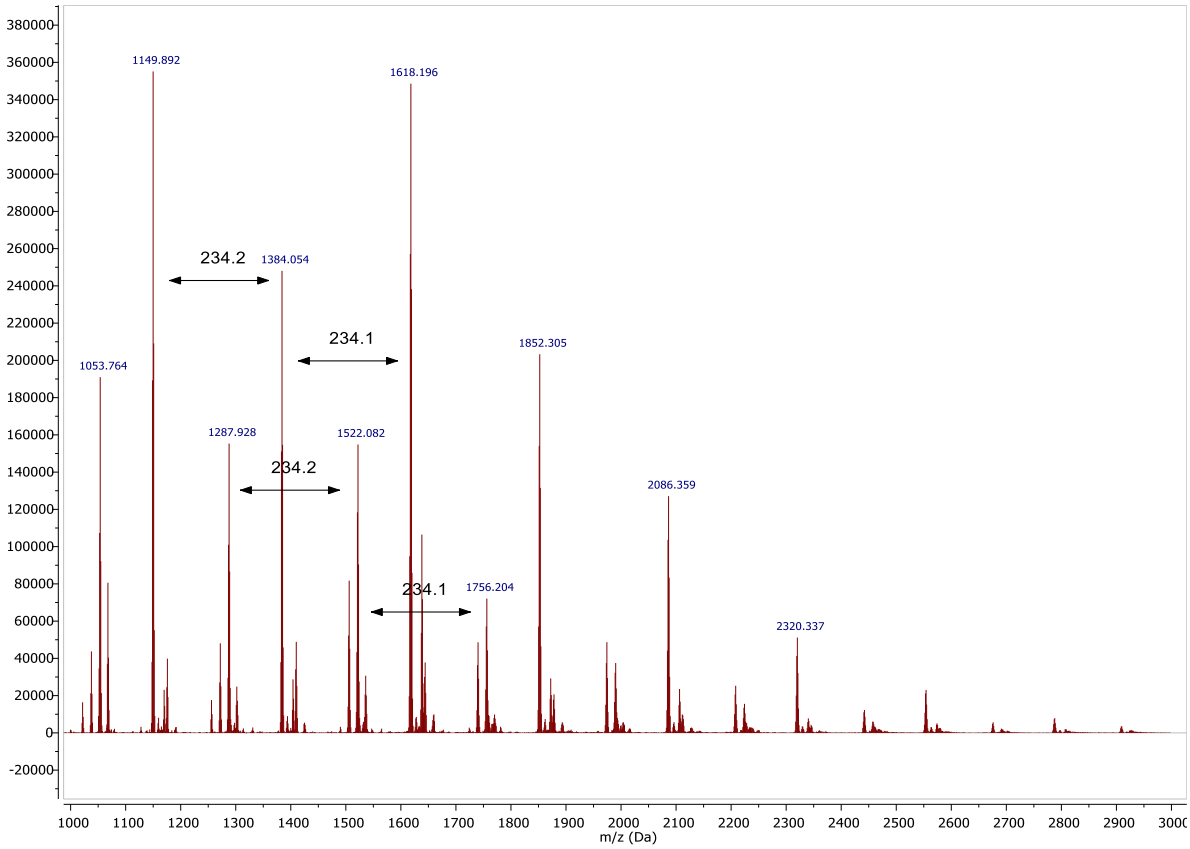

Figure S2.28 ESI-MS (+) spectrum of **2.2c** in DCM.

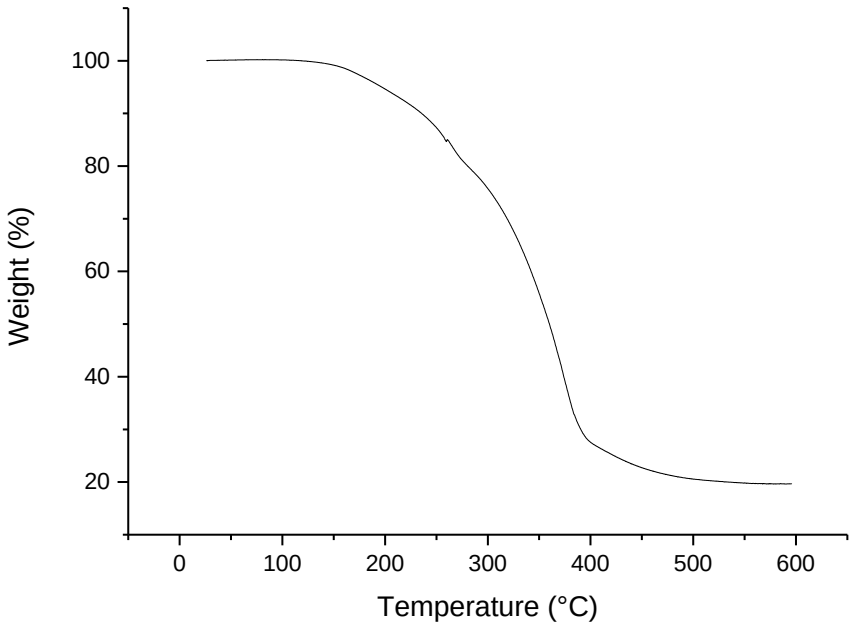

Figure S2.29 TGA thermogram of **2.2c** (heating rate: 10 °C min^{-1}).

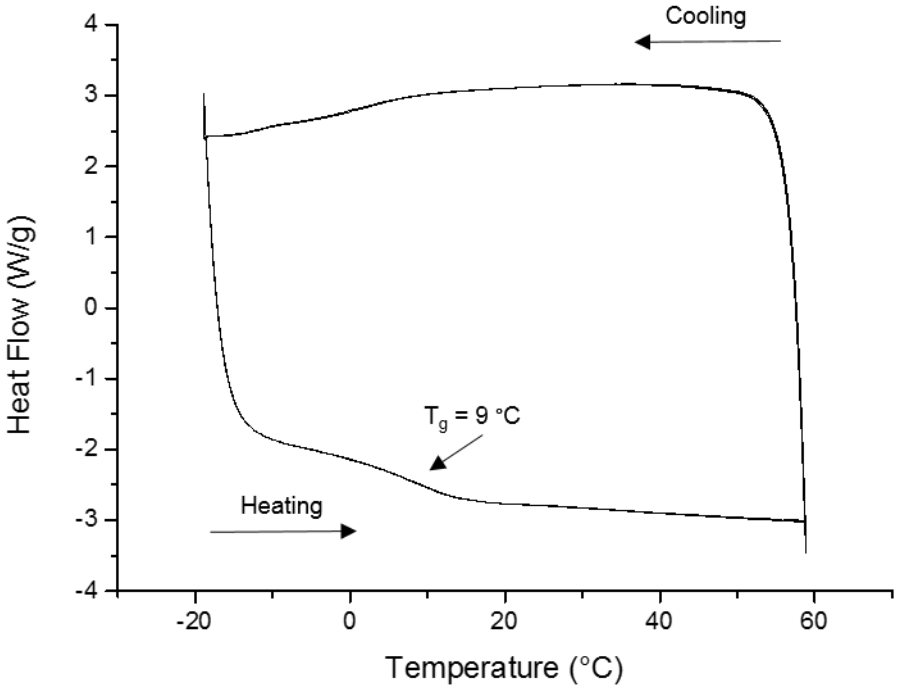

Figure S2.30 DSC thermogram of **2.2c**, first cycle excluded (heating rate: 10 °C min^{-1}).

Figure S2.31 Photographs of isolated **2.2c.**

2.5.4.5 Synthesis and characterisation of polymer 2.2d

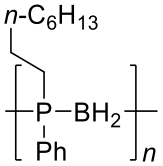

2.1 (244 mg, 2 mmol), 1-octene (159 μL, 4 mmol), DMPA (51 mg, 0.2 mmol), TEMPO (31 mg, 0.2 mmol), and THF (5 mL) were added to a 14 mL vial equipped with a magnetic stirrer. The resultant solution was irradiated ca. 3 cm away from a mercury lamp for 24 h. Volatiles were then removed under vacuum and the resultant solid was purified by precipitation from THF into H_2O/isopropanol (1:1 v/v) at −20 °C (3 × 25 mL). The polymer was then dried under vacuum at 40 °C for 48 h yielding **2.2d** as a gummy orange solid (conversion: 100%; yield: 297 mg, 63 %).

Spectroscopic data:

^{1}H NMR (400 MHz, $CDCl_3$) δ 7.64 – 6.89 (br m, Ar*H*), 2.02 – 0.59 (br m, CH_2, CH_3, BH_2).

^{11}B NMR (128 MHz, $CDCl_3$) δ −32.5 (br s).

^{31}P NMR (162 MHz, $CDCl_3$) δ −24.0 (s, 76%, PhR*P*-BH_2).

GPC (2 mg mL^{-1}) M_n = 112,000 g mol^{-1}, PDI = 1.1.

$T_{5\%}$ = 216 °C; ceramic yield = 6%; T_g = 4 °C.

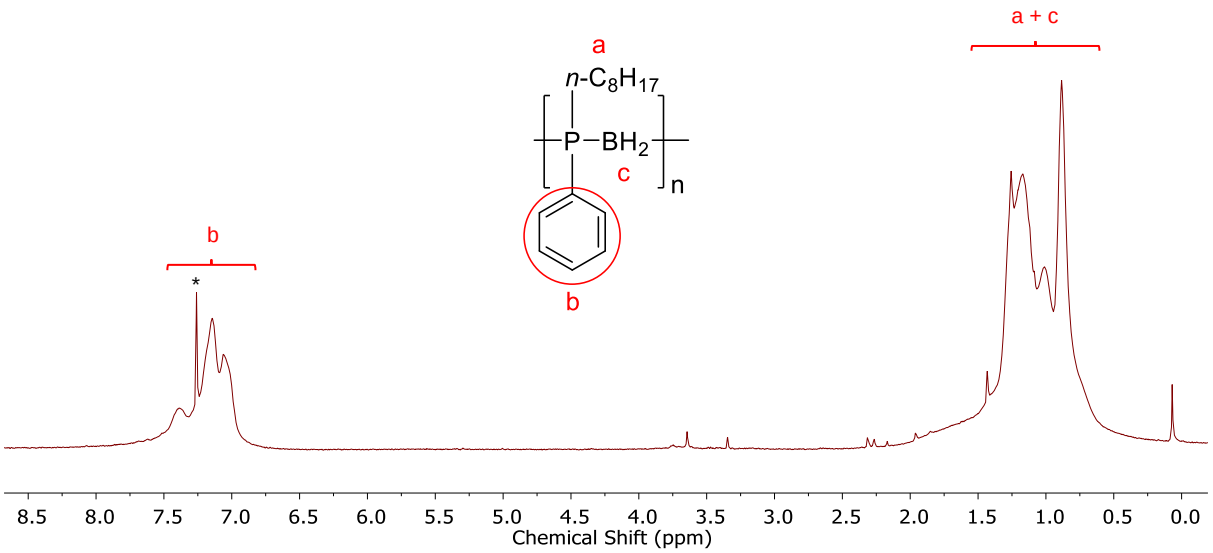

Figure S2.32 ^{1}H NMR spectrum (400 MHz, 25 °C, $CDCl_3$) of **2.2d**. Deuterated chloroform residual signal denoted by *.

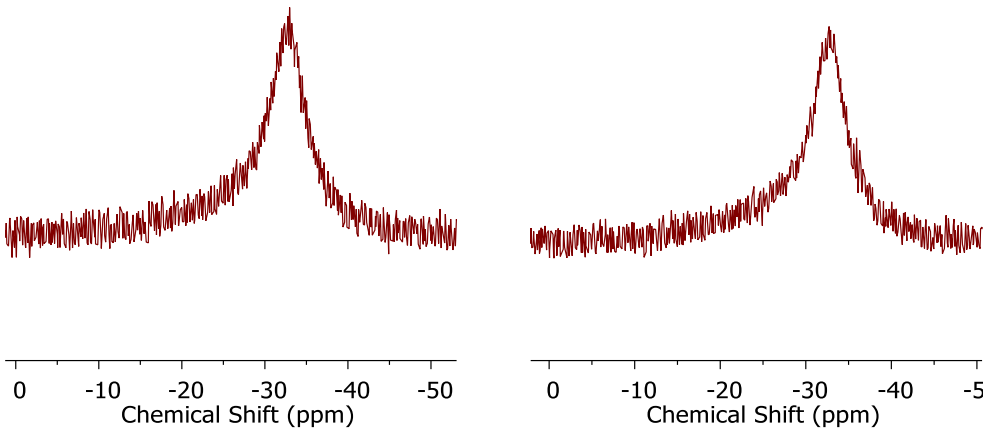

Figure S2.33 ^{11}B (left) and ^{11}B{H} (right) NMR spectra (128 MHz, 25 °C, $CDCl_3$) of **2.2d**.

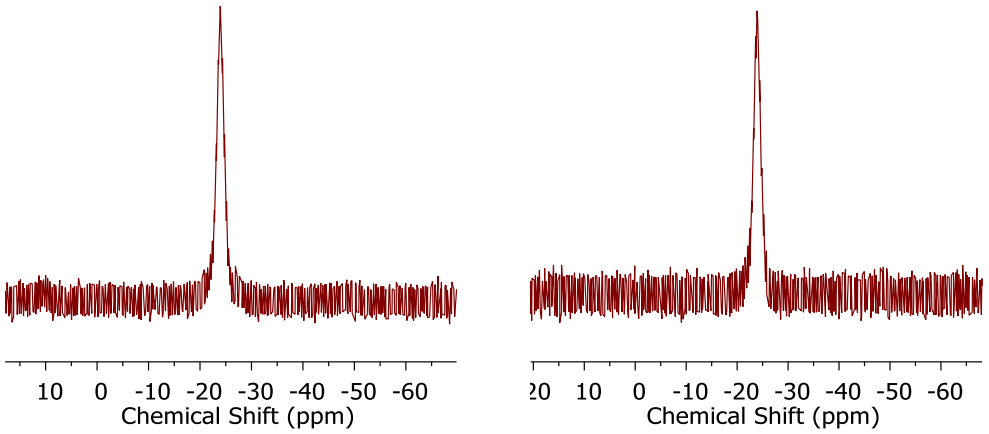

Figure S2.34 ^{31}P (left) and ^{31}P{H} (right) NMR spectra (162 MHz, 25 °C, $CDCl_3$) of **2.2d**.

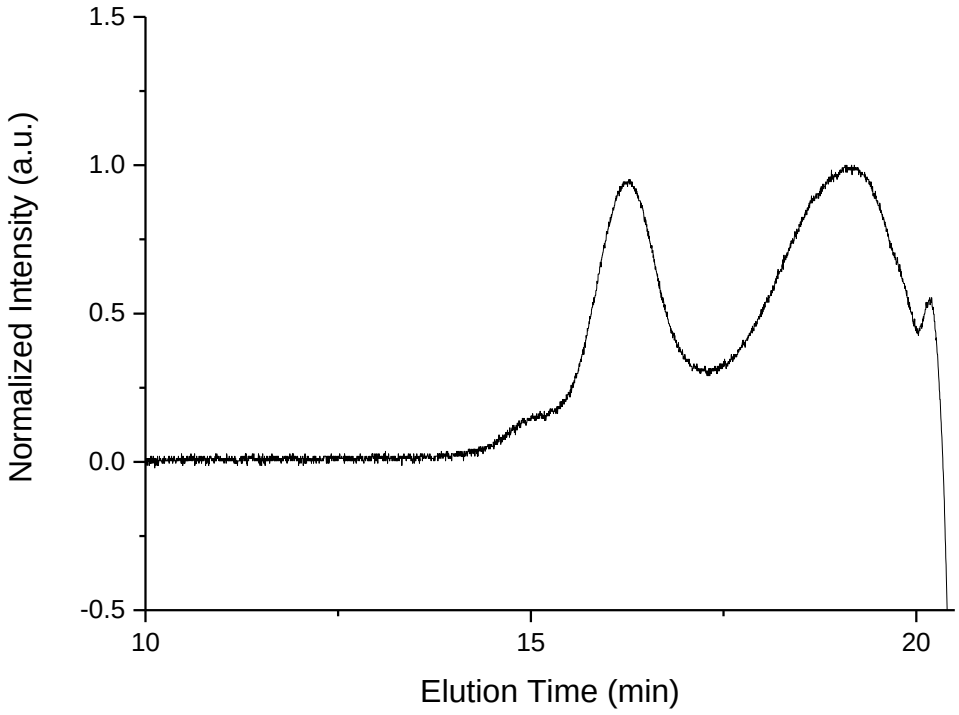

Figure S2.35 GPC chromatogram of **2.2d** (2 mg mL^{-1} in THF, 0.1 w/w % $n$$Bu_4NBr$ in the THF eluent).

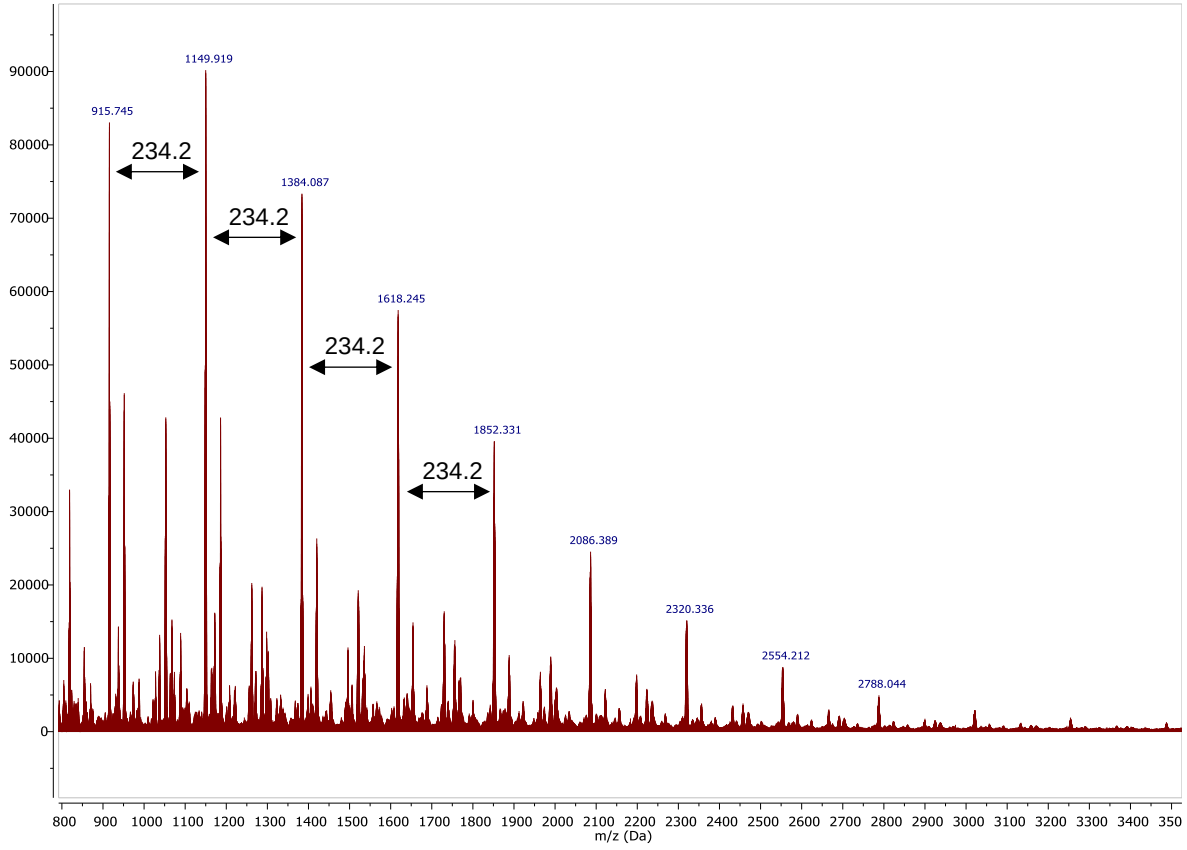

Figure S2.36 ESI-MS (+) spectrum of **2.2d** in DCM.

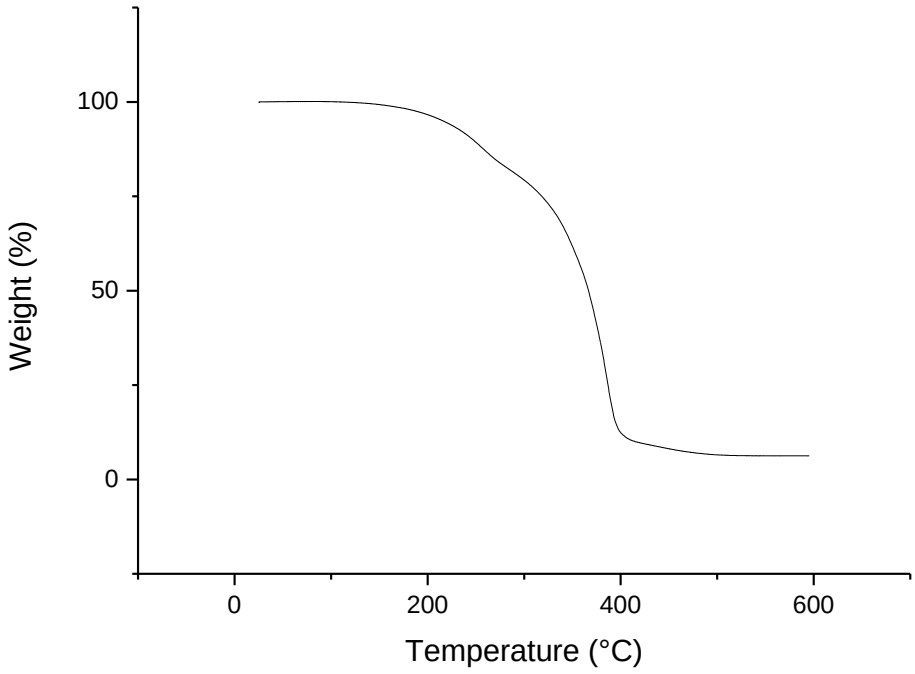

Figure S2.37 TGA thermogram of **2.2d** (heating rate: 10 °C min^{-1}).

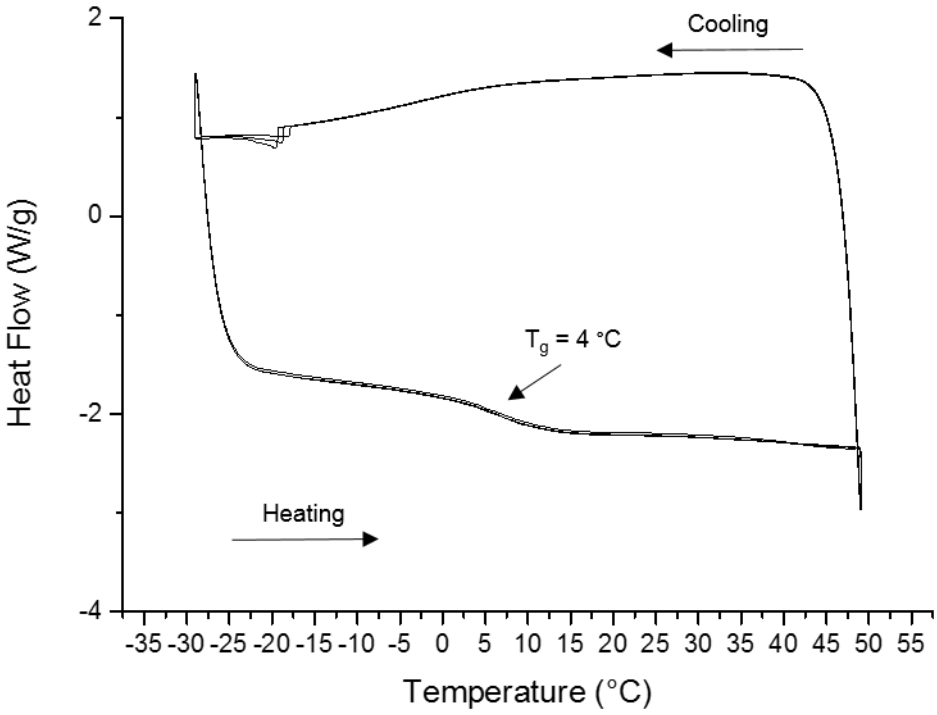

Figure S2.38 DSC thermogram of **2.2d**, first cycle excluded (heating rate: 10 °C min^{-1}).

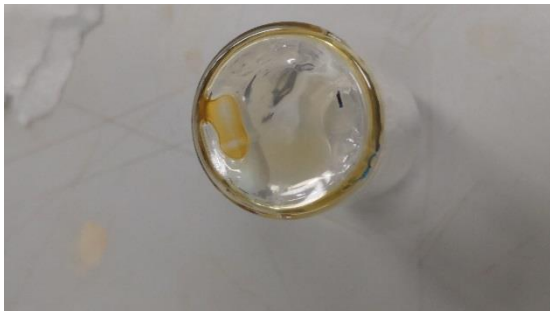

Figure S2.39 Photograph of isolated **2.2d**.

2.5.4.6 Synthesis and characterisation of polymer 2.3

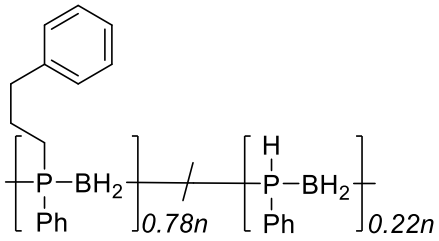

2.1 (244 mg, 2 mmol), allylbenzene (265 μL, 2 mmol), DMPA (51 mg, 0.2 mmol), TEMPO (31 mg, 0.2 mmol), and THF (5 mL) were added to a 14 mL vial equipped with a magnetic stirrer. The resultant solution was irradiated ca. 3 cm away from a mercury lamp for 2 h. Volatiles were then removed under vacuum and the resultant solid was purified by precipitation from DCM into pentane at −78 °C (3 × 25 mL). The polymer was then dried under vacuum at 40 °C for 48 h yielding **2.3** as an orange solid (conversion: 78%; yield: 249 mg, 57%).

Spectroscopic data:

^{1}H NMR (400 MHz, $CDCl_3$) δ 7.48 – 6.80 (m, Ar*H*), 4.10 (br d, *J* = 349 Hz, PhP*H*), 2.10 (br s, PhCH_2), 1.79 – 0.80 (br m, PCH_2, PCH_2CH_2, and BH_2).

^{11}B NMR (128 MHz, $CDCl_3$) δ −33.4 (br s).

^{31}P NMR (162 MHz, $CDCl_3$) δ −23.9 (s, 78%, PhR*P*-BH_2), −48.5 (d, *J* = 354 Hz, 22%, PhH*P*-BH_2).

GPC (2 mg mL^{-1}) M_n = 104,000 g mol^{-1}, PDI = 1.3.

$T_{5\%}$ = 194 °C; ceramic yield = 19%; T_g = 50 °C.

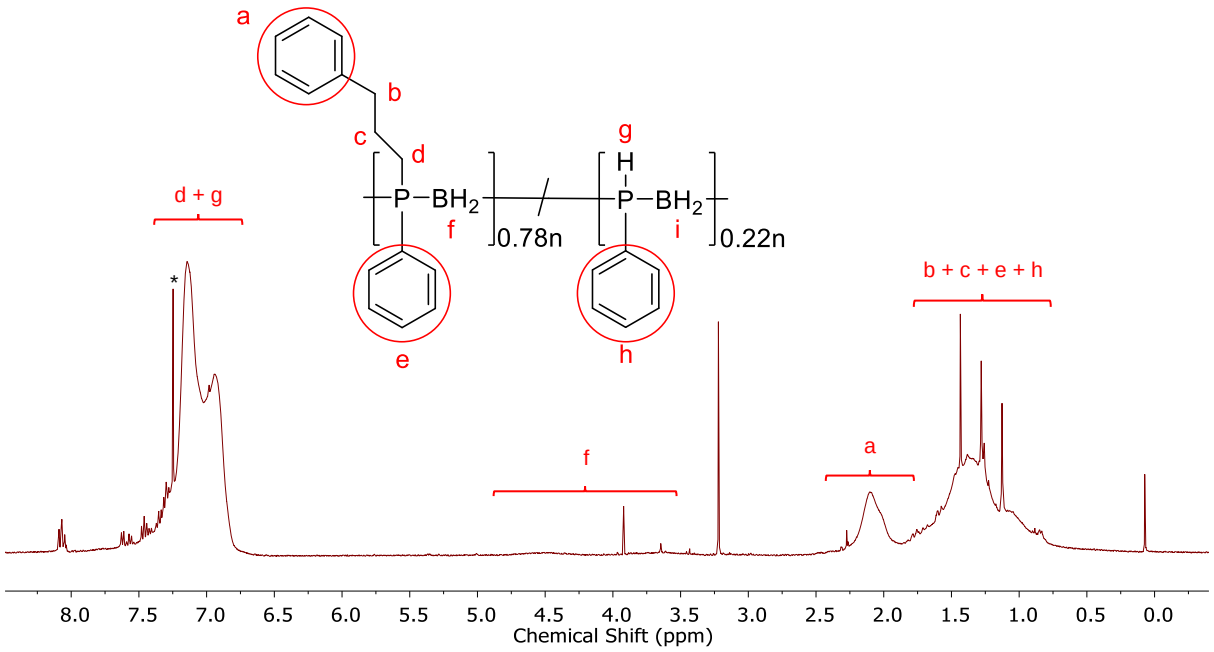

Figure S2.40 ^{1}H NMR spectrum (400 MHz, 25 °C, $CDCl_3$) of **2.3**. Deuterated chloroform residual signal denoted by *.

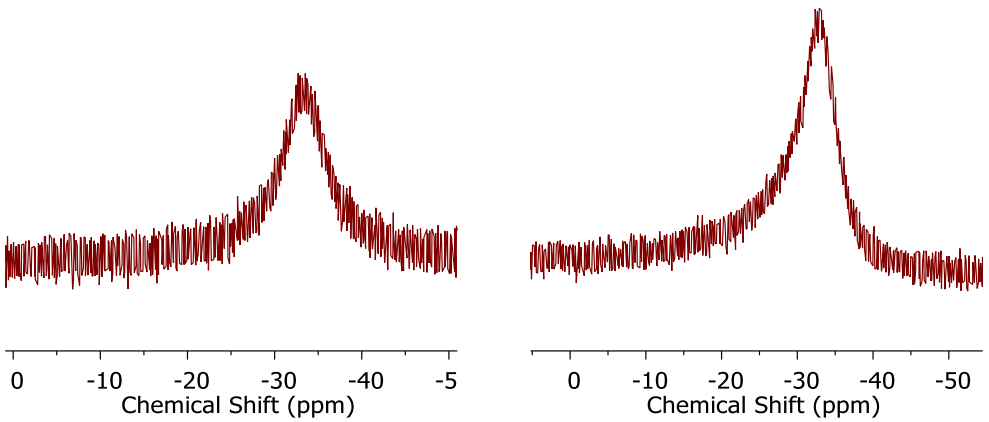

Figure S2.41 ^{11}B (left) and ^{11}B{H} (right) NMR spectra (128 MHz, 25 °C, $CDCl_3$) of **2.3**.

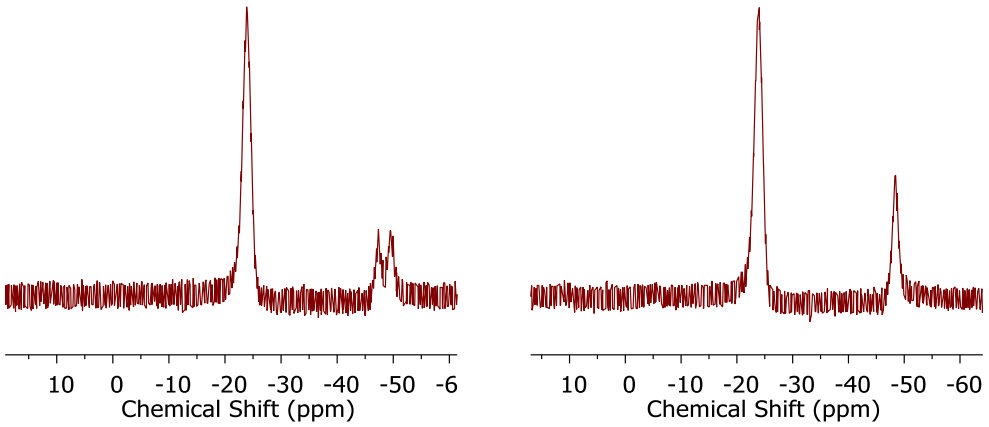

Figure S2.42 ^{31}P NMR (left) and ^{31}P{H} (162 MHz, 25 °C, $CDCl_3$) of **2.3**.

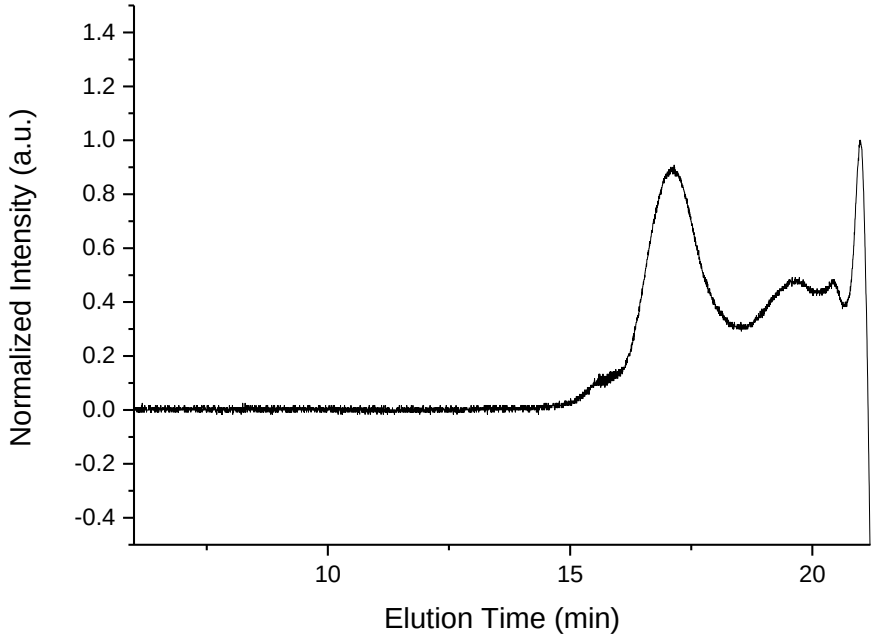

Figure S2.43 GPC chromatogram of **2.3** (2 mg mL^{-1} in THF, 0.1 w/w % *n*Bu_4NBr in the THF eluent).

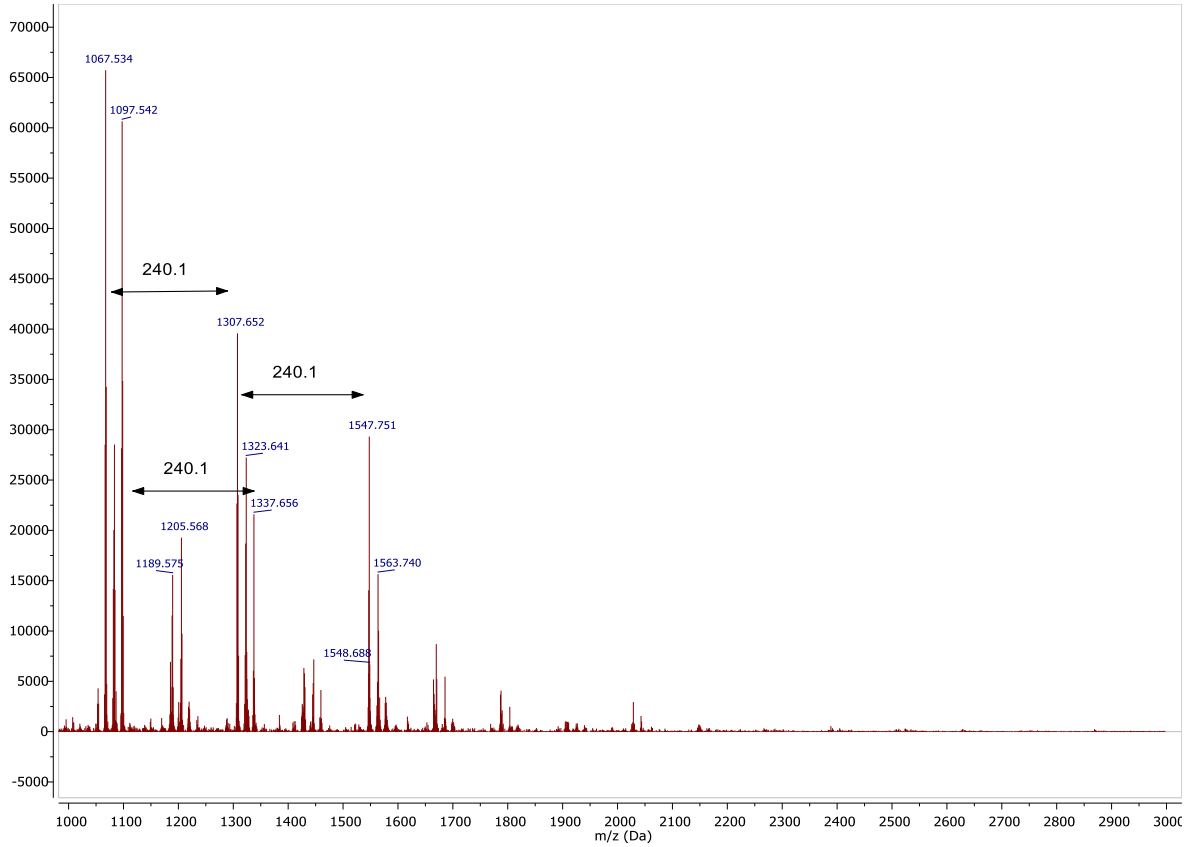

Figure S2.44 ESI-MS (+) spectrum of **2.3** in DCM.

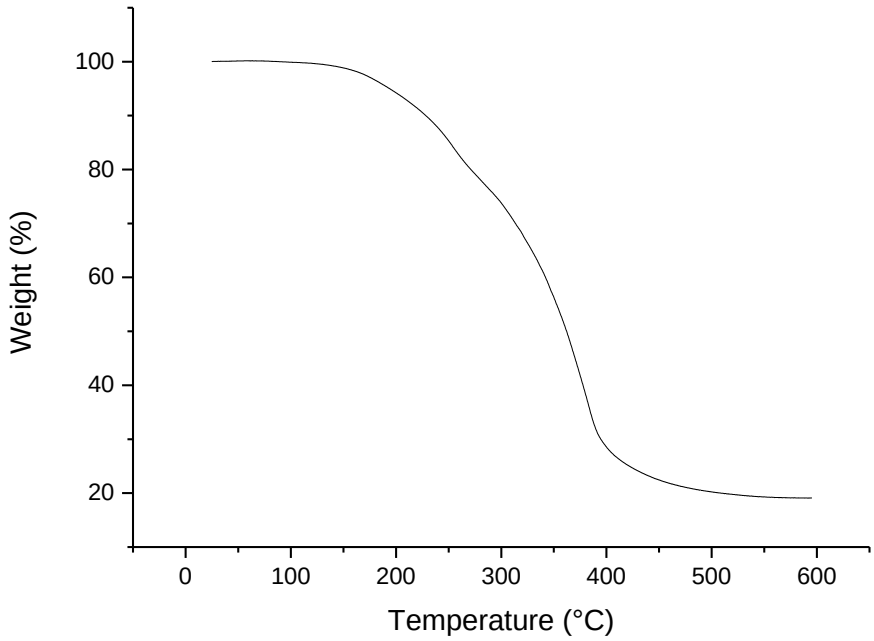

Figure S2.45 TGA thermogram of **2.3** (heating rate: 10 °C min^{-1}).

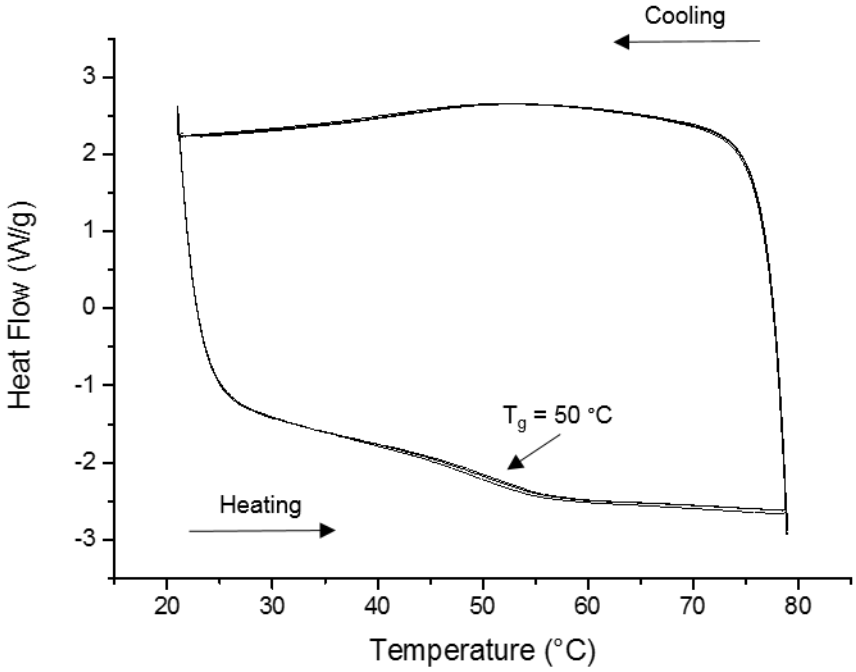

Figure S2.46 DSC thermogram of **2.3**, first cycle excluded (heating rate: 10 °C min^{-1}).

Figure S2.47 Photograph of isolated **2.3**.

2.5.4.7 Synthesis and characterisation of polymer 2.4

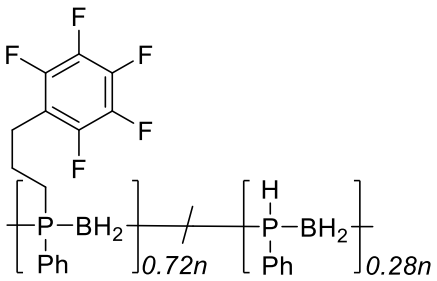

2.1 (244 mg, 2 mmol), allyl pentafluorobenzene (307 μL, 2 mmol), DMPA (51 mg, 0.2 mmol), TEMPO (31 mg, 0.2 mmol), and THF (5 mL) were added to a 14 mL vial equipped with a magnetic stirrer. The

resultant solution was irradiated ca. 3 cm away from a mercury lamp for 2 h. Volatiles were then removed under vacuum and the resultant solid was purified by precipitation from DCM into pentane at −78 °C (3 × 25 mL). The polymer was then dried under vacuum at 40 °C for 48 h yielding **2.4** as an orange solid (conversion: 72%; yield: 204 mg, 37%).

Spectroscopic data:

^{1}H NMR (400 MHz, $CDCl_3$) δ 7.52 – 6.80 (br m, Ar*H*), 4.09 (br d, *J* = 344 Hz, PhP*H*), 2.24 (br s, $C_6F_5CH_2$), 1.68 – 0.92 (br m, CH_2, CH_3, BH_2).

^{11}B NMR (128 MHz, $CDCl_3$) δ −34.3 (br s).

^{31}P NMR (162 MHz, $CDCl_3$) δ −24.0 (s, 72%, PhR*P*-BH_2), −48.6 (d, *J* = 368 Hz, 28%, PhH*P*-BH_2).

^{19}F NMR (283 MHz, $CDCl_3$) δ −143.63 (s), −157.72 (s), −162.83 (s).

GPC (2 mg mL^{-1}) M_n = 130,000 g mol^{-1}, PDI = 1.5.

$T_{5\%}$ = 209 °C; ceramic yield = 34%; T_g = 67 °C.

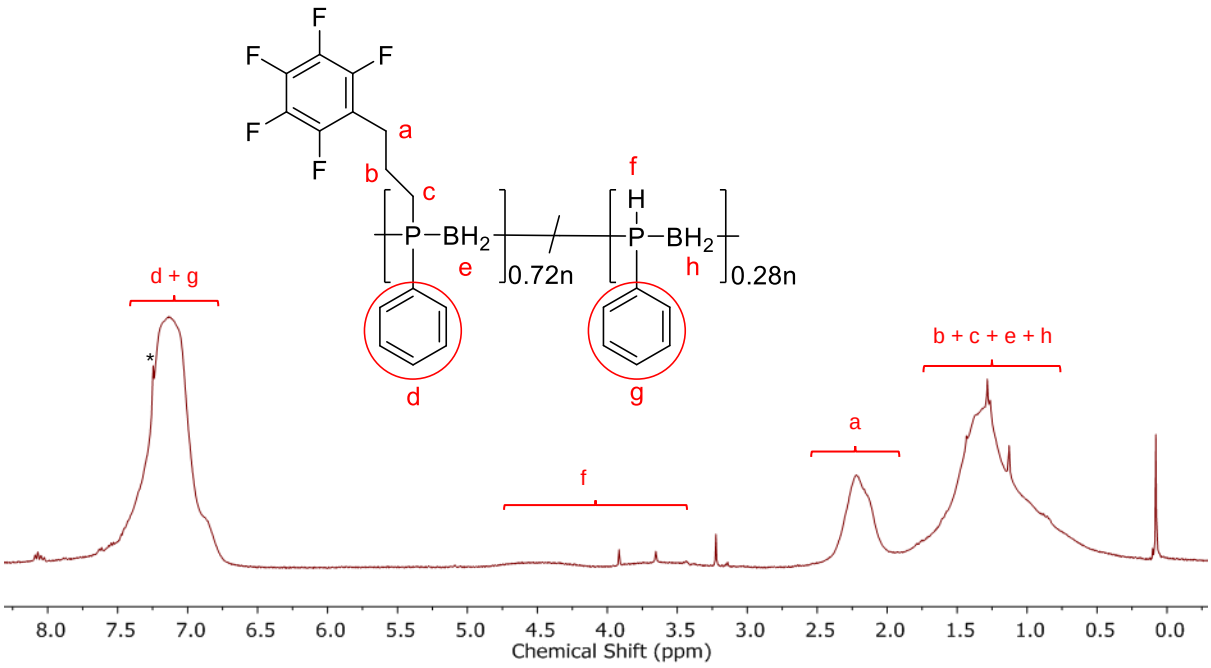

Figure S2.48 ^{1}H NMR spectrum (400 MHz, 25 °C, $CDCl_3$) of 2.4. Deuterated chloroform residual signal denoted by *****.

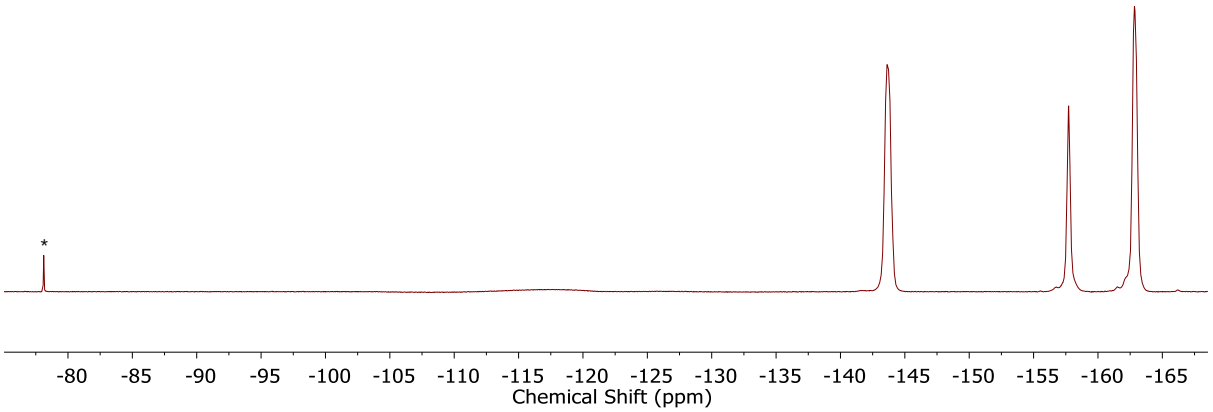

Figure S2.49 ^{19}F NMR (283 MHz, 25 °C, $CDCl_3$) of **2.4**. Signal arising from OTf group originating from $CpFe(CO)_2OTf$ used in the polymerisation of $PhH_2P{\cdot}BH_3$ denoted by *.

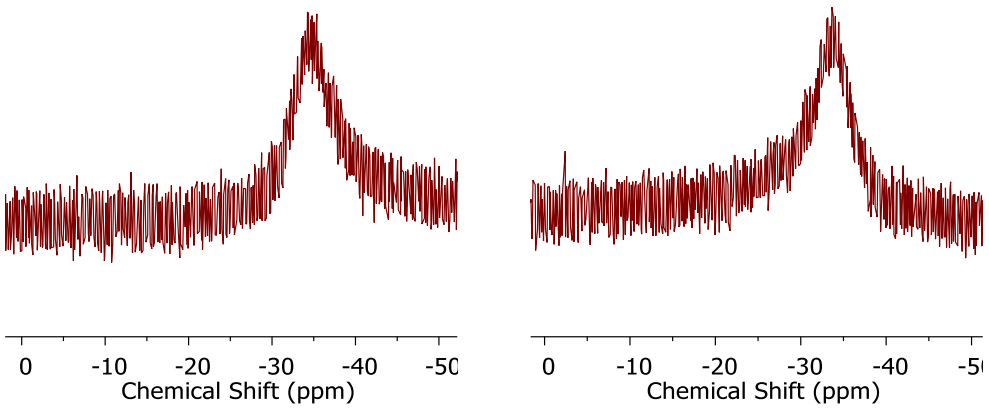

Figure S2.50 ^{11}B (left) and $^{11}B\{H\}$ (right) NMR spectra (128 MHz, 25 °C, $CDCl_3$) of **2.4**.

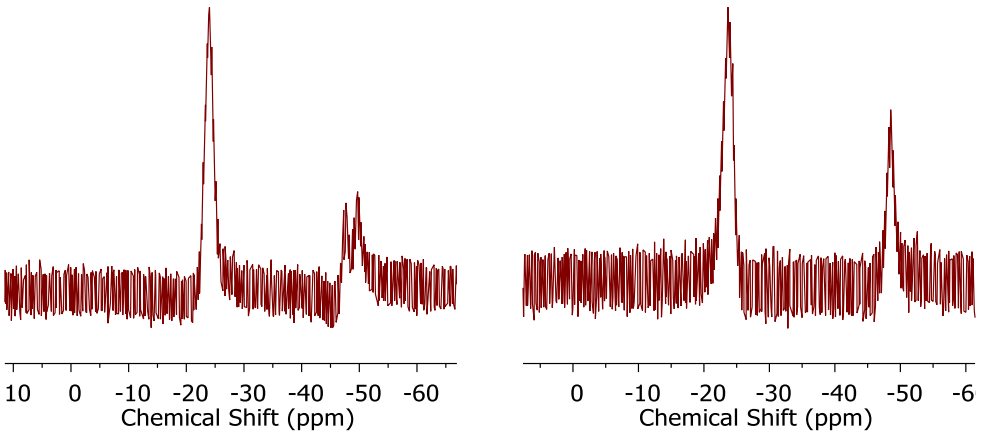

Figure S2.51 ^{31}P (left) and $^{31}P\{H\}$ (right) NMR spectra (162 MHz, 25 °C, $CDCl_3$) of **2.4**.

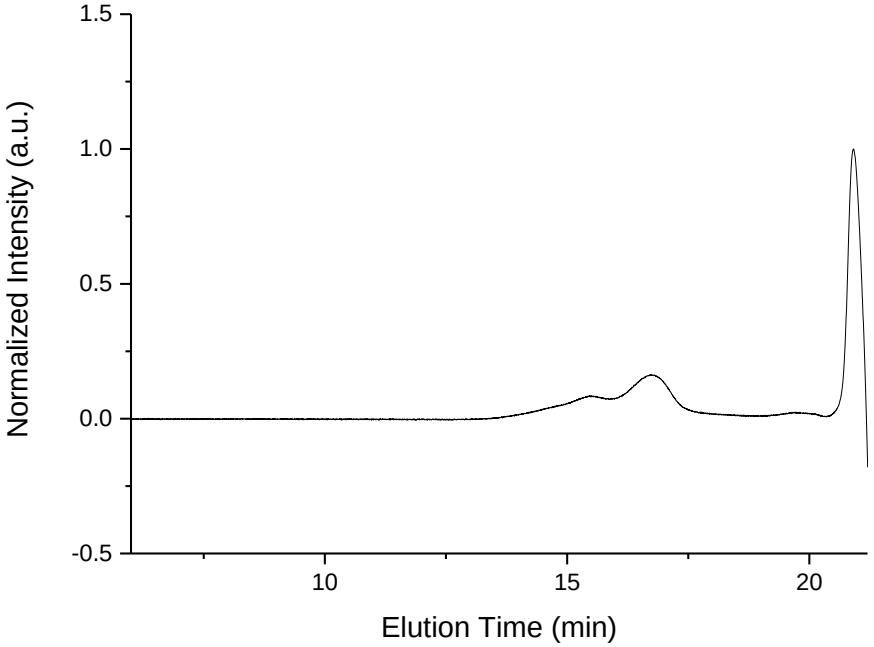

Figure S2.52 GPC chromatogram of **2.4** (2 mg mL^{-1} in THF, 0.1 w/w % *n*Bu_4NBr in the THF eluent).

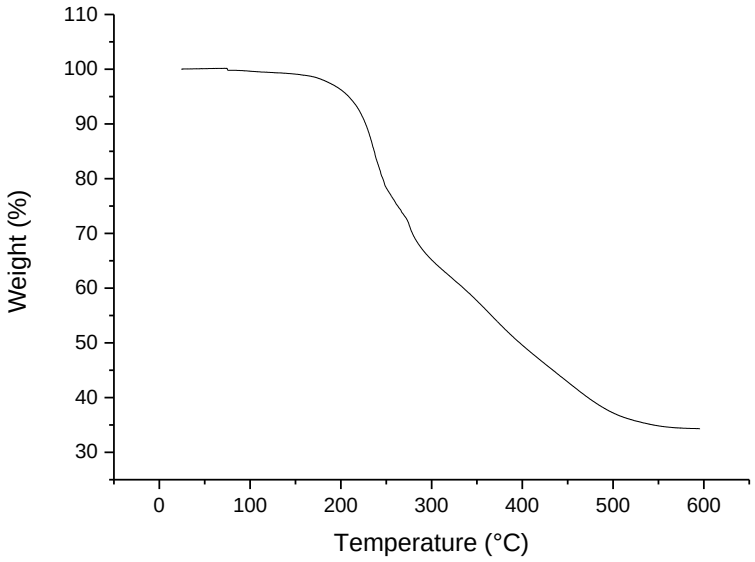

Figure S2.53 TGA thermogram of **2.4** (heating rate: 10 °C min^{-1}).

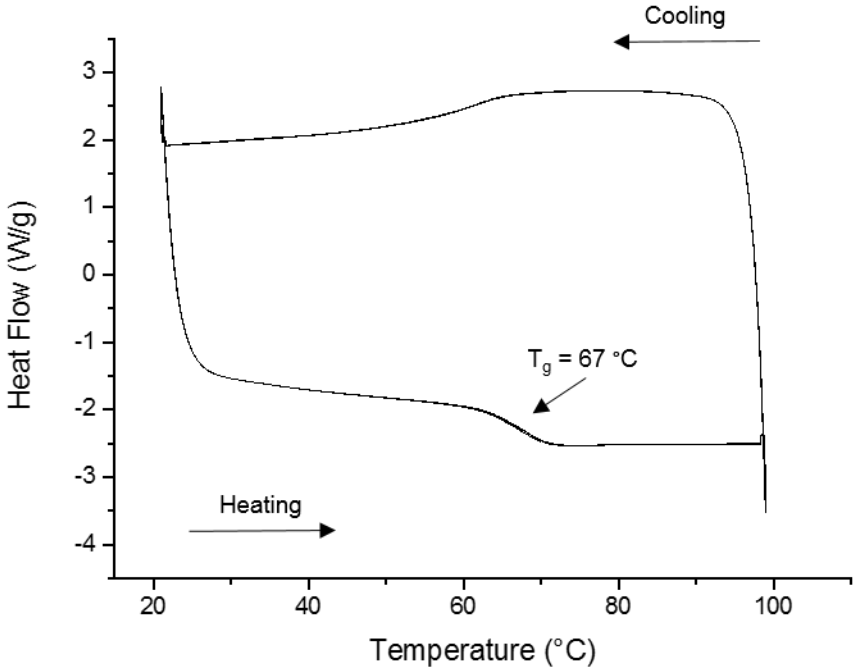

Figure S2.54 DSC thermogram of **2.4**, first cycle excluded (heating rate: 10 °C min^{-1}).

2.5.4.8 Synthesis and characterisation of polymer 2.5

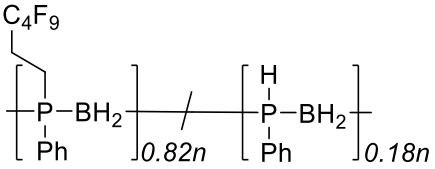

2.1 (244 mg, 2 mmol), 1H,1H,2H-perfluoro-1-hexene (339 mg, 2 mmol), DMPA (51 mg, 0.2 mmol), TEMPO (31 mg, 0.2 mmol), and THF (5 mL) were added to a 14 mL vial equipped with a magnetic stirrer. The resultant solution was irradiated ca. 3 cm away from a mercury lamp for 2 h. Volatiles were then removed under vacuum and the resultant solid was purified by precipitation from THF into H_2O/isopropanol (1:1 v/v) at −20 °C (3 × 25 mL). The polymer was then dried under vacuum at 40 °C for 48 h yielding **2.5** as an orange solid (conversion: 82%; yield: 479 mg, 74%).

Spectroscopic data:

^{1}H NMR (400 MHz, $CDCl_3$) δ 7.54 – 6.80 (br m, Ar*H*), 4.16 (br d, *J* = 357 Hz, PhP*H*) 2.28 – 0.94 (br m, CH_2, BH_2).

^{11}B NMR (128 MHz, $CDCl_3$) δ −34.1 (br s).

^{31}P NMR (162 MHz, $CDCl_3$) δ −23.7 (s, 82%, PhR*P*-BH_2), −49.9 (d, *J* = 357 Hz, 18%, PhH*P*-BH_2).

^{19}F NMR (377 MHz, $CDCl_3$) δ −81.31, −115.17, −124.30, −126.30.

GPC (2 mg mL^{-1}) M_n = 92,000 g mol^{-1}, PDI = 1.4.

$T_{5\%}$ = 173 °C; ceramic yield = 8%; T_g = 43 °C.

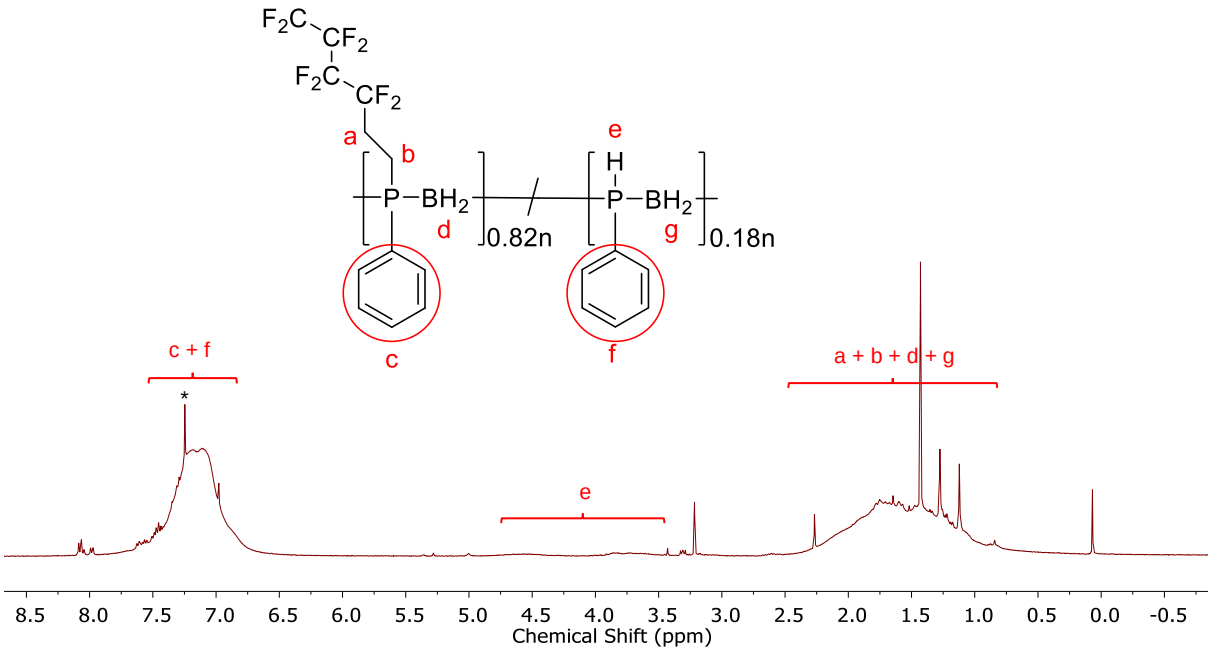

Figure S2.55 ^{1}H NMR spectrum (400 MHz, 25 °C, $CDCl_3$) of **2.5**. Deuterated chloroform residual signal denoted by *.

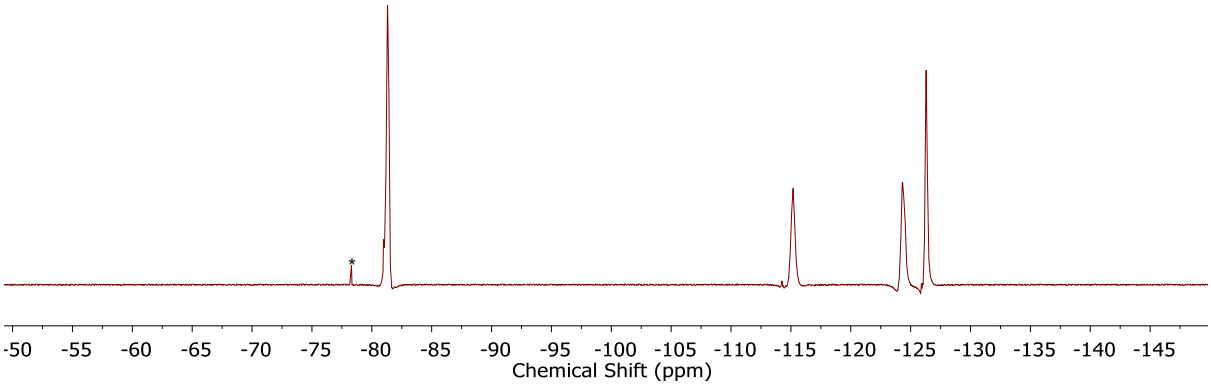

Figure S2.56 ^{19}F NMR (377 MHz, 25 °C, $CDCl_3$) of **2.5**. Signal arising from OTf group originating from $CpFe(CO)_2OTf$ used in the polymerisation of $PhH_2P{\cdot}BH_3$ denoted by *.

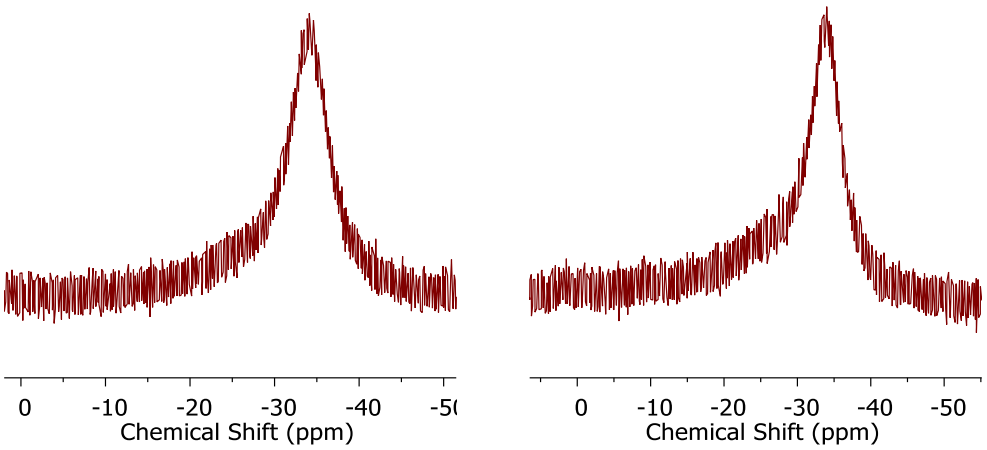

Figure S2.57 ^{11}B (left) and ^{11}B{H} NMR spectra (128 MHz, 25 °C, $CDCl_3$) of **2.5**.

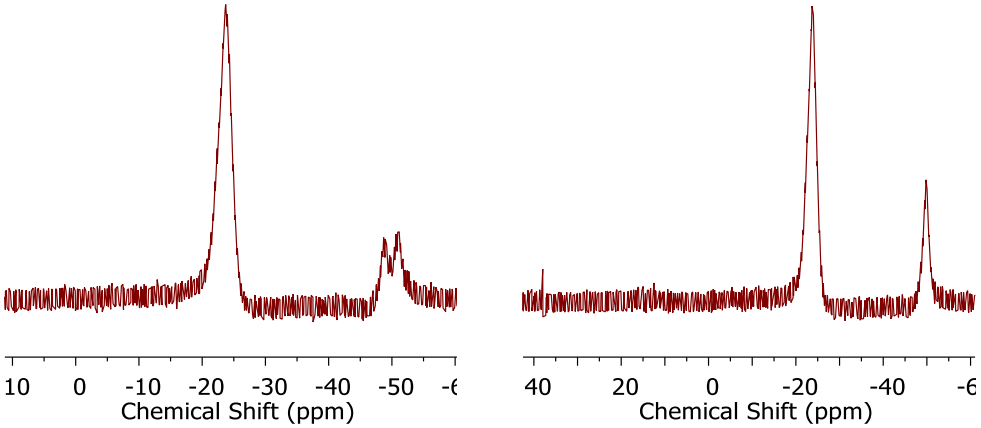

Figure S2.58 ^{31}P (left) and ^{31}P{H} (right) NMR spectra (162 MHz, 25 °C, $CDCl_3$) of **2.5**.

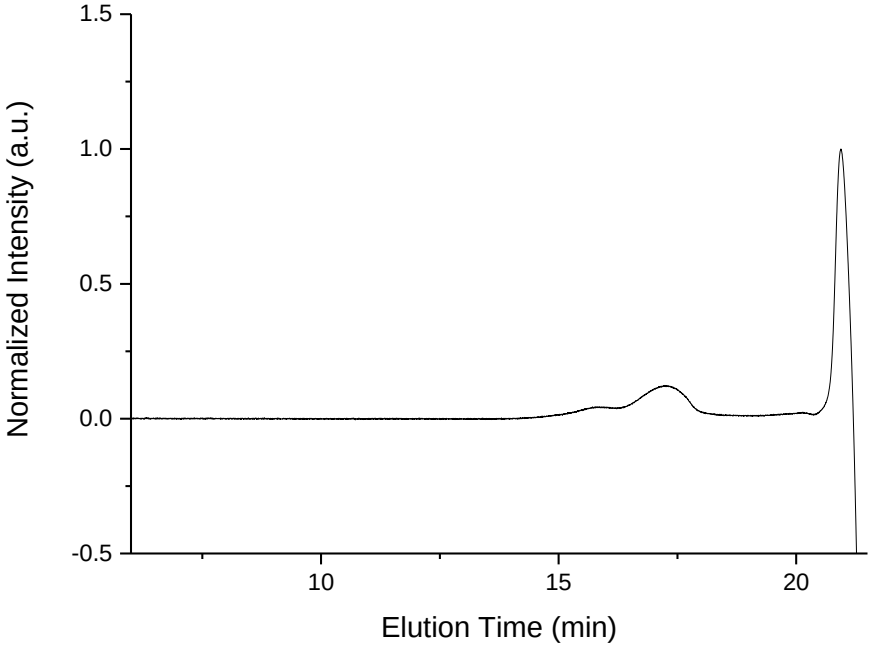

Figure S2.59 GPC chromatogram of **2.5** (2 mg mL^{-1} in THF, 0.1 w/w % *n*Bu_4NBr in the THF eluent).

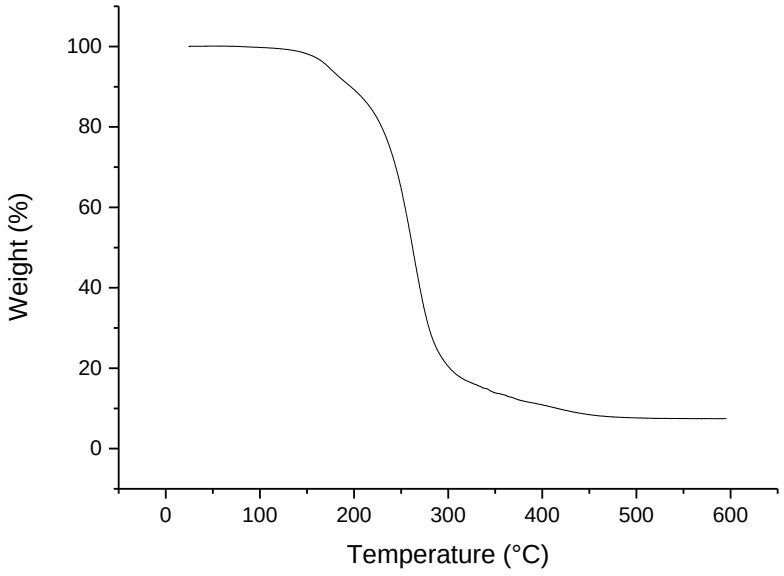

Figure S2.60 TGA thermogram of **2.5** (heating rate: 10 °C min^{-1}).

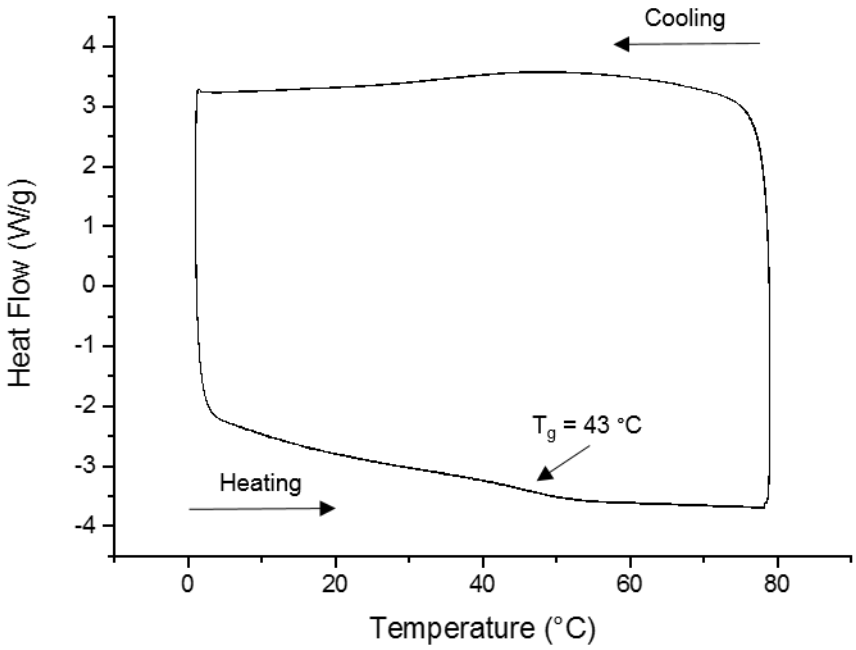

Figure S2.61 DSC thermogram of **2.5**, first cycle excluded (heating rate: 10 °C min^{-1}).

Figure S2.62 Photograph of isolated **2.5**.

2.5.5 Synthesis and characterisation of crosslinked polyphosphinoborane

2.5.5.1 Irradiation of [PhHP-BH_2]$_n$ with DMPA (10 mol%) in the absence of alkene.

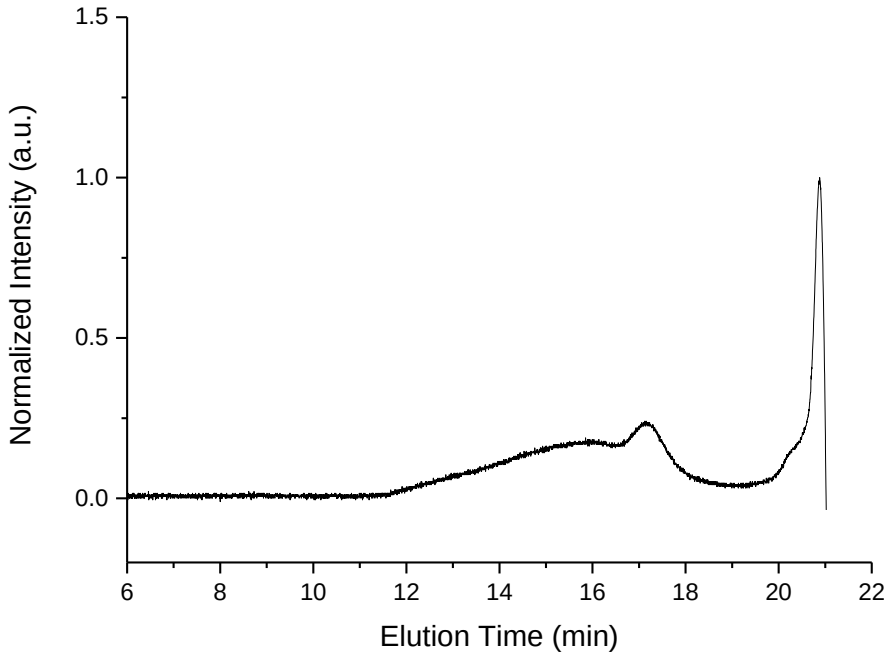

Figure S2.63 GPC chromatogram in THF (2 mg mL^{-1}, 0.1 w/w % *n*-Bu_4NBr in the THF eluent) of material obtained via irradiation of [PhHP-BH_2]$_n$ with DMPA (10 mol%) in the absence of alkene.

2.5.5.2 Synthesis and characterisation of crosslinked poly(phenylphosphinoborane)

2.1 (122 mg, 1 mmol), 1,5-hexadiene (17.8 μL, 0.15 mmol), DMPA (25 mg, 0.1 mmol), TEMPO (15 mg, 0.1 mmol), and THF (1 mL) were added to a 14 mL vial. The resultant solution was irradiated ca. 3 cm away from a mercury lamp for 2 h resulting in the formation of an insoluble gel with exclusion of orange coloured solvent. Excess solvent was decanted away, and volatiles were removed under vacuum yielding an orange solid. This solid was purified by swelling in THF for 6 hours followed by decanting away of excess solvent until no colouration of the solvent was observed (2 × 5 mL). Volatiles were removed under vacuum yielding a brittle orange solid (yield: 89 mg).

Spectroscopic data:

^{31}P NMR (202 MHz, THF-d_8) δ −23.6 (s, 7%, PhR*P*-BH_2), −49.1 (d, *J* = 345.3 Hz, 93%, PhH*P*-BH_2).

$T_{5\%}$ = 138 °C; ceramic yield = 53%.

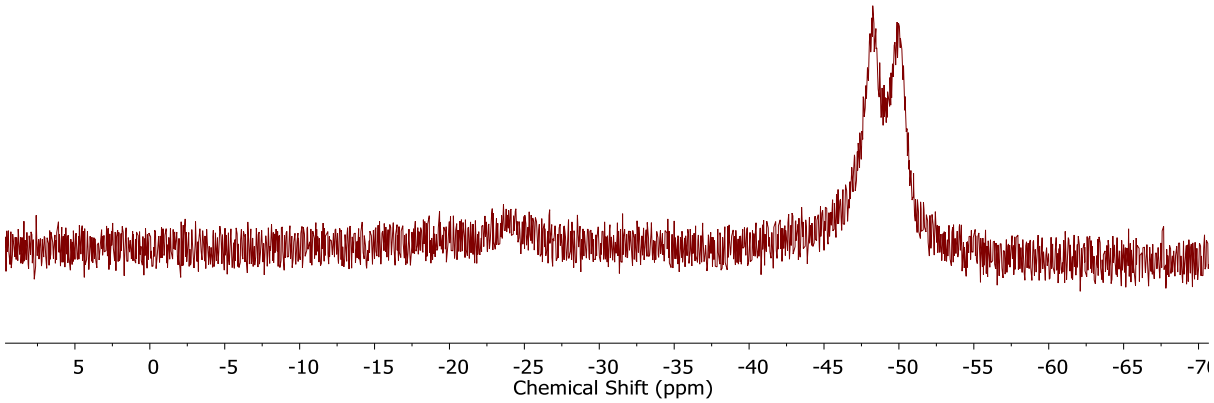

Figure S2.64 ^{31}P NMR spectrum (202 MHz, 25 °C, THF-d_8) of crosslinked poly(phenylphosphinoborane) swelled in THF-d_8.

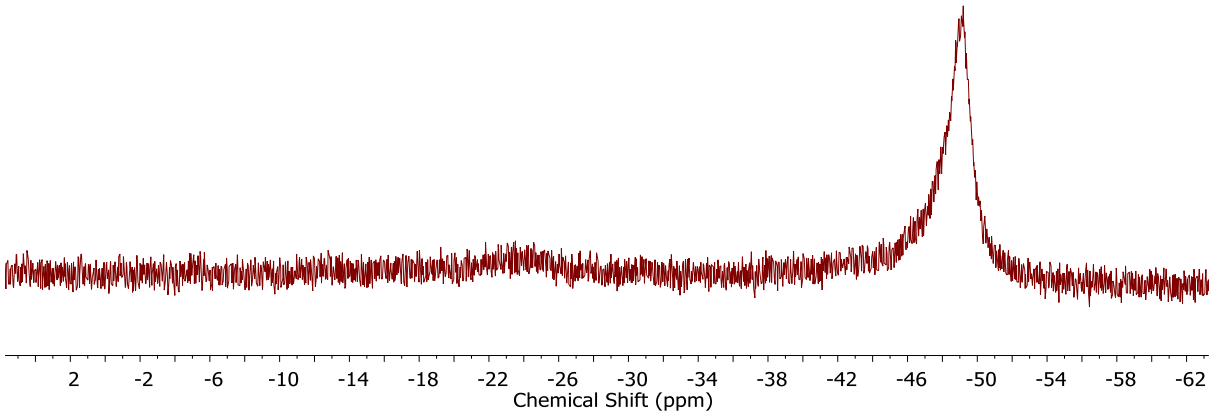

Figure S2.65 ^{31}P{H} NMR spectrum (202 MHz, 25 °C, THF-d_8) of crosslinked poly(phenylphosphinoborane) swelled in THF-d_8.

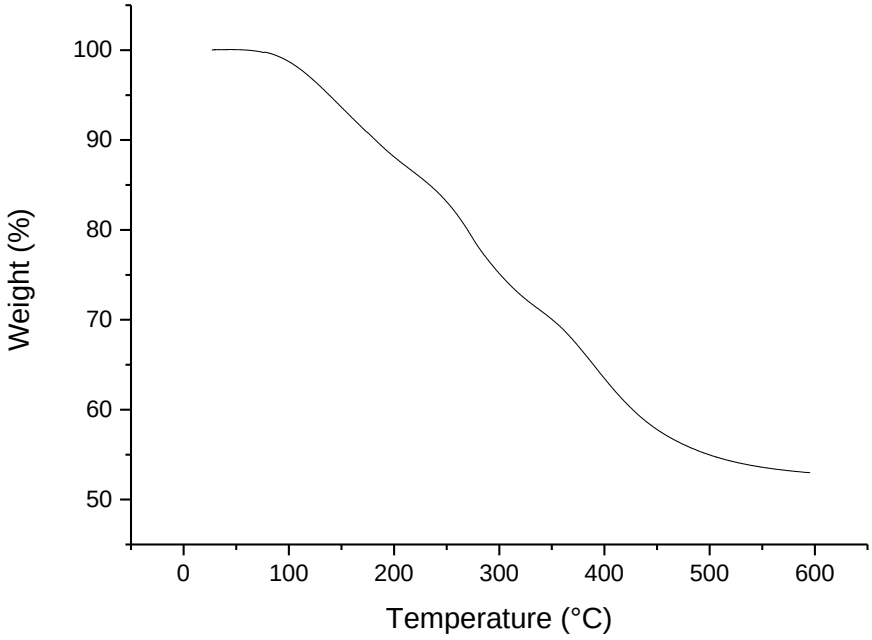

Figure S2.66 TGA thermogram of crosslinked poly(phenylphosphinoborane) (heating rate: 10 °C min^{-1}).

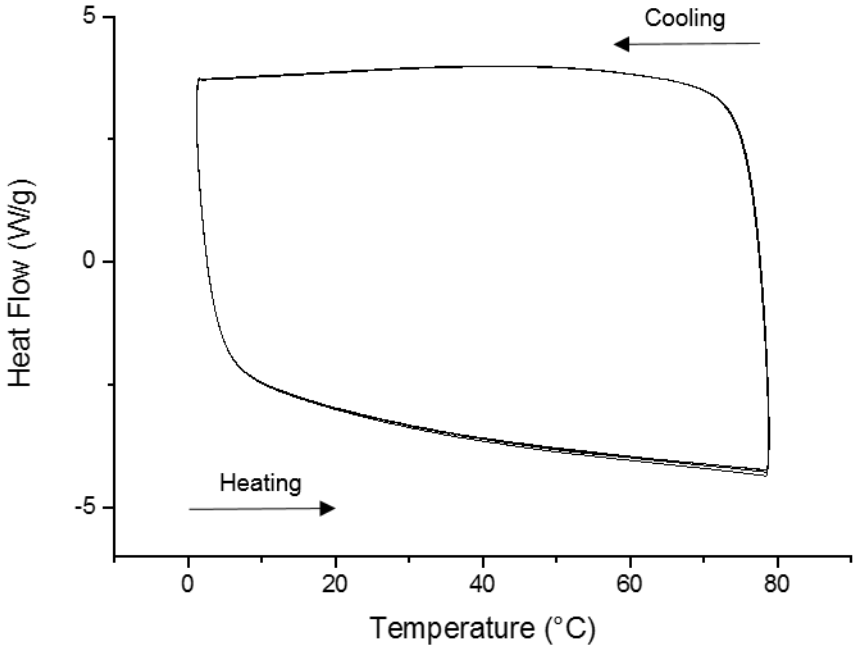

Figure S2.67 DSC thermogram of crosslinked poly(phenylphosphinoborane), first cycle excluded (heating rate: 10 °C min^{-1}).

Figure S2.68 Photograph of crosslinked poly(phenylphosphinoborane) after irradiation (left) and after drying under vacuum for 48 h (right).

2.5.5.3 Swellability of crosslinked poly(phenylphosphinoborane)

A sample of dry crosslinked poly(phenylphosphinoborane) was weighed (54 mg) and swelled in THF for 48 h. No coloration of the THF was observed after this time. Excess solvent was decanted away, and surface solvent removed by careful swabbing with a Kimwipe. After this, the sample was reweighed (114 mg) and the swellability in THF calculated (210% mass increase).

2.5.6 Synthesis of a water-soluble bottlebrush polymer

2.5.6.1 Synthesis and characterisation of bottlebrush polymer 2.6

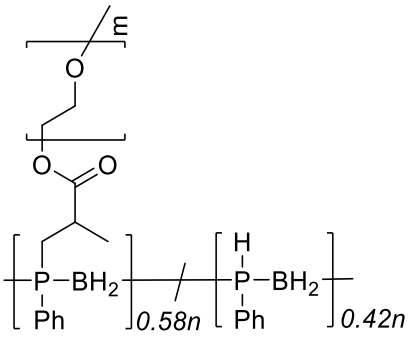

2.1 (244 mg, 2 mmol), poly(ethylene glycol) methyl ether methacrylate (average M_n = 950 g mol^{-1}, 1.90 g, 2 mmol), DMPA (51 mg, 0.2 mmol), TEMPO (31 mg, 0.2 mmol), and THF (5 mL) were added to a 14 mL vial equip with a magnetic stirrer. The resultant solution was irradiated ca. 3 cm away from a mercury lamp for 2 h. Volatiles were removed under vacuum and the resultant material was dissolved in water. The yellow solution obtained was transferred into a dialysis tube (Molecular weight cut off: 12,000 – 14,000 g mol^{-1}) and dialysis was performed against water for 48 h in order to remove excess poly(ethylene glycol) methyl ether methacrylate. No colouring of the medium outside the dialysis

tubing was observed. The yellow solution remaining inside the dialysis tubing was dried under vacuum at 40 °C for 48 h yielding **2.6** as an orange solid (grafting density: 0.58; yield: 0.93 g, 69%).

Spectroscopic data:

^{11}B NMR (128 MHz, $CDCl_3$) δ −34.6 (br s).

^{31}P NMR (162 MHz, $CDCl_3$) δ −24.2 (s, PhR*P*-BH_2), −48.9 (d, *J* = 352 Hz, PhH*P*-BH_2).

GPC (2 mg mL^{-1}) M_n = 156,000 g mol^{-1}, PDI = 1.3.

$T_{5\%}$ = 301 °C; ceramic yield = 2.4%; T_m (PEG side chains) = 40.0 °C.

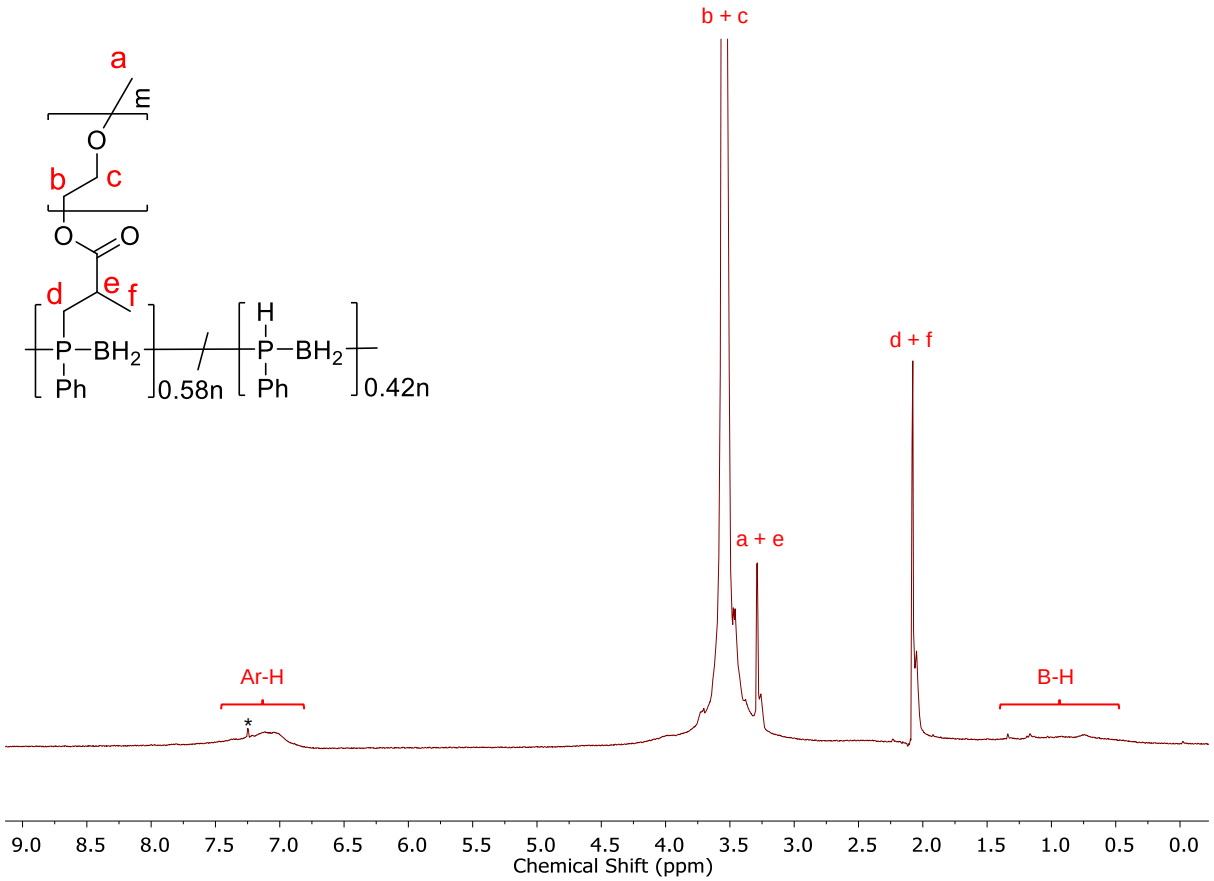

Figure S2.69 ^{1}H NMR spectrum (400 MHz, 25 °C, $CDCl_3$) of 2.6. Deuterated chloroform residual signal denoted by *.

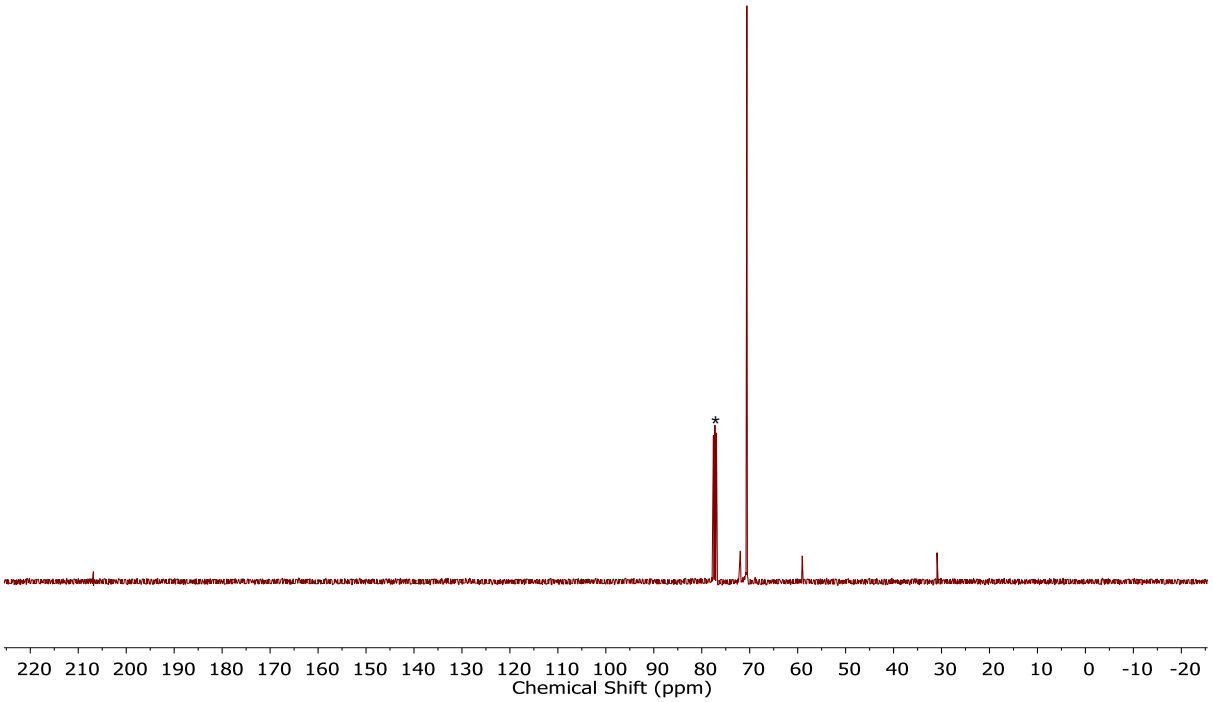

Figure S2.70 ^{13}C NMR spectrum (126 MHz, 25 °C, $CDCl_3$) of **2.6**. Deuterated chloroform residual signal denoted by *.

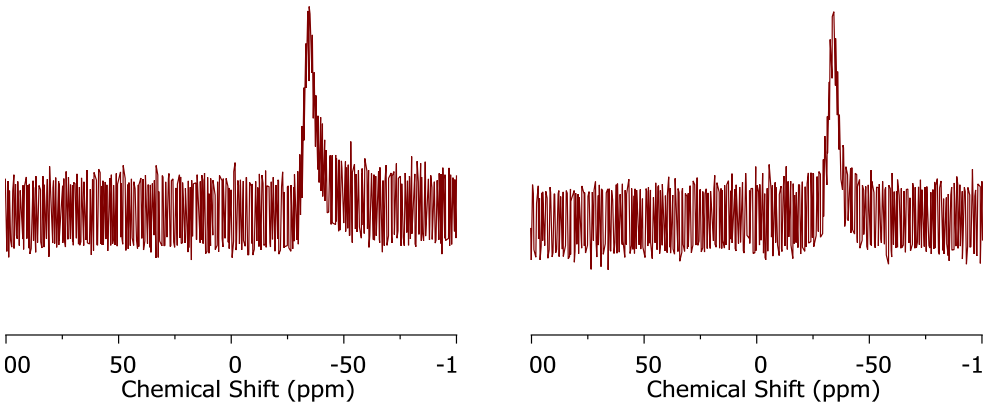

Figure S2.71 ^{11}B (left) and $^{11}B\{H\}$ NMR spectra (128 MHz, 25 °C, $CDCl_3$) of **2.6**.

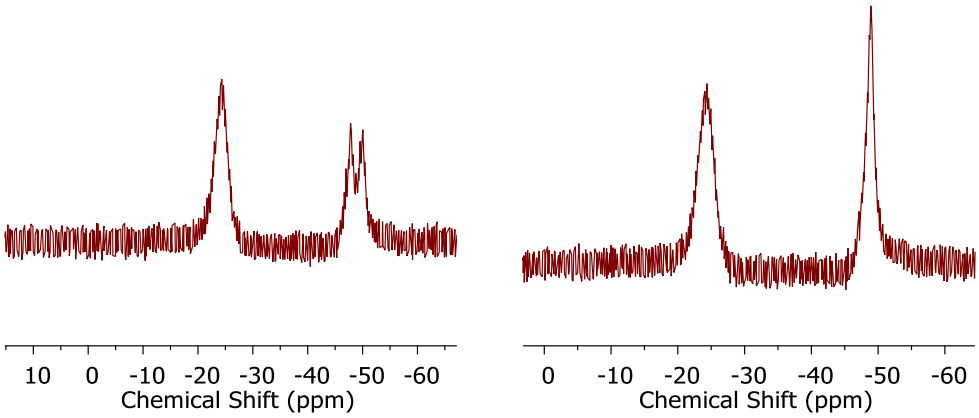

Figure S2.72 ^{31}P (left) and ^{31}P{H} (right) NMR spectra (162 MHz, 25 °C, $CDCl_3$) of **2.6**.

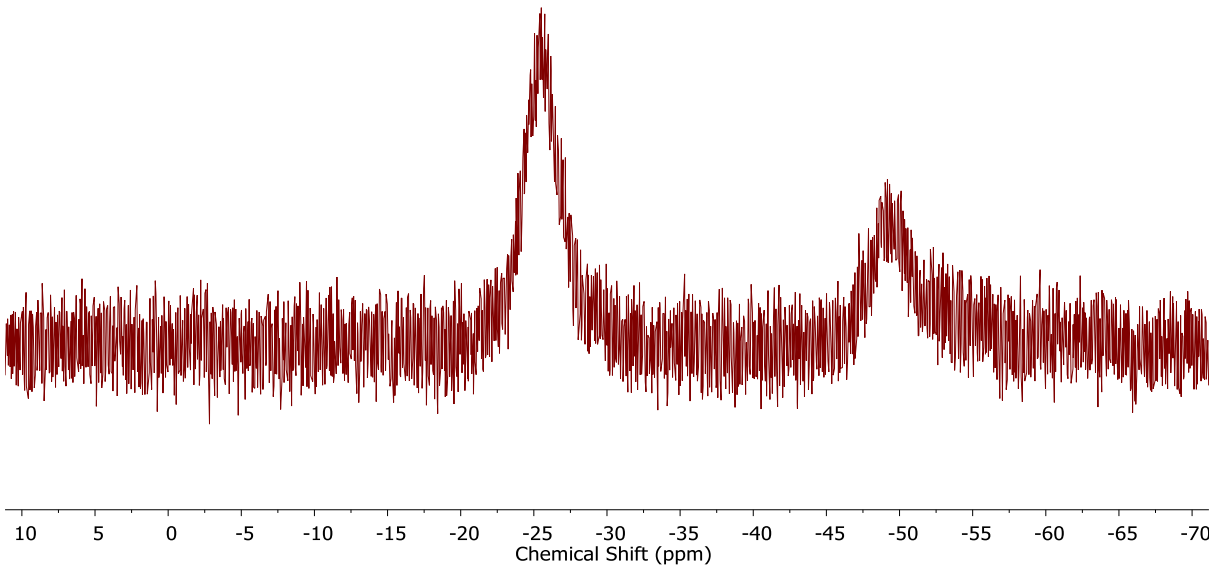

Figure S2.73 ^{31}P NMR spectrum (203 MHz, 25 °C, D_2O) of **2.6**. Peak broadening in D_2O prevents the observation of P-H coupling.

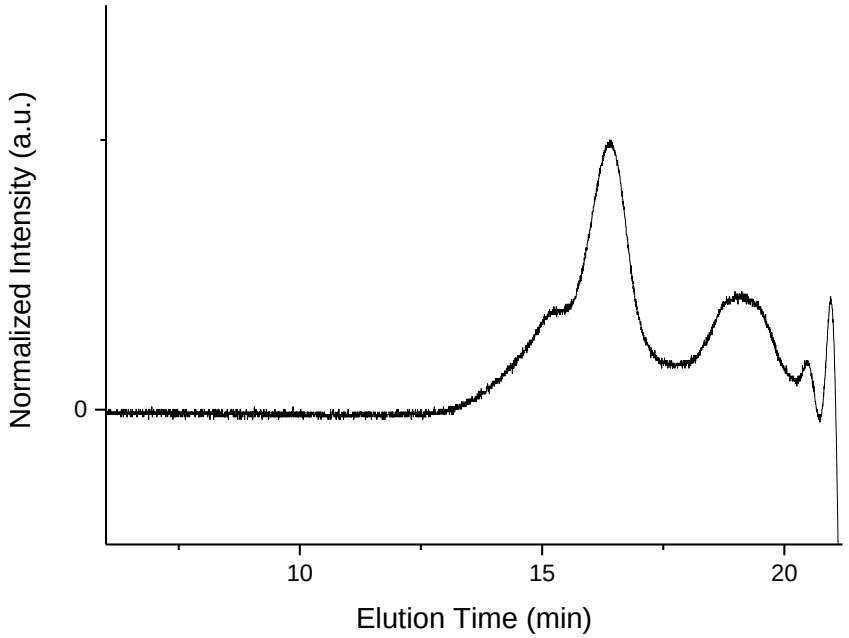

Figure S2.74 GPC chromatogram of **2.6** in THF (2 mg mL^{-1}, 0.1 w/w % *n*Bu$_4$NBr in the THF eluent).

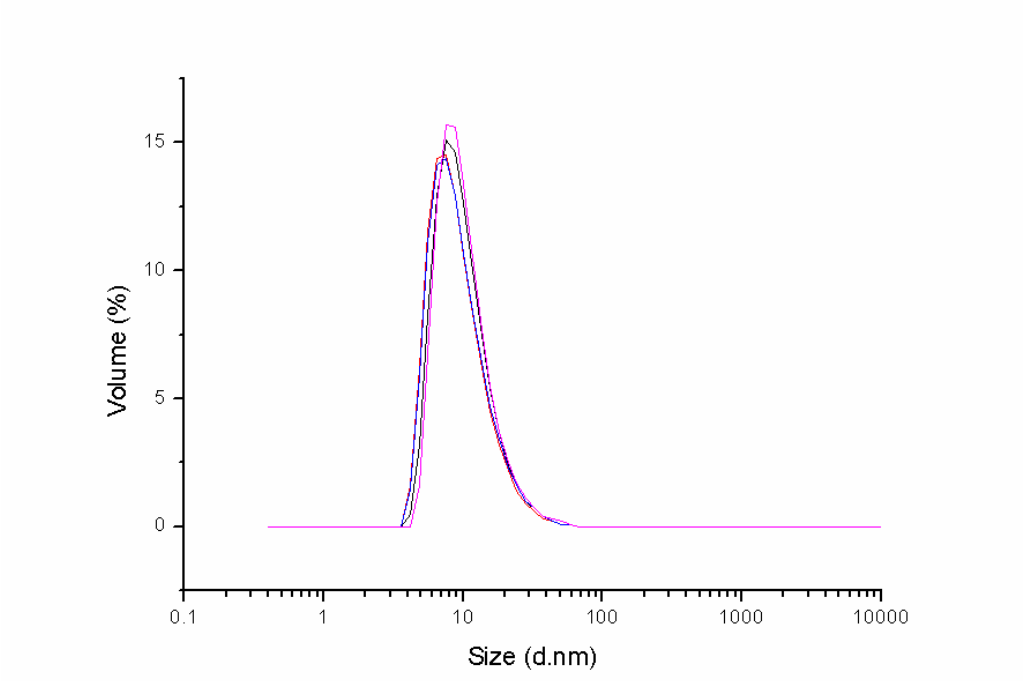

Figure S2.75 DLS size distribution by volume of **2.6** in THF (1 mg mL^{-1}). Multiple measurements in different colours show that the measured diameter is stable.

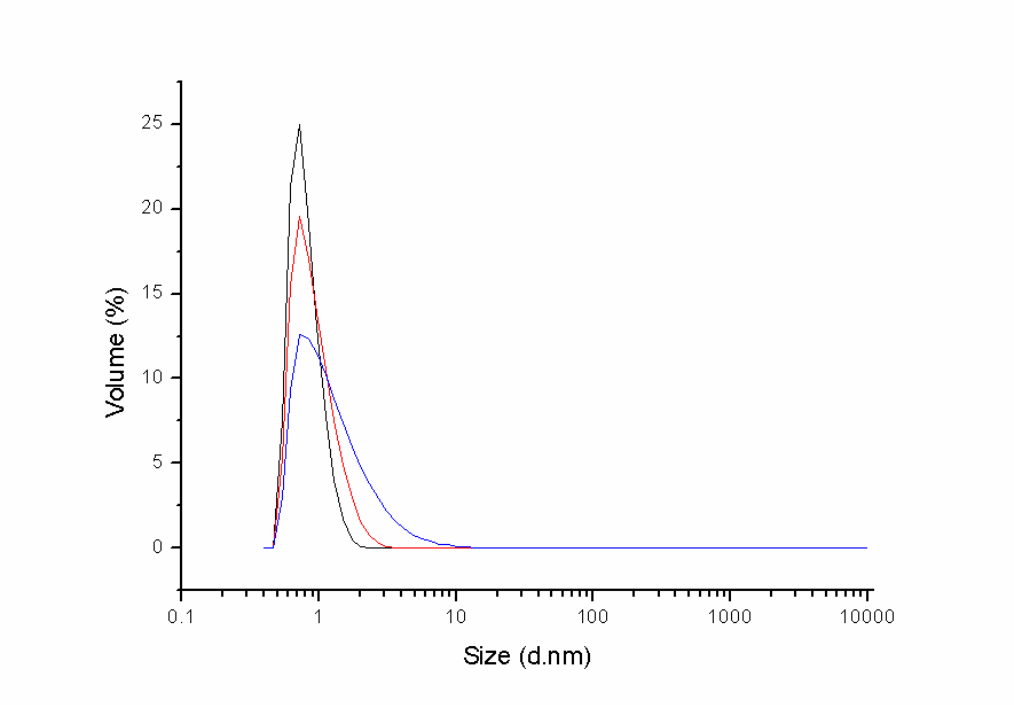

Figure S2.76 DLS size distribution by volume of poly(ethylene glycol) methyl ether methacrylate (average M_n 950 g mol^{-1}) in THF (1 mg mL^{-1}). Multiple measurements in different colours show that the measured diameter is stable.

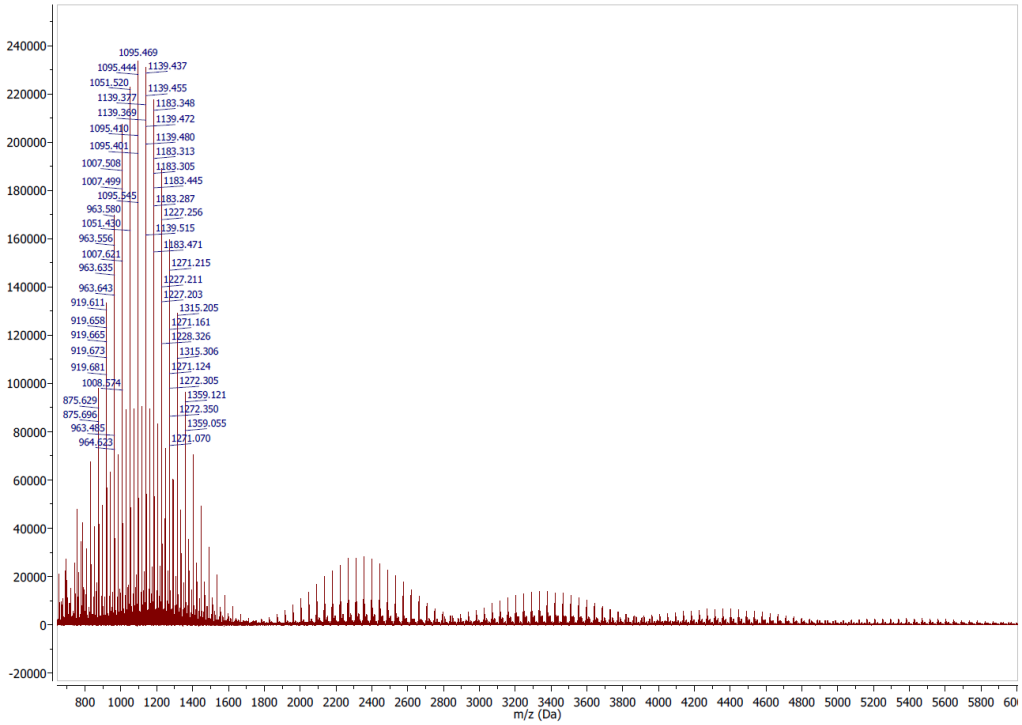

Figure S2.77 MALDI-MS spectrum of **2.6**. A complex spectrum is observed due to the presence of both a polymeric backbone and side chains. Each envelope arises from the distribution of molar mass of the poly(ethylene glycol) side chains (molar mass of repeat unit = 44.1 g mol^{-1}). Multiple envelopes are observed due to ionisation of the poly(phosphinoborane) main chain units ([PhRP-BH_2], R = $CH_2CH(CH_3)C(O)O[CH_2CH_2O]_mCH_3$, molar mass of repeat unit = 1072 g mol^{-1}).

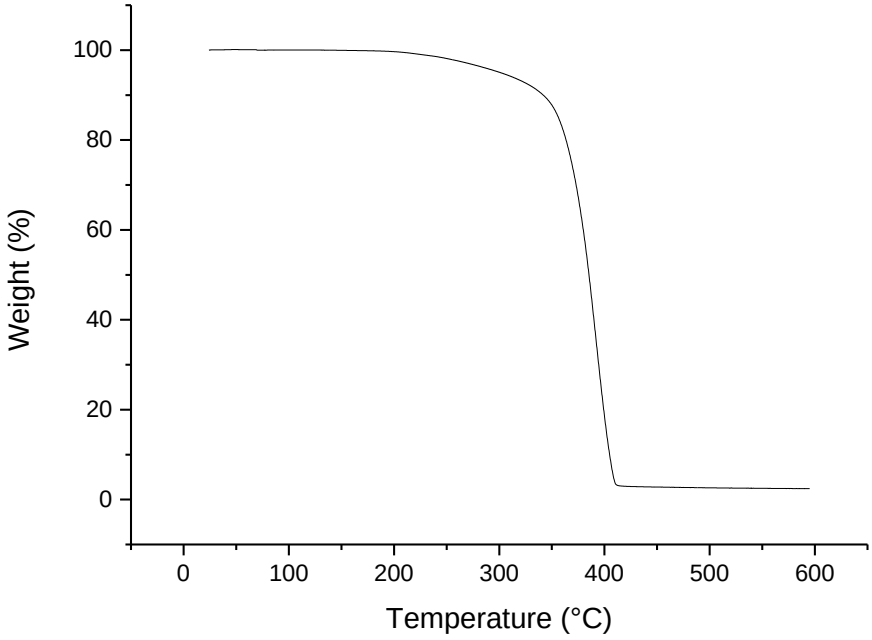

Figure S2.78 TGA thermogram of **2.6** (heating rate: 10 °C min^{-1}).

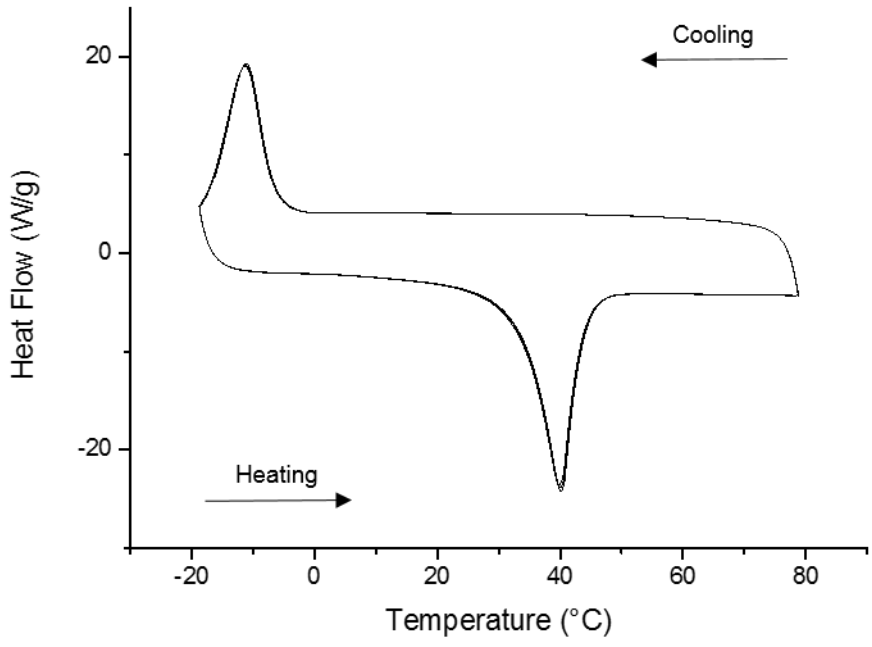

Figure S2.79 DSC thermogram of **2.6**, first cycle excluded (heating rate: 10 °C min^{-1}).

Figure S2.80 Photograph of isolated **2.6**.

2.6 References

1. Caminade, A.-M., *Chem. Soc. Rev.* **2016,** *45*, 5174-5186.
2. Yan, Y.; Zhang, J.; Ren, L.; Tang, C., *Chem. Soc. Rev.* **2016,** *45*, 5232-5263.
3. Hailes, R. L. N.; Oliver, A. M.; Gwyther, J.; Whittell, G. R.; Manners, I., *Chem. Soc. Rev.* **2016,** *45*, 5358-5407.
4. Priegert, A. M.; Rawe, B. W.; Serin, S. C.; Gates, D. P., *Chem. Soc. Rev.* **2016,** *45*, 922-53.
5. Monge, S.; Canniccioni, B.; Graillot, A.; Robin, J.-J., *Biomacromolecules* **2011,** *12*, 1973-1982.
6. Jäkle, F., *Chem. Rev.* **2010,** *110*, 3985-4022.
7. Baumgartner, T.; Réau, R., *Chem. Rev.* **2006,** *106*, 4681-4727.
8. Nunns, A.; Gwyther, J.; Manners, I., *Polymer* **2013,** *54*, 1269-1284.
9. Jäkle, F.; Vidal, F., *Angew. Chem. Int. Ed.* **2019,** *58*, 5846-5870.
10. Dorn, H.; Singh, R. A.; Massey, J. A.; Lough, A. J.; Manners, I., *Angew. Chem. Int. Ed.* **1999,** *38*, 3321-3323.
11. Dorn, H.; Singh, R. A.; Massey, J. A.; Nelson, J. M.; Jaska, C. A.; Lough, A. J.; Manners, I., *J. Am. Chem. Soc.* **2000,** *122*, 6669-6678.
12. Dorn, H.; Rodezno, J. M.; Brunnhöfer, B.; Rivard, E.; Massey, J. A.; Manners, I., *Macromolecules* **2003,** *36*, 291-297.
13. Clark, T. J.; Rodezno, J. M.; Clendenning, S. B.; Aouba, S.; Brodersen, P. M.; Lough, A. J.; Ruda, H. E.; Manners, I., *Chem. Eur. J.* **2005,** *11*, 4526-4534.
14. Jacquemin, D.; Lambert, C.; Perpète, E. A., *Macromolecules* **2004,** *37*, 1009-1015.
15. Nakhmanson, S. M.; Nardelli, M. B.; Bernholc, J., *Phys. Rev. Lett.* **2004,** *92*, 115504.
16. Han, D.; Anke, F.; Trose, M.; Beweries, T., *Coord. Chem. Rev.* **2019,** *380*, 260-286.
17. Staubitz, A.; Hoffmann, J.; Gliese, P., Group 13–Group 15 Element Bonds Replacing Carbon–Carbon Bonds in Main Group Polyolefin Analogs. In *Smart Inorganic Polymers*, Hey-Hawkins, E.; Hissler, M., Eds. Wiley-VCH: Weinheim, Germany, 2019; pp 17-39.
18. Schäfer, A.; Jurca, T.; Turner, J.; Vance, J. R.; Lee, K.; Du, V. A.; Haddow, M. F.; Whittell, G. R.; Manners, I., *Angew. Chem. Int. Ed.* **2015,** *54*, 4836-41.
19. Paul, U. S. D.; Braunschweig, H.; Radius, U., *Chem. Commun.* **2016,** *52*, 8573-8576.
20. Marquardt, C.; Jurca, T.; Schwan, K.-C.; Stauber, A.; Virovets, A. V.; Whittell, G. R.; Manners, I.; Scheer, M., *Angew. Chem. Int. Ed.* **2015,** *54*, 13782-13786.
21. Pandey, S.; Lönnecke, P.; Hey-Hawkins, E., *Eur. J. Inorg. Chem.* **2014**, 2456-2465.
22. Hooper, T. N.; Weller, A. S.; Beattie, N. A.; Macgregor, S. A., *Chem. Sci.* **2016,** *7*, 2414-2426.
23. Denis, J.-M.; Forintos, H.; Szelke, H.; Toupet, L.; Pham, T.-N.; Madec, P.-J.; Gaumont, A.-C., *Chem. Commun.* **2003**, 54-55.
24. Cavaye, H.; Clegg, F.; Gould, P. J.; Ladyman, M. K.; Temple, T.; Dossi, E., *Macromolecules* **2017,** *50*, 9239-9248.
25. Turner, J. R.; Resendiz-Lara, D. A.; Jurca, T.; Schäfer, A.; Vance, J. R.; Beckett, L.; Whittell, G. R.; Musgrave, R. A.; Sparkes, H. A.; Manners, I., *Macromol. Chem. Phys.* **2017,** *218*, 1700120.

26. Thoms, C.; Marquardt, C.; Timoshkin, A. Y.; Bodensteiner, M.; Scheer, M., *Angew. Chem.* **2013,** *125*, 5254-5259.
27. Thoms, C.; Marquardt, C.; Timoshkin, A. Y.; Bodensteiner, M.; Scheer, M., *Angew. Chem. Int. Ed.* **2013,** *52*, 5150-5154.
28. Stauber, A.; Jurca, T.; Marquardt, C.; Fleischmann, M.; Seidl, M.; Whittell, G. R.; Manners, I.; Scheer, M., *Eur. J. Inorg. Chem.* **2016**, 2684-2687.
29. Burg, A. B., *J. Inorg. Nucl. Chem.* **1959,** *11*, 258.
30. Wagner, R. I.; Caserio, F. F., *J. Inorg. Nucl. Chem.* **1959,** *11*, 259.
31. Burg, A. B.; Wagner, R. I. Phosphinoborine compounds and their preparation. Patent, U. S. 3071553, 1963.
32. Burg, A. B.; Wagner, R. I. Phosphinoborine compounds and their preparation. Patent, U. S. 2948689, 1960.
33. We have recently shown that treatment of P-disubstituted phosphine borane adducts with stoichiometric amounts of cyclic alkylaminocarbenes can give oligo- and polyphosphinoboranes with two organic groups at phosphorus. See: N. L. Oldroyd, S. C. Chitnis, V. T. Annibale, M. I. Arz, H. A. Sparkes, I. Manners; *Nat. Comm.* **2019**, 10, 1370.
34. Pouget, E.; Tonnar, J.; Lucas, P.; Lacroix-Desmazes, P.; Ganachaud, F.; Boutevin, B., *Chem. Rev.* **2010,** *110*, 1233-1277.
35. Ren, Z.; Yan, S., *Prog. Mater Sci.* **2016,** *83*, 383-416.
36. Rothemund, S.; Teasdale, I., *Chem. Soc. Rev.* **2016,** *45*, 5200-5215.
37. Banovetz, J. P.; Hsiao, Y. L.; Waymouth, R. M., *J. Am. Chem. Soc.* **1993,** *115*, 2540-2541.
38. Lee, P. T. K.; Skjel, M. K.; Rosenberg, L., *Organometallics* **2013,** *32*, 1575-1578.
39. Kato, N.; Tamura, Y.; Kashiwabara, T.; Sanji, T.; Tanaka, M., *Organometallics* **2010,** *29*, 5274-5282.
40. Lee, P. T. K.; Rosenberg, L., *Dalton Trans.* **2017,** *46*, 8818-8826.
41. Zechel, D. L.; Hultzsch, K. C.; Rulkens, R.; Balaishis, D.; Ni, Y.; Pudelski, J. K.; Lough, A. J.; Manners, I.; Foucher, D. A., *Organometallics* **1996,** *15*, 1972-1978.
42. Lunn, D. J.; Boott, C. E.; Bass, K. E.; Shuttleworth, T. A.; McCreanor, N. G.; Papadouli, S.; Manners, I., *Macromol. Chem. Phys.* **2013,** *214*, 2813-2820.
43. Gauthier, M. A.; Gibson, M. I.; Klok, H.-A., *Angew. Chem. Int. Ed.* **2009,** *48*, 48-58.
44. Allcock, H. R., *Soft Matter* **2012,** *8*, 7521-7532.
45. Allcock, H. R., *J. Polym. Sci.* **1983,** *70*, 71-77.
46. Allcock, H. R., *Chem. Mater.* **1994,** *6*, 1476-1491.
47. Liu, X.; Tian, Z.; Chen, C.; Allcock, H. R., *Macromolecules* **2012,** *45*, 1417-1426.
48. Rosenberg, L., *ACS Catal.* **2013,** *3*, 2845-2855.
49. Bange, C. A.; Waterman, R., *Chem. Eur. J* **2016,** *22*, 12598-12605.
50. Guterman, R.; Rabiee Kenaree, A.; Gilroy, J. B.; Gillies, E. R.; Ragogna, P. J., *Chem. Mater.* **2015,** *27*, 1412-1419.
51. Béland, V. A.; Wang, Z.; Sham, T.-K.; Ragogna, P. J., *Angew. Chem. Int. Ed.* **2018,** *57*, 13252-13256.
52. Mimeau, D.; Delacroix, O.; Gaumont, A.-C., *Chem. Commun.* **2003**, 2928-2929.
53. Yousif, E.; Haddad, R. J. S., *SpringerPlus* **2013,** *2*, 398.
54. Staubitz, A.; Sloan, M. E.; Robertson, A. P. M.; Friedrich, A.; Schneider, S.; Gates, P. J.; Schmedt auf der Günne, J.; Manners, I., *J. Am. Chem. Soc.* **2010,** *132*, 13332-45.
55. Colebatch, A. L.; Weller, A. S., *Chem. Eur. J.* **2019,** *25*, 1379-1390.
56. Georges, M. K.; Veregin, R. P. N.; Kazmaier, P. M.; Hamer, G. K., *Macromolecules* **1993,** *26*, 2987-2988.
57. Hawker, C. J.; Bosman, A. W.; Harth, E., *Chem. Rev.* **2001,** *101*, 3661-3688.
58. Goto, A.; Ohtsuki, A.; Ohfuji, H.; Tanishima, M.; Kaji, H., *J. Am. Chem. Soc.* **2013,** *135*, 11131-11139.
59. Mucci, V.; Vallo, C., *J. Appl. Polym. Sci.* **2011,** *123*, 418-425.
60. Hawker, C. J., *J. Am. Chem. Soc.* **1994,** *116*, 11185-11186.
61. Heurich, T.; Qu, Z.-W.; Nožinović, S.; Schnakenburg, G.; Matsuoka, H.; Grimme, S.; Schiemann, O.; Streubel, R., *Chem. Eur. J.* **2016,** *22*, 10102-10110.
62. Verduzco, R.; Li, X.; Pesek, S. L.; Stein, G. E., *Chem. Soc. Rev.* **2015,** *44*, 2405-2420.

63. Bourumeau, K.; Gaumont, A.-C.; Denis, J.-M., *J. Organomet. Chem.* **1997,** *529*, 205-213.
64. Liston, D. J.; Lee, Y. J.; Scheidt, W. R.; Reed, C. A., *J. Am. Chem. Soc.* **1989,** *111*, 6643-6648.

Chapter 3

Investigations into the iron-catalysed dehydropolymerisation of phenylphosphine-borane and the synthesis of polyphosphinoboranes using non-metal precatalysts

3.1 Abstract

Although a range of precatalysts are known to facilitate the transition metal-mediated dehydropolymerisation of primary phosphine-borane monomers, the materials produced are often highly polydisperse or possess multimodal molar mass distributions, and mechanistic insight is often severely lacking. Herein we describe detailed studies of the dehydropolymerisation of phenylphosphine-borane ($PhH_2P{\cdot}BH_3$) using $CpFe(CO)_2OTf$ (OTf = CF_3SO_3) as a precatalyst in solution at 80 – 150 °C. We were able to significantly increase the proportion of high molar mass polymer produced compared to previously reported conditions by increasing the reaction concentration to 4 M. Studies into the effect of conversion on the molar mass of the resulting polymer suggest that the reaction proceeds via a combination of chain-growth and step-growth mechanisms rather than the purely chain-growth pathway that was previously postulated based on preliminary results. Triflic acid released from the precatalyst appears to be involved in this hybrid mechanism. Investigations into the effect of conversion on molar mass using $CpFe(CO)_2R$ (R = OTf, I, $PPhHBH_3$) and TfOH precatalysts, and studies into the reaction of oligophosphinoboranes with these precatalysts have aided our understanding of the polymerisation mechanism. Triflic acid or 1,8-bis(dimethylamino)naphthalene (proton sponge®) were found to be active precatalysts for the polymerisation of $PhH_2P{\cdot}BH_3$ in solution providing a catalytic metal-free route to these macromolecules giving polymer with $M_n \approx 5{,}000$ g mol^{-1} and PDI = 2.2 – 2.4. Triflic acid was also found to be a proficient precatalyst for the polymerisation of

tert-butylphosphine-borane; however, sluggish reaction rates and the formation of by-products hinder the dehydrocoupling of *n*-hexyl- and diethylphosphine-borane.

3.2 Introduction

Polymers containing inorganic elements in their main chains are of growing interest owing to their fascinating properties, such as high thermooxidative stability, low temperature elasticity, flame retardancy, and optoelectronic tunability, many of which are challenging to access for all-organic polymers.[1-6] Despite the many potential uses of inorganic polymers, the field remains in a state of infancy compared to organic polymer chemistry. Catalytic routes to organic polymers have been extensively developed as evidenced by the award of a Nobel prize for the development of the synthesis of polyolefins.[7] The controlled synthesis of a wide range of organic polymers has been facilitated by the development of a number of different methods to form C-C[8-10] and C-E bonds (E = O, N, Si, B etc);[11-14] however, the use of similar methods to form bonds between main group elements remains a significant challenge.[15]

Traditional routes to inorganic polymers involve reductive coupling and ring-opening polymerisations, and while these routes allow the formation of a number of interesting inorganic polymer classes such as polysiloxanes $[R_2SiO]_n$,[16, 17] polysilanes $[R_2Si]_n$,[18, 19] and polyphosphazenes $[R_2PN]_n$,[20, 21] they frequently suffer from a number of limitations including poor functional group tolerance, low atom efficiency, and the formation of toxic by-products. More recently, catalytic methods to form bonds between main group elements have been developed.[15] Of particular note are dehydrogenative coupling reactions which have been reported as a general, atom economic tool in the formation of bonds between main group elements.[18, 22, 23] This has provided a route to interesting inorganic polymers such as polyaminoboranes $[RHN\text{-}BH_2]_n$ and polyphosphinoboranes $[RR'P\text{-}BH_2]_n$.[24] These macromolecules consist of main chains formed of alternating group 13 and 15 elements and are formally isoelectronic to polyolefins but possess vastly different properties owing to the presence of inorganic *p*-block elements in the polymer main chains.[25]

The synthesis of high molar mass polyphosphinoboranes were first reported by our group in 1999 via rhodium catalysed dehydrocoupling of phenylphosphine-borane ($PhH_2P{\cdot}BH_3$).[26, 27] The potential use of

polyphosphinoboranes as precursors to PB semiconductor-based ceramics, etch-resists, flame-retardant materials, and as piezoelectrics has fuelled significant scientific interest in these macromolecules, resulting in the development of a number of routes to P-monosubstituted polyphosphinoboranes $[RHP\text{-}BH_2]_n$ where R is an alkyl or aryl substituent using Rh, Ir or Fe precatalysts (Scheme 3.1 a);[28-39] metal-free dehydropolymerisation using a stoichiometric amount of cyclic(alkyl)(amino)carbenes (CAACs) as hydrogen acceptors (Scheme 3.1 b);[40] or thermally-induced Lewis-base elimination routes (Scheme 3.1 c).[41, 42] The development of catalytic metal-free routes to polyphosphinoboranes remains an important target for polymer chemists. To date, the only reported non-metal catalysed route to oligophosphinoboranes made use of tris(pentafluorophenyl)borane ($B(C_6F_5)_3$) as a precatalyst; however, this gave a multimodal molar mass material (M_w = 3,900 and 800 g mol^{-1}) (Scheme 3.1d).[43]

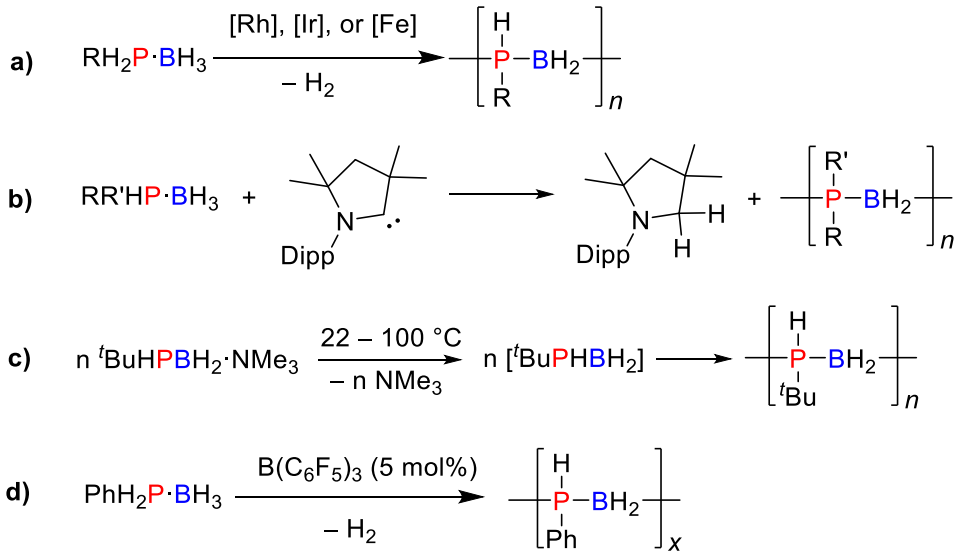

Scheme 3.1 Selected routes to polyphosphinoboranes.

While a number of routes to polyphosphinoboranes have been reported, mechanistic understanding of these polymerisations is often incomplete. Whereas the monomer used in the formation of isoelectronic polyolefins is a stable alkene, polyphosphinoboranes are made up of phosphinoborane monomer units which have only been isolated as molecular species when stabilised by bulky groups on either phosphorus or boron.[44-46] Any precatalyst must be capable of facilitating the loss of hydrogen from the phosphine-borane precursor while also mediating P-B coupling events if this takes place on-metal.[24] Another possibility is the in situ formation of free phosphinoborane by dehydrogenation of a phosphine-borane precursor which will then undergo spontaneous polymerisation.[40] The presence of different

potential pathways to polyphosphinoboranes makes it challenging to obtain a full mechanistic picture of the polymerisation process. Furthermore, several of the reported systems for the formation of polyphosphinoboranes take place in the melt and/or at elevated temperatures, hindering mechanistic insight. For the control of the dehydropolymerisation process and design of improved catalytic systems, a deeper understanding of the fundamental steps that take place in catalysis is essential.

We recently reported the synthesis of poly(phenylphosphinoborane), $[PhHP\text{-}BH_2]_n$ using the precatalyst $CpFe(CO)_2OTf$.[32] Subsequently, this precatalyst has been shown to be proficient in the catalysis of a number of P-monosubstituted phosphine-boranes featuring either alkyl or aryl side groups.[37, 47, 48] This catalytic system has a number of advantages over many of the previously reported systems. The catalysis takes place in toluene rather than the melt allowing for more detailed reaction monitoring. It also makes use of earth abundant iron and gives mostly linear high molar mass material (although formation of a low molar mass fraction was also observed). Some preliminary experimental and computational studies suggested that this polymerisation operates via a homogeneous chain-growth coordination-type mechanism. It was suggested that loss of CO and TfOH initially occurs giving a phosphido-borane iron complex which facilitates B-H/P-H activation and P-B coupling via multiple σ-complex assisted metathesis steps (Scheme 3.2).[49]

In this chapter, we report our investigations into the polymerisation of $PhH_2P{\cdot}BH_3$ using $CpFe(CO)_2OTf$ and related species, and the consequences of these findings on the mechanism previously postulated. Furthermore, we report the synthesis of $[PhHP\text{-}BH_2]_n$ using simple p-block non-metal catalysts and the dehydrocoupling of alkyl phosphine-boranes using triflic acid.

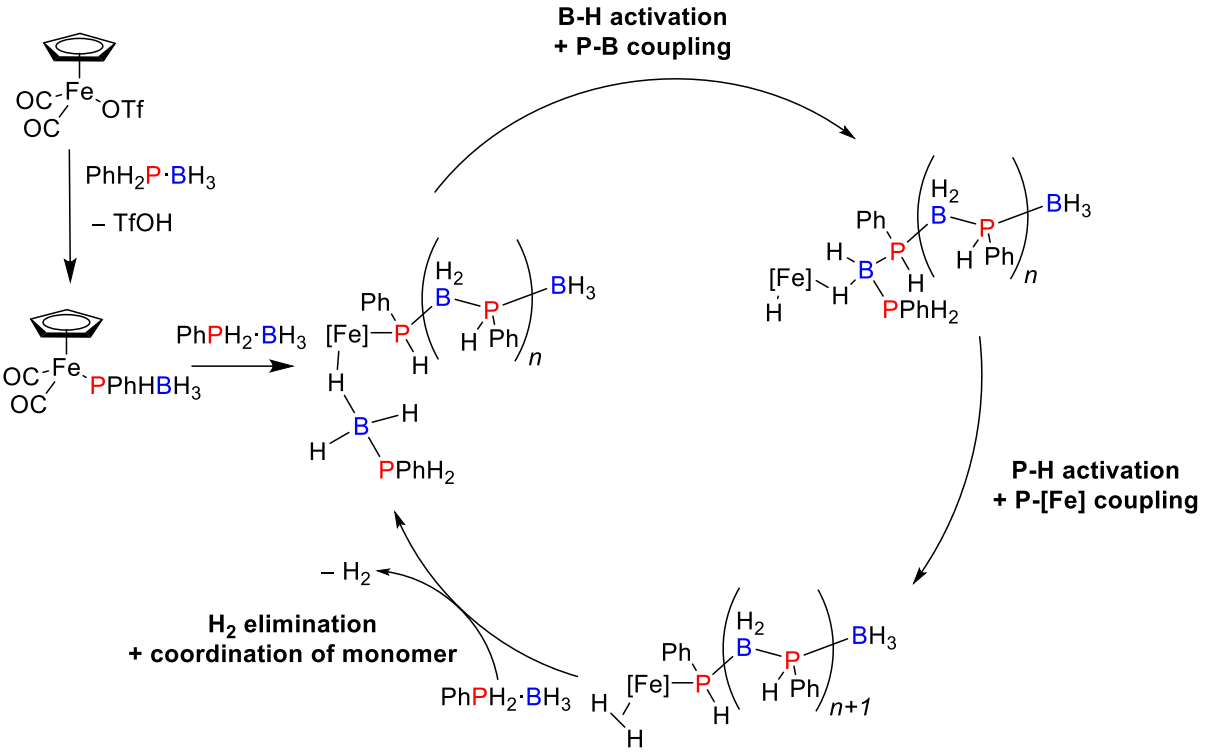

Scheme 3.2 Proposed mechanism for the dehydropolymerisation of $PhH_2P{\cdot}BH_3$.[32]

3.3 Results and discussion

3.3.1 Investigations into the effect of changing reaction conditions on the polymerisation of phenylphosphine-borane using a $CpFe(CO)_2OTf$ precatalyst

The polymerisation of $PhH_2P{\cdot}BH_3$ using $CpFe(CO)_2OTf$ (0.1 – 10 mol%) in toluene or dioxane (0.8 M) at 100 °C for 24 h has previously been reported by our group.[32] When the formed poly(phenylphosphinoborane), $[PhHP\text{-}BH_2]_n$ was analysed by NMR spectroscopy, a broad doublet was observed in the ^{31}P NMR spectrum at ca. −49 ppm (Figure 3.1), and a broad singlet at ca. −35 ppm in the ^{11}B NMR spectrum. According to gel permeation chromatography (GPC) analysis, the material produced has a bimodal molar mass distribution with a significant amount of low molar mass polymer (M_n = 2,000 g mol^{-1}) formed along with a high molar mass fraction (M_n = 59,000 g mol^{-1}, Figure 3.2, 0.8 M). The formation of monomodal product is desirable for further utility of polyphosphinoboranes in a range of applications, for example, in post polymerisation modification of these polymers and crosslinking to form gels (see Chapters 2 and 4 respectively). Furthermore, although a preliminary mechanism has been postulated,[32] there is much scope to fully understand how this mechanism operates and the role that other components of the reaction mixture have in the polymerisation e.g. triflic acid liberated from the iron precatalyst.

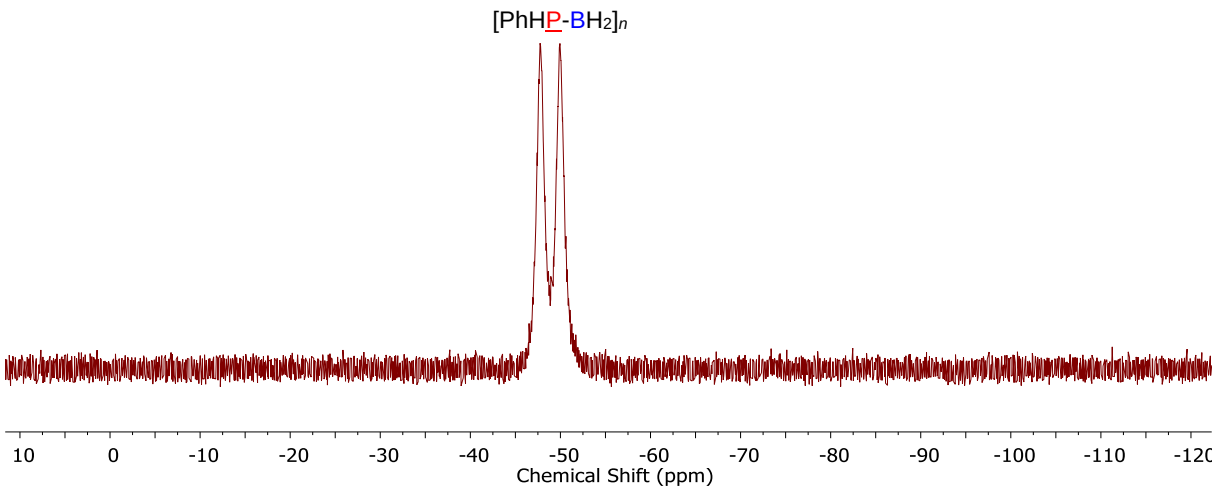

Figure 3.1 ^{31}P NMR (122 MHz, 25 °C, $CDCl_3$) spectrum of $[PhHP\text{-}BH_2]_n$ synthesised using previously reported conditions ($CpFe(CO)_2OTf$ (1 mol%), toluene, 0.8 M, 100 °C, 24 h).[32]

Initially, reactions were undertaken to investigate reaction conditions using the following general procedure: $CpFe(CO)_2OTf$ (1 mol%) was added to $PhH_2P{\cdot}BH_3$ (2 mmol), and the mixture was dissolved in the solvent and stirred at room temperature for 5 min. The reaction mixture was heated to the specified temperature under a positive pressure of nitrogen. After workup, the polymers were analysed by ^{11}B and ^{31}P NMR spectroscopy and unless stated otherwise, all NMR data matched that previously reported.[32] The materials were also analysed by GPC to obtain molar masses and polydispersity indices (PDIs) by comparison to polystyrene standards.

3.3.1.1 Effect of reaction concentration on the polymerisation of $PhH_2P{\cdot}BH_3$ using $CpFe(CO)_2OTf$

We examined the effect of three initial substrate concentrations (0.1 M, 2 M, and 4 M) on the polymerisation of $PhH_2P{\cdot}BH_3$ (Figure 3.2) in toluene 100 °C for 24 h. Complete monomer consumption was observed in each reaction within 24 h determined by ^{11}B NMR spectroscopy. For comparison, the GPC chromatogram for $[PhHP\text{-}BH_2]_n$ using conditions outlined in previously published work is also shown below (Figure 3.2, 0.8 M).[32] Reaction at 0.8 M resulted in formation of high molar mass polymer with M_n = 59,000 g mol^{-1} (PDI = 1.6); however, a significant amount of low molar mass material (≈ 2,000 g mol^{-1}) was also produced.

We observed an increase in the ratio of high molar mass polymer to lower molar mass material when higher reaction concentrations are used. An increase in molar mass of this high molar mass fraction (M_n = 74,000 g mol^{-1}) was also observed at substrate concentrations of 2 M or 4 M (M_n = 74,000 and

69,000 g mol^{-1} respectively) compared to reaction 0.8 M (M_n = 59,000 g mol^{-1}). Reaction at very low concentration (0.1 M) results in the formation of mainly low molar mass material. Due to the improvement in the amount of high molar mass fraction at higher concentration, all subsequent investigations were carried out at a concentration of 4 M unless stated otherwise.

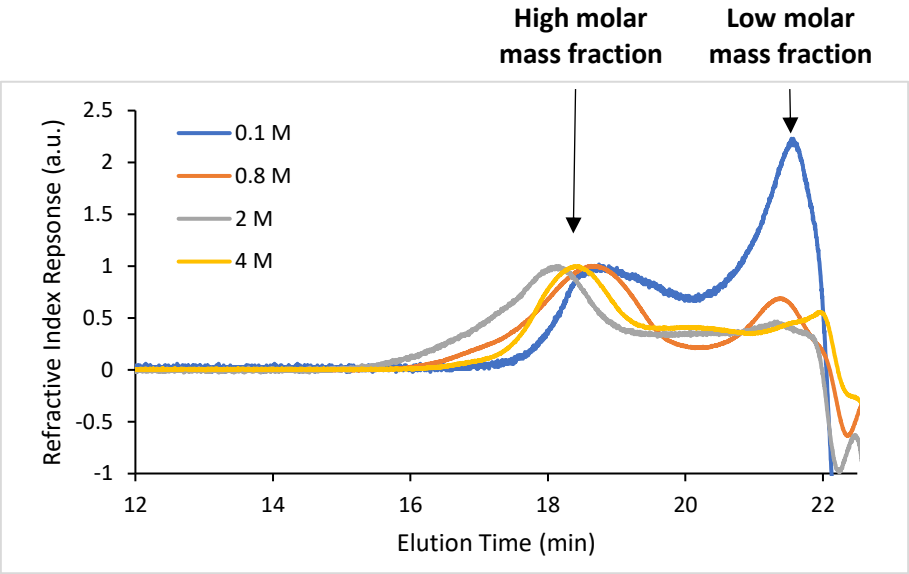

Figure 3.2 GPC chromatograms (2 mg mL^{-1} in THF, 0.1 w/w % nBu$_4$NBr in the THF eluent) showing the effect of changing reaction concentration on the molar mass of [PhHP-BH$_2$]$_n$. Conditions: PhH$_2$P·BH$_3$ (2 mmol), CpFe(CO)$_2$OTf (1 mol%), toluene, 100 °C, 24 h.

3.3.1.2 Effect of reaction temperature on the polymerisation of PhH$_2$P·BH$_3$ using CpFe(CO)$_2$OTf

We next sought to examine the effect of temperature on the polymerisation. We reasoned that by performing this reaction at 80 °C rather than 100 °C, any potential competing thermal non-catalysed dehydrocoupling may be avoided. We found that when the reaction temperature was reduced to 80 °C, the molar mass of the polymer formed decreased significantly (M_n = 18,000 g mol^{-1}) compared to when the reaction was carried out at 100 °C (72,000 g mol^{-1}; Figure 3.3). Attempts to lower the polymerisation temperature to 60 °C resulted in no reaction taking place. We also investigated the effect of increasing reaction temperature to above 100 °C. This required the use of a solvent with a higher boiling point than toluene. Mesitylene was chosen because it has similar properties to toluene but boils at 165 °C. When the polymerisation was carried out at 150 °C in mesitylene, PhH$_2$P·BH$_3$ was consumed within 1 h (determined by ^{11}B NMR spectrometry) forming a material with a M_n = 95,500 g mol^{-1}, but with a higher PDI (1.92). A significant shoulder of high molar mass was observed in the GPC chromatogram.

The material was also found to be sparingly soluble in THF and chloroform. Together, these observations indicate the formation of cross-linked material.

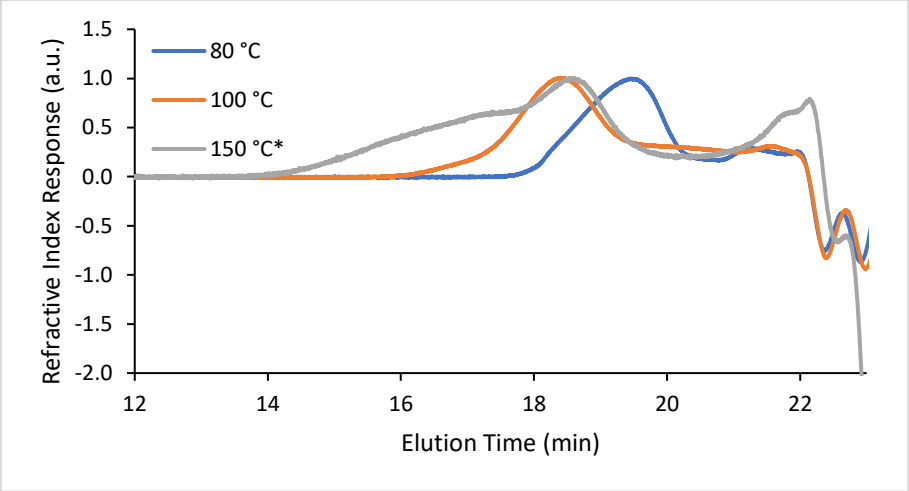

Figure 3.3 GPC chromatograms (2 mg mL^{-1} in THF, 0.1 w/w % *n*Bu$_4$NBr in the THF eluent) showing the effect of changing reaction temperature on the molar mass of [PhHP-BH$_2$]$_n$. Conditions: PhH$_2$P·BH$_3$ (2 mmol), CpFe(CO)$_2$OTf (1 mol%), toluene, 4 M, 24 h. *CpFe(CO)$_2$OTf (1 mol%), mesitylene, 4 M, 1 h.

3.3.1.3 Effect of solvent on the polymerisation of PhH$_2$P·BH$_3$ using CpFe(CO)$_2$OTf

Experiments to investigate the effect of solvent were performed at 80 °C as many of the solvents we used boil at temperatures between 80 °C and 100 °C. We examined the effect of changing the solvent from toluene to 1,2-difluorobenzene, 1,2-dimethoxyethane (DME), 1,4-dioxane, and acetonitrile. The reaction in acetonitrile was unsuccessful; the ^{31}P NMR spectrum did not show any diagnostic doublet at around −50 ppm which corresponds to [PhHP-BH$_2$]$_n$, nor a triplet at around −50 ppm which would indicate that starting material remained. Instead a single triplet was observed at −122.8 ppm indicating dissociation of PhH$_2$P·BH$_3$ to PPhH$_2$. A number of unassigned peaks were observed in the ^{11}B NMR spectrum.

The GPC chromatograms for experiments using 1,2-difluorobenzene, DME, 1,4-dioxane, and toluene are shown below (Figure 3.4). Toluene and 1,4-dioxane gave rise to a similar ratio of high molar mass polymer to oligomers, although dioxane resulted in the formation of slightly higher molar mass material (1,4 dioxane: M_n = 25,000 g mol^{-1}, toluene: M_n = 18,000). The use of DME resulted in a higher amount of oligomeric material forming. 1,2-Difluorobenzene gave the highest polymer to oligomer ratio; however, the lowest molar mass polymer is formed using this solvent (M_n = 16,000 g mol^{-1}), and incomplete reaction was observed (only around 70% of monomer was consumed after 24 h) and so this

is not an optimum solvent for the polymerisation. These results suggest that increasing solvent polarity has a negative effect on the polymerisation, either retarding the reaction in the case of 1,2-difluorobenzene; or resulting in the formation of more oligomeric material when DME is used.

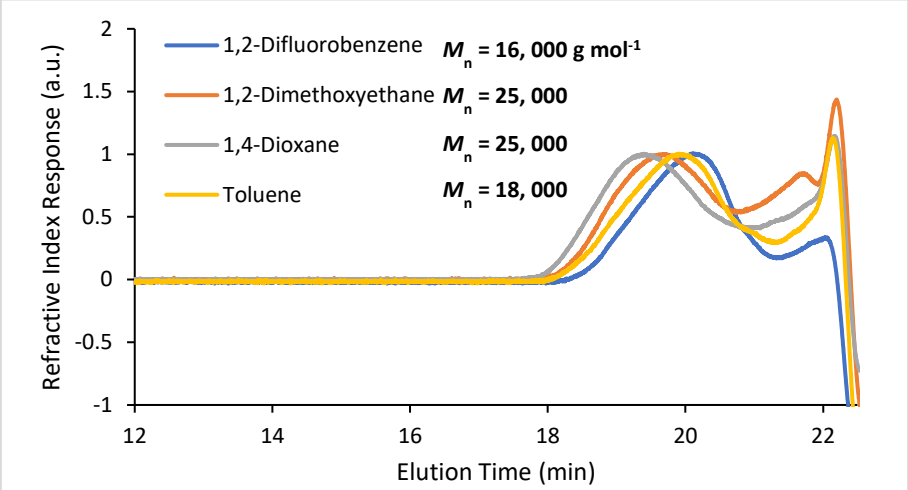

Figure 3.4 GPC chromatograms (2 mg mL^{-1} in THF, 0.1 w/w % *n*Bu$_4$NBr in the THF eluent) showing the effect of changing reaction solvent on the molar mass of [PhHP-BH$_2$]$_n$. Conditions: PhH$_2$P·BH$_3$ (2 mmol), CpFe(CO)$_2$OTf (1 mol%), 80˚C, 4 M, 24 h.

3.3.1.4 Molar mass dependence on reaction time for the polymerisation of PhH$_2$P·BH$_3$ using CpFe(CO)$_2$OTf

Lastly, in our studies to optimise the polymerisation of PhH$_2$P·BH$_3$ to form uniform high molar mass material, we sought to examine the effect of time on the polymerisation. At a concentration of 4 M, the reaction is significantly faster than previously reported, with complete consumption of the monomer within 4 h determined by ^{11}B NMR spectroscopy. Previously, the polymerisation was postulated to operate via a chain-growth mechanism because high molar mass material is formed at low conversion. GPC analysis of reaction aliquots taken between 0.5 h and 3 h supports this previous hypothesis as high molar mass polymer (ca. 27,000 g mol^{-1}) is observed at low conversion (Figure 3.5). However, characterisation of the material obtained after 24 h revealed a further increase in molar mass (77,000 g mol^{-1}). We therefore sought to study the molar mass of material obtained from a time period corresponding to high monomer consumption (2 – 24 h). GPC chromatograms of aliquots taken during this time frame are shown below (Figure 3.6). From these results, it is clear that there is continued polymer growth after complete consumption of the monomer. From 4 h (after monomer has been consumed completely) to 24 h, polymer molar mass increased from 46,000 to 69,000 g mol^{-1}. Continued heating did not result in any further increase in molar mass, nor did the addition of more catalyst

(additional 1 mol%) to the reaction mixture after 24 h and heating at 100 °C for 24 h. Plotting monomer consumption vs molar mass, we found that molar mass reaches a plateau of around 25,000 g mol^{-1} after 45% conversion (1 h), until high consumption of monomer (>90%), at which point a significant increase in molar mass is observed (Figure 3.7). These results suggest that there is also a competing process operating rather than solely the chain-growth mechanism previously postulated. Dehydrocoupling polymerisations operating via a combination of chain- and step-growth mechanisms have previously been postulated for the dehydrocoupling of $PhH_2P{\cdot}BH_3$ using Rh and Ir precatalysts.[33, 35]

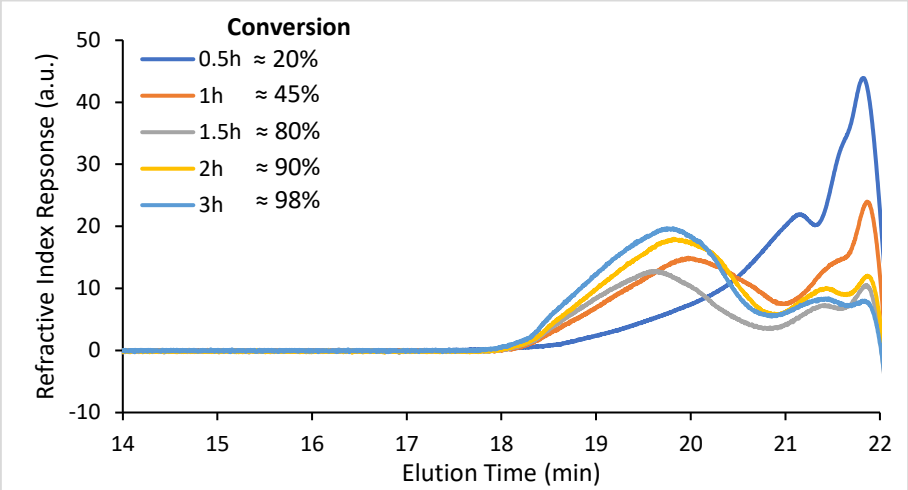

Figure 3.5 GPC chromatograms (2 mg mL^{-1} in THF, 0.1 w/w % nBu$_4$NBr in the THF eluent) showing the effect of reaction times of up to 3 h on the molar mass of [PhHP-BH$_2$]$_n$. Conditions: $PhH_2P{\cdot}BH_3$ (2 mmol), CpFe(CO)$_2$OTf (1 mol%), toluene, 100 °C, 4M.

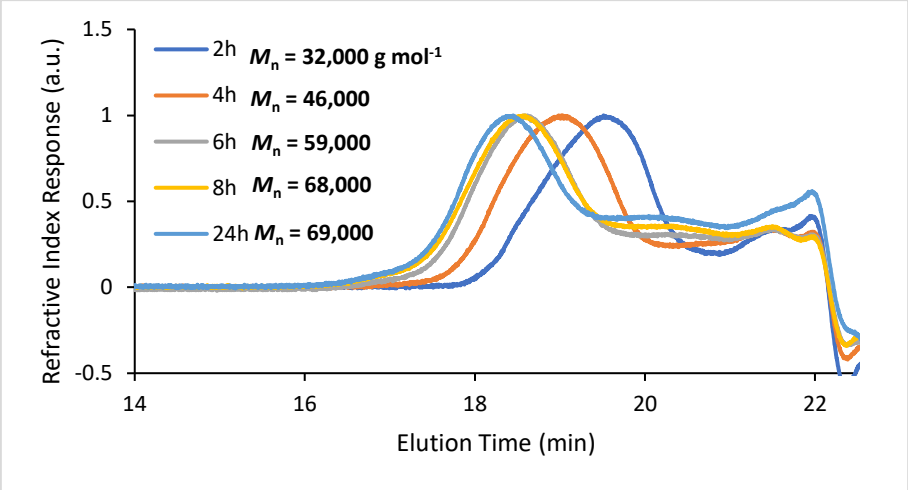

Figure 3.6 GPC chromatograms (2 mg mL^{-1} in THF, 0.1 w/w % nBu$_4$NBr in the THF eluent) showing the effect of reaction times of 2 – 24 h on the molar mass of [PhHP-BH$_2$]$_n$. Conditions: $PhH_2P{\cdot}BH_3$ (2 mmol), CpFe(CO)$_2$OTf (1 mol%), toluene, 100 °C, 4M.

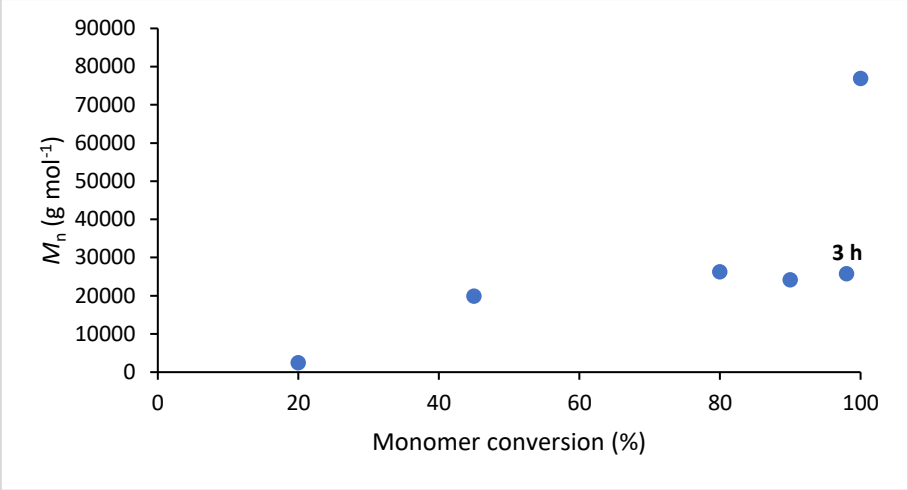

Figure 3.7 Conversion vs M_n plot for the dehydropolymerisation of $PhH_2P{\cdot}BH_3$ using $CpFe(CO)_2OTf$. Conditions: $PhH_2P{\cdot}BH_3$ (2 mmol), $CpFe(CO)_2OTf$ (1 mol%), toluene, 100 °C, 4M.

3.3.2 Elucidating the role of "Fe" in catalysis

In order to explain the apparent mechanistic complexity of the polymerisation of $PhH_2P{\cdot}BH_3$, we consider three possible dehydropolymerisation pathways arising when $CpFe(CO)_2OTf$ is used as the precatalyst: catalysis by the "Fe" centre; catalysis from TfOH released from the precatalyst; and a non-catalysed thermally-induced polymerisation.

3.3.2.1 Non-metal thermally induced dehydrocoupling of phenylphosphine-borane

It has previously been reported that heating $PhH_2P{\cdot}BH_3$ in the absence of solvent for 3 h at 90 °C followed by 3 h at 130 °C results in the formation of oligomers with M_n = ca. 2000 g mol^{-1}.[26] In order to elucidate whether non-catalysed thermally induced dehydrocoupling plays a significant role in the solution-phase polymerisation, we heated $PhH_2P{\cdot}BH_3$ to 100 °C in toluene (4 M) for 48 h. We consistently found incomplete monomer consumption with ca. 25% $PhH_2P{\cdot}BH_3$ according to integration of the ^{11}B NMR spectrum. The formation of mostly oligomeric material with a small amount of high molar mass polymer was determined by GPC (Figure S3.3). The material formed was sparingly soluble suggesting the formation of very high molar mass or crosslinked material. Analysis of the reaction mixture by ^{31}P NMR spectroscopy showed the formation of $PhPH_2$, along with a number of overlapping peaks assigned to $PhH_2P{\cdot}BH_3$, $[PhHP\text{-}BH_2]_n$, and small cyclic phosphinoborane species (δ = −43.9 – −59.1 ppm) along with a broad unassigned doublet at ca. −80 ppm (Figure 3.8). The differences in rate of polymerisation, and the molar mass and properties of the material obtained by heating $PhH_2P{\cdot}BH_3$ differ significantly from those from iron-catalysed dehydropolymerisation,

suggesting that uncatalysed thermal dehydrocoupling is not competent in the formation of [PhHP-BH_2]$_n$ using CpFe(CO)$_2$OTf; however, this could still be significant in the later stages of polymerisation after monomer has been fully consumed because only a few reaction events linking together oligomer chains would be required to explain the large increase in molar mass observed.

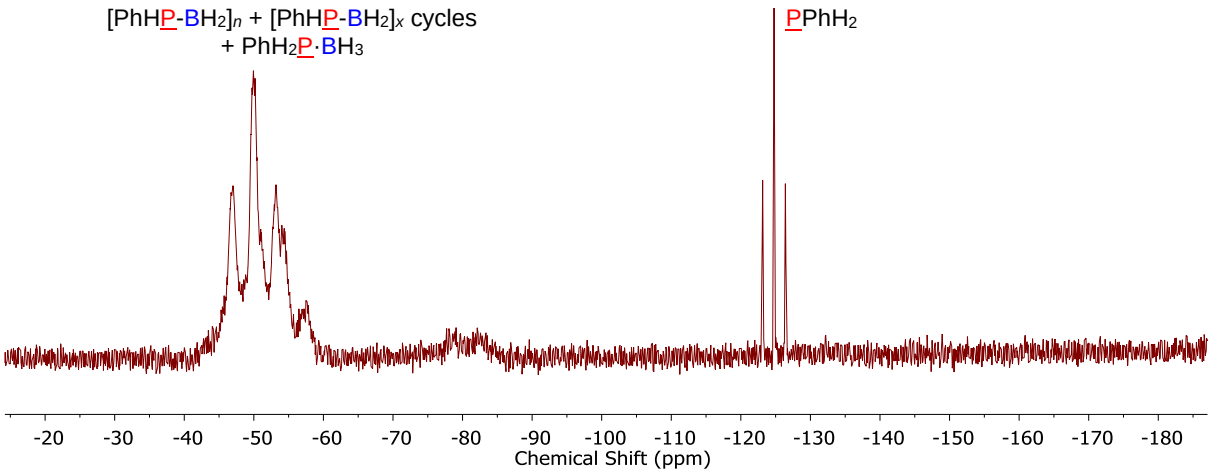

Figure 3.8 In situ ^{31}P NMR spectrum (122 MHz, 25 °C) after heating $PhH_2P{\cdot}BH_3$ in toluene (3 M) at 100 °C for 22 h.

3.3.2.2 Use of triflic acid as a precatalyst

In the previously reported mechanism for the dehydropolymerisation of $PhH_2P{\cdot}BH_3$ using the precatalyst CpFe(CO)$_2$OTf, the first step is the formation of CpFe(CO)$_2$PPhHBH_3 with the concomitant loss of triflic acid. To investigate whether triflic acid reacted with $PhH_2P{\cdot}BH_3$ under similar reaction conditions to those used in the polymerisation using CpFe(CO)$_2$OTf, we carried out a reaction using a catalytic amount of triflic acid (1 mol%) and heated the reaction mixture to 100 °C (Scheme 3.3). To our surprise, after 24 h we found complete consumption of the monomer determined by ^{11}B NMR spectroscopy and analysis of the products by NMR spectroscopy confirmed the formation of [PhHP-BH_2]$_n$. The ^{31}P NMR spectrum showed the diagnostic doublet at −49 ppm assigned to PH*P* units of [PhHP-BH_2]$_n$ alongside a minor peak at −56 ppm which has been reported to correspond to small cyclic species (Figure 3.9).[27] The polymer was found to be high molar mass (M_n = 49,700 g mol^{-1}) determined by GPC analysis with a PDI of 1.5. Further discussion on the use of triflic acid in the polymerisation of phosphine-boranes is provided in Section 3.3.5.

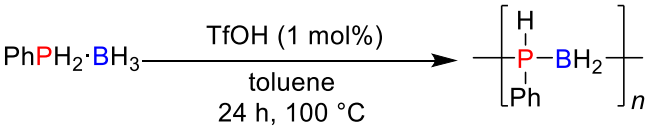

Scheme 3.3 The synthesis of $[PhHP\text{-}BH_2]_n$ using triflic acid as a precatalyst.

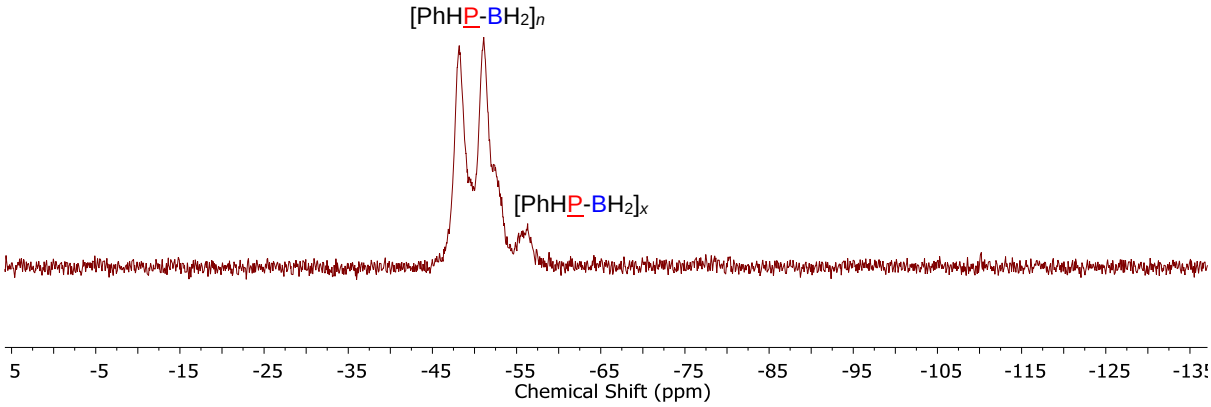

Figure 3.9 ^{31}P NMR (122 MHz, 25 °C, $CDCl_3$) of the product of polymerisation of $PhH_2P{\cdot}BH_3$ in the presence of triflic acid (1 mol%).

The observation that triflic acid is a proficient precatalyst for the polymerisation of $PhH_2P{\cdot}BH_3$, indicates that this could potentially have a significant role to play when $CpFe(CO)_2OTf$ is used as the precatalyst. We therefore sought to identify the roles of triflic acid and the iron centre. Firstly, we attempted the reaction of $PhH_2P{\cdot}BH_3$ with $CpFe(CO)_2OTf$ (5 mol%) in the presence of a bulky base, either 2,6-di-*tert*-butylpyridine (DTBP) or proton sponge® (5 mol%). We anticipated that these H^+ scavengers might negate any acid-catalysed polymerisation. The dehydropolymerisation was found to proceed in the presence of either of these bases (Table 3.1). Addition of DTBP (5 or 10 mol%) was found to have little effect on the molar mass of polymer produced using $CpFe(CO)_2OTf$ (5 mol%) (compare Table 3.1, entry 1 with entries 2 and 3); whereas, the addition of an excess of proton sponge® did result in lower molar mass material (entry 4). All reactions were found to be complete after heating at 100 °C for 24 h and analysis of the reaction mixture by ^{11}B and ^{31}P NMR spectroscopy all showed formation of $[PhHP\text{-}BH_2]_n$.

Significantly, analogous studies using triflic acid as a precatalyst revealed similar results (Table 3.2): Addition of DTBP (5 or 10 mol%) was found to have little effect on the molar mass of polymer produced (compare Table 3.2, entry 1 with entries 2 and 3); whereas, the addition of an excess of proton sponge®

did result in lower molar mass material (entry 4). Premixing an equimolar amount of triflic acid and DTBP for 2 h before addition to $PhH_2P{\cdot}BH_3$ also had little effect on the polymerisation (entry 5), whereas the analogous experiment using triflic acid and proton sponge® resulted in a lowering of the polymer molar mass (entry 6). Again, all reactions were found to be complete after heating at 100 °C for 24 h.

Table 3.1 Effect of DTBP and proton sponge® on the polymerisation of $PhH_2P{\cdot}BH_3$ using $CpFe(CO)_2OTf$.

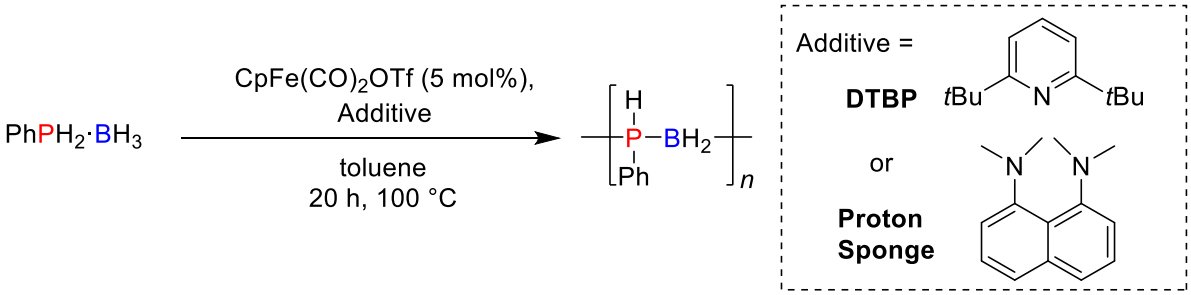

Entry	Additive	M_n (g mol^{-1})	PDI
1	None	29,000	1.6
2	DTBP (5 mol%)	28,000	1.7
3	DTBP (10 mol%)	27,800	1.6
4	Proton sponge® (10 mol%)	12,200	1.7

Reaction conditions: A J. Young NMR tube was charged with $PhH_2P{\cdot}BH_3$ (0.1 mmol), $CpFe(CO)_2OTf$ (5 mol%), toluene (0.5 mL) and any additive stated. The tube was sealed and heated to 100 °C for 20 h after which the reaction was analysed by ^{11}B and ^{31}P NMR, and the reaction mixture dried and analysed by GPC.

Table 3.2 Effect of DTBP and proton sponge® on the polymerisation of $PhH_2P{\cdot}BH_3$ using triflic acid.

Entry	Additive	M_n (g mol^{-1})	PDI
1	None	19,500	1.5
2	DTBP (5 mol%)	19,500	1.7
3	DTBP (10 mol%)	19,600	2.2
4	Proton sponge® (10 mol%)	3,400	2.2
5	DTBP (5 mol%)[a]	21,700	1.8
6	Proton sponge® (5 mol%)[a]	5,700	2.4

Reaction conditions: A J. Young NMR tube was charged with $PhH_2P{\cdot}BH_3$ (0.1 mmol,), TfOH (5 mol%), toluene (0.5 mL) and any additive stated. The tube was sealed and heated to 100 °C for 20 h after which the reaction was analysed by ^{11}B and ^{31}P NMR, and the reaction mixture dried and analysed by GPC. [a]TfOH and the additive stated were premixed in toluene prior to addition to $PhH_2P{\cdot}BH_3$.

Remarkably, it was also found that $PhH_2P{\cdot}BH_3$ would polymerise in the presence of a catalytic amount of proton sponge® providing an alternative base-catalysed route to access polyphosphinoboranes (see Section 3.3.4.1). In contrast, no change in the ^{31}P NMR spectrum was observed when $PhH_2P{\cdot}BH_3$ was heated to 100 °C in the presence of DTBP (5 mol%) in toluene for 24 h and no polymeric material was detected from the GPC chromatogram of the product mixture. A possible reason for this is that DTBP is a weaker base than proton sponge® (pKa $(Me_3C)_2C_5H_3NH^+$ = 4.95 in water; pKa $C_{14}H_{18}N_2H^+$ = 12.1 in water).

3.3.2.3 Conversion versus molar mass studies

Given the interesting conversion vs molar mass profile of the polymerisation of $PhH_2P{\cdot}BH_3$ using $CpFe(CO)_2OTf$ (Figure 3.7), we were interested in examining if there were any differences using related precatalysts. It was previously reported that dehydrocoupling of $PhH_2P{\cdot}BH_3$ could also be facilitated using the precatalyst $CpFe(CO)_2I$; however, this was found to give only moderate molar mass polymer (M_n = 18,000, PDI = 2.0).[32] This difference between $CpFe(CO)_2I$ and $CpFe(CO)_2OTf$ was postulated to be due to the more weakly coordinating trifluoromethanesulfonate anion resulting in a more active precatalyst. Given the reported differences between the polymer produced using these two precatalysts, we sought to compare the effect of conversion on molar mass for polymerisation of $PhH_2P{\cdot}BH_3$ using $CpFe(CO)_2I$ to the above study using $CpFe(CO)_2OTf$.

When $CpFe(CO)_2I$ (1 mol%) was used as a precatalyst for the polymerisation of $PhH_2P{\cdot}BH_3$, low molar mass polymeric material was observed in the GPC at low conversion ($M_n \approx 3{,}500$ g mol^{-1}). As with the case of $CpFe(CO)_2OTf$, the molar mass of the material obtained using $CpFe(CO)_2I$ remained fairly constant until high monomer consumption (>95%) at which point a large increase in molar mass was observed (Figure 3.10). The absence of high molar mass material at lower conversion is more reminiscent of step-growth polymerisation rather than chain-growth. The polymerisation using $CpFe(CO)_2I$ as a precatalyst was found to be slower than when $CpFe(CO)_2OTf$ was used, taking 10 h for complete monomer consumption (cf. <4 h when $CpFe(CO)_2OTf$ is used).

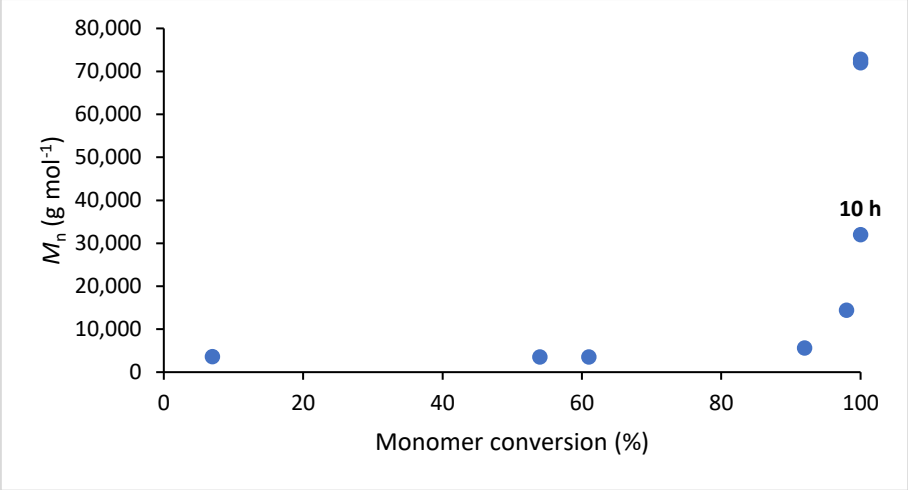

Figure 3.10 Conversion vs M_n plot for the dehydropolymerisation of $PhH_2P{\cdot}BH_3$ using $CpFe(CO)_2I$. Conditions: $PhH_2P{\cdot}BH_3$ (2 mmol), $CpFe(CO)_2I$ (1 mol%), toluene, 100 °C, 4 M.

The first step in the dehydropolymerisation using $CpFe(CO)_2OTf$ is reported to be the formation of the iron phosphidoborane species $CpFe(CO)_2PPhHBH_3$. The stoichiometric reaction between $CpFe(CO)_2OTf$ and $PhH_2P{\cdot}BH_3$ resulted in clean conversion to $CpFe(CO)_2PPhHBH_3$ after 7 d. This species can also be selectively formed and isolated by the reaction $CpFe(CO)_2I$ with $LiPPhHBH_3$.[32] We postulated that absence of any triflate leaving group would allow us to evaluate the role of iron in the catalysis of $PhH_2P{\cdot}BH_3$ more clearly.

When $CpFe(CO)_2PPhHBH_3$ (1 mol%) was used as a precatalyst, the effect of monomer conversion on the molar mass of the isolated material is shown below (Figure 3.11). At monomer consumptions of less than 60%, the molar mass of material was below the detection limit of the GPC (M_n = 1,200 g mol^{-1}). Monomer was fully consumed after around 10 h (similar to the time taken for $CpFe(CO)_2I$ dehydropolymerisation) and as with the previous catalysts, a large increase in molar mass was observed at high conversion. The time taken for monomer consumption using $CpFe(CO)_2PPhHBH_3$ is significantly longer than when $CpFe(CO)_2OTf$ is used. This suggests that the iron-phosphidoborane is not a kinetically competent catalyst. The absence of high molar mass material is also more reminiscent of step-growth polymerisation rather than a chain-growth mechanism. These findings are significant because while $CpFe(CO)_2PPhHBH_3$ was postulated to be the active catalyst for the polymerisation of $PhH_2P{\cdot}BH_3$ using $CpFe(CO)_2OTf$ as a precatalyst (Scheme 3.2), the rate of polymerisation and the extent of molar mass growth with monomer consumption for the two precatalysts do not match, which

suggests that they either operate via different catalytic pathways or that there is an additional accessible mechanism for the $CpFe(CO)_2OTf$ precatalyst.

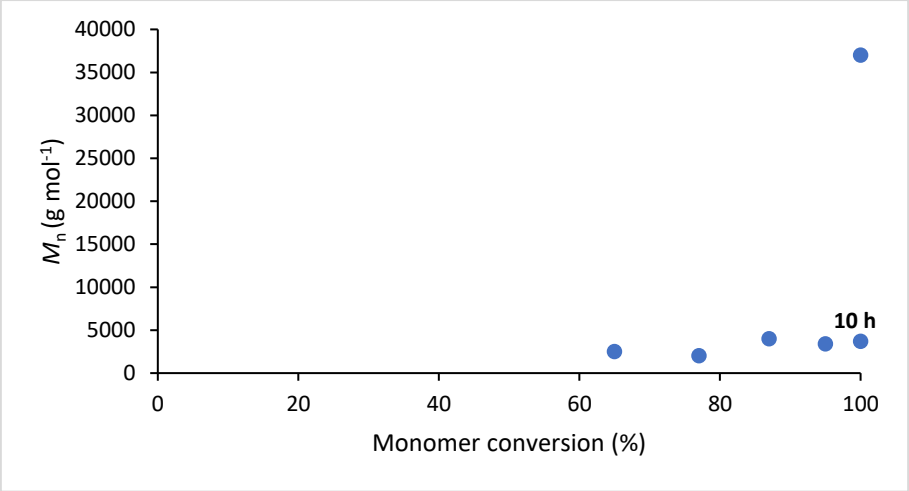

Figure 3.11 Conversion vs M_n plot for the dehydropolymerisation of $PhH_2P{\cdot}BH_3$ using $CpFe(CO)_2PPhHBH_3$. Conditions: $PhH_2P{\cdot}BH_3$ (2 mmol), $CpFe(CO)_2PPhHBH_3$ (1 mol%), toluene, 100 °C, 4 M.

We lastly studied the effect of conversion on molar mass for the triflic acid-catalysed polymerisation of $PhH_2P{\cdot}BH_3$. Use of triflic acid (1 mol%) as a precatalyst gave a molar mass growth profile that closely matches step-growth mechanism (Figure 3.12). The molar mass of the isolated material was below 1,500 g mol^{-1} up to ca. 50% conversion and only significantly increases at very high monomer consumption. The time taken for complete monomer consumption (10 h: conversion = 96%, 24 h: conversion = 100%) was significantly higher than when $CpFe(CO)_2OTf$ was used as a precatalyst (<4 h).

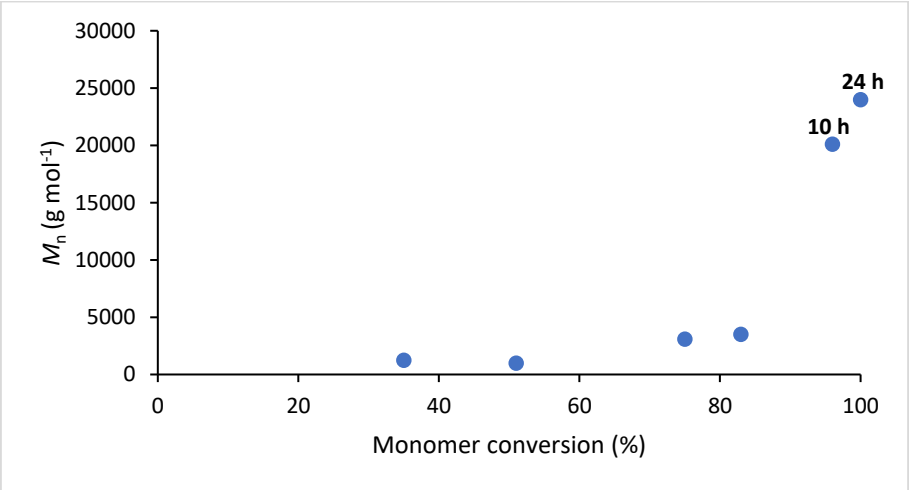

Figure 3.12 Conversion vs M_n plot for the dehydropolymerisation of $PhH_2P{\cdot}BH_3$ using TfOH. Conditions: $PhH_2P{\cdot}BH_3$ (2 mmol), TfOH (1 mol%), toluene, 100 °C, 4 M.

These studies reveal that while a number of precatalysts are capable of catalysing the dehydropolymerisation of $PhH_2P{\cdot}BH_3$ to give high molar mass material at high conversion, only $CpFe(CO)_2OTf$ forms high molar mass material at lower degrees of monomer consumption. This difference in conversion vs M_n suggest that there is a significant chain-growth component for the polymerisation using $CpFe(CO)_2OTf$ which is absent for other catalysts.

3.3.3 The effect of HOTf loading on the polymerisation of phenylphosphine-borane and comparison with [$CpFe(CO)_2OTf$]

It was previously reported that the molar mass of $[PhHP\text{-}BH_2]_n$ formed using $[CpFe(CO)_2OTf]$ is inversely related to the precatalyst loading.[32] We sought to determine if the same relationship between precatalyst loading and polyphosphinoborane molar mass was observed when triflic acid was used. Heating of $PhH_2P{\cdot}BH_3$ (0.8 mmol) in toluene (0.4 mL, 2 M) in the presence of varied amounts of triflic acid at 100 °C for 24 h and subsequent analysis of the material formed by GPC showed that there was an almost negligible effect of triflic acid loading on the molar mass of the resultant polymer (Table 3.3) which is inconsistent with a chain-growth mechanism.

Table 3.3 Effect of triflic acid loading on the molar mass of polymer produced from the dehydrocoupling of $PhH_2P{\cdot}BH_3$

Conditions	M_n (g mol^{-1})	M_w (g mol^{-1})	PDI
1 mol% TfOH	49,700	75,500	1.52
5 mol% TfOH	51,600	77,300	1.49
10 mol% TfOH	41,300	62, 600	1.51

Reaction conditions: A J. Young NMR tube was charged with $PhH_2P{\cdot}BH_3$ (0.8 mmol), TfOH, toluene (0.4 mL). The tube was sealed and heated to 100 °C for 24 h after which the material was analysed by GPC.

3.3.4 Reaction of oligomeric material with $CpFe(CO)_2OTf$ and TfOH

For each of the polymerisation precatalysts that we have investigated, a significant increase in polymer molar mass is observed at very high conversion and after the monomer has been fully consumed. To further elucidate the reason for this, we sought to synthesise well-defined low molar mass material which we could then subject to catalytic conditions to examine if there is any molar mass increase.

While it has been reported that the thermal dehydrocoupling of $PhH_2P{\cdot}BH_3$ yielded oligomeric material, we consistently found that some high molar mass material was formed when attempting to replicate this

reaction either in the melt or in toluene. Material synthesised from the thermal dehydrocoupling of $PhH_2P{\cdot}BH_3$ was also found to be sparingly soluble and likely somewhat crosslinked and was therefore not suitable for further studies.

Another method for producing low molar mass material was reported by Gaumont and co-workers using $B(C_6F_5)_3$ as a catalyst.[43] This was reported to give material with a bimodal mass distribution (M_w = 3,900 and 800 g mol^{-1}); however, we could not reproduce these results following the reported reaction conditions (0.5 mol% $B(C_6F_5)_3$, 20 °C, 3 d, toluene). The use of more forcing condition (5 mol% $B(C_6F_5)_3$, 95 °C) did result in complete monomer consumption after 44 h and the formation of material with M_n = 8,000 g mol^{-1}. As with the $[PhHP\text{-}BH_2]_n$ polymer reported by Gaumont, the ^{31}P NMR spectrum of this material showed a doublet at around −49 ppm and a number of unresolved peaks between −50 and −59 ppm. A significant amount of $PPhH_2$ was also formed during the course of this reaction, suggesting monomer decomposition under these conditions. Despite this, we endeavoured to examine whether heating this material further in toluene in the presence of $CpFe(CO)_2OTf$ (1 mol%, 100 °C, 18 h) had any effect on molar mass compared to heating without any catalyst; however, the results were inconclusive. The molar mass profiles of the material obtained with and without catalyst do vary (Figure S3.7) but it is unclear whether this is significant variation.

The polymerisation of $PhH_2P{\cdot}BH_3$ using $CpFe(CO)_2I$ results in the formation of fairly low molar mass material until very high conversion (Figure 3.10). We therefore anticipated that we could isolate low molar mass material by quenching this reaction at 60% conversion. Indeed, material isolated by precipitation into cold pentane and washing with diethyl ether to remove any remaining $PhH_2P{\cdot}BH_3$ was found to have an M_n = 15,000 g mol^{-1} (PDI = 1.7) and was determined to be monomer free from the ^{11}B NMR spectrum. To analyse the difference between the reaction with $CpFe(CO)_2OTf$, triflic acid, and any thermal reaction occurring at 100 °C, three J. Young NMR tubes were charged with the isolated low molar mass material (0.475 mmol) and dissolved in toluene (0.25 mL). To the first, no catalyst was added, to the second was added $CpFe(CO)_2OTf$ (5 mol% based on the monomer molar mass), and to the third was added triflic acid (5 mol%). The reaction mixtures were heated at 100 °C for 20 h. Volatiles were removed from the reaction mixtures and the residues analysed by GPC. The addition of triflic acid was found to have little effect on the molar mass (M_n = 17,000 g mol^{-1}, PDI = 2.6); whereas, the presence

of $CpFe(CO)_2OTf$ resulted in a significant increase in molar mass (M_n = 54,100 g mol^{-1}, PDI = 1.8). However, a significant increase in molar mass was also observed for the reaction heated to 100 °C in the absence of catalyst (M_n = 83,400, PDI = 3.8). These results show that while triflic acid is capable of polymerising monomeric $PhH_2P{\cdot}BH_3$, it will not facilitate the linking of preformed polymeric chains together. The lack of molar mass increase when oligomeric material was heated in the presence of triflic acid suggests that TfOH could be acting to modify the polymer end group and preventing coupling between them.

The difference between the reaction in the absence of catalyst and when $CpFe(CO)_2OTf$ is present are less obvious. Molar mass increase was observed in each case, which can be interpreted as indicating that a thermally induced reaction is responsible for the increase in molar mass of $[PhHP\text{-}BH_2]_n$ after complete monomer consumption rather than an on-metal reaction; however, the presence of $CpFe(CO)_2OTf$ does have a significant effect on the PDI of the resultant polymer which suggests that $CpFe(CO)_2OTf$ is imparting an increased degree of control over reactivity leading to molar mass increase. Additionally one limitation of this study is that we cannot rule out the presence of an active iron species remaining in the polymer from the initial $CpFe(CO)_2I$ polymerisation. Despite repeated precipitations, the material remained strongly coloured suggesting that iron-containing species remain. The difficulty in removing iron species from polyphosphinoboranes subsequent to their formation using $CpFe(CO)_2OTf$ as a precatalyst has previously been reported.[37]

In summary, these results suggest that the polymerisation of $PhH_2P{\cdot}BH_3$ using $CpFe(CO)_2OTf$ occurs via a hybrid mechanism rather than the simple chain-growth previously postulated. A similar hybrid mechanism was reported for the rhodium-catalysed polymerisation of phenylphosphinoborane[35] and N-methylamine-borane,[50] and has also been implicated in a number of other polymerisation processes.[51-53] There are a few possibilities for this proposed step-growth component. i) head-to-tail linking of end groups giving a phosphinoborane linkage (Figure 3.13a); ii) chain branching through P-B coupling giving triphosphinoborane units or phosphinotriborane linkages (Figure 3.13b); iii) homoatomic linking e.g. P-P coupling (Figure 3.13c). While homoatomic coupling is conceivable, and has previously been reported using iron precatalysts,[54] this would lead to differences to the observed ^{31}P NMR spectra and therefore is ruled out as a significant process. Given that we only observe one

signal in the ^{11}B and ^{31}P NMR, the data tentatively points towards end group linking (Figure 3.13a) as this would give linkages indistinguishable from the chain-growth mechanism previously postulated while any alternatives would likely be detectable by either ^{11}B or ^{31}P NMR spectroscopy.

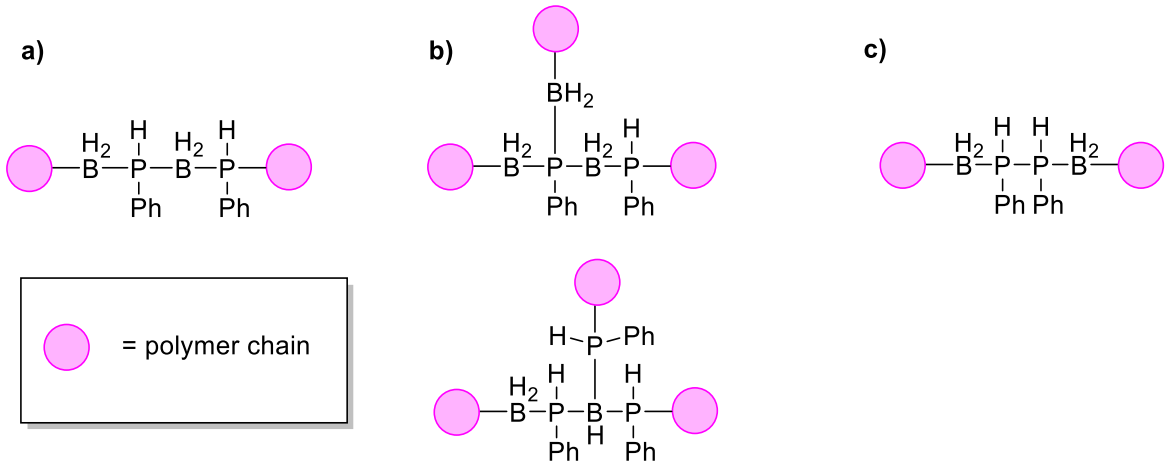

Figure 3.13 Possible polymer chain coupling motifs during the polymerisation of $PhH_2P{\cdot}BH_3$.

3.3.5 Catalytic Dehydrocoupling of phenylphosphine-borane using non-metal catalysts

As discussed in Section 3.3.2.2 it is possible to facilitate the dehydrocoupling of $PhH_2P{\cdot}BH_3$ using both acidic and basic non-metal precatalysts. The development of non-metal catalysts is of significant importance both to eliminate the need for the use of toxic, expensive transition metals in favour of more benign and earth abundant species and because the presence of metals in polymers can have significant deleterious effects on their material properties. We therefore endeavoured to investigate the catalytic dehydrocoupling of phosphine-boranes using proton sponge® and triflic acid.

3.3.5.1 The synthesis of $[PhHP\text{-}BH_2]_n$ using proton sponge® as a precatalyst

The polymerisation of $PhH_2P{\cdot}BH_3$ using proton sponge® was investigated (Scheme 3.4). Analysis of the material formed stirring for 24 h in toluene at 100 °C by ^{31}P NMR revealed the formation of $PhPH_2$ alongside a doublet at ca. −50 ppm which corresponds to $[PhHP\text{-}BH_2]_n$.[32] A broad unassigned signal was also observed at −80 ppm, along with several overlapping signals with chemicals shifts between −50 and −60 ppm. These signals in the ^{31}P NMR spectrum have previously been observed in rhodium catalysed dehydropolymerisation of $PhH_2P{\cdot}BH_3$ and are reported to correspond to small cyclic species.[27] Analysis of this material by GPC showed high molar mass material revealed that mostly low molar mass polydisperse polymer was formed (Figure S3.3, M_n = 4,700, PDI = 2.2).

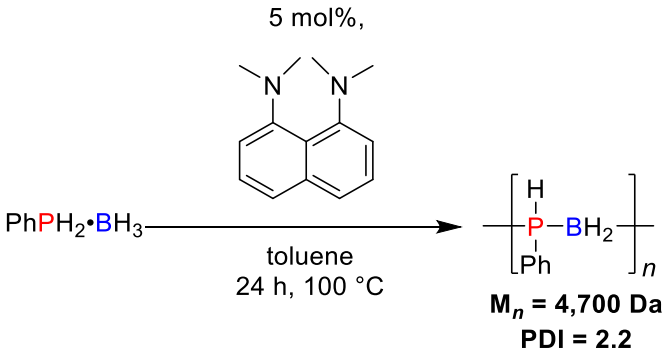

Scheme 3.4 The synthesis of [PhHP-BH_2]$_n$ using proton sponge® as a precatalyst.

3.3.5.2 Large scale synthesis and isolation of [PhHP-BH_2]$_n$ using triflic acid precatalyst

In order to synthesise sufficient material which is metal-free for use in further applications e.g. in the synthesis of crosslinked polyphosphinoborane, we targeted the synthesis [PhHP-BH_2]$_n$ on a 4 mmol scale using triflic acid as a precatalyst (Scheme 3.3). To this end, $PhH_2P{\cdot}BH_3$ was dissolved in toluene (2 M) and heated to 100 °C in the presence of triflic acid (1 mol%). After 2 d, volatiles were removed under vacuum and the residue dissolved in DCM and precipitated into pentane at −78 °C. The resultant material was dried under vacuum for 2 d yielding a colourless solid (yield = 0.37 g, 75%). The NMR spectra of this material were consistent with the formation of [PhHP-BH_2]$_n$.[32] The molar mass was determined by GPC and was found to be significantly lower than the molar mass of previous smaller scale reactions (Figure S3.14, M_n = 5,200, PDI = 2.4). The reason for this remains unclear but the material produced is of sufficient molar mass for further functionalisation and as a precursor to polyphosphinoborane gels (see Chapter 4).

3.3.6 Catalytic dehydrocoupling of alkylphosphine-boranes

3.3.6.1 Polymerisation of *t*$BuH_2P{\cdot}BH_3$ using triflic acid as a precatalyst

Heating *t*$BuH_2P{\cdot}BH_3$ in toluene (2 M) in the presence of triflic acid (10 mol%) at 100 °C resulted in complete consumption of the monomer after 64 h (determined by ^{11}B NMR). After workup, analysis by ^{31}P NMR spectroscopy revealed several signals in the range −10 ppm to −30 ppm (Figure S3.17). A similar set of signals was observed in a thermally-induced Lewis-base elimination route to poly(*tert*-butylphosphinoborane) and was tentatively attributed to polymer tacticity.[41] Analysis of the material by GPC revealed the formation of polymeric material (Figure S3.19, M_n = 15,000 g mol^{-1}, PDI = 1.7).

3.3.6.2 Polymerisation of *n*HexH$_2$P·BH$_3$ using triflic acid as a precatalyst

Heating *n*HexH$_2$P·BH$_3$ in toluene (2 M) in the presence of triflic acid (5 mol%) to 100 °C resulted in a sluggish reaction. After 5 d, the reaction was stopped at ca. 75% monomer consumption. After workup, analysis of this material by ^{31}P NMR spectroscopy showed signals corresponding to the polymer (δ = −60 ppm);[36] however, some *n*HexH$_2$P·BH$_3$ remained (δ = −55 ppm) along with a number of other unidentified signals (Figure S3.21). The molar mass of the material was determined by GPC chromatography (Figure S3.25, M_n of 6,400 g mol^{-1}, PDI = 2.5).

3.3.6.3 Dehydrocoupling of Et$_2$HP·BH$_3$ using CpFe(CO)$_2$OTf and TfOH precatalysts

Given the successful dehydrocoupling of primary alkylphosphine–boranes using [CpFe(CO)$_2$(OTf)],[47] we decided to examine the dehydrocoupling of a P-disubstituted dialkylphosphine-borane. To this end, Et$_2$HP·BH$_3$ was heated to 100 °C in the presence of [CpFe(CO)$_2$(OTf)] (1 mol% precatalyst, toluene, 2.0 M) for 14 days, after which ~30% conversion of the starting material was detected by ^{31}P NMR spectroscopy. After removal of the volatiles under vacuum, including unreacted Et$_2$HP·BH$_3$, the material was analysed by NMR spectroscopy. This analysis revealed the major product to be the linear dimer Et$_2$HP·BH$_2$-PEt$_2$·BH$_3$. The ^{31}P{^{1}H} and ^{11}B{^{1}H} NMR spectra each contain two major peaks in a 1:1 ratio by integration corresponding to internal (δ_P = –26.7, δ_B = –37.5 ppm) and terminal (δ_P = –2.7, δ_B = –38.9 ppm) P- and B-centers within the linear dimeric chain (Figure S3.27 and Figure S3.29). Further analysis of the dehydrocoupling product mixture by ESI-MS uncovered trace amounts of oligomeric [Et$_2$P–BH$_2$]$_x$ (x <5) with expected repeat unit of Δ(m/z) = 102 Da (Figure S3.33), but no high molar mass material was observed in the GPC chromatogram of the product where the peak was below the limit of the lowest molecular weight polystyrene standard (2,300 g mol^{-1}; Figure S3.34).

Heating Et$_2$HP·BH$_3$ in toluene in the presence of triflic acid (5 mol%) to 100 °C in a J. Young NMR tube resulted in a sluggish reaction. After 10 d, analysis of the reaction by ^{31}P NMR spectroscopy showed a broad doublet at −2.8 ppm (J = 339 Hz) and a broad singlet at −25.4 ppm which have been reported to correspond to the linear dimer Et$_2$HP·BH$_2$-Et$_2$P·BH$_3$; however a significant amount of starting material remained (δ = 1.6 ppm, J = 364.5 Hz), and a number of other products were also formed (Figure S3.35). Due to the poor selectivity and slow reaction rate, this reaction was stopped after 10 d and not pursued further.

3.4 Conclusions

In summary, we have significantly increased the amount of high molar mass polymer produced from a high molar mass:low molar mass ratio of 3:7 to 7:3. from the dehydropolymerisation of $PhH_2P{\cdot}BH_3$ using the precatalyst $CpFe(CO)_2OTf$ by thorough investigation of reaction conditions on the polymerisation. While this reaction was previously postulated to operate via a chain-growth mechanism, our studies suggest that the reaction proceeds instead via a mixture of chain-growth and step-growth pathways. The evidence for this hybrid mechanism comes from studies into conversion vs molar mass for $CpFe(CO)_2OTf$ and related catalysts with continued molar mass increase observed after complete monomer consumption.

Triflic acid and proton sponge® were found to be active precatalysts in their own right for the polymerisation of $PhH_2P{\cdot}BH_3$ and the dehydrocoupling of other phosphine-borane monomers was also facilitated by triflic acid; however, while triflic acid is a proficient precatalyst for the polymerisation of *tert*-butylphosphine-borane, issues with selectivity, and a slow reaction rate hinder the dehydrocoupling of *n*-hexyl- and diethylphosphine-borane. There is therefore significant scope for improving non-metal catalysed dehydrocoupling of phosphine-boranes to compete with the efficacy of $CpFe(CO)_2OTf$.

3.5 Experimental

3.5.1 General procedures, reagents, and equipment

All air- and water-sensitive manipulations were carried out in glassware under a nitrogen atmosphere using standard Schlenk line and glovebox techniques. Glassware was dried in an oven at 200 °C overnight prior to use. Polymer workup was carried out under air. Anhydrous solvents were dried via a Grubbs design purification system. Anhydrous, deuterated solvents were purchased from Sigma Aldrich, and stored over activated molecular sieves (4Å). $PhH_2P{\cdot}BH_3$,[55] $t\text{BuH}_2\text{P}{\cdot}BH_3$,[41] $Et_2HP{\cdot}BH_3$,[56] and $CpFe(CO)_2OTf$[57] were synthesised via literature procedures. All other compounds were purchased from commercial sources and used as received unless stated otherwise.

NMR spectra were recorded using Oxford Jeol ECS 400 MHz, Bruker Nano 400 MHz, Bruker Avance III HD 500 MHz Cryo, Bruker Advance 500 MHz, or Varian VNMR 500 MHz spectrometers. ^1H and ^{13}C NMR spectra were reference to residual signals of the solvent ($CDCl_3$: ^1H: $\delta = 7.24$, ^{13}C: $\delta = 77.0$;

C_6D_5H: ^1H: δ = 7.20, ^{13}C: δ = 128.0). ^{11}B and ^{31}P NMR spectra were referenced to external standards (^{11}B: $BF_3{\cdot}OEt_2$ (δ = 0.0); ^{31}P: 85% H_3PO_4 (aq.) (δ = 0.0)). Chemical shifts (δ) are given in parts per million (ppm) and coupling constants (*J*) are given in Hertz (Hz), rounded to the nearest 0.5 Hz.

Electrospray ionisation mass spectrometry (ESI-MS) was performed on a MSQ Plus single quadrupole mass spectrometer (Thermo, MA) with a flow rate of 0.2 mL min^{-1}. A 50:50 solvent mixture was prepared of Mili-Q™ water (Millipore) and Optima™ Methanol (Fisher Chemical). 200 uL of sample was injected using a manual injector. The instrument cone voltage was set to 75 V and a scan time of 1 s used.

Gel permeation chromatography (GPC) was performed on a Malvern RI max Gel Permeation Chromatograph, equipped with an automatic sampler, pump, injector, and inline degasser. The columns (2xT5000) were contained within an oven (35°C) and consisted of styrene/divinyl benzene gels. Sample elution was detected by means of a differential refractometer. The calibration was conducted using monodisperse polystyrene standards obtained from Aldrich. The lowest and highest molecular weight standards used were 2,300 Da and 994,000 g mol^{-1} respectively.

Additional GPC was performed on an Omnisec Resolve TDA 305 GPC system, equipped with an automatic sampler, pump, injector, and inline degasser. The columns (T3000 and T5000 in sequence) were contained within an oven (35°C) and consisted of styrene/divinyl benzene gels. Sample elution was detected by means of a differential refractometer. The calibration was conducted using monodisperse polystyrene standards obtained from Aldrich. The lowest and highest molecular weight standards used were 1,200 Da and 4,200,000 g mol^{-1} respectively.

For GPC analysis, THF (Fisher) containing 0.1 w/w % [nBu$_4$N][Br] was used as the eluent for GPC at a flow rate of 1 mL min^{-1}. Samples were dissolved in THF (2 mg mL^{-1}) and filtered with a Ministart SRP15 filter (poly(tetrafluoroethylene) membrane of 0.45 μm pore size) before analysis.

3.5.2 Investigations of monomer conversion on molar mass for $CpFe(CO)_2OTf$ and related catalysts

In a glovebox, a vial was charged with $PhH_2P{\cdot}BH_3$ (2 mmol), catalyst (1 mol%), and toluene (1 mL). The reaction mixture was transferred to a J. Young flask, sealed, removed from the glovebox, and connected to a Schlenk manifold. The flask was opened to nitrogen and heated to 100 °C. At regular

time intervals, a few drops of material were removed via syringe. The aliquot was analysed by ^{11}B NMR to determine the monomer conversion and subsequently dried under vacuum and analysed by GPC to determine the molar mass of the material.

3.5.3 Catalytic dehydrocoupling with different precatalyst loadings of HOTf

Under a dinitrogen atmosphere $PhH_2P{\cdot}BH_3$ (0.8 mmol) was dissolved in toluene (0.4 mL), and TfOH added directly. Each colourless reaction mixture was transferred to a J. Young NMR tube, sealed, and heated at 100 °C in an oil bath. The conversion was monitored by $^{31}P\{^1H\}$ and $^{11}B\{^1H\}$ NMR spectroscopy. Upon complete consumption of monomer, each J. Young tube was opened in air carefully to vent H_2 generated in the dehydropolymerisation reaction, and the solvent was removed under vacuum. For each reaction, the crude colourless residue was dissolved in CH_2Cl_2 (0.5 mL) and washed with a 0.1 M $NaHCO_3$ solution, the organic phase was separated and dried over a short pad of $MgSO_4$ within a glass microfiber plugged pipette and was eluted with CH_2Cl_2 (5 mL), afterwards the solvent was removed by rotary evaporation and the pale yellow to colourless solid polymeric product was dried under vacuum overnight followed by in 40 °C vacuum oven for a minimum of 2 days (quantitative yield). The material was subsequently analysed by GPC to determine molar mass (Table 3.3).

3.5.4 Synthesis and reactivity of oligo(phenylphosphinoborane)

3.5.4.1 Thermal dehydrocoupling of phenylphosphine-borane

In a glovebox, a J. Young flask was charged with $PhH_2P{\cdot}BH_3$ (2 mmol) and toluene (1 mL). The flask was sealed and transferred to a Schlenk manifold and then heated at 100 °C for 2 d. The progress of the reaction was monitored by ^{11}B and ^{31}P NMR spectroscopy. After 2 d, a monomer conversion of 75% was determined by ^{11}B NMR spectroscopy. At this point, volatiles were removed from the reaction mixture and the molar mass of the material determined by GPC.

GPC: M_n = 10,800 g mol^{-1}, M_w = 24,600 g mol^{-1}, PDI = 2.3.

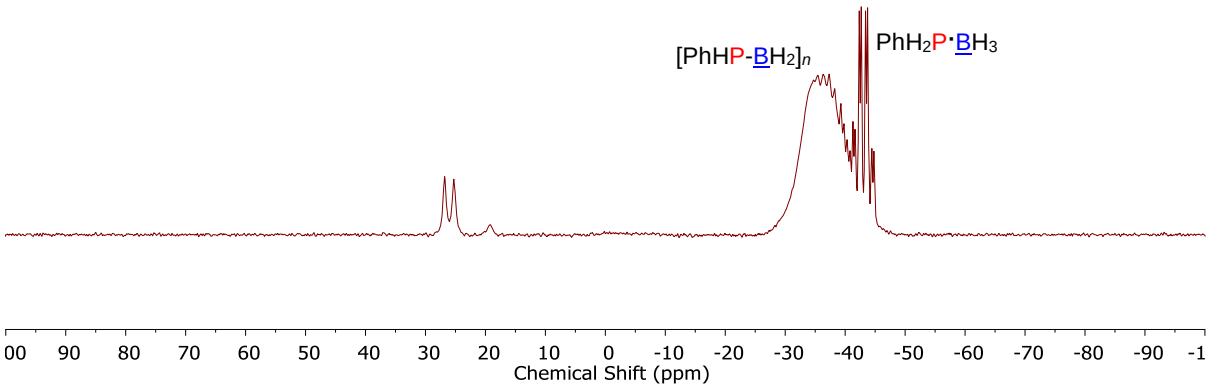

Figure S3.1 In situ ^{11}B NMR (96 MHz, 25 °C, toluene) of the thermal reaction of $PhH_2P{\cdot}BH_3$ after 2 d.

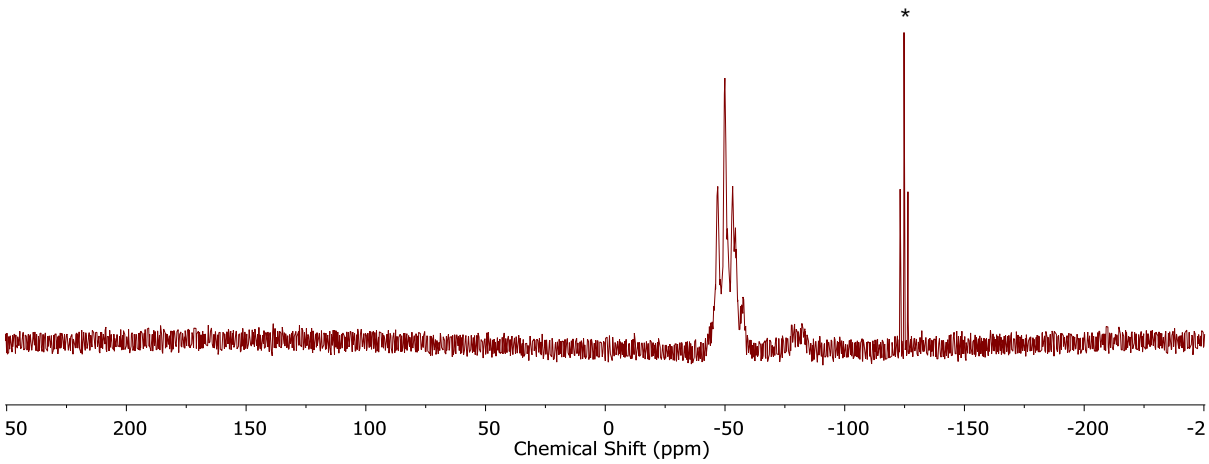

Figure S3.2 In situ ^{31}P NMR spectrum (122 MHz, 25 °C, toluene) of the thermal reaction of $PhH_2P{\cdot}BH_3$ after 2 d. Signal corresponding to $PhPH_2$ is denoted by *.

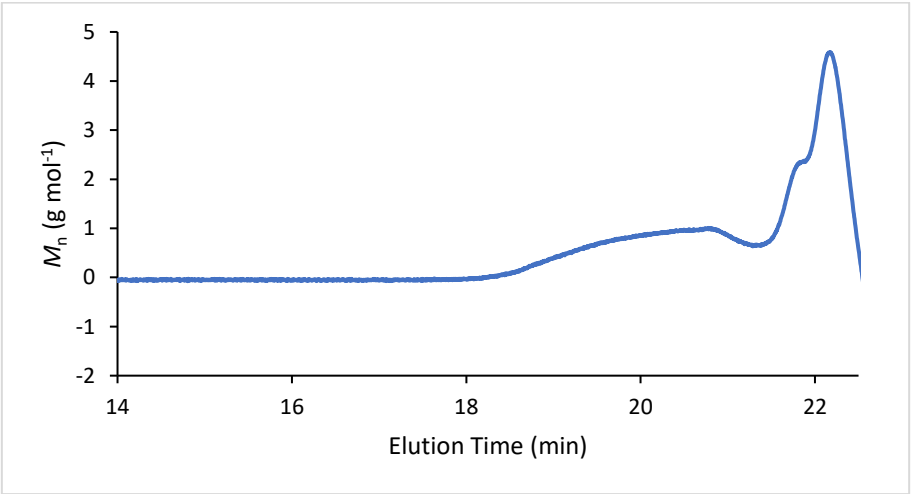

Figure S3.3 GPC chromatogram (2 mg mL^{-1} in THF, 0.1 w/w % nBu$_4$NBr in the THF eluent) of material isolated from the thermal reaction of $PhH_2P{\cdot}BH_3$ after 2 d.

3.5.4.2 Dehydrocoupling of phenylphosphine-borane using $B(C_6F_5)_3$ as a precatalyst

In a glovebox, a flask was charged with $PhH_2P{\cdot}BH_3$ (0.3 g, 2.4 mmol), $B(C_6F_5)_3$ (0.06 g, 0.12 mmol), and toluene (4 mL). The flask was sealed and transferred to a Schlenk manifold and then heated at 95 °C for 44 h open to a nitrogen atmosphere. Volatiles were then removed under vacuum and the residue dried overnight in a vacuum oven at 40 °C. The resultant material was analysed by GPC to determine the molar mass: M_n = 7,800 g mol^{-1}, M_w = 15,100 g mol^{-1}, PDI = 1.9 (yield = 0.124 g, 42%).

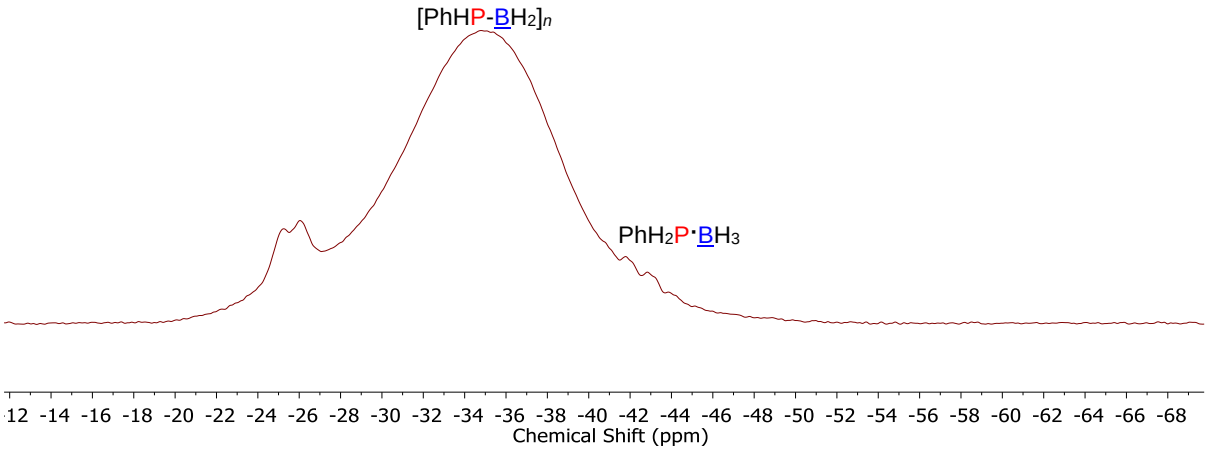

Figure S3.4 In situ ^{11}B NMR spectrum (96 MHz, 25 °C, toluene) of the $B(C_6F_5)_3$ catalysed polymerisation of $PhH_2P{\cdot}BH_3$.

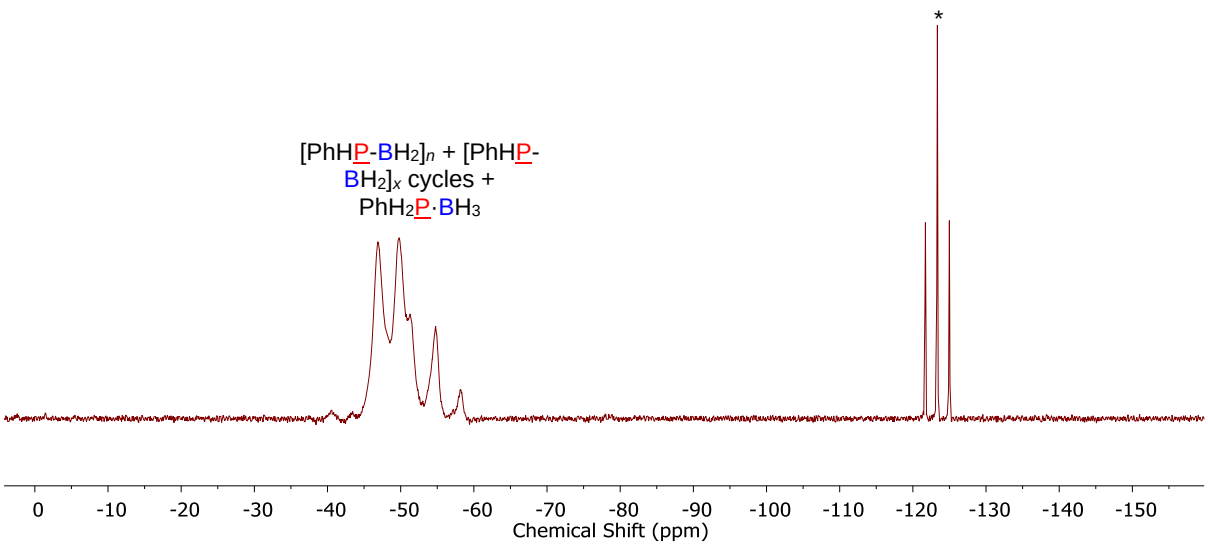

Figure S3.5 In situ ^{31}P NMR spectrum (122 MHz, 25 °C, toluene) of the $B(C_6F_5)_3$ catalysed polymerisation of $PhH_2P{\cdot}BH_3$. Signal corresponding to $PhPH_2$ is denoted by *.

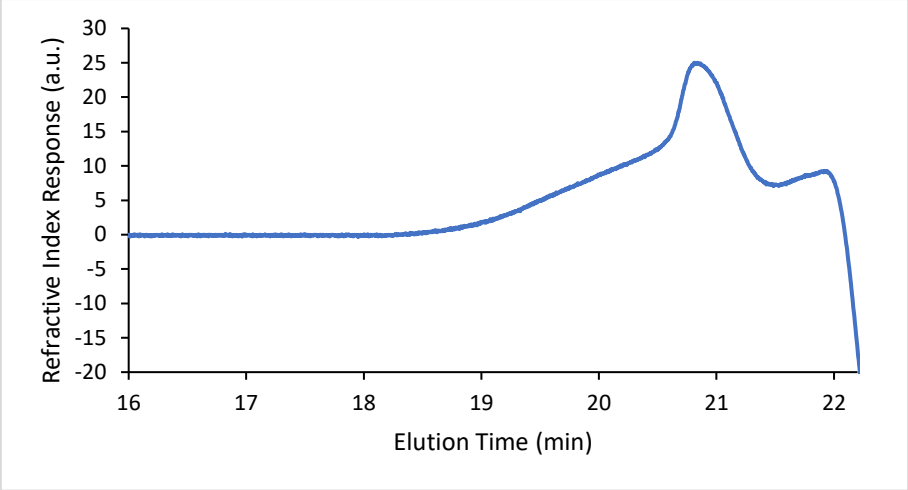

Figure S3.6 GPC chromatogram of material isolated from the $B(C_6F_5)_3$ catalysed polymerisation of $PhH_2P{\cdot}BH_3$ (2 mg mL^{-1} in THF, 0.1 w/w % nBu$_4$NBr in the THF eluent).

3.5.4.3 Reaction of oligo(phenylphosphinoborane) formed using $B(C_6F_5)_3$

To oligo(phenylphosphinoborane) (M_n = 7,800 g mol^{-1}, 61 mg, 0.49 mmol based on monomer) was added $CpFe(CO)_2OTf$ (2 mg, 4.9 × 10^{-3} mmol), and toluene (0.5 mL). The reaction mixture was transferred to a J. Young NMR tube and heated at 100 °C for 18 h, after which, volatiles were removed under vacuum and the residue dried overnight in a vacuum oven at 40 °C. The material was analysed by GPC to determine any molar mass increase from the starting material (Figure S3.7). An analogous thermal reaction was carried out without the addition of catalyst.

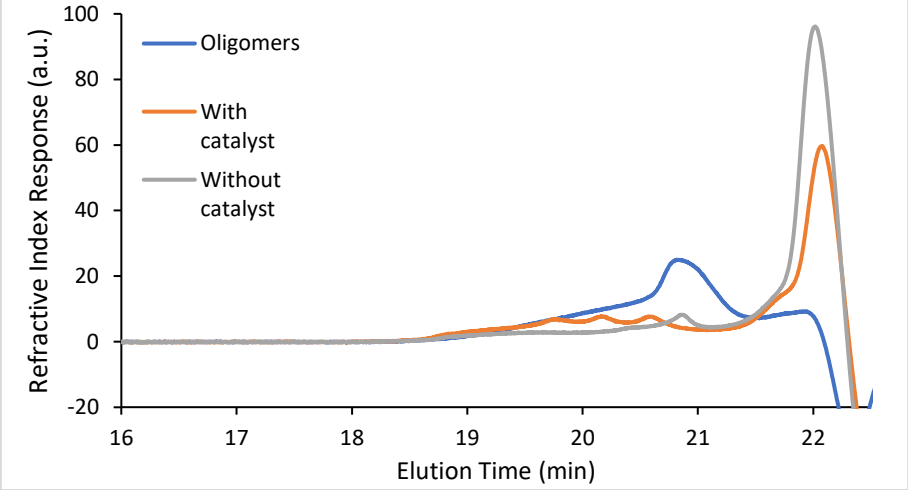

Figure S3.7 GPC chromatograms (2 mg mL^{-1} in THF, 0.1 w/w % nBu$_4$NBr in the THF eluent) showing the molar mass of the materials obtained by $B(C_6F_5)_3$ dehydrocoupling of $PhH_2P{\cdot}BH_3$ (oligomers), the material obtained after heating the oligomers in the presence of $CpFe(CO)_2OTf$ at 100 °C for 18 h (with catalyst), and heating to 100 °C for 18 h in the absence of any $CpFe(CO)_2OTf$ (without catalyst).

3.5.4.4 Synthesis of low molar mass poly(phenylphosphinoborane) using $CpFe(CO)_2I$ as a precatalyst

In a glovebox under a dinitrogen atmosphere, a J. Young flask was charged with $PhH_2P{\cdot}BH_3$ (712 mg, 6 mmol), $CpFe(CO)_2I$ (18.2 mg, 0.06 mmol) and toluene (2 mL, 3 M). The flask was sealed and transferred to a Schlenk manifold and the reaction subsequently heated at 100 °C open to an atmosphere of nitrogen. After 6 h, the reaction mixture was precipitated into cold pentane (−78 °C). Volatiles were removed under vacuum and the residue washed with diethyl ether. The material was determined to be monomer free by ^{11}B NMR analysis. The resultant material was dried under vacuum for 2 d yielding a light grey solid. M_n = 15,000 g mol^{-1}, M_w = 25,500 g mol^{-1}, PDI = 1.7 (yield = 348 mg, 48%).

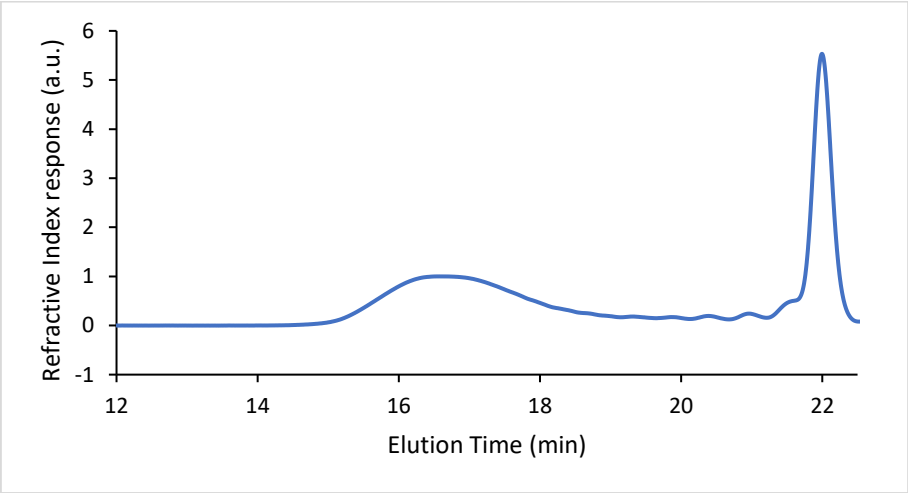

Figure S3.8 GPC chromatogram (2 mg mL^{-1} in THF, 0.1 w/w % nBu$_4$NBr in the THF eluent) of material isolated from the polymerisation of $PhH_2P{\cdot}BH_3$ using $CpFe(CO)_2I$.

3.5.4.5 Reaction of low molar mass poly(phenylphosphinoborane) formed using $CpFe(CO)_2I$

In a glovebox, three vials were each charged with low molar mass $[PhHP\text{-}BH_2]_n$ (M_n = 15,000 g mol^{-1}) 58 mg, 0.48 mmol) formed using $CpFe(CO)_2I$. To the first was added nothing, to the second was added $CpFe(CO)_2OTf$ (8 mg, 0.024 mmol), and to the third was added TfOH (2.1 μL, 0.024 mmol). To each vial was added toluene (0.24 mL, 2 M) and the contents transferred to separate J. Young NMR tubes. The three NMR tubes were heated at 100 °C for 20 h, after which, volatiles were removed under vacuum and the residue dried overnight in a vacuum oven at 40 °C. A GPC was taken of this material to determine any molar mass increase from the starting material. The molar masses are given in Table S3.1.

Table S3.1 Molar mass (M_n) and polydispersity of $[PhHP\text{-}BH_2]_n$ obtained from the polymerisation of $PhH_2P{\cdot}BH_3$ using $CpFe(CO)_2I$ and subsequent reactions using this material.

Reaction	**M_n (g mol^{-1})**	**PDI**
Oligo(phenylphosphinoborane) formed using $CpFe(CO)_2I$	15,000	1.7
Thermal	83,400	3.8
$CpFe(CO)_2OTf$	54,100	1.8
TfOH	17,000	2.6

3.5.5 Polymerisation of phenylphosphine-borane using proton sponge®

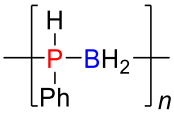

In a glovebox, a J. Young NMR tube was charged with $PhH_2P{\cdot}BH_3$ (0.1 mmol) and proton sponge® stock solution in toluene (0.5 ml, 0.01 M, 5 mol%). The NMR tube was sealed and heated to 100 °C. The reaction was monitored by ^{31}P NMR spectroscopy. After 1 d, volatiles were removed under vacuum and the molar mass of the residue determined by GPC: M_n = 4,700 g mol^{-1}, M_w =10,400 g mol^{-1}, PDI = 2.2.

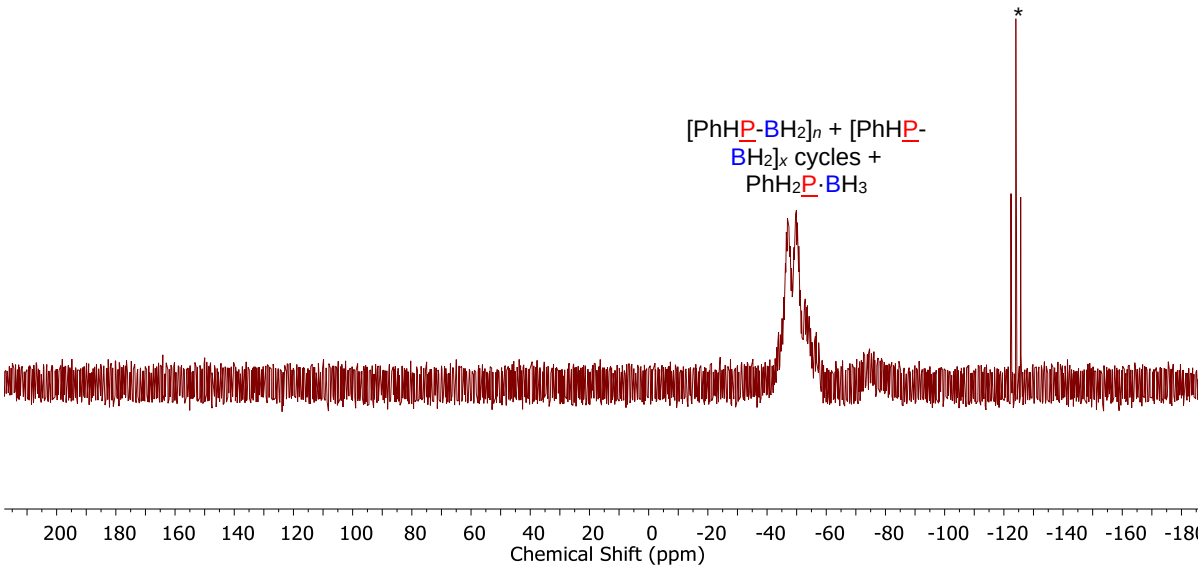

Figure S3.9 In situ ^{31}P NMR spectrum (122 MHz, 25 °C, toluene) after the dehydrocoupling of $PhH_2P{\cdot}BH_3$ using proton sponge®. Signal corresponding to $PhPH_2$ are denoted by *.

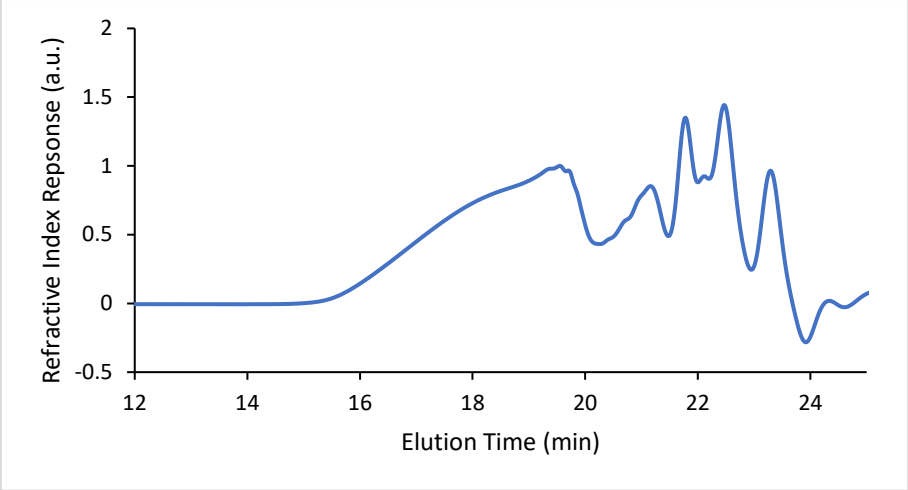

Figure S3.10 GPC chromatogram (2 mg mL^{-1} in THF, 0.1 w/w % *n*Bu$_4$NBr in the THF eluent) of material isolated from the dehydrocoupling reaction of PhH$_2$P·BH$_3$ in the presence of proton sponge®.

3.5.6 Larger scale synthesis of poly(phenylphosphinoborane) using triflic acid

Under a dinitrogen atmosphere PhH$_2$P·BH$_3$ (496 mg, 4 mmol) was dissolved in toluene (2 mL). Directly to this solution, HOTf (17 μL, 0.2 mmol, 5 mol%) was added. The colourless reaction mixture was transferred to a Schlenk flask and heated at 100 °C open to an atmosphere of nitrogen. After 2 d, volatiles were removed under vacuum and the residue dissolved in DCM and precipitated into pentane at −78 °C. The resultant material was dried under vacuum for 2 d yielding a colourless solid (yield = 0.37 g, 75%). NMR data matched those previously reported for [PhHP-BH$_2$]$_n$.

GPC: M_n = 5,200 g mol^{-1}, M_w = 12,600 g mol^{-1}, PDI = 2.4).

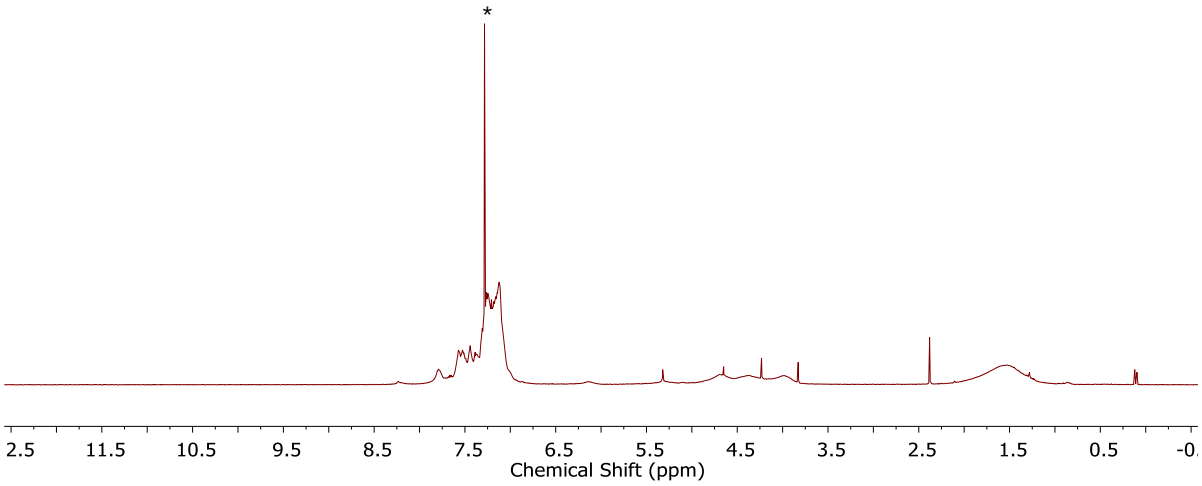

Figure S3.11 ^{1}H NMR (300 MHz, CDCl$_3$) of isolated [PhHP-BH$_2$]$_n$ formed using TfOH catalyst. Deuterated chloroform residual signal denoted by *.

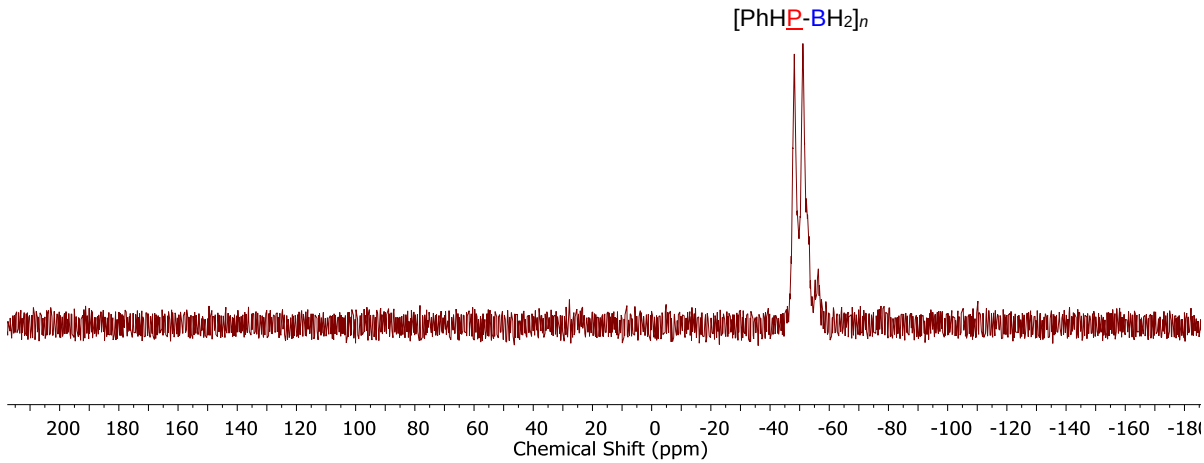

Figure S3.12 ^{31}P NMR (122 MHz, 25 °C, $CDCl_3$) of isolated $[PhHP\text{-}BH_2]_n$ formed using TfOH catalyst.

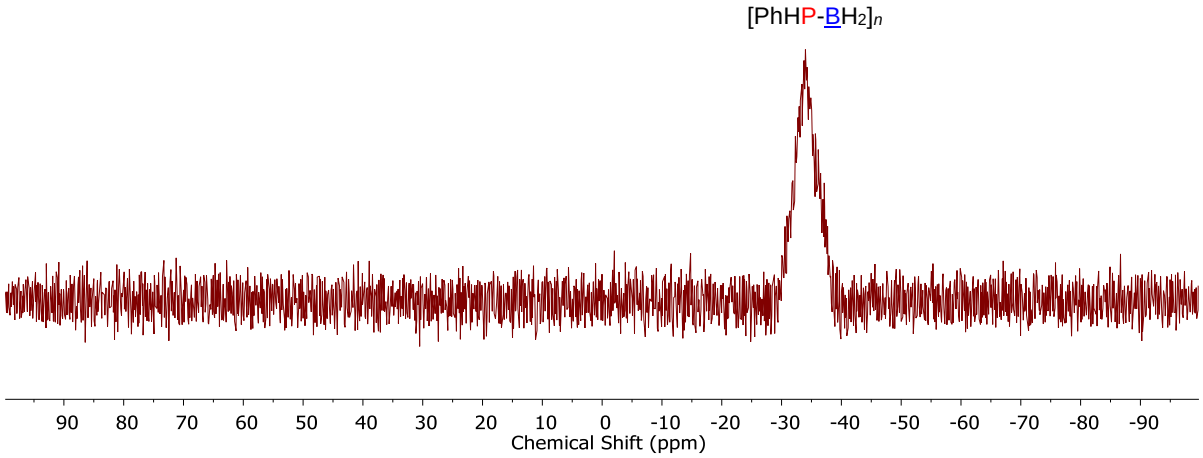

Figure S3.13 ^{11}B NMR (96 MHz, 25 °C, $CDCl_3$) of isolated $[PhHP\text{-}BH_2]_n$ formed using TfOH catalyst.

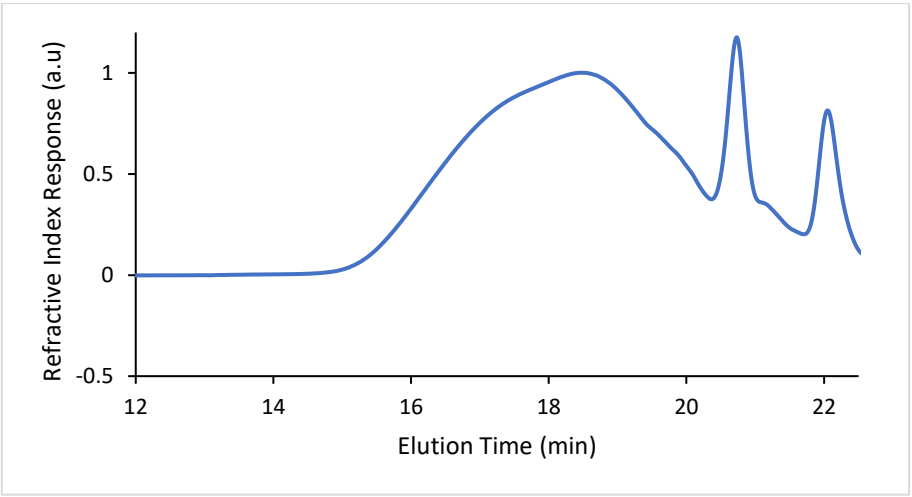

Figure S3.14 GPC chromatogram ((2 mg mL^{-1} in THF, 0.1 w/w % nBu$_4$NBr in the THF eluent)) of isolated $[PhHP\text{-}BH_2]_n$ formed using TfOH catalyst.

3.5.7 Synthesis of poly(tert-butylphosphinoborane) using triflic acid

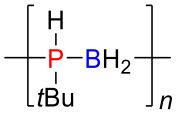

Under a dinitrogen atmosphere 1 mmol of *t*BuH$_2$P·BH$_3$ was dissolved in 0.5 mL of toluene. Directly to this solution, 8 μL of HOTf (10 mol %) was added. The colourless reaction mixture was transferred to a J. Young NMR tube, sealed, and heated at 100 °C in an oil bath. The conversion was monitored by ^{31}P and ^{11}B NMR spectroscopy. Upon complete consumption of monomer (64 h), the J. Young tube was opened in air carefully to vent H_2 generated in the dehydropolymerisation reaction, and the solvent was removed by rotary evaporation. The crude colourless residue was dissolved in CH_2Cl_2 (0.5 mL) and washed with a 0.1 M $NaHCO_3$ solution, the organic phase was separated and dried over a short pad of $MgSO_4$ within a glass microfiber plugged pipette and was eluted with CH_2Cl_2 (5 mL), afterwards the solvent was removed by rotary evaporation and the pale yellow to colourless solid polymeric product was dried under vacuum for 24 h followed by in 40 °C vacuum oven for 24 h. NMR data matched those previously reported for poly(*t*-butylphosphinoborane).

GPC: M_n = 15,000 g mol^{-1}, M_w = 26,200 g mol^{-1}, PDI = 1.7.

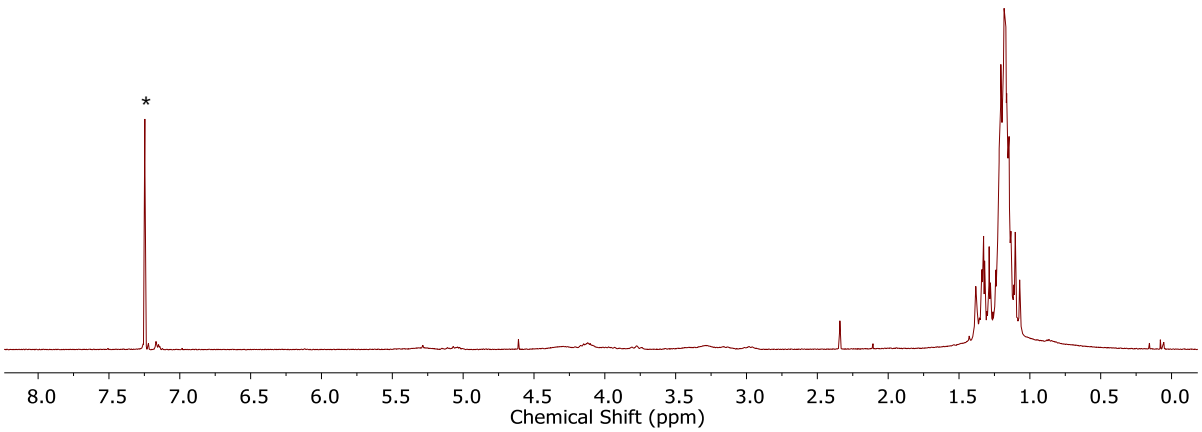

Figure S3.15 ^{1}H NMR (400 MHz, 25 °C, $CDCl_3$) of isolated [*t*BuHP-BH$_2$]$_n$. Deuterated chloroform residual signal denoted by *.

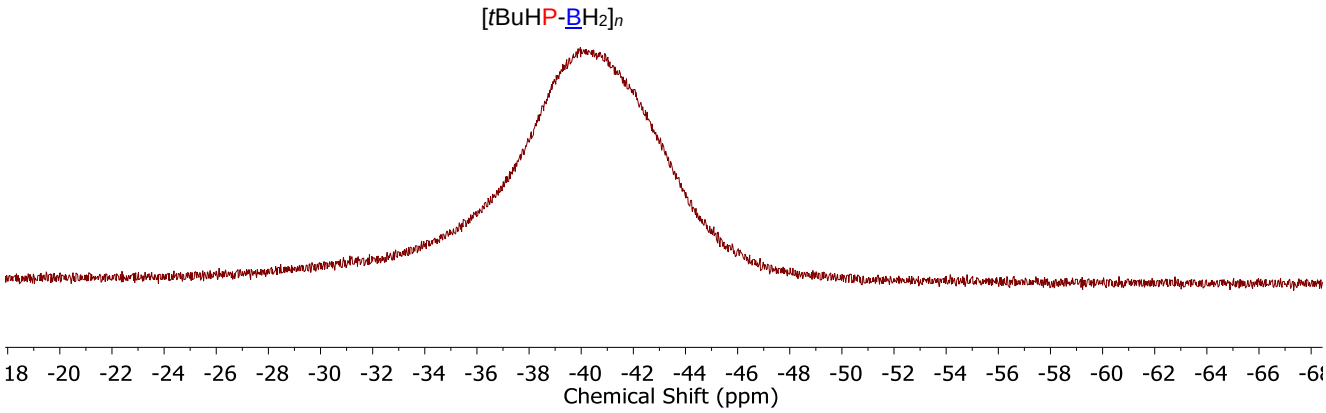

Figure S3.16 ^{11}B NMR (96 MHz, 25 °C, $CDCl_3$) of isolated [*t*BuHP-BH_2]$_n$.

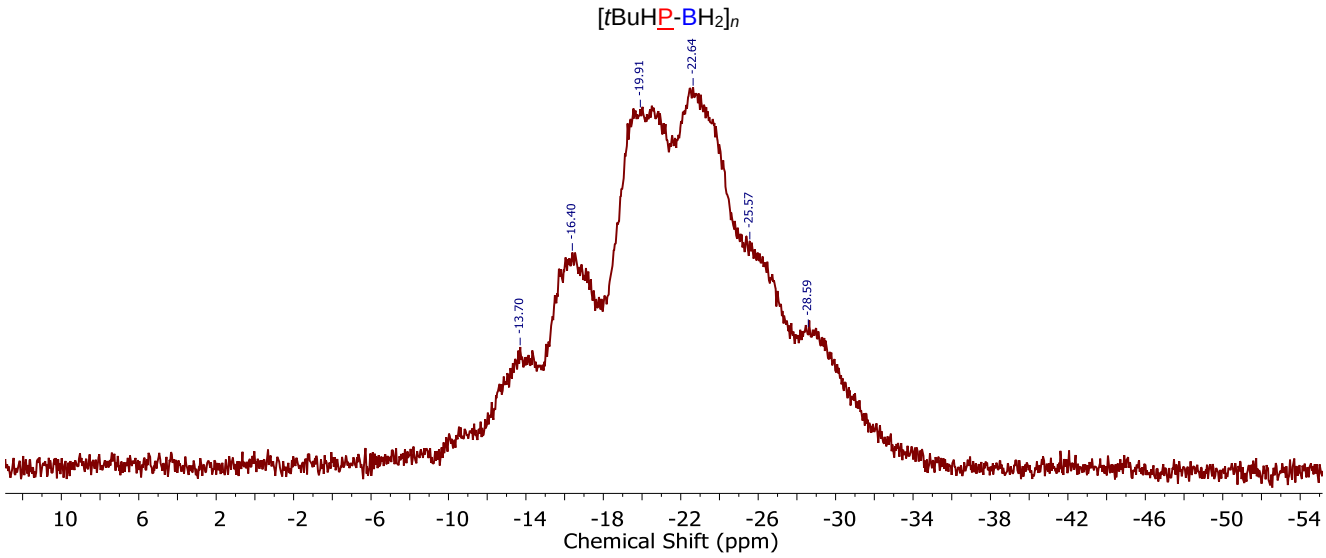

Figure S3.17 ^{31}P NMR (122 MHz, 25 °C, $CDCl_3$) of isolated [*t*BuHP-BH_2]$_n$.

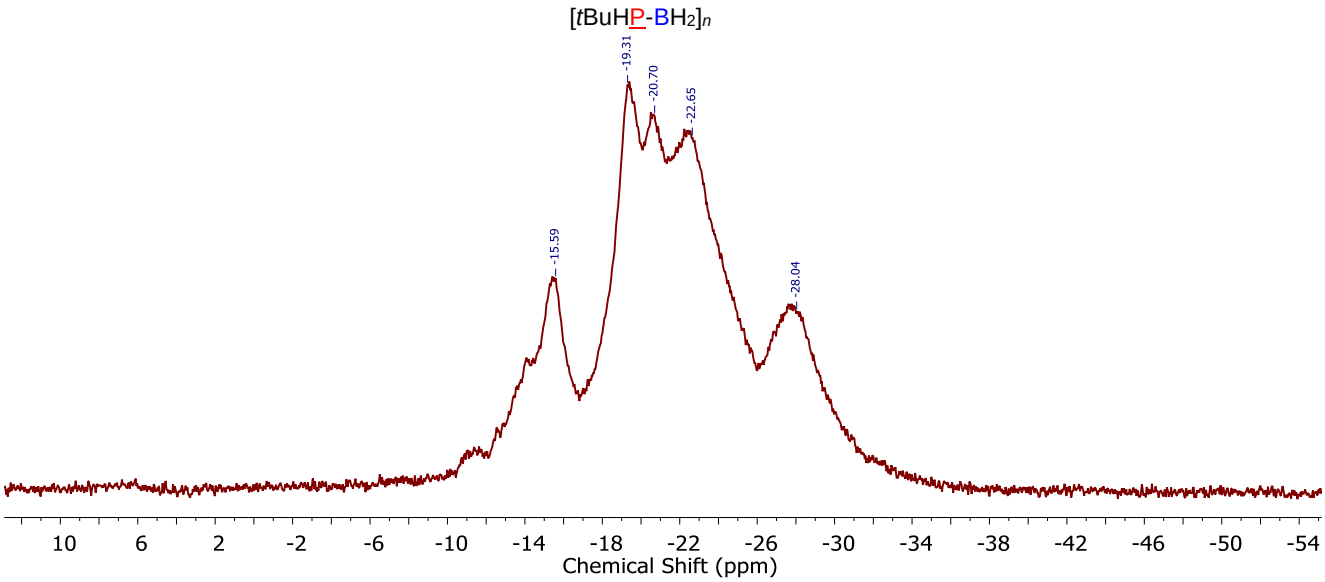

Figure S3.18 $^{31}P\{H\}$ NMR (122 MHz, 25 °C, $CDCl_3$) of isolated $[t\text{BuHP-BH}_2]_n$.

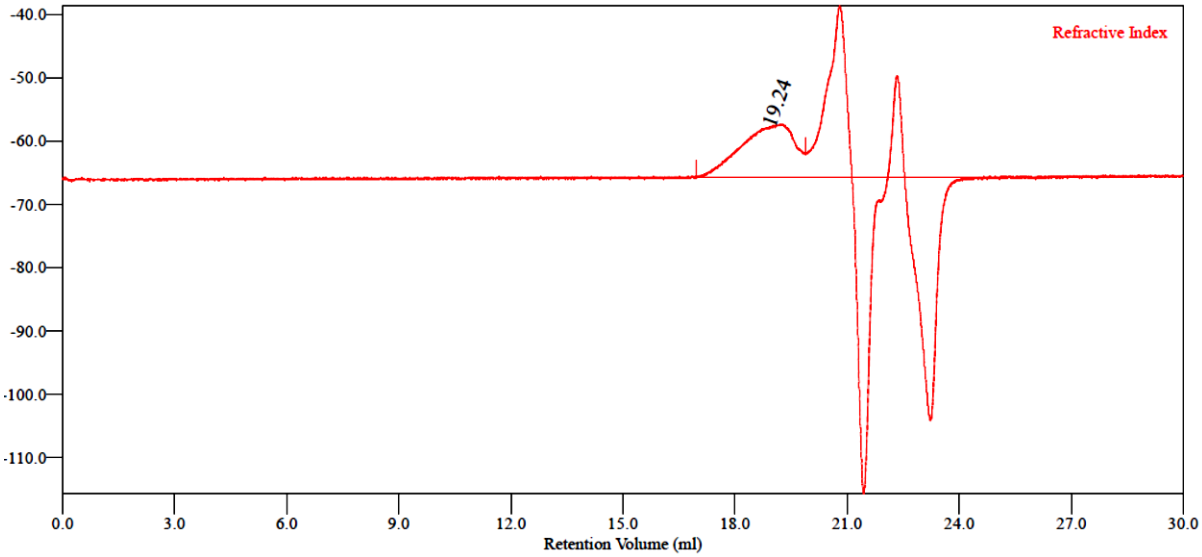

Figure S3.19 GPC chromatogram (2 mg mL^{-1} in THF, 0.1 w/w % $n\text{Bu}_4\text{NBr}$ in the THF eluent) of isolated $[t\text{BuHP-BH}_2]_n$.

3.5.8 Synthesis of poly(*n*-hexylphosphinoborane) using triflic acid

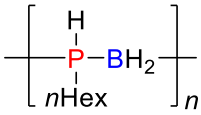

Under a dinitrogen atmosphere 4 mmol of $n\text{HexH}_2\text{P}\cdot\text{BH}_3$ (528 mg, 4 mmol) was dissolved in 2 mL of toluene, directly to this solution was added HOTf (17.7 µL, 0.2 mmol). The pale-yellow reaction mixture was transferred to a J. Young flask and heated at 100 °C under an atmosphere of nitrogen. The

conversion was monitored by ^{11}B NMR and ^{31}P spectroscopy. After 5 d, the reaction was stopped (ca. 75% consumption of the monomer). Volatiles were removed under vacuum and the reaction mixture was dissolved in a small amount of THF (ca. 1 mL) and precipitated into 50 mL water/isopropanol (v/v 1:1). The material was dried under vacuum for 2 d. This yielded a colourless gummy solid.

GPC: M_n = 6,400 g mol^{-1}, M_w = 15,700, PDI = 2.5.

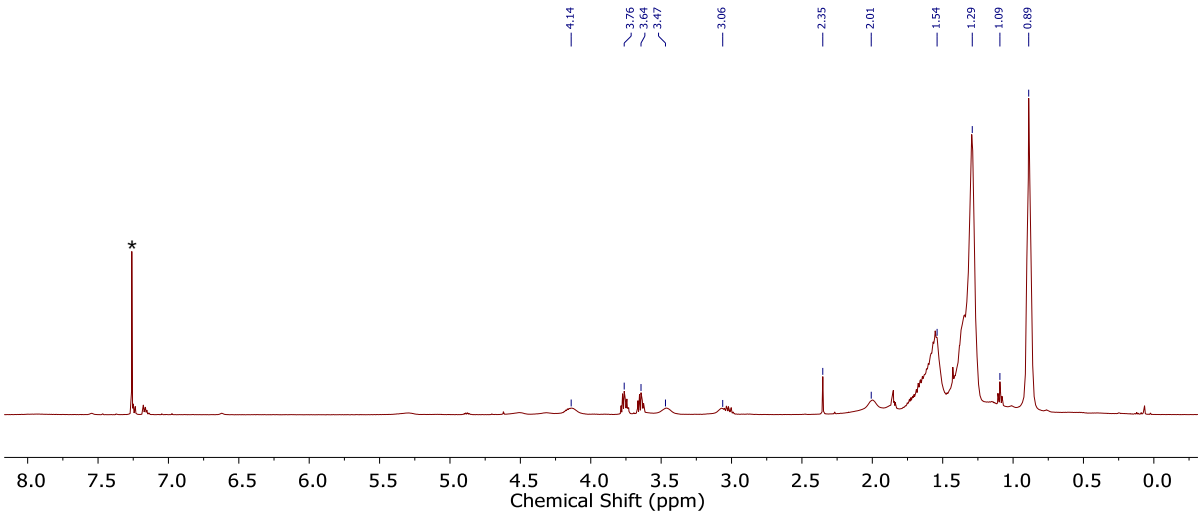

Figure S3.20 ^{1}H NMR spectrum (500 MHz, 25 °C, $CDCl_3$) of material isolated from the dehydrocoupling of *n*HexH_2P·BH_3 using TfOH. Deuterated chloroform residual signal denoted by *.

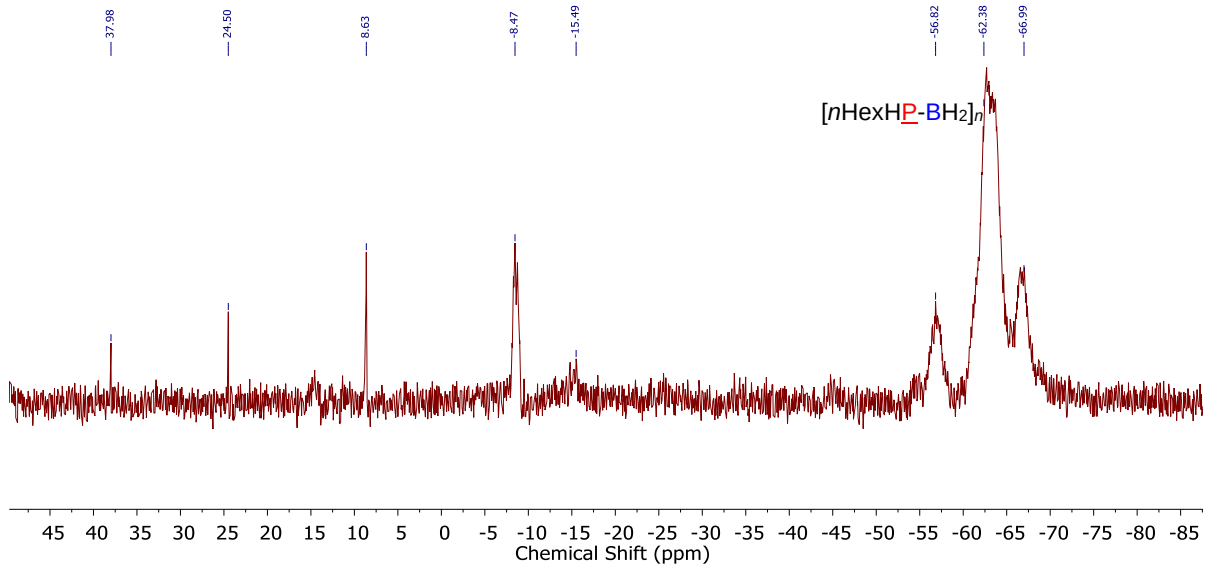

Figure S3.21 ^{31}P{H} NMR (203 MHz, 25 °C, $CDCl_3$) spectrum of material isolated from the dehydrocoupling of *n*HexH_2P·BH_3 using TfOH.

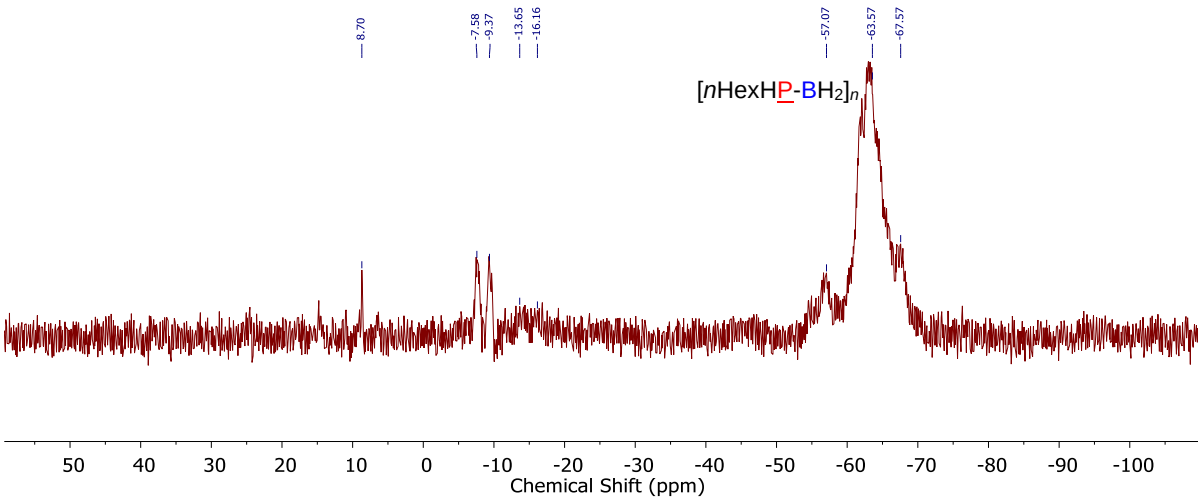

Figure S3.22 ^{31}P NMR spectrum (203 MHz, 25 °C, $CDCl_3$) of material isolated from the dehydrocoupling of *n*HexH_2P·BH_3 using TfOH.

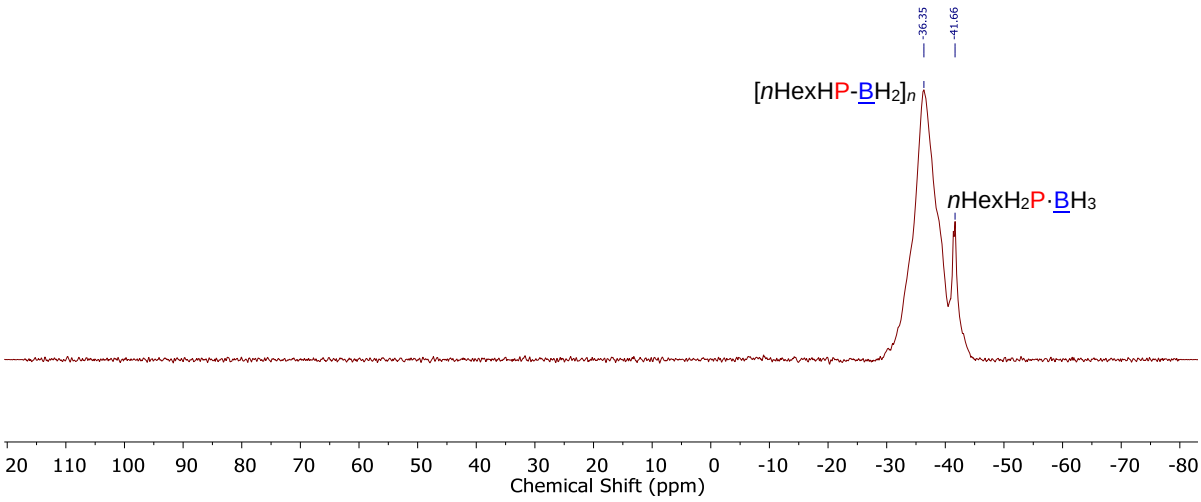

Figure S3.23 ^{11}B{H} NMR spectrum (161 MHz, 25 °C, $CDCl_3$) of material isolated from the dehydrocoupling of *n*HexH_2P·BH_3 using TfOH.

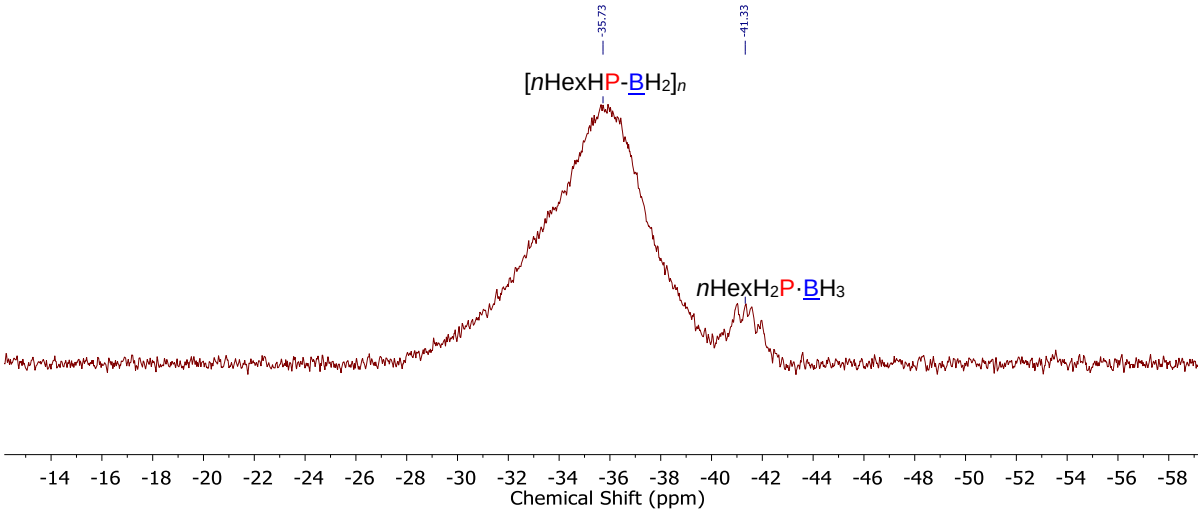

Figure S3.24 ^{11}B NMR spectrum (161 MHz, 25 °C, $CDCl_3$) of material isolated from the dehydrocoupling of *n*$HexH_2P{\cdot}BH_3$ using TfOH.

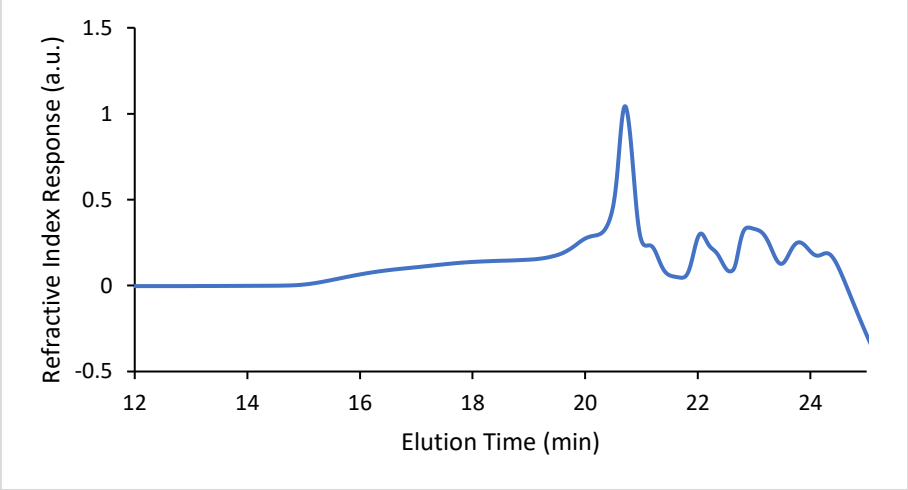

Figure S3.25 GPC chromatogram (2 mg mL^{-1} in THF, 0.1 w/w % *n*Bu_4NBr in the THF eluent) of material isolate from the dehydrocoupling of *n*$HexH_2P{\cdot}BH_3$ using TfOH.

3.5.9 Dehydrocoupling of $Et_2HP{\cdot}BH_3$ to the Linear Dimer $Et_2HP{\cdot}BH_2{-}PEt_2{\cdot}BH_3$, and Minor Amounts of Oligomeric $[Et_2P{-}BH_2]_x$.

In a glovebox, $Et_2HP{\cdot}BH_3$ (1 mmol, 104 mg), was dissolved in 400 µL of toluene. To the phosphine−borane solution 100 µL of a stock solution of $[CpFe(CO)_2(OTf)]$ in toluene (0.1 M) was added. The initially red-orange reaction mixture was transferred to a J. Young NMR tube, sealed, and removed from the glovebox and heated to 100 °C after which the reaction mixture changed color to yellow. After heating at 100 °C for 14 days the conversion as determined by $^{31}P\{^1H\}$ NMR spectroscopy was ca. 30% and the volatiles including unreacted $Et_2HP{\cdot}BH_3$ were then removed under vacuum for 3 days to obtain 10 mg (~10% yield) of yellow oily product mixture. The product mixture was analyzed

by ^{1}H, ^{11}B, ^{13}C and ^{31}P NMR spectroscopy indicating the formation of primarily linear dimer $Et_2HP{\cdot}BH_2{-}PEt_2{\cdot}BH_3$, ESI-MS revealed minor amounts of low molecular weight oligomers $[Et_2P{-}BH_2]_x$, and GPC revealed that no high molecular weight polymer is formed.

Spectroscopic analysis:

^{1}H NMR (500 MHz, $CDCl_3$): δ (ppm) 4.76 (d, *J* = 380 Hz, 1H, $(CH_3CH_2)_2\mathit{H}P{\cdot}BH_2$-$P(CH_2CH_3)_2{\cdot}BH_3$), 1.96 (br d, *J* = 40.5 Hz 4H, $(CH_3C\mathit{H_2})_2HP{\cdot}BH_2$-$P(CH_2CH_3)_2{\cdot}BH_3$)), 1.56 – 1.43 (m, 4H, $(CH_3CH_2)_2HP{\cdot}BH_2$-$P(C\mathit{H_2}CH_3)_2{\cdot}BH_3$)), 1.31 – 1.19 (m, *J* = 15.0, 7.0 Hz, 6H, $(C\mathit{H_3}CH_2)_2HP{\cdot}BH_2$–$P(CH_2CH_3)_2{\cdot}BH_3$)), 1.16 – 1.03 (m, 6H, $CH_3CH_2)_2HP{\cdot}BH_2$-$P(CH_2C\mathit{H_3})_2{\cdot}BH_3$)), 0.42 (br q, *J* = 88.0 Hz, 3H, $(CH_3CH_2)_2HP{\cdot}BH_2$-$P(CH_2CH_3)_2{\cdot}B\mathit{H_3}$)).

Peaks corresponding to internal BH_2 are hidden under alkyl-derived peaks and could not be located.

$^{11}B\{^{1}H\}$ NMR (161 MHz, $CDCl_3$): δ (ppm) −37.5 (t, *J* = 77.0 Hz, $Et_2HP{\cdot}\mathit{B}H_2$-$PEt_2{\cdot}BH_3$), −38.9 (d, *J* = 64.0 Hz, $Et_2HP{\cdot}BH_2$-$PEt_2{\cdot}\mathit{B}H_3$).

^{11}B NMR (161 MHz, $CDCl_3$): δ (ppm) −33.4 – −39.9 (br m).

$^{31}P\{^{1}H\}$ NMR (203 MHz, $CDCl_3$): δ (ppm) −2.2 – −3.2 (m, $Et_2H\mathit{P}{\cdot}BH_2$-$PEt_2{\cdot}BH_3$), −26.7 (m, $Et_2HP{\cdot}BH_2$-$\mathit{P}Et_2{\cdot}BH_3$).

^{31}P NMR (203 MHz, $CDCl_3$): δ (ppm) −0.43 – −4.78 (m, *J* = 384.5 Hz, $Et_2H\mathit{P}{\cdot}BH_2$-$PEt_2{\cdot}BH_3$), −26.7 (m, $Et_2HP{\cdot}BH_2$-$\mathit{P}Et_2{\cdot}BH_3$).

$^{13}C\{^{1}H\}$ NMR (126 MHz, $CDCl_3$): δ (ppm) 18.16 (dd, *J* = 33.5 Hz, $(CH_3CH_2)_2HP{\cdot}BH_2$-$P(\mathit{C}H_2CH_3)_2{\cdot}BH_3$), 12.45 (dd, *J* = 38.5 Hz, $(CH_3\mathit{C}H_2)_2HP{\cdot}BH_2$-$P(CH_2CH_3)_2{\cdot}BH_3$), 8.68 (d, *J* = 5 Hz, $(CH_3\mathit{C}H_2)_2HP{\cdot}BH_2$-$P(CH_2CH_3)_2{\cdot}BH_3$)), 7.90 (d, *J* = 3 Hz, $(CH_3CH_2)_2HP{\cdot}BH_2$-$P(CH_2\mathit{C}H_3)_2{\cdot}BH_3$)).

Attempted characterization of higher oligomers/polymer:

GPC (2 mg mL^{-1}): Peak is below the limit of the lowest molecular weight polystyrene standard (2,300 g mol^{-1}).

ESI-MS: Difference of 102 m/z ($[Et_2P{-}BH_2]$ subunit) confirms presence of linear oligo(diethylphosphinoborane) with a phosphine end group $[H{-}[Et_2P{-}BH_2]_x{-}PHEt_2]^+$ up to 5 repeat units.

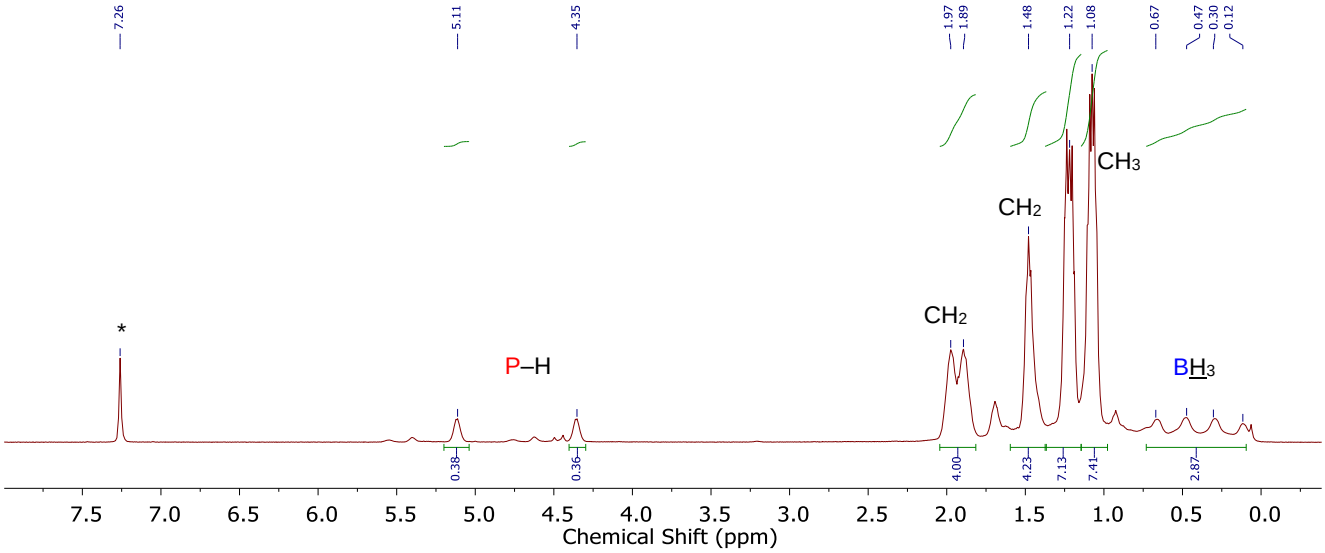

Figure S3.26 ^{1}H NMR spectrum (500 MHz, 25 °C, $CDCl_3$) of the product mixture from dehydrocoupling of $Et_2HP{\cdot}BH_3$ yielding mostly linear dimer $Et_2HP{\cdot}BH_2$-$PEt_2{\cdot}BH_3$. Deuterated chloroform residual signal denoted by *.

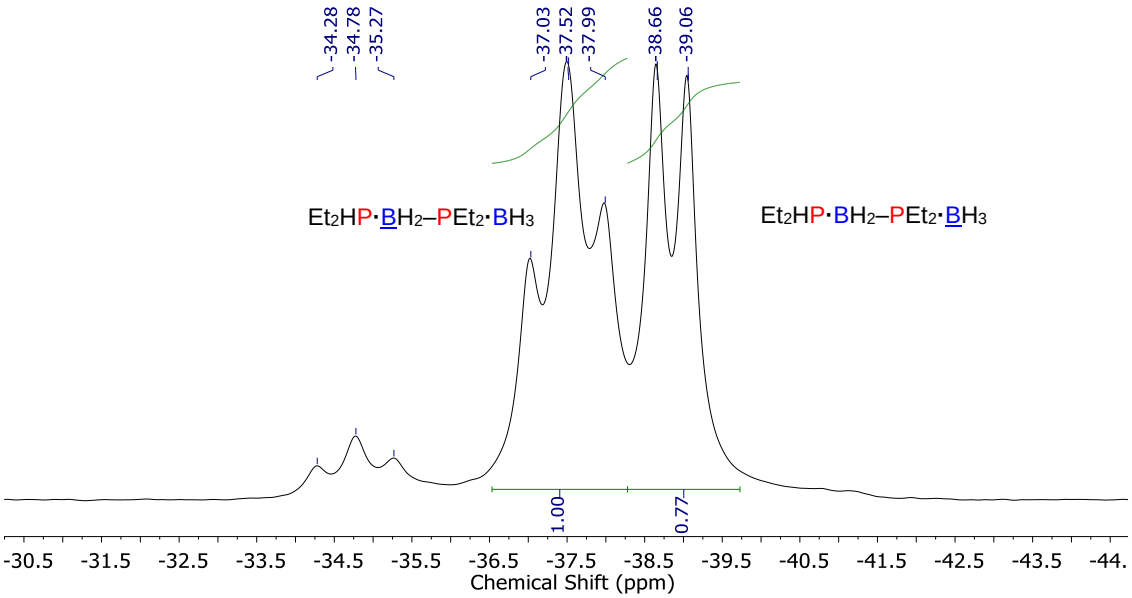

Figure S3.27 ^{11}B{H} NMR spectra (161 MHz, 25 °C, $CDCl_3$) of the product mixture from dehydrocoupling of $Et_2HP{\cdot}BH_3$ yielding mostly linear dimer $Et_2HP{\cdot}BH_2$-$PEt_2{\cdot}BH_3$.

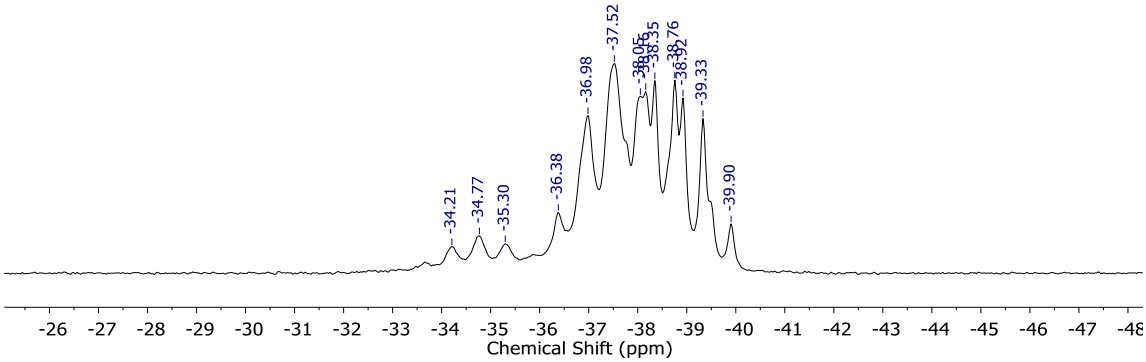

Figure S3.28 ^{11}B NMR spectra (161 MHz, 25 °C, $CDCl_3$) of the product mixture from dehydrocoupling of $Et_2HP{\cdot}BH_3$ yielding mostly linear dimer $Et_2HP{\cdot}BH_2$-$PEt_2{\cdot}BH_3$.

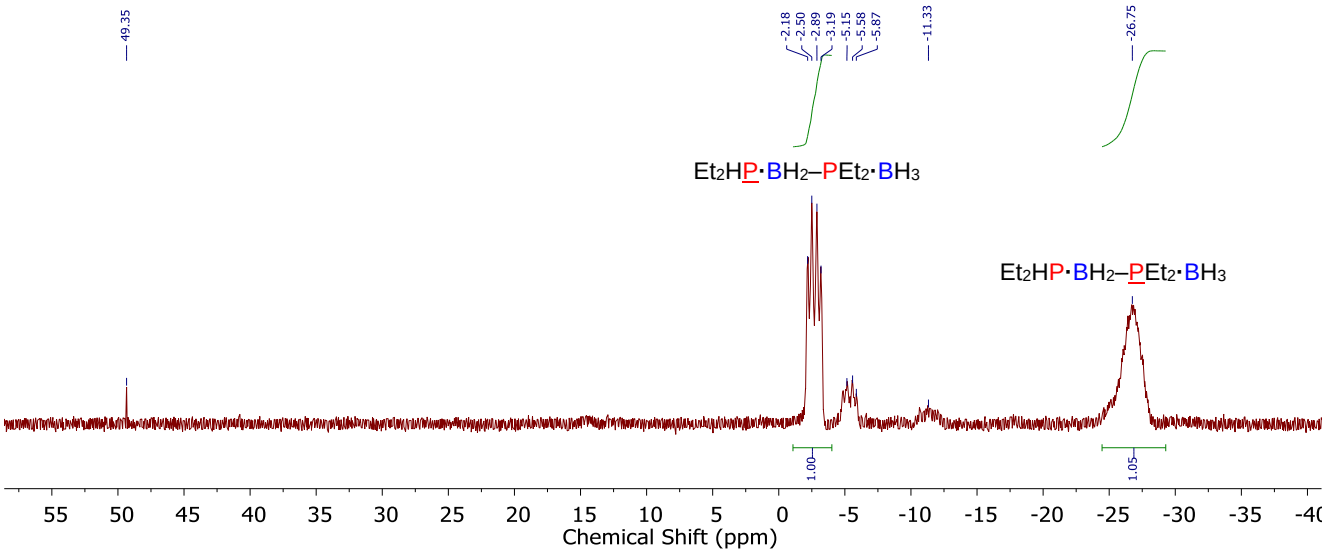

Figure S3.29 $^{31}P\{H\}$ NMR spectra (203 MHz, 25 °C, $CDCl_3$) of the product mixture from dehydrocoupling of $Et_2HP{\cdot}BH_3$ yielding mostly linear dimer $Et_2HP{\cdot}BH_2$-$PEt_2{\cdot}BH_3$.

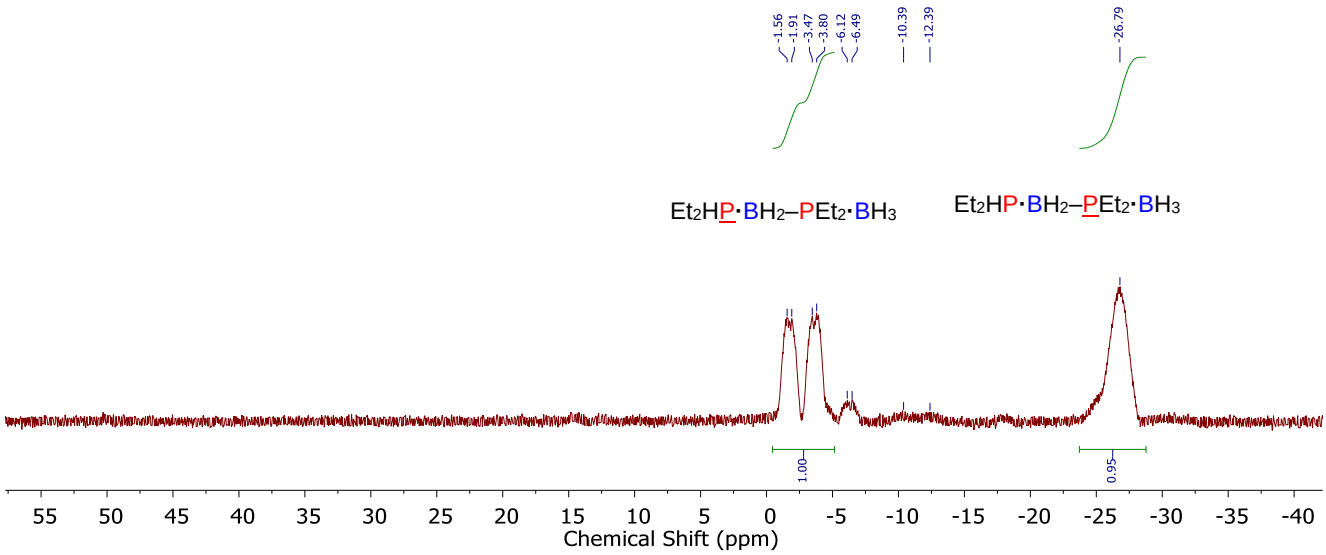

Figure S3.30 ^{31}P NMR spectra (203 MHz, 25 °C, $CDCl_3$) of the product mixture from dehydrocoupling of $Et_2HP{\cdot}BH_3$ yielding mostly linear dimer $Et_2HP{\cdot}BH_2$-$PEt_2{\cdot}BH_3$.

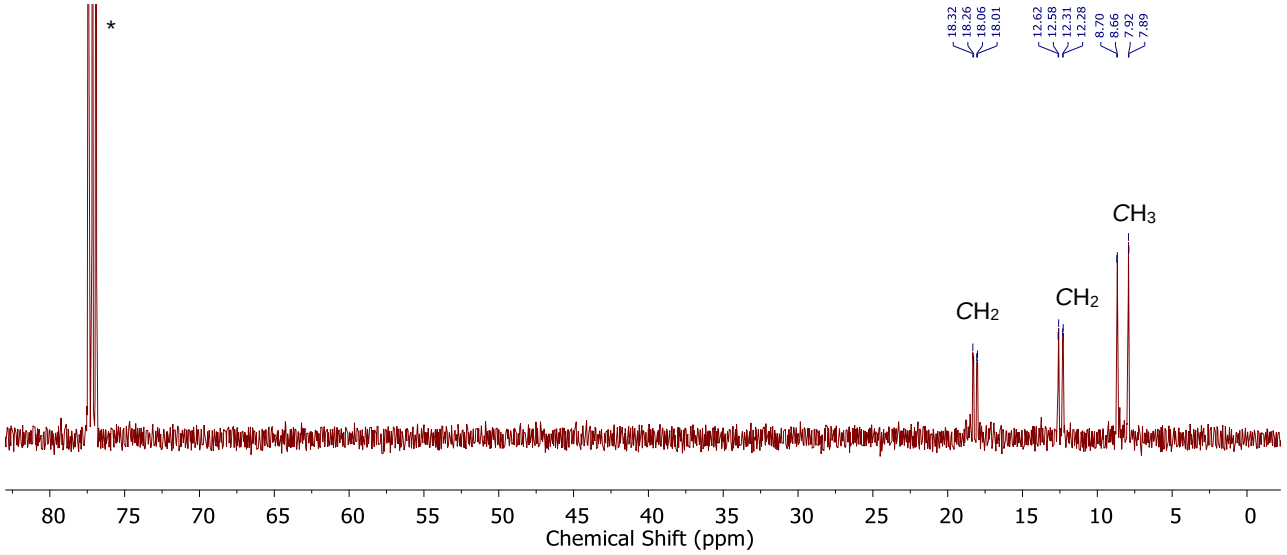

Figure S63. $^{13}C\{^1H\}$ NMR spectrum (126 MHz, 25 °C, $CDCl_3$) of the product mixture from dehydrocoupling of $Et_2HP{\cdot}BH_3$ yielding mostly linear dimer $Et_2HP{\cdot}BH_2$-$PEt_2{\cdot}BH_3$. Deuterated chloroform residual signal denoted by *.

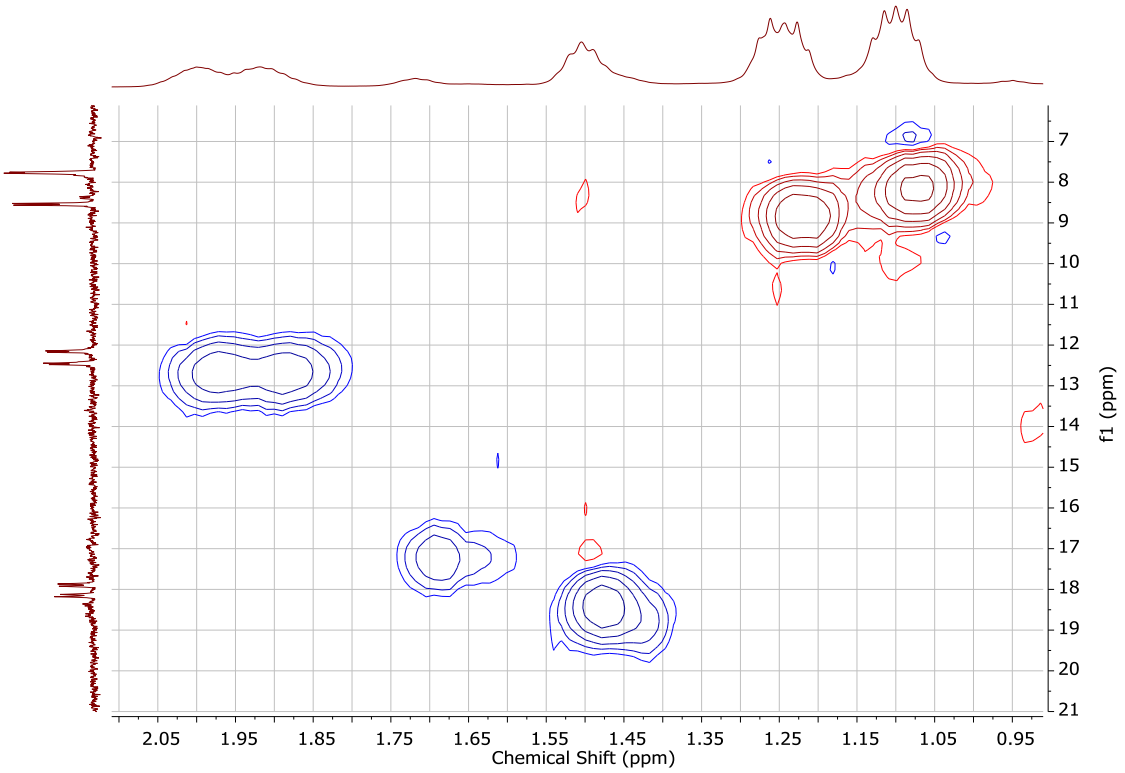

Figure S3.31 $^{1}H,^{13}C$-HSQC NMR spectrum of the product mixture from dehydrocoupling of $Et_2HP{\cdot}BH_3$ yielding mostly linear dimer $Et_2HP{\cdot}BH_2$-$PEt_2{\cdot}BH_3$.

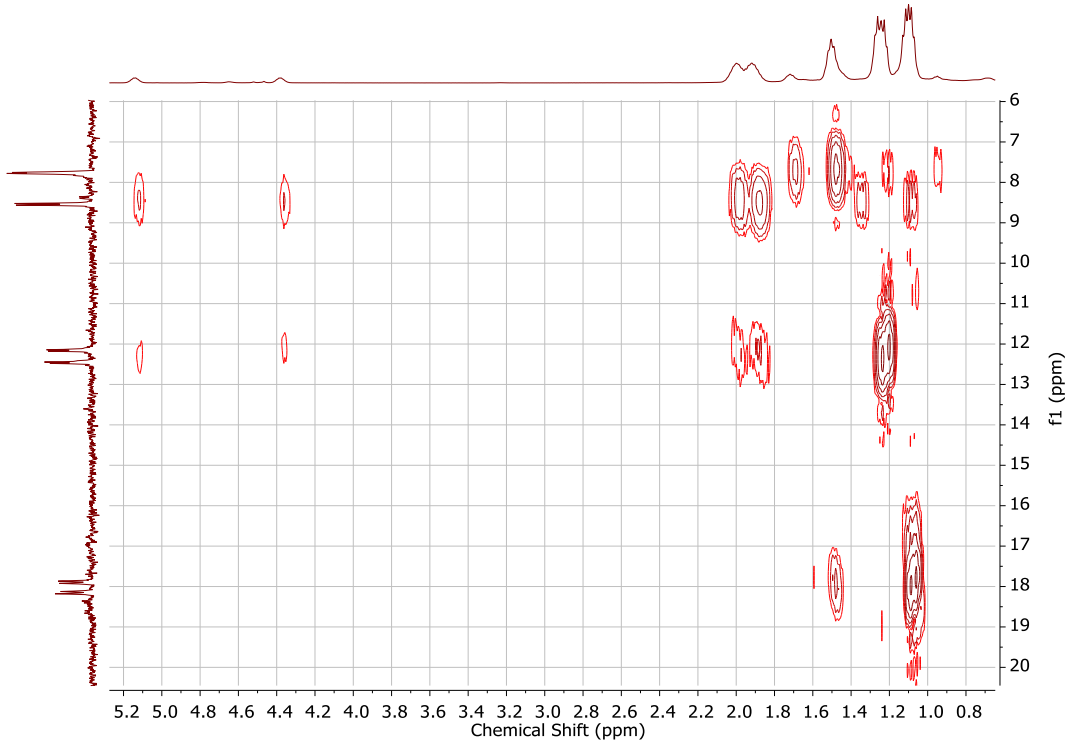

Figure S3.32 $^{1}H,^{13}C$-HMBC NMR spectrum of the product mixture from dehydrocoupling of $Et_2HP{\cdot}BH_3$ yielding mostly linear dimer $Et_2HP{\cdot}BH_2$-$PEt_2{\cdot}BH_3$.

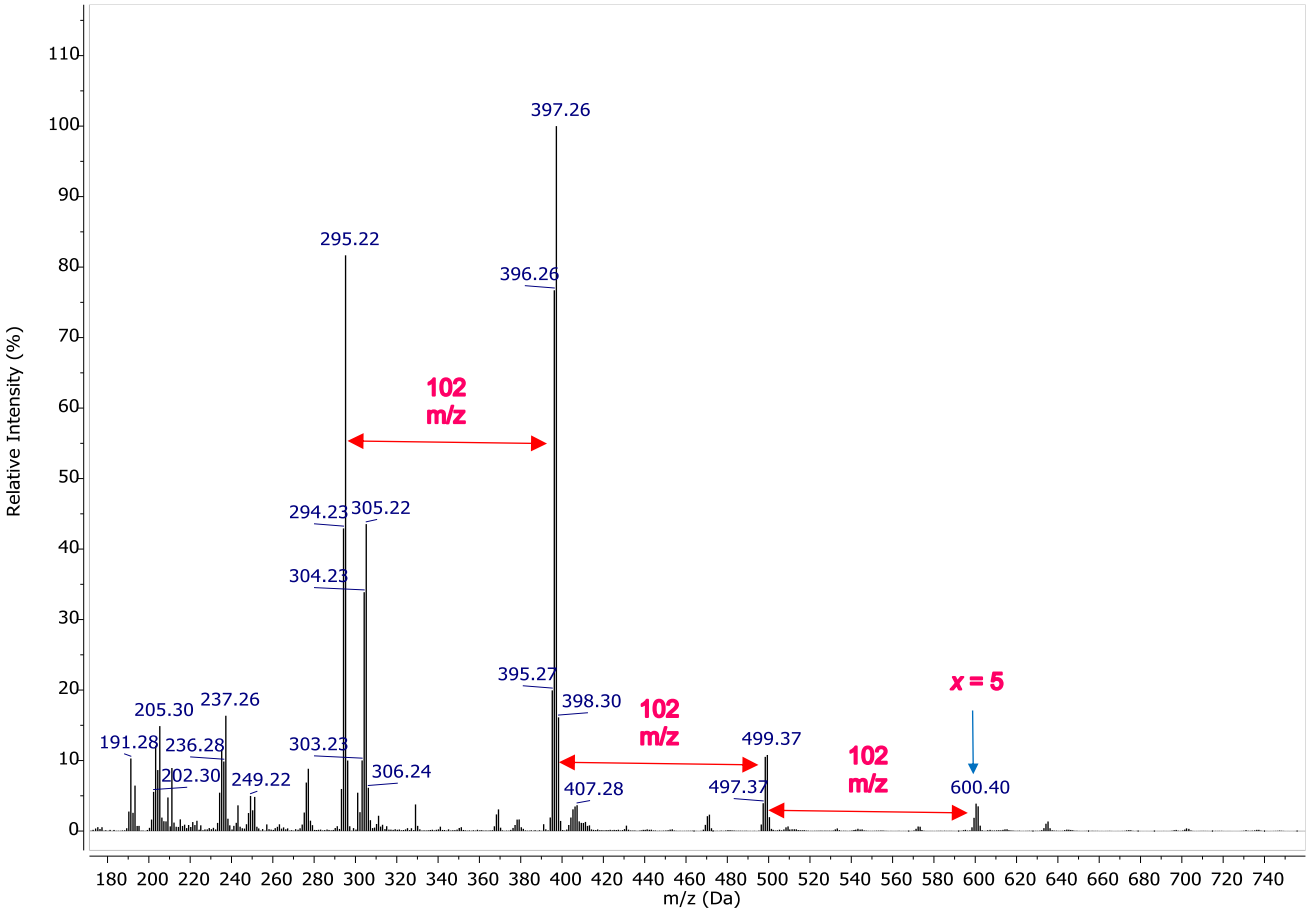

Figure S3.33 ESI-MS (1 mg mL^{-1} in CH_2Cl_2) in positive mode of $[Et_2P–BH_2]_x$ oligomers present in sample containing primarily linear dimer $Et_2HP{\cdot}BH_2$-$PEt_2{\cdot}BH_3$.

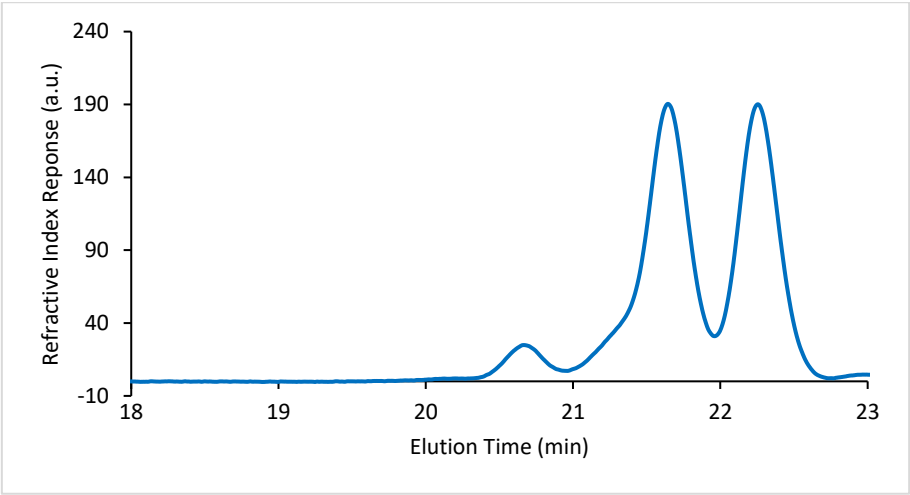

Figure S3.34 GPC chromatogram (2 mg mL^{-1} in THF, 0.1 w/w % nBu$_4$NBr in the THF eluent) of the product mixture from the dehydrocoupling of $Et_2HP{\cdot}BH_3$ in THF. Molar mass of $[Et_2P–BH_2]_x$ oligomers is below the limit of the lowest molecular weight polystyrene standard (2,300 g mol^{-1}).

3.5.10 Attempted dehydrocoupling of $Et_2HP{\cdot}BH_3$ using triflic acid

In a glovebox, a J. Young NMR tube was charged with $Et_2HP{\cdot}BH_3$ (0.1 mmol), TfOH (5 mol%), and toluene (0.5 mL). The NMR tube was sealed and heated to 100 °C. After 10 d, analysis of the reaction

by ^{31}P NMR spectroscopy showed signals that correspond to formation linear dimer (ca. 60% of total ^{31}P integration), along with significant amount of starting material remained (ca. 25% total ^{31}P integration), and a number of other signals. This reaction was not pursued further.

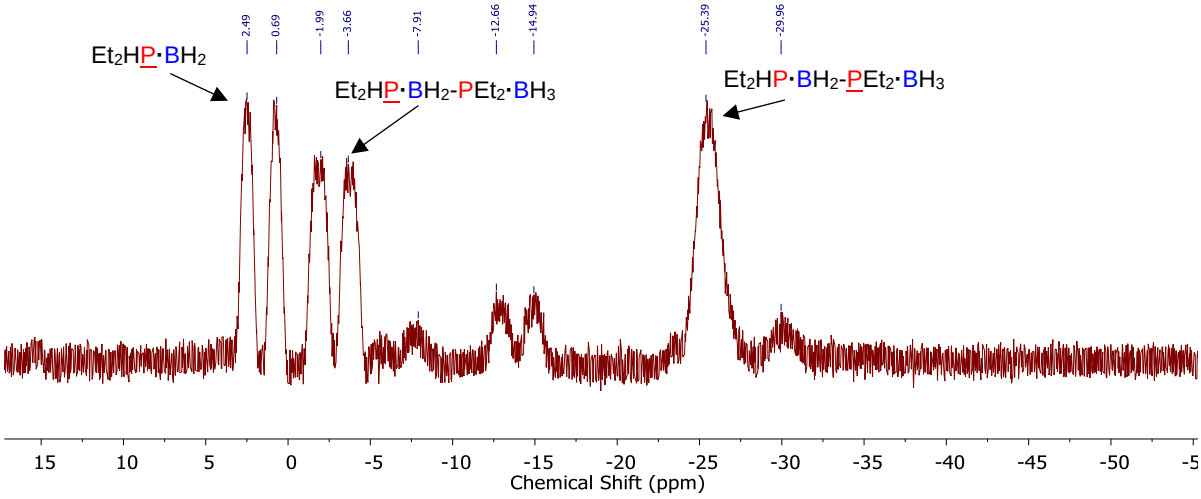

Figure S3.35 ^{31}P NMR (202 MHz, toluene) of the crude reaction mixture of the attempted dehydrocoupling of $Et_2HP{\cdot}BH_3$ using triflic acid

3.6 References

1. Priegert, A. M.; Rawe, B. W.; Serin, S. C.; Gates, D. P., *Chem. Soc. Rev.* **2016,** *45*, 922-53.
2. Manners, I., *Angew. Chem. Int. Ed.* **1996,** *35*, 1602-1621.
3. Neilson, R. H.; Wisian-Neilson, P., *Chem. Rev.* **1988,** *88*, 541-562.
4. Jäkle, F.; Vidal, F., *Angew. Chem. Int. Ed.* **2019,** *58*, 5846-5870.
5. Entwistle, C. D.; Marder, T. B., *Angew. Chem. Int. Ed.* **2002,** *41*, 2927-2931.
6. Hissler, M.; Dyer, P. W.; Réau, R., *Coord. Chem. Rev.* **2003,** *244*, 1-44.
7. https://www.nobelprize.org/prizes/lists/all-nobel-prizes-in-chemistry.
8. Grubbs, R. H., *Angew. Chem. Int. Ed.* **2006,** *45*, 3760-3765.
9. Miyaura, N.; Suzuki, A., *Chem. Rev.* **1995,** *95*, 2457-2483.
10. Beletskaya, I. P.; Cheprakov, A. V., *Chem. Rev.* **2000,** *100*, 3009-3066.
11. Troegel, D.; Stohrer, J., *Coord. Chem. Rev.* **2011,** *255*, 1440-1459.
12. Delacroix, O.; Gaumont, A. C., *Curr. Org. Chem.* **2005,** *9*, 1851-1882.
13. Wolfe, J. P.; Wagaw, S.; Marcoux, J.-F.; Buchwald, S. L., *Acc. Chem. Res.* **1998,** *31*, 805-818.
14. Hartwig, J. F., *Nature* **2008,** *455*, 314-322.
15. Leitao, E. M.; Jurca, T.; Manners, I., *Nat. Chem.* **2013,** *5*, 817-829.
16. Abe, Y.; Gunji, T., *Prog. Polym. Sci.* **2004,** *29*, 149-182.
17. Mark, J. E.; Schaefer, D. W.; Gui, L., *The Polysiloxanes*. Oxford University Press: New York, 2015.
18. Corey, J., *Adv. Organomet. Chem.* **2004,** *51*, 1-52.
19. Miller, R. D.; Michl, J., *Chem. Rev.* **1989,** *89*, 1359-1410.
20. Rothemund, S.; Teasdale, I., *Chem. Soc. Rev.* **2016,** *45*, 5200-5215.
21. Allcock, H. R., *Dalton Trans.* **2016,** *45*, 1856-1862.
22. Melen, R. L., *Chem. Soc. Rev.* **2016,** *45*, 775-788.
23. Greenberg, S.; Stephan, D. W., *Chem. Soc. Rev.* **2008,** *37*, 1482-1489.
24. Han, D.; Anke, F.; Trose, M.; Beweries, T., *Coord. Chem. Rev.* **2019,** *380*, 260-286.
25. Staubitz, A.; Robertson, A. P. M.; Sloan, M. E.; Manners, I., *Chem. Rev.* **2010,** *110*, 4023-4078.

26. Dorn, H.; Singh, R. A.; Massey, J. A.; Lough, A. J.; Manners, I., *Angew. Chem. Int. Ed.* **1999,** *38,* 3321-3323.
27. Dorn, H.; Singh, R. A.; Massey, J. A.; Nelson, J. M.; Jaska, C. A.; Lough, A. J.; Manners, I., *J. Am. Chem. Soc.* **2000,** *122,* 6669-6678.
28. Dorn, H.; Rodezno, J. M.; Brunnhöfer, B.; Rivard, E.; Massey, J. A.; Manners, I., *Macromolecules* **2003,** *36,* 291-297.
29. Clark, T. J.; Rodezno, J. M.; Clendenning, S. B.; Aouba, S.; Brodersen, P. M.; Lough, A. J.; Ruda, H. E.; Manners, I., *Chem. Eur. J.* **2005,** *11,* 4526-4534.
30. Jacquemin, D.; Lambert, C.; Perpète, E. A., *Macromolecules* **2004,** *37,* 1009-1015.
31. Nakhmanson, S. M.; Nardelli, M. B.; Bernholc, J., *Phys. Rev. Lett.* **2004,** *92,* 115504.
32. Schäfer, A.; Jurca, T.; Turner, J.; Vance, J. R.; Lee, K.; Du, V. A.; Haddow, M. F.; Whittell, G. R.; Manners, I., *Angew. Chem. Int. Ed.* **2015,** *54,* 4836-41.
33. Paul, U. S. D.; Braunschweig, H.; Radius, U., *Chem. Commun.* **2016,** *52,* 8573-8576.
34. Pandey, S.; Lönnecke, P.; Hey-Hawkins, E., *Eur. J. Inorg. Chem.* **2014,** 2456-2465.
35. Hooper, T. N.; Weller, A. S.; Beattie, N. A.; Macgregor, S. A., *Chem. Sci.* **2016,** *7,* 2414-2426.
36. Cavaye, H.; Clegg, F.; Gould, P. J.; Ladyman, M. K.; Temple, T.; Dossi, E., *Macromolecules* **2017,** *50,* 9239-9248.
37. Turner, J. R.; Resendiz-Lara, D. A.; Jurca, T.; Schäfer, A.; Vance, J. R.; Beckett, L.; Whittell, G. R.; Musgrave, R. A.; Sparkes, H. A.; Manners, I., *Macromol. Chem. Phys.* **2017,** *218,* 1700120.
38. Thoms, C.; Marquardt, C.; Timoshkin, A. Y.; Bodensteiner, M.; Scheer, M., *Angew. Chem.* **2013,** *125,* 5254-5259.
39. Thoms, C.; Marquardt, C.; Timoshkin, A. Y.; Bodensteiner, M.; Scheer, M., *Angew. Chem. Int. Ed.* **2013,** *52,* 5150-5154.
40. Oldroyd, N. L.; Chitnis, S. S.; Annibale, V. T.; Arz, M. I.; Sparkes, H. A.; Manners, I., *Nat. Commun.* **2019,** *10,* 1370.
41. Marquardt, C.; Jurca, T.; Schwan, K.-C.; Stauber, A.; Virovets, A. V.; Whittell, G. R.; Manners, I.; Scheer, M., *Angew. Chem. Int. Ed.* **2015,** *54,* 13782-13786.
42. Stauber, A.; Jurca, T.; Marquardt, C.; Fleischmann, M.; Seidl, M.; Whittell, G. R.; Manners, I.; Scheer, M., *Eur. J. Inorg. Chem.* **2016,** 2684-2687.
43. Denis, J.-M.; Forintos, H.; Szelke, H.; Toupet, L.; Pham, T.-N.; Madec, P.-J.; Gaumont, A.-C., *Chem. Commun.* **2003,** 54-55.
44. LaFortune, J. H. W.; Qu, Z.-W.; Bamford, K. L.; Trofimova, A.; Westcott, S. A.; Stephan, D. W., *Chem. Eur. J.* **2019,** *25,* 12063-12067.
45. Geier, S. J.; Gilbert, T. M.; Stephan, D. W., *Inorg. Chem.* **2011,** *50,* 336-344.
46. Geier, S. J.; Gilbert, T. M.; Stephan, D. W., *J. Am. Chem. Soc.* **2008,** *130,* 12632-12633.
47. Resendiz-Lara, D.; Annibale, V. T.; Knights, A. W.; Chitnis, S. S.; Manners, I., *Manuscript submitted* **2020**.
48. Arz, M. I.; Knights, A. W.; Manners, I., *Macromol. Rapid Commun.* **2019,** 1900468.
49. Perutz, R. N.; Sabo-Etienne, S., *Angew. Chem. Int. Ed.* **2007,** *46,* 2578-2592.
50. Colebatch, A. L.; Hawkey Gilder, B. W.; Whittell, G. R.; Oldroyd, N. L.; Manners, I.; Weller, A. S., *Chem. Eur. J.* **2018,** *24,* 5450-5455.
51. Mizutani, M.; Satoh, K.; Kamigaito, M., *J. Am. Chem. Soc.* **2010,** *132,* 7498-7507.
52. Mizuntani, M.; Satoh, K.; Kamigaito, M., *Macromolecules* **2011,** *44,* 2382-2386.
53. Zhang, X.; Dou, H.; Zhang, Z.; Zhang, W.; Zhu, X.; Zhu, J., *J. Polym. Sci., Part A: Polym. Chem.* **2013,** *51,* 3907-3916.
54. King, A. K.; Buchard, A.; Mahon, M. F.; Webster, R. L., *Chem. Eur. J.* **2015,** *21,* 15960-15963.
55. Bourumeau, K.; Gaumont, A.-C.; Denis, J.-M., *J. Organomet. Chem.* **1997,** *529,* 205-213.
56. Baban, J. A.; Roberts, B. P., *J. Chem. Soc., Perkin Trans. 2* **1986,** 1607-1611.
57. Liston, D. J.; Lee, Y. J.; Scheidt, W. R.; Reed, C. A., *J. Am. Chem. Soc.* **1989,** *111,* 6643-6648.

Chapter 4

Applications of polyphosphinoboranes in the formation of hydrogels and as flame retardants

4.1 The synthesis of hydrogels from polyphosphinoboranes

4.1.1 Abstract

Recently there has been significant interest in the development of new hydrogels for a range of applications. Herein we report a novel class of inorganic hydrogel consisting of a network of crosslinked polyphosphinoborane chains. These hydrogels were synthesised via UV-light induced reaction of poly(phenylphosphinoborane) $[PhHP\text{-}BH_2]_n$ with methacrylate and acrylate capped poly(ethylene glycol), and dimethacrylate crosslinkers in the presence of the photoinitiator 2,2-dimethoxy-2-phenylacetophenone. These materials were found to be highly swellable in water and the swellability was tunable by the length and amount of crosslinker used. This could also be influenced by choice of end capping for PEG side groups, with methoxy-terminated PEG resulting in more swellable materials than hydroxy-terminated analogues. Furthermore, the formation of a colourless hydrogel was achieved from poly(phenylphosphinoborane) synthesised using a triflic acid precatalyst rather than iron-based catalysts.

4.1.2 Introduction

Polymer gels are semi-solid systems consisting of three-dimensional cross-linked polymer networks capable of absorbing large amounts of solvent in their swollen state. These materials are known as hydrogels if the solvent is water, and can be classified as either physical or chemical gels: physical gels are formed when secondary forces, for example H-bonding, ionic, or hydrophobic forces are responsible for formation of a physical network; and chemical gels result from covalent linkages are formed between polymer chains.[1] Physical hydrogels, are often designed to form under physiological

conditions and can be dissolved by changes in, for example, pH and temperature; whereas chemical hydrogels tend to be robust when formed.[2] Due to their high water content, the properties of hydrogels often closely resemble those of biological tissues resulting in excellent biocompatibility.[1] Since the first report on hydrogels and their use as soft contact lenses in 1960,[3] these materials have found uses in a wide variety of biomedical applications, including controlled drug delivery[4] and tissue engineering.[5, 6] The vast majority of hydrogels that have been hitherto reported are derived from organic polymers, for example, poly(ethylene glycol) (PEG)[7, 8] and poly(vinyl alcohol),[9] or natural polymers such as chitosan.[10] Recently there has been interest in the development of new classes of inorganic hydrogels with improved properties and functionality, such as redox responses.[11, 12] However, examples of hydrogels featuring networks based on polymers derived from main group elements are still extremely scarce and mostly confined to the well-established polyphosphazenes and polysiloxanes. Poly(dimethylsiloxanes) (PDMS) possesses a number of properties that make it well suited to biomedical applications, including chemical and thermal stability, optical transparency, high flexibility, and nontoxicity and biocompatibility although the development of techniques to overcome its inherent hydrophobicity have been required.[13] Polyphosphazene gels have been investigated and found to have interesting properties e.g. thermoresponsive swelling as well as strong biocompatibility.[14-17] Recently, polyphosphazenes hydrogels have been developed as injectable materials for biomedical applications,[18-21]

These examples showcase the need for continued research into the formation of p-block element-containing hydrogels from different polymer systems in order to form novel materials with unique and useful properties. An interesting class of inorganic polymer are polyphosphinoboranes $[RHP\text{-}BH_2]_n$. These are isoelectronic with polyolefins but possess significantly different properties owing to the presence of phosphorus and boron units in the polymer chains. These materials can be formed via a number of metal- and non-metal-based polymerisation techniques,[22-39] and these have been shown to have potential applicability as precursors to semiconductor-based ceramics, etch resists, and as piezoelectronics.[24-27] However, until recently research into their applicability has been hindered by access to polyphosphinoboranes with controlled structures via scalable routes. With this in mind, we have recently developed the iron-catalysed synthesis of a number of polyphosphinoboranes featuring

both aryl and alkyl side chains,[28, 35, 40, 41] and we have also described the synthesis of water-soluble polyphosphinoboranes through the post-polymerisation functionalisation of poly(phenylphosphinoborane) (**4.1a**) by UV-induced hydrophosphination with poly(ethylene glycol) methyl ether methacrylate (**4.2**), and of crosslinked organogels through reaction with 1,5-hexadiene (Scheme 4.1).[42] Herein, we report our findings on the use of post-polymerisation functionalisation of alkenes and dienes for the formation of hydrogel networks.

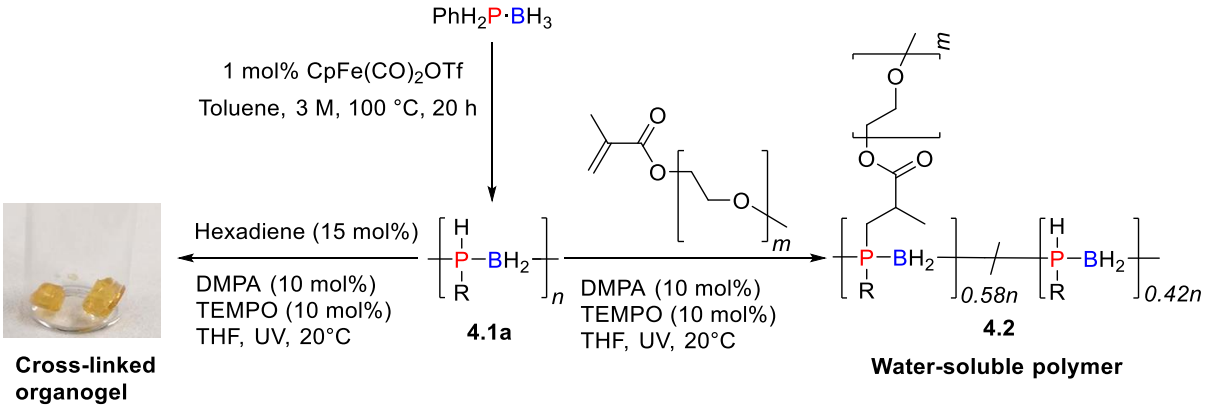

Scheme 4.1 Post-polymerisation of poly(phenylphosphinoborane) to yield organogels (left) and water-soluble polymers (right).

4.1.3 Results and discussion

Following our recent report of the synthesis of water-soluble polymer **4.2** from **4.1a**,[42] we initially attempted to form a hydrogel from **4.2** via UV induced crosslinking by hydrophosphination of 1,5-hexadiene. To this end, we irradiated **4.2** with 1,5-hexadiene (10 mol%) in the presence of the photoinitiator 2,2-dimethoxy-2-phenylacetophenone (DMPA) in THF at 20 °C for 20 h; however, this did not result in any gelation taking place. A possible explanation is that the sterical encumbrance afforded by the PEG containing side groups is sufficient to prevent reaction with the 1,5-hexadiene. We therefore postulated that a three-component reaction of **4.1a** with PEG methyl ether acrylate (M_n = 480 g mol^{-1}) (50 mol%, as polar functions to induce water solubility) and 1,5-hexadiene (15 mol%, to induce crosslinking) in THF would facilitate the formation of a gel. Although irradiation of this reaction mixture for 20 h did result in the formation of an insoluble material, no swelling behaviour was observed in water.

We also investigated the incorporation of smaller side groups to induce water solubility rather than long PEG moieties in order to reduce any potential steric clashes that might be preventing crosslinking.

Reaction of **4.1a** with DL-allylglycine and 2-(dimethylamino)ethyl methacrylate were both investigated; however, issues with solubility in THF prevented the hydrophosphination of these alkenes using **4.1a** under UV-induced conditions. In each case, an insoluble material was formed but swelling in either THF or water was not detected.

The breakthrough came when we changed the crosslinking agent from 1,5-hexadiene to a PEG dimethacrylate crosslinker. This has three significant differences to 1,5-hexadiene: Firstly, PEG dimethacrylate is more reactive; secondly, it is more hydrophilic; and thirdly, the longer chains allow for more flexibility possibly circumventing any repulsive steric interactions between polymer side groups when a short chain crosslinker is used. The three-component reaction between **4.1a**, PEG dimethacrylate (Figure 4.2, **A**, M_n = 550 g mol^{-1}, 15 mol%) and PEG methyl ether acrylate (**D**, M_n = 480 g mol^{-1}, 50 mol%) in the presence of DMPA (10 mol%) was therefore investigated. After UV irradiation of a THF solution of these species for 20 h, an orange insoluble gel (**4.3a**) was formed with the exclusion of an orange coloured supernatant (Scheme 4.2). The supernatant was decanted, and volatiles removed from the solid residue via exposure to air for 24 h followed by drying under vacuum for 24 h. **4.3a** was purified by swelling in THF for 6 h followed by decanting away of the liquid until no colouration of the supernatant was observed (2 × 5 mL). Volatiles were again removed from the gel via air exposure (24 h) followed by drying under vacuum (24 h) to yield the isolated unswollen gel. **4.3a** was a tacky solid, shaped by the reaction vial (Figure 4.1).

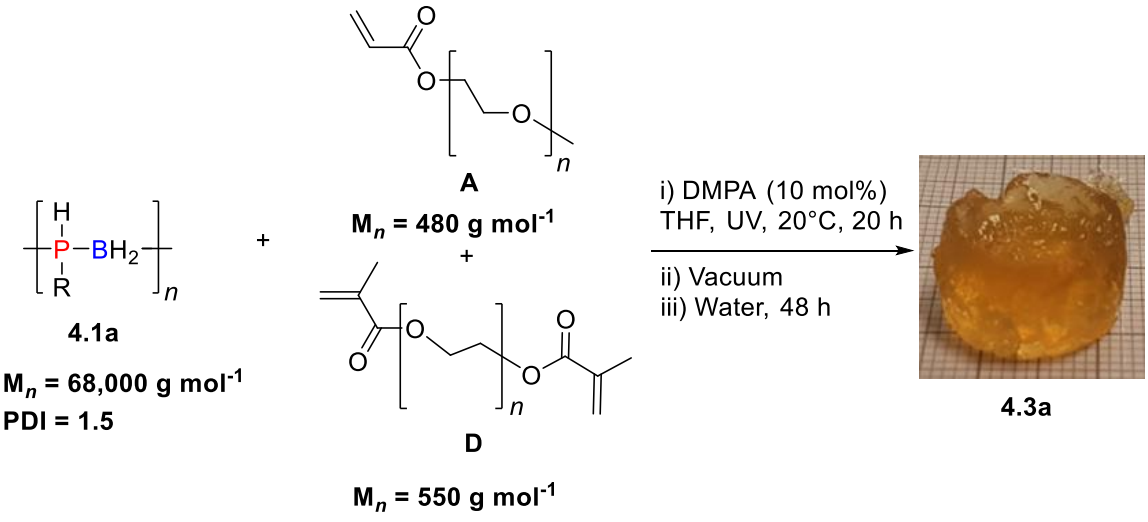

Scheme 4.2 Synthesis of hydrogel **4.3a** from the reaction of **4.1a** with PEG dimethacrylate (**A**) and PEG methyl ether acrylate (**D**).

Next, we explored potential hydrogel formation by submersion in water for 48 h. The gel was observed to swell under these conditions (Figure 4.1) giving a swollen material which was lighter in colour than the unswollen analogue and was very soft and fragile. The swellability of **4.3a** was quantified by measuring the mass of a swollen piece of hydrogel, drying under vacuum for 48 h, and reweighing to calculate the swellability by mass. This swelling, deswelling process was repeated two further times and the average swelling was found to be 647% of the unswollen mass (Table 4.1, hydrogel **4.3a**). The successful repeated swelling of this material demonstrates that the integrity of the hydrogel and the crosslinked network is not disrupted.

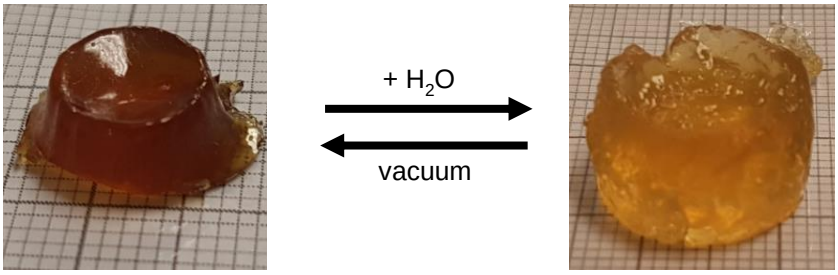

Figure 4.1 Left: Tacky unswollen **4.3a**; Right: Soft yellow gel obtained after soaking **4.3a** in water for 48 h.

To confirm that this hydrogel behaviour arises from the anticipated formation of a crosslinked polyphosphinoborane polymer containing PEG side groups, two important control reactions were performed. Firstly, the UV-induced reaction of **4.1a** with PEG dimethacrylate (M_n = 550 g mol^{-1}, 15 mol%) in the presence of DMPA (10 mol%) in THF was investigated. After irradiation for 20 h, an insoluble gel was formed, accompanied by an orange coloured solution; however, this material was not found to swell in water. This suggests that **4.1a** is crosslinked by PEG dimethacrylate to form an organogel but without the presence of hydrophilic PEG side groups, the material is too hydrophobic to swell in water. Secondly, to investigate the possibility that the hydrogel consists of a crosslinked network formed from copolymerisation of **A** and **D** with **4.1a** trapped in the material rather than directly incorporated into the polymer network, a 1:2 molar ratio of **A** and **D** were irradiated in THF in the presence of DMPA; however, no gel formation was observed after irradiation for 20 h. These results confirm that the formation of a hydrogel via the reaction of **4.1a**, **A**, and **D** is due to the anticipated crosslinking of polyphosphinoborane chains.

Having determined that reaction of **4.1a** with **A** and **D** results in the formation of a water-swellable network of polyphosphinoborane chains, we endeavoured to examine the effect of the side group moieties and the crosslinker length on the properties and swellability of the hydrogels. We therefore synthesised a series of hydrogels from the reaction of **4.1a** with different dimethacrylates (**A** – **C**), and PEG methyl ether acrylate (**D**) or PEG methacrylate (**E**) (Figure 4.2). The results of these swelling experiments are summarised in Table 4.1.

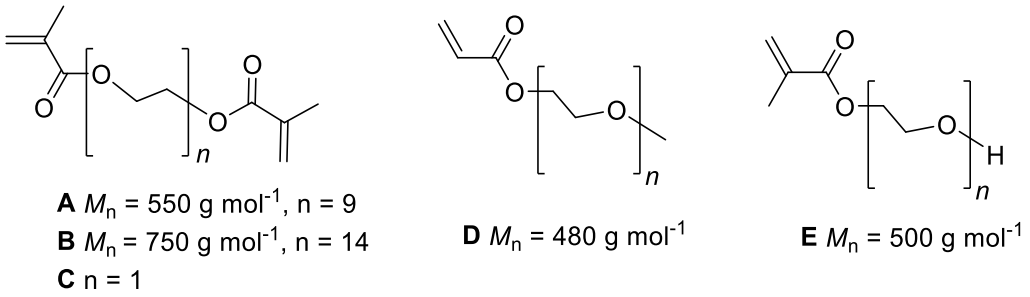

Figure 4.2 Crosslinking dimethacrylates and hydrophilic PEG acrylate and methacrylate employed in this study.

Increasing the amount of crosslinker **A** from 15 mol% to 25 mol% was found to significantly reduce the swellability of the gel (Table 4.1, compare hydrogels **4.3a** and **4.3b**), which is consistent with the formation of a more tightly crosslinked network. **4.3b** was found to have greater structural integrity than **4.3a**: whereas unswollen **4.3a** was found to sink over time, unswollen **4.3b** kept its shape even after several days. The shape was also retained after multiple swelling cycles even though the hydrogel was removed from the mould (the reaction vial) for these swelling experiments. The formation of shaped materials and the retention of this shape during swelling and deswelling is promising for device fabrication using these materials. We therefore used 25 mol% crosslinker in subsequent experiments.

Changing the length of the crosslinker from n = 9 (**A**) to 14 (**B**) was found to have little impact on the swelling (417 and 387% for hydrogels **4.3b** and **4.3c**, respectively). The use of a shorter ethylene glycol dimethacrylate (**C**) resulted in the formation of a hydrogel (**4.3d**) with a swellability of 521%. This swellability is higher than for hydrogels prepared using longer crosslinkers despite the expectation of a more tightly packed network when a short crosslinker is used. We postulate that this is because steric interactions between polymer chains inhibit efficient crosslinking taking place and so only a very lightly crosslinked hydrogel is formed. Further evidence for this is that the material did not assume the shape

of the reaction vial during formation instead several insoluble masses formed rather than one solid material.

Table 4.1 Synthesis of hydrogels from reaction of poly(phenylphosphinoborane) with a dimethacrylate crosslinker and PEG acrylate and their swellability in water.

Hydrogel	Crosslinker (mol%)	PEG monoacrylate (mol%)	Swellability[a] (%)
4.3a	**A** (15)	**D** (50)	647[b]
4.3b	**A** (25)	**D** (50)	417[b]
4.3c	**B** (25)	**D** (50)	387[b]
4.3d	**C** (25)	**D** (50)	521[b]
4.3e	**A** (25)	**D** (40)	385
4.3f	**A** (25)	**D** (60)	518
4.3g	**A** (25)	**E** (50)	274[b]

[a]Swellability = (mass of swollen gel/mass of unswollen gel) × 100%; [b]Average swelling over three swelling-deswelling cycles

The swellability of the hydrogel was found to be dependent on the amount of PEG methyl ether acrylate (**D**) used. Whereas the swellability of **4.3b** is 417%, when the amount of **D** was decreased to 40 mol%, a gel was formed which swells by 385% (hydrogel **4.3e**) and when increased to 60 mol%, the swellability also increases to 518% (hydrogel **4.3f**). This indicates that the presence of a larger amount of PEG side groups on the polymer chains induces greater water uptake, either due to the hydrophilicity of PEG or an increase in pore size due to the presence of more side groups forcing the polymer main chains apart. However, another possibility that cannot be discounted is that the presence of a great proportion of P-disubstituted units reduces the number of available sites for crosslinking and therefore a more lightly crosslinked network is formed.

Use of PEG methacrylate (**E**, M_n = 500 g mol^{-1}) instead of **D** was found to significantly reduce the swellability of the resultant gel (**4.3 g**, swelling = 274%). This is postulated to be due to the possibility of hydrogen bond formation between polymer chains owing to the presence of hydroxyl groups

resulting in a more compact network structure. This material was also found to be brittle in both its unswollen and swollen states.

One drawback with these materials is that they are strongly coloured which is likely to be due to the presence of residual iron arising from the catalyst used for the dehydropolymerisation of phenylphosphine-borane.[28, 35] The presence of metal is undesirable because of the possible impact on the mechanical properties and possible side effect on any biomedical applications of the hydrogels. We therefore attempted to form hydrogels from polyphosphinoborane which do not contain any metal species. We very recently found that triflic acid can be used to catalyse the polymerisation of phosphine-boranes producing colourless polymers (Scheme 4.3 I, see Chapter 3).

Reaction of poly(phenylphosphinoborane) (**4.1b**) prepared using a triflic acid precatalyst with **A** (25 mol%) and **D** (50 mol%) in the presence of DMPA (10 mol%) in THF led to the formation of a gel (**4.4**) after UV irradiation for 20 h (Scheme 4.3 II). The material was purified by repeated swelling in THF (2 × 5 mL). After drying the material overnight, a light yellow coloured solid was isolated. Upon submerging **4.4** in water for 48 h, a swollen hydrogel was formed that was colourless (Figure S4.8). The average swellability of **4.4** over three swelling-deswelling cycles was found to be 632%. This is significantly higher than the swellability of gel **4.3b** prepared under analogous conditions from **4.1a.** This may be because the molar mass of **4.1b** (M_n = 5,200 g mol^{-1}) is markedly lower than **4.1a** (M_n = 68,000 g mol^{-1}) which could affect the pore sizes in the crosslinked network formed or because the polydispersity is higher (**4.1a**, PDI = 1.5; **4.1b**, PDI = 2.4). The absence of any metal in this hydrogel should serve to improve the applicability of these materials, and future work will involve an in-depth study of the mechanical and biotoxicity of hydrogels synthesised via this methodology.

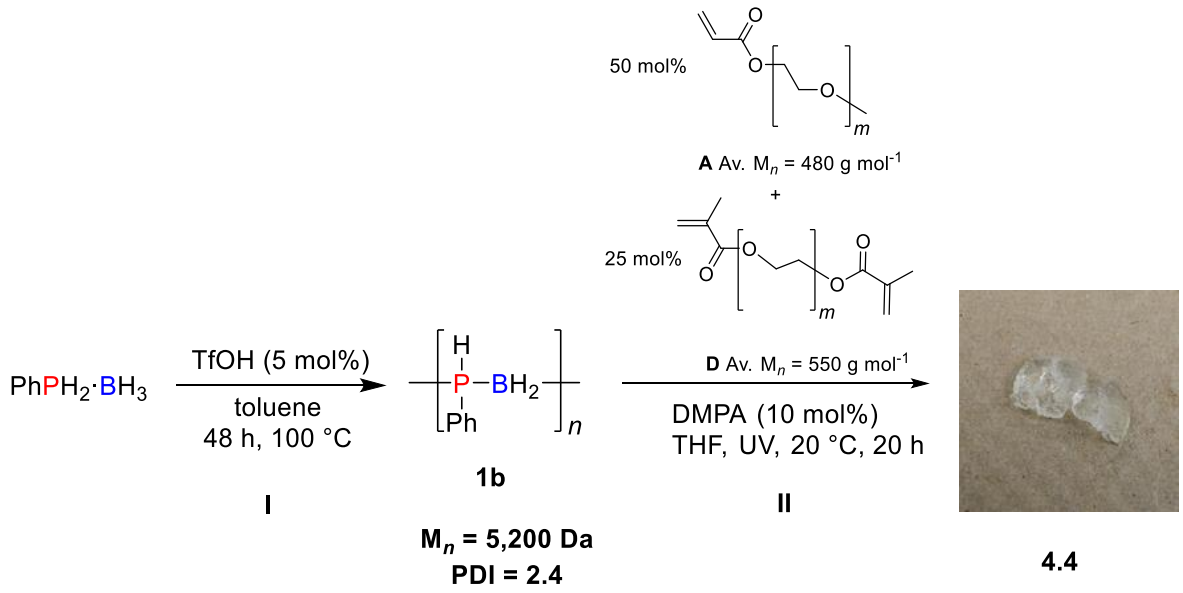

Scheme 4.3 I Synthesis of poly(phenylphosphinoborane) (**1b**) using triflic acid as a precatalyst; **II** Synthesis of a hydrogel (**4.4**) via UV-induced hydrophosphination reaction of **1B** with **A** and **D**.

4.1.4 Conclusions

We report the synthesis of the first hydrogels featuring polyphosphinoborane chains. These materials were synthesised via UV-light induced reaction of poly(phenylphosphinoborane) with acrylate capped PEG, and dimethacrylate crosslinkers in the presence of the photoinitiator 2,2-dimethoxy-2-phenylacetophenone. The hydrogels were found to be highly swellable in water, with the swellability dependent on both the crosslinker loading and length, and the amount of PEG containing side-groups present. The end capping of the hydrophilic PEG side groups was found to have an effect on the swellability: hydrogels containing methoxy-terminated PEG side groups resulted in more swellable materials than analogues with hydroxy-terminated PEG We also describe the synthesis of colourless hydrogels from poly(phenylphosphinoborane) synthesised using a triflic acid precatalyst rather than iron-based catalysts. Further work will focus on quantifying the mechanical properties of these hydrogels and investigating their applicability in biomedical applications.

4.1.5 Experimental

4.1.5.1 General procedure, reagents and equipment

Unless otherwise noted, chemicals were obtained from commercial suppliers and used as received. **4.1a** and **4.2** were synthesised via literature procedures.[42] **4.1b** was synthesised via the procedure reported in Chapter 3.

Photoirradiation experiments under ultraviolet (UV) light were carried out in a Luzchem LZC-ICH2 photoreactor featuring 8 side and 8 top lamps – 8 W lamps with emission centred at 352 nm.

4.1.5.2 Attempted crosslinking of 4.2 using 1,5-hexadiene

A 14 mL vial was charged with **4.2** (95 mg, 0.14 mmol), DMPA (2.5 mg, 0.01 mmol), 1,5-hexadiene (1.7 μL, 0.014 mmol), and THF (2 mL). The orange solution was irradiated ca. 5 cm away from a UV lamp for 20 h; however, no observation of gelation was observed and so this reaction was not pursued further.

4.1.5.3 Attempted reaction of poly(phenylphosphinoborane) (4.1a) with 1,5-hexadiene and poly(ethylene glycol) methyl ether acrylate

A vial was charged with **4.1a** (12 mg, 0.1 mmol), poly(ethylene glycol) methyl ether acrylate (**D**, M_n = 480, 22 μL, 0.05 mmol), DMPA (2.5 mg, 0.01 mmol), 1,5-hexadiene (1.8 μL, 0.015 mmol), and THF (5 mL). The orange solution was irradiated ca. 5 cm away from a UV lamp for 20 h. This resulted in the formation of an insoluble gel with the exclusion of an orange coloured solution. The solution was decanted away, and volatiles removed under vacuum yielding an orange solid. Attempts to swell this solid in water were unsuccessful.

4.1.5.4 Reaction of 4.1a with DL-allylglycine

A vial equipped with a magnetic stirrer was charged with **4.1a** (12 mg, 0.1 mmol), DL-allylglycine (5.76 mg, 0.05 mmol), DMPA (2.5 mg, 0.01 mmol), and THF (2 mL). The resultant suspension was irradiated ca. 5 cm away from a UV lamp for 20 h resulting in the formation of an insoluble material. This was insoluble in THF and water and was not found to swell in either solvent.

4.1.5.5 Reaction of 4.1a with 2-(Dimethylamino)ethyl methacrylate (DMAEMA)

A vial equipped with a magnetic stirrer was charged with **4.1a** (12 mg, 0.1 mmol), DMAEMA (8.42 μL, 0.05 mmol), DMPA (2.5 mg, 0.01 mmol), and THF (5 mL). The resultant solution was irradiated ca. 5 cm away from a UV lamp for 20 h resulting in the formation of an insoluble material. This was insoluble in THF and water and was not found to swell in either solvent.

4.1.5.6 Reaction of 4.1a with ethylene glycol dimethacrylate

A vial was charged with **4.1a** (12 mg, 0.1 mmol), ethylene glycol dimethacrylate (**A**, 1.88 μL, 0.01 mmol), DMPA (2.5 mg, 0.01 mmol), and THF (5 mL). The resultant solution was irradiated ca. 5 cm

away from a UV lamp for 20 h. This resulted in the formation of an insoluble gel with the exclusion of an orange coloured solution. The solution was decanted away, and volatiles removed under vacuum yielding an orange solid. Attempts to swell this solid in water were unsuccessful.

4.1.5.7 General procedure for the formation of hydrogels

A vial was charged with **4.1a** (122 mg, 1 mmol), dimethacrylate (**A** – **C**, 0.15 or 0.25 mmol), acrylate terminated poly(ethylene glycol) (**D,** 0.4 – 0.6 mmol or **E,** 0.5 mmol), DMPA (26 mg, 0.1 mmol), and THF (2 mL). The orange solution was irradiated ca. 5 cm away from a UV lamp for 20 h. This resulted in the formation of insoluble gels with the exclusion of an orange coloured supernatant. The liquid was decanted away, and volatiles removed opening the vial to air for 24 h followed by drying under vacuum for 24 h yielding orange solids. These solids were purified by swelling in THF for 6 hours followed by decanting away of excess solvent until no colouration of the solvent was observed (2 × 5 mL). Volatiles were removed by opening the vial to air for 24 h followed by drying under vacuum for 24 h to yield the isolated unswollen gel (**4.3a** – **g**).

4.1.5.8 General swelling procedure

A sample of unswollen gel (**4.3a** – **g**) was submerged in water (10 mL) for 48 h. No colouration of the water was observed after this time. Excess solvent was decanted away, and surface solvent removed by careful swabbing with a Kimwipe. The sample was weighed and then the vial opened to air for 24 h followed by drying under vacuum for 24 h, after which the sample was reweighed and the swellability in water calculated: swellability = (swollen mass/unswollen mass) x 100%. The procedure was repeated a further two times.

4.1.5.9 Synthesis and properties of hydrogel 4.3a

Alkene: poly(ethylene glycol) methyl ether acrylate (**D**, M_n = 480 g mol^{-1}, 20 μL, 0.5 mmol).

Diene: poly(ethylene glycol) dimethacrylate (**A**, M_n = 550 g mol^{-1}, 75 μL, 0.15 mmol).

Yield: 422 mg

Gel properties

Unswollen: Very sticky solid, easily broken when handling. Does not hold shape over time.

Swollen: Soft material, easily broken when handling.

Swellability

Swelling 1: 648%

Swelling 2: 769%

Swelling 3: 525%

Average swelling: 647%

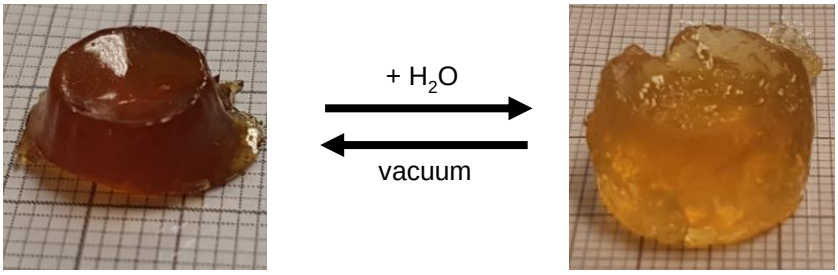

Figure S4.1 Left: Tacky unswollen **5.3a**; Right: Soft yellow gel obtained after soaking **5.3a** in water for 48 h.

4.1.5.10 Synthesis and properties of hydrogel 4.3b

Alkene: poly(ethylene glycol) methyl ether acrylate (**D**, M_n = 480 g mol^{-1}, 220 μL, 0.5 mmol).

Diene: poly(ethylene glycol) dimethacrylate (**A**, M_n = 550 g mol^{-1}, 125 μL, 0.25 mmol).

Yield: 470 mg

Gel properties

Unswollen: Tacky solid, holds shape over time (3 d).

Swollen: Soft solid, requires mechanical pressure to break apart rather than breaking apart during normal handling.

Swellability

Swelling 1: 434%

Swelling 2: 449%

Swelling 3: 369%

Average swelling: 417%

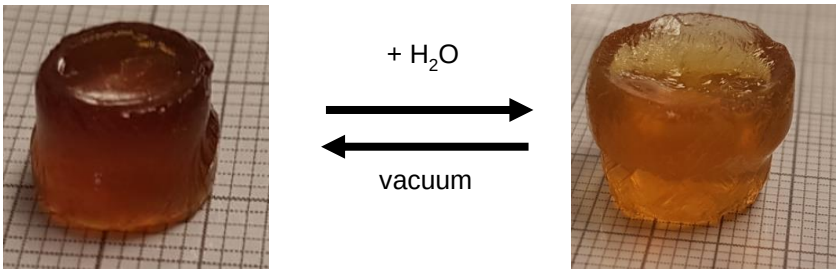

Figure S4.2 Left: Tacky unswollen **5.3b**; Right: Soft yellow gel obtained after soaking **5.3b** in water for 48 h.

4.1.5.11 Synthesis and properties of hydrogel 4.3c

Alkene: poly(ethylene glycol) methyl ether acrylate (**D**, M_n = 480 g mol^{-1}, 220 µL, 0.5 mmol).

Diene: poly(ethylene glycol) dimethacrylate (**B**, M_n = 750 g mol^{-1}, 169 µL, 0.25 mmol).

Yield: 493 mg

Gel properties

Unswollen: Tacky solid, holds shape over time (3 d).

Swollen: Soft solid, requires mechanical pressure to break apart rather than breaking apart during normal handling.

Swellability

Swelling 1: 379%

Swelling 2: 398%

Swelling 3: 385%

Average swelling: 387%

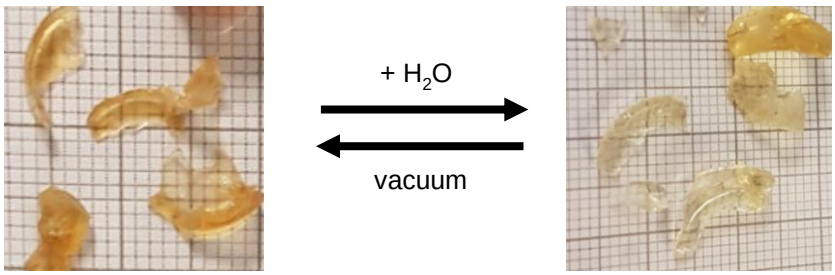

Figure S4.3 Left: Tacky unswollen **5.3c**; Right: Soft yellow gel obtained after soaking **5.3c** in water for 48 h.

4.1.5.12 Synthesis and properties of hydrogel 4.3d

Alkene: poly(ethylene glycol) methyl ether acrylate (**D**, M_n = 480 g mol^{-1}, 220 µL, 0.5 mmol).

Diene: ethylene glycol dimethacrylate (**C**, 47 µL, 0.25 mmol).

Yield: 322 mg

Gel properties

Unswollen: Very sticky solid elastic solid. Did not mould to vial shape during formation.

Swollen: Soft material, easily broken when handling.

Swellability

Swelling 1: 638%

Swelling 2: 452%

Swelling 3: 473%

Average swelling: 521%

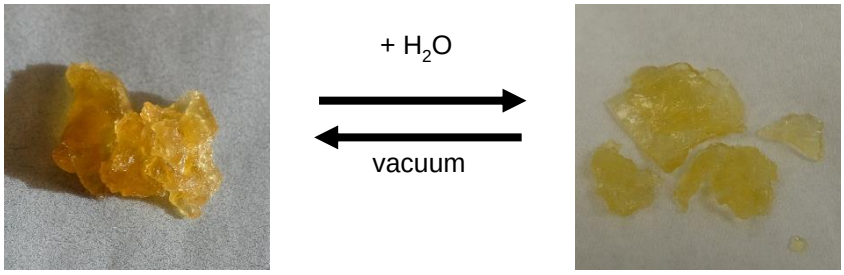

Figure S4.4 Left: Tacky unswollen **5.3d**; Right: Soft yellow gel obtained after soaking **5.3d** in water for 48 h.

4.1.5.13 Synthesis and properties of hydrogel 4.3e

Alkene: poly(ethylene glycol) methyl ether acrylate (**D**, M_n = 480 g mol^{-1}, 220 µL, 0.4 mmol).

Diene: poly(ethylene glycol) dimethacrylate (**A**, M_n = 550 g mol^{-1}, 125 µL, 0.25 mmol).

Yield: 344 mg

Gel properties

Unswollen: Tacky solid, holds shape over time (3 d).

Swollen: Soft solid, requires mechanical pressure to break apart rather than breaking apart during normal handling.

Swellability

Swelling 1: 385%

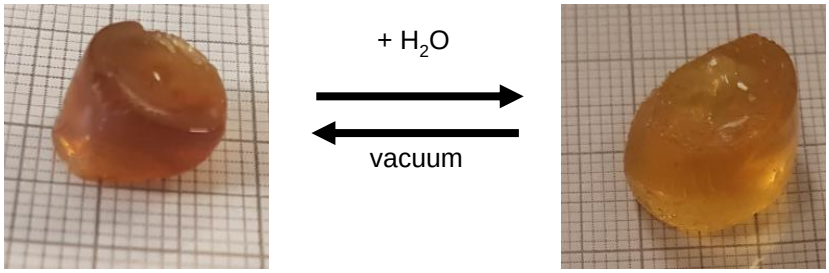

Figure S4.5 Left: Tacky unswollen **5.3f**; Right: Soft yellow gel obtained after soaking **5.3f** in water for 48 h.

4.1.5.14 Synthesis and properties of hydrogel 4.3f

Alkene: poly(ethylene glycol) methyl ether acrylate (**D**, M_n = 480 g mol^{-1}, 220 µL, 0.6 mmol).

Diene: poly(ethylene glycol) dimethacrylate (**A**, M_n = 550 g mol^{-1}, 125 µL, 0.25 mmol).

Yield: 461 mg

Gel properties

Unswollen: Tacky solid, holds shape over time (3 d).

Swollen: Soft solid, requires mechanical pressure to break apart rather than breaking apart during normal handling.

Swellability

Swelling 1: 518%

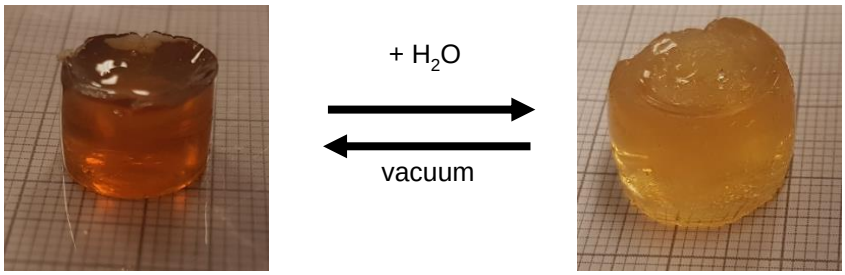

Figure S4.6 Left: Tacky unswollen **5.3g**; Right: Soft yellow gel obtained after soaking **5.3g** in water for 48 h.

4.1.5.15 Synthesis and properties of hydrogel 4.3g

Alkene: poly(ethylene glycol) methacrylate (**E**, M_n = 500 g mol^{-1}, 227 µL, 0.5 mmol).

Diene: poly(ethylene glycol) dimethacrylate (**A**, M_n = 550 g mol^{-1}, 125 µL, 0.25 mmol).

Yield: 572 mg

Gel properties

Unswollen: Tacky brittle solid.

Swollen: Soft solid, easily broken when handling.

Swellability

Swelling 1: 299%

Swelling 2: 263%

Swelling 3: 261%

Average swelling: 274%

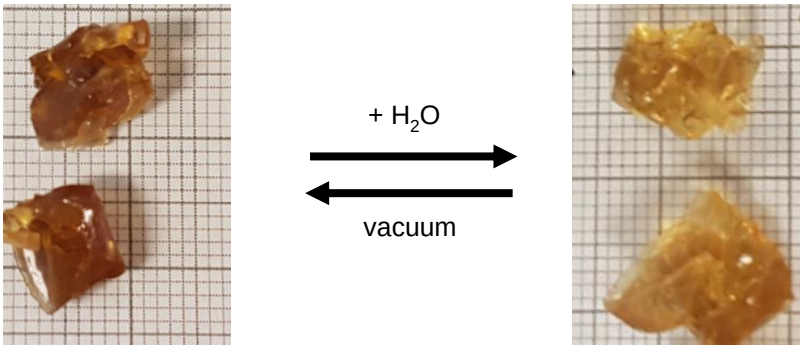

Figure S4.7 Left: Tacky unswollen **5.3e**; Right: Soft yellow gel obtained after soaking **5.3e** in water for 48 h.

4.1.5.16 Formation of hydrogel from polymer synthesised using triflic acid

A vial was charged with **4.1b** (122 mg, 1 mmol), poly(ethylene glycol) methyl ether acrylate (**D**, M_n = 480 g mol^{-1}, 220 µL, 0.5 mmol), poly(ethylene glycol) dimethacrylate (**A**, M_n = 550 g mol^{-1}, 125 µL, 0.25 mmol), DMPA (26 mg, 0.1 mmol), and THF (2 mL). The colourless solution was irradiated ca. 5 cm away from a UV lamp for 20 h. This resulted in the formation of an insoluble gel with the exclusion of a small amount of light-yellow solution. The solution was decanted away, and volatiles removed under vacuum yielding a yellow solid. This solid was purified by swelling in THF for 6 hours followed by decanting away of excess solvent until no colouration of the solvent was observed (2 × 5 mL). Removal of volatiles under vacuum yielded a lightly colourless solid (Yield: 412 mg). The gel was subjected to analogous swelling conditions as above.

Yield: 412 mg

Polymer properties

Unswollen: Tacky light-yellow solid.

Swollen: Soft colourless solid,

Swellability

Swelling 1: 617%

Swelling 2: 646%

Swelling 3: 632%

Average swelling: 632%

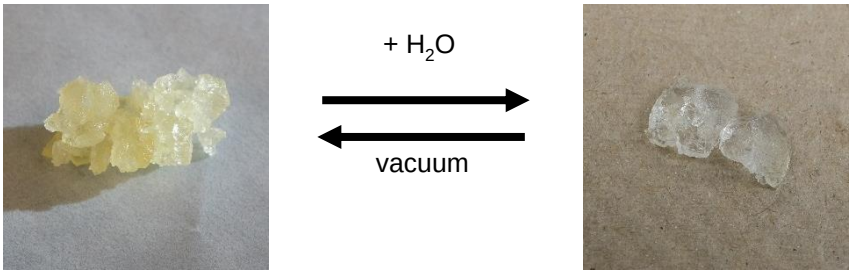

Figure S4.8 Left: Tacky unswollen **5.4**; Right: Soft yellow gel obtained after soaking **5.4** in water for 48 h.

4.2 Applications of polyphosphinoboranes as flame-retardant materials

4.2.1 Abstract

Phosphorus-containing polymers are of significant interest as flame-retardant additives that provide an alternative to halogenated species, many of which are banned due to environmental and health reasons, whilst also avoiding leaching issues commonly observed for molecular phosphorus species. We report investigations into the flame-retardant properties of polyphosphinoboranes $[RR'P\text{-}BH_2]_n$. When cotton towel was impregnated with a variety of polyphosphinoboranes and exposed to a flame, the presence of polyphosphinoborane was found to result in self-extinguishing of the flame leaving behind a charred material. In contrast, under analogous conditions, untreated cotton and cotton treated with polystyrene burnt completely. Analysis of the char revealed the formation of phosphoric and boric acids, species commonly invoked for action of related flame-retardant species. The use of P-disubstituted polyphosphinoboranes was found to slightly slow burning; however, the presence of halogenated groups in the side chain had little effect suggesting that it is the main chain that imparts any flame-retardant effect. Exposure of cotton treated with poly(phenylphosphinoborane) to water was not found to have any effect on flame-retardancy demonstrating the non-leachability of these polymers in aqueous media.

4.2.2 Introduction

Many of the materials ubiquitous to everyday life are inherently flammable, for example, materials found in housing, furnishings, clothing, and transportation. These common commercial products must therefore contain high loadings of flame-retardant additives to permit their safe usage.[43] Traditionally brominated flame retardants have fulfilled this role owing to their excellent extinguishing properties, generally through vapour phase reaction with radicals produced during combustion.[44] However, concerns about persistence, bioaccumulation, and toxicity have prompted a move away from these materials, many of which are now banned. The development of alternative flame retardants is therefore of significant fundamental and commercial interest.[45-47] One such class are phosphorus-containing materials which tend to have reduced toxicity compared to halogenated flame retardants while maintaining a high propensity for flame retardance.[43] These compounds have been shown to act primarily in the condensed phase, forming a non-flammable surface char protecting the bulk material;

however, vapour phase action has also been found to play an important role for some systems.[44, 46, 48] Many molecular phosphorus flame retardants (PFRs) have been utilised as additives to both natural and synthetic products;[49] however, one significant disadvantage of many of these materials is that they are prone to leach out of the product over time and after contact with water which both reduces their flame retardancy and leads to environmental and toxicity concerns.[49, 50]

One potential method to overcome this limitation is through the use of polymeric phosphorus-containing flame-retardants which have significantly decreased leachability compared to molecular species. Indeed, several phosphorus-based polymers have found applicability in the area of flame retardancy such as polyphosphazenes $[R_2P{=}N]_n$,[51-53] polyphosphonates,[54-56] and polyphosphines $[R_2P]_n$ (Figure 4.3).[57-59] Another class of flame-retardants are those containing boron moieties, for example, boric acid and borates. These have been shown to exhibit flame retardancy, particular in synergy with halogenated materials.[60-62] Boron containing materials typically act in the condensed phase by inducing the formation of carbon rather than CO or CO_2 resulting in the formation of a protective char.[46]

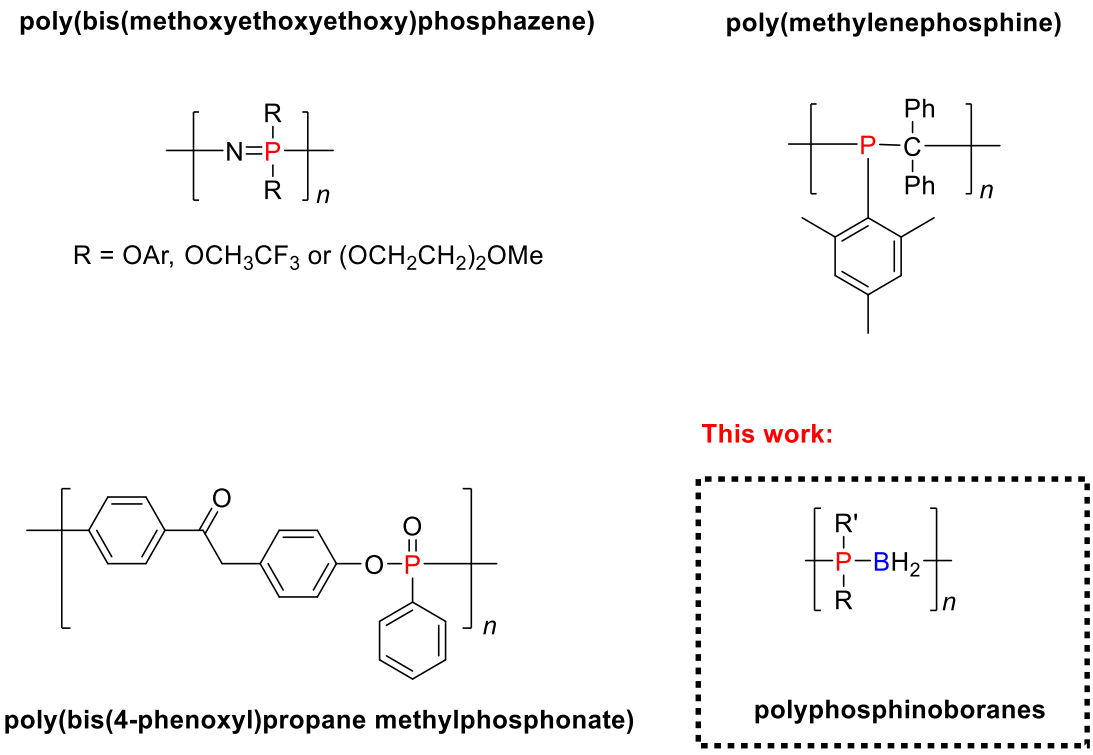

Figure 4.3 Examples of previously reported phosphorus containing polymeric flame-retardants and polyphosphinoboranes which are investigated in this work.

Polyphosphinoboranes, $[RR'P\text{-}BH_2]_n$ are a class of inorganic polymer that are formally isoelectronic with polyolefins.[63] First investigated in the 1950s, these macromolecules were first isolated as high

molar mass materials in 1999,[22] and have since attracted growing attention owing to their interesting properties and potential applications.[22-38, 64-67] One such application that has long been proposed but to the best of our knowledge never examined experimentally is as flame-retardants owing to their high phosphorus and boron content.[68] In part, this is because until recently it was not possible to access high molar mass polyphosphinoboranes on a sufficient scale to be utilised for flame retardant research. Recently, Manners and co-workers reported an iron-catalysed polymerisation of a variety of phosphine-boranes with control over the molar mass.[28, 35, 40] The post-polymerisation functionalisation of polyphosphinoboranes has also recently been reported giving access to a wide variety of polymers with different side groups.[41, 42]

With ready access to a range of polymers with different substituents, we have been able to investigate the potential utility of polyphosphinoboranes as a flame-retardant additive for cotton towel. This material was selected because it is excellent mimic for clothing and a number of other materials that have significant commercial application.[69] Flame-retardant systems for cotton are a well-documented challenge in this field owing to issues associated with leaching, and the modification of the material characteristics and appearance of the treated cotton.[50] It is therefore of significant importance for development of novel flame-retardants in an attempt to overcome these issues.

4.2.3 Results and discussion

4.2.3.1 Use of poly(phenylphosphinoborane) (4.1a) as a flame-retardant

The synthesis of poly(phenylphosphinoborane) **4.1a** was recently reported by our group using the precatalyst $CpFe(CO)_2OTf$ (Tf = CF_3SO_3).[28] While this polymerisation was reported on a relatively small scale (2.8 mmol monomer, 350 mg), we have found that it is amenable to scale up to 0.020 mol (2.5 g) using slightly modified conditions (toluene, 3M, 1 mol% $CpFe(CO)_2OTf$, 100 °C, 20 h) without any detrimental effects on yield (65%) or molar mass (Scheme 4.4). NMR data for the polymer after precipitation into cold pentane (−78 °C) matched that previously reported,[28] and the molar mass of the material was determined by gel permeation chromatography (GPC) (M_n = 68,000 Da, polydispersity index (PDI) = 1.5). This compares to M_n = 59,000 g mol^{-1} and a PDI of 1.6 for polymer previously reported using 1 mol% of precatalyst on a 2.8 mmol scale.[28]

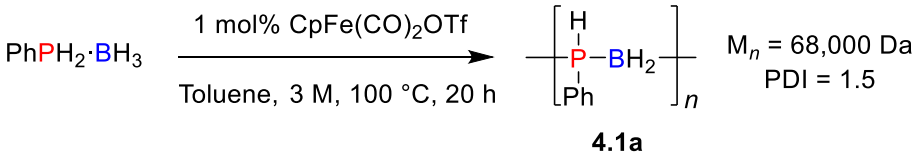

4.1a

Scheme 4.4 The dehydropolymerisation of poly(phenylphosphinoborane) using a $CpFe(CO)_2OTf$ precatalyst

In order to assess the flame-retardant properties of **4.1a**, a sample of cotton (5 × 10 cm, Figure 4.4a) was treated by pipetting **4.1a** (164 mg) dissolved in DCM (5 mL) over the cotton sample with frequent turning to ensure an even covering. A control sample was also prepared by pipetting DCM (5 mL) over cotton. The samples were then dried for 24 h in a vacuum oven at 40 °C. The discolouring of the cotton sample after loading of **4.1a** arises from the slight yellow colour of the polymer which is reported to come from residual iron species that remains even after repeated precipitation (Figure 4.4b). The increase in mass of this treated cotton sample after loading with **4.1a** and drying for 24 h in a vacuum oven was 158 mg (cf. 164 mg of polymer used), showing that minimal polymer mass is lost during this process.

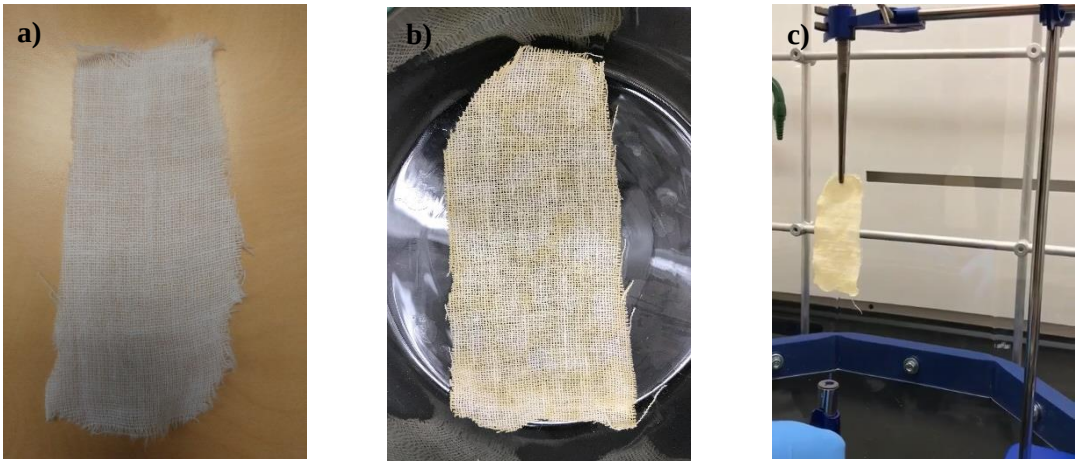

Figure 4.4 a) Standard cotton towel sample used prior to any addition of polyphosphinoborane; b) cotton towel sample impregnated with **4.1a** after drying overnight in a vacuum oven at 40 °C; c) Standard experimental set up for flame tests.

The cotton samples were suspended 10 cm above a blow torch (Figure 4.4 c). The flame was moved under the sample and then slowly moved upwards until the sample ignited. Whereas the control cotton sample with no polyphosphinoborane burned completely leaving minimal char, the sample loaded with **4.1a** was found to catch fire but then to self-extinguish leaving a significant amount of charred residue remaining (Figure 4.5 and Figure S4.10). The char remained intact throughout the flame-test with no

dripping observed, a key requirement of flame-retardant materials. The material did not disintegrate on removing from the clamp stand; however, it was found to be brittle and could be easily broken by manipulating the char. The duration that the cotton sample treated with **4.1a** burnt with a flame was significantly lower (8 s) than for the untreated cotton (17 s). Both samples ignited quickly before the blow torch was raised completely to the bottom of the sample.

A further cotton sample was impregnated with ca. two times the mass of **4.1a** (305 mg) in 5 mL DCM, dried in a vacuum oven for 24 h at 40 °C and subjected to flame testing (Figure S4.11); however, this did not show any increased flame-retardancy.

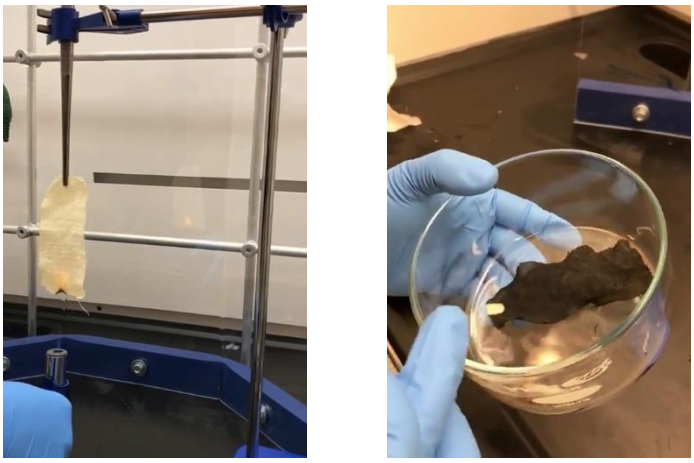

Figure 4.5 Flame testing of cotton sample impregnated with **4.1a** showing the ignition of the sample (left) and the charred material remaining after self-extinguishing of the flame (right).

4.2.3.2 Analysis of char material

A key step in the operation of phosphorus-containing flame-retardants commonly involves the formation of phosphorus oxides and/or acids. Boric acid has been invoked in the operation of boron containing flame retardants.[46] To investigate if any of these were forming in flame testing of cotton treated with **4.1a**, the char formed upon burning cotton treated with **4.1a** was extracted into deionised water (10 mL) over 72 h. The pH of the water was then tested and found to be around pH 1 indicating the presence of highly acidic species. The water was removed by rotary evaporation and the residue dissolved in D_2O. Analysis of this material by ^{31}P NMR spectroscopy revealed a major peak of 90% relative intensity at $\delta = 0$ ppm, consistent with the formation of phosphoric acid H_3PO_4 ($\delta = 0$ ppm, 85% H_3PO_4 in H_2O).[70] Several other unidentified minor products were also observed. The ^{11}B NMR spectrum showed a broad singlet with a chemical shift of −19.4 ppm which consistent with the formation of boric

acid (Figure 4.6). The formation of these acidic species along with significant amounts of char suggest that the poly(phenylphosphinoborane) is operating as a flame-retardant via a similar condensed phase mechanism to that reported for previously developed PFRs.

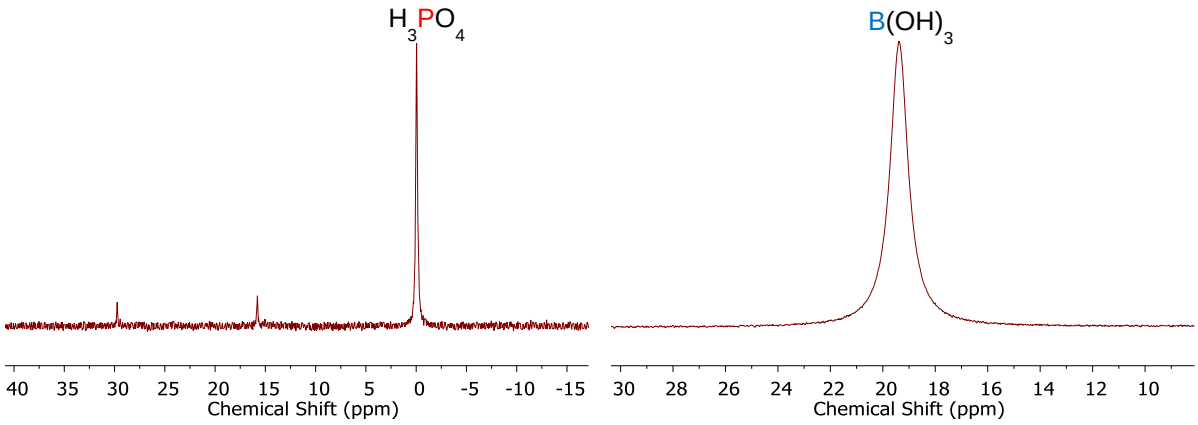

Figure 4.6 ^{31}P NMR spectrum (122 MHz, 25 °C, D_2O) (left) and ^{11}B NMR spectrum (96 MHz, 25 °C, D_2O) (right) of the residue following aqueous extraction from the char formed from burning cotton treated with **4.1a**.

4.2.3.3 Comparison with cotton treated with polystyrene

Given that poly(phenylphosphinoborane) is isoelectronic with polystyrene, we endeavoured to compare the flammability of material impregnated with **4.1a** with a cotton sample treated with polystyrene. A 5 × 10 cm sample of cotton was loaded with polystyrene (162 mg in 5 mL DCM). This gave an inflexible material after drying overnight. Subjecting this material to our flame-test resulted in complete consumption of the material without the formation of a char. The material also disintegrated during the flame-testing with dripping of burning material to the ground (Figure S4.12). This showcases that while many inorganic polymers may have isoelectronic organic analogues, they possess properties that are not accessible for many organic macromolecules.

4.2.3.4 The use of P-disubstituted polyphosphinoboranes as flame-retardants

Following our investigation into the use of **4.1a** as a flame-retardant additive for cotton towel, we examined the effect of the presence of different side groups on the flame-retardant properties. To this end we synthesised two polymers from **4.1a** using a recently reported post-polymerisation modification via the hydrophosphination of olefins (Scheme 4.5).[42] **4.5** was synthesised via reaction with 1-octene and was chosen to investigate the effect of replacing the P-H (which under combustion conditions has the potential to release reactive hydrogen radicals) with a second organic side chain. A number of PFRs also contain halogenated moieties. The presence of these are postulated to have a synergic effect

resulting in more proficient flame-retardants because phosphorus mainly acts in the condensed phase with halogens offering a gas phase contribution to extinguishing a flame.[71] We therefore synthesised a halogen containing polymer (**4.6**) by hydrophosphination of 1H,1H,2H-perfluoro-1-hexene using **4.1a**. As with previous cases, cotton towel samples (5 × 10 cm) were impregnated with polyphosphinoborane (ca. 150 mg), dried overnight and then subjected to flame testing.

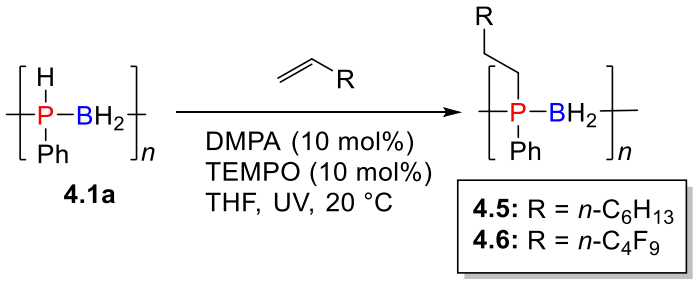

Scheme 4.5 The post-polymerisation modification of poly(phenylphosphinoborane) via the radical hydrophosphination of olefins to give P-disubstituted polymers

Cotton treated with **4.5** took longer to catch fire compared to cotton treated with **4.1a,** taking around 2 s of flame contact with the material to ignite; however, it burnt for slightly longer (12 s compared to 8 s for sample impregnated with **4.1a**) (Figure S4.13). This slower burning may be due to the absence of reactive P-H groups that can release radicals that can accelerate combustion. Again, the flame was found to self-extinguish with the formation of a char. Polymer treated with **4.6** showed very similar results to **4.5,** taking around 2 s to ignite and subsequently burning for 13 s (Figure S4.14). This suggests that the presence of halogens does not impart any additional flame-retardancy and it is the condensed phase action of phosphorus/boron that is most important for the flame-retardancy of these polymers.

4.2.3.5 Leaching study

A common issue with molecular PFRs is that they are prone to leach out of the product when placed in contact with water or moisture. To assess the leachability of **4.1a** in aqueous media, we treated a cotton sample with **4.1a** (5 × 10 cm cotton sample, 152 mg of **4.1a** in 5 mL DCM) and dried the sample in a vacuum oven overnight at 40 °C (mass after drying = 0.701 g). This sample was then placed in a deionised water bath for 6 h with the water changed every 2 h. The sample was again dried overnight under vacuum at 40 °C yielding material with a mass of 0.697 g. The mass change between the sample before and after exposure to water is negligible suggesting that there is minimal leaching of the polymer

from the cotton sample in water. To assess whether there is any change in the flame-retardant properties of this material compared to other samples which have not been submerged in water, an analogous flame test was carried out (Figure S4.15). As with previous cases, the flame was found to self extinguish leaving a char showing that the flame-retardancy properties are retained after exposure to water. This property is especially promising for the application of polyphosphinoboranes as flame-retardants because leaching is a common issue for many additives currently used.

4.2.4 Conclusions

Polyphosphinoboranes, **4.1a**, **4.5**, and **4.6** were each found to be effective flame retardants for cotton towel. Flame-tests show that these polymers are capable of inducing a char which inhibits burning and prevents complete combustion of the material. This is in contrast to untreated cotton and cotton treated with polystyrene which burnt completely. Analysis of the char material revealed the formation of phosphoric and boric acids, species commonly invoked for action of related flame-retardant species. Polymers **4.5** and **4.6** formed by modification of **4.1a** via hydrophosphination of 1-octene or 1H,2H,2H-perfluorohexene respectively, were found to have similar flame-retardant proficiency to **4.1a,** indicating that it is the condensed phase action of phosphorus and boron in the polymer main chain that imparts this property. Exposure of cotton treated with **4.1a** to water was not found to have any effect on flame-retardancy demonstrating the non-leachability of these polymers, in contrast to many commercial used molecular flame retardants which commonly have leachability issues.

4.2.5 Experimental Section

4.2.5.1 General procedures, reagents, and equipment

Polymers **4.5** and **4.6** were synthesised via literature procedure.[42] Poly(styrene) (average M_w = 250,000 Da) was purchased from Fisher Scientific and used as received. Cotton towel was purchase from Canadian Tire and cut into 5x10 cm segments. For flame experiments, an Iroda PT-200 Butane Torch with a flame temperature of 1300 °C flame was used. This was purchased from Canadian Tire. The blow torch was operated at its maximum setting.

NMR spectra were recorded using a Bruker Avance III 300 spectrometer. ^{11}B, and ^{31}P NMR spectra were referenced to external standards (^{11}B: $BF_3{\cdot}OEt_2$ (δ = 0.0); ^{31}P: 85% H_3PO_4 (aq.) (δ = 0.0)). Chemical shifts (δ) are given in parts per million (ppm).

4.2.5.2 Preparation of poly(phenylphosphinoborane) 4.1a

A Schlenk flask was charged with $PhH_2P{\cdot}BH_3$ (2.5 g. 0.020 mol), $FeCp(CO)_2OTf$ (69 mg, 0.2 mmol, 1 mol%) and toluene (6.8 mL, 3 M). The orange solution was heated to 100 °C for 20 h after which the reaction mixture was precipitated into cold pentane (−78 °C, 250 mL). The polymer was precipitated a further two times from DCM (5 mL) into pentane (−78 °C, 250 mL) after which volatiles were removed under vacuum and the polymer dried in a vacuum oven at 40 °C for 24 h giving a pale yellow solid (yield = 1.60 g, 65%). NMR data matched literature values[28] and the molar mass was determined by GPC (M_n = 68,000 g mol^{-1}, PDI = 1.5). The discolouration of this polymer is reported to come from residual iron species remaining despite repeated precipitation from DCM into cold pentane (−78 °C).[28]

4.2.5.3 General procedure for preparation of cotton samples treated with polymer

Cotton flour towel was cut into ca. 5 × 10 cm samples. The cotton sample was weighed and then treated with a polymer solution (ca. 150 mg unless stated otherwise) in DCM (5 mL) via pipetting with frequent turning to give an even loading. The resultant material was dried for 24 h in a vacuum oven at 40 °C and subsequently reweighed to determine polymer loading.

4.2.5.4 General flame testing methodology

A clamp stand was set up as shown in Figure 4.4. The bottom of the cotton sample was held 10 cm above a blow torch. The blow torch was switched on and moved under the sample. This was then slowly moved up until the polymer sample ignited and then removed to observe the combustion process.

4.2.5.5 Specific flame test details

Untreated cotton

DCM (5 mL) was pipetted over cotton. The sample was then dried in a vacuum oven overnight prior to flame testing (mass of cotton sample = 0.586 g).

Burning time (time from catching fire to extinguishing of flame) = 17 s.

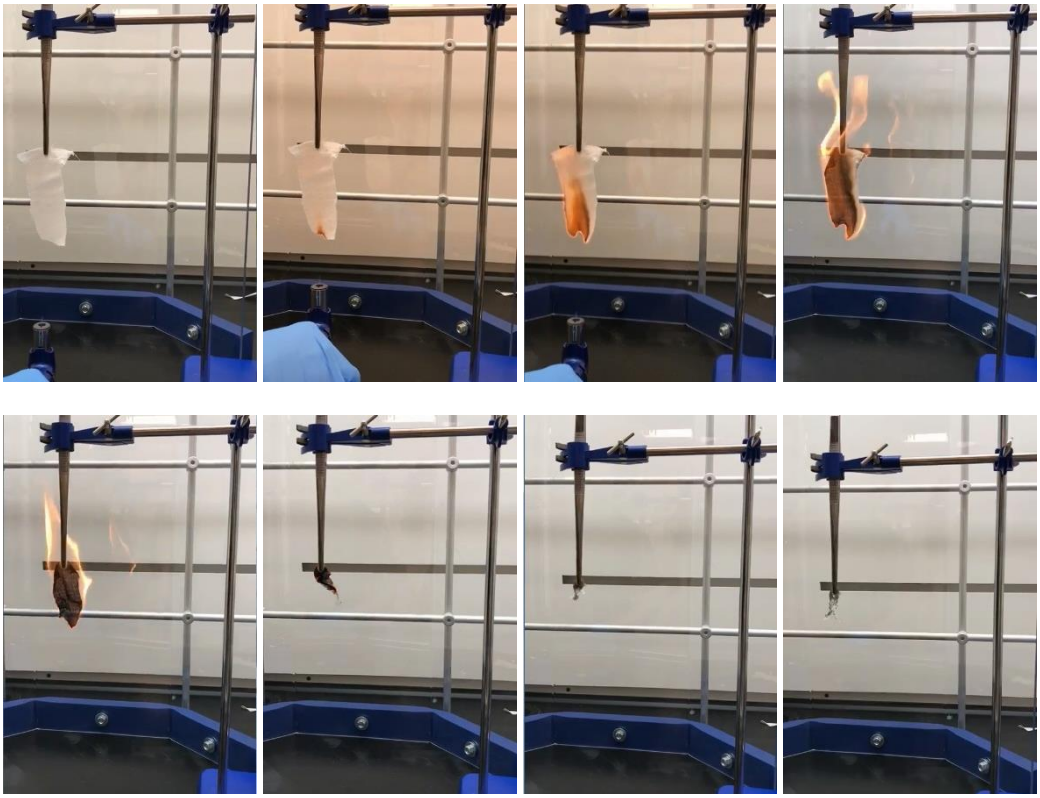

Figure S4.9 Flame test on cotton sample without any poly(phosphinoborane) additive.

Poly(phenylphosphinoborane) (4.1a)

<u>164 mg loading</u>

Mass of polymer added = 164 mg.

Mass of cotton sample after drying = 716 mg.

Increase in cotton sample mass after loading and drying = 158 mg.

Burning time = 8 s.

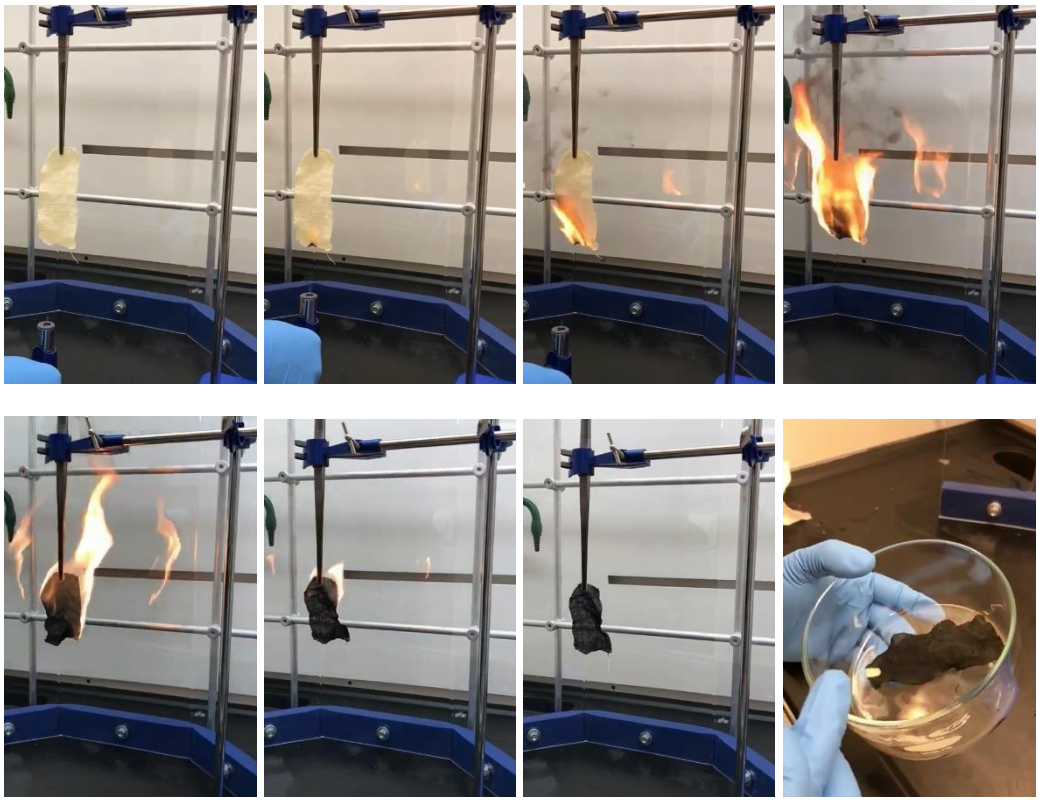

Figure S4.10 Flame test on cotton sample loaded with **4.1a** (164 mg).

305 mg loading

Mass of polymer added = 305 mg.

Mass of cotton sample after drying = 781 mg.

Increase in cotton sample mass after loading and drying = 269 mg.

Burning time = 5 s.

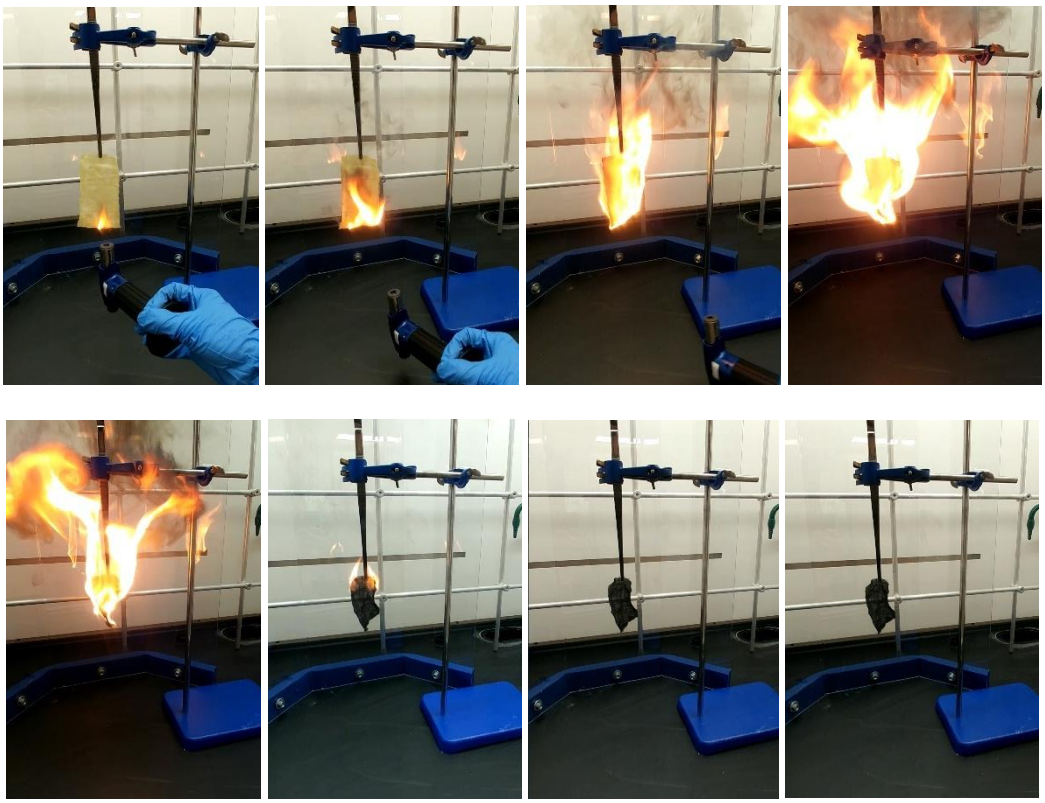

Figure S4.11 Flame test on cotton sample loaded with **4.1a** (305 mg).

Polystyrene

Mass of polymer added = 162 mg.

Mass of cotton sample after drying = 736 mg.

Increase in cotton sample mass after loading and drying = 136 mg.

Burning time = 20 s.

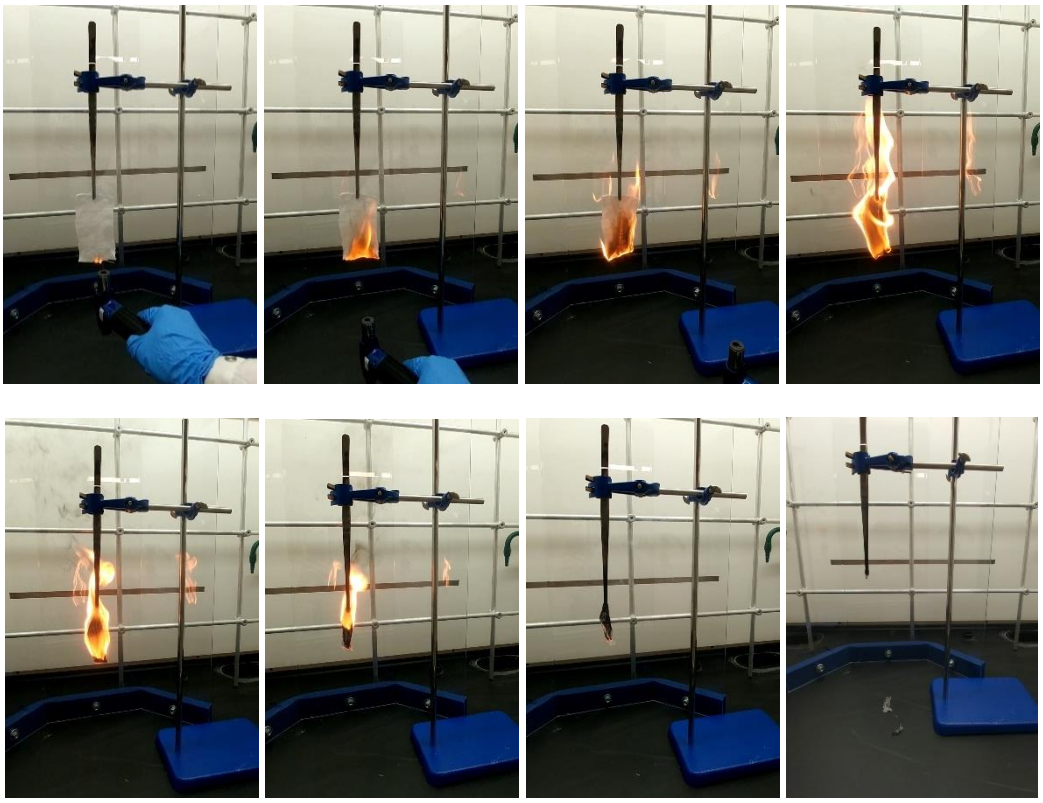

Figure S4.12 Flame test on cotton sample loaded with polystyrene (162 mg).

Poly(octyl(phenyl)phosphinoborane) (4.5)

Mass of polymer added = 149 mg.

Mass of cotton sample after drying = 705 mg.

Increase in cotton sample mass after loading and drying = 127 mg.

Burning time = 12 s.

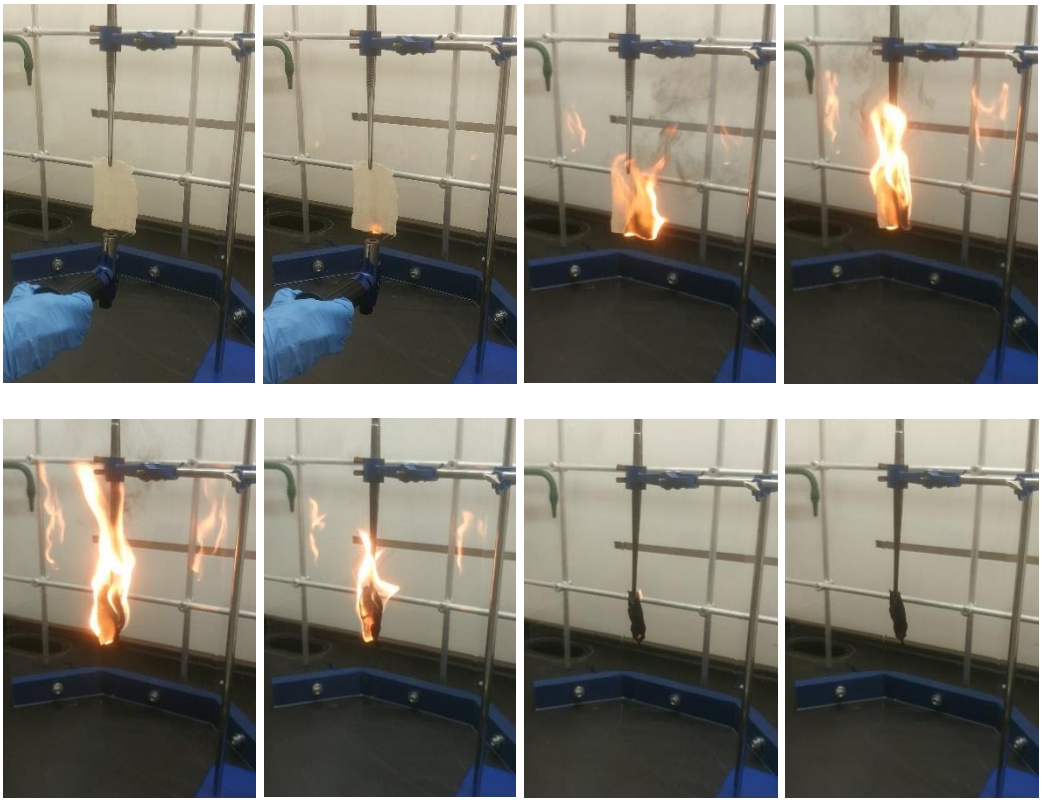

Figure S4.13 Flame test on cotton sample loaded with **4.5** (149 mg).

Poly((3,3,4,4,5,5,6,6,6-nonafluorohexyl)(phenyl)phosphinoborane) (4.6)

Mass of polymer added = 160 mg.

Mass of cotton sample after drying = 651 mg.

Increase in cotton sample mass after loading and drying = 91 mg.

Burning time = 13 s.

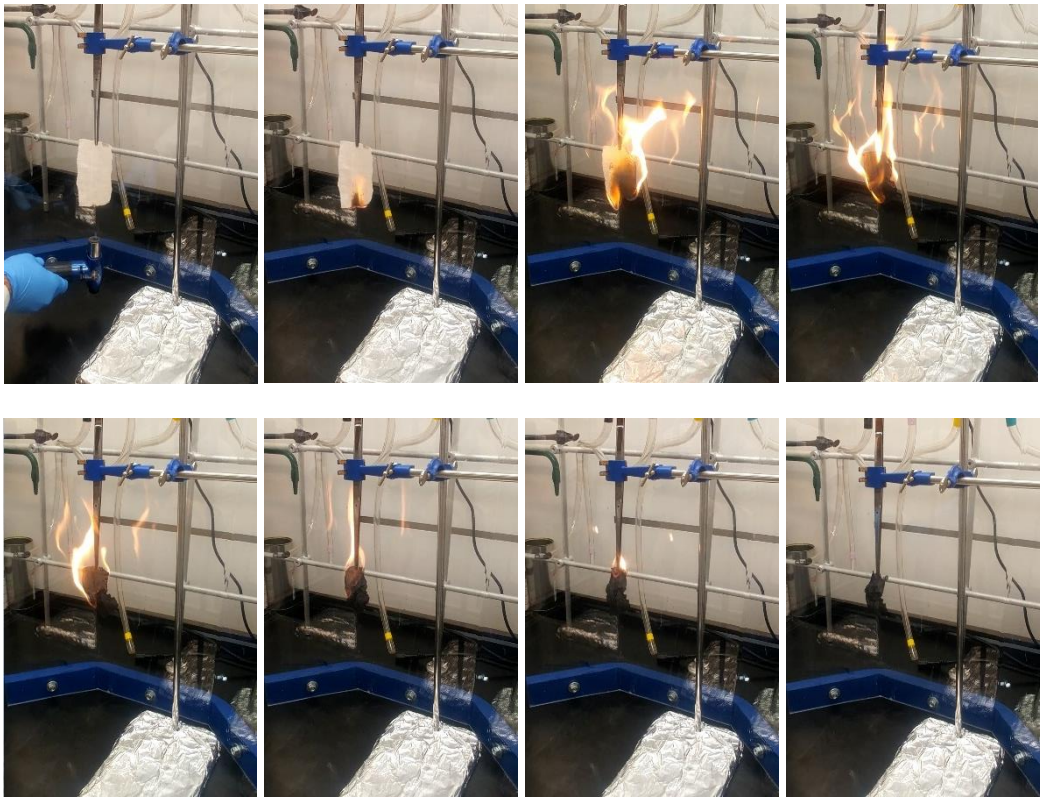

Figure S4.14 Flame test on cotton sample loaded with **4.6** (149 mg).

4.2.5.6 Char analysis

The char formed during combustion was placed in water for 2 days after which, the pH of the water was tested and found to be very acidic (pH 1). The water was transferred to a round bottom flask and dried using a rotary evaporator. The remaining material was dissolved in D_2O and ^{11}B and ^{31}P NMR spectra measured (Figure 4.6).

4.2.5.7 Leaching test

A sample of cotton towel impregnated in **4.1a** was prepared using the above method. This sample was placed in a deionised water bath for 6 h with the water changed every 2 h. The sample was then dried

in a vacuum oven overnight at 40 °C. Sample mass before submersion in water = 0.701 g, sample mass after submersion in water = 0.697 g. The flame-retardant properties of this material were tested using an analogous method to above and found to be indistinguishable from a sample impregnated with **1** and not exposed to water.

Mass of polymer added = 152 mg.

Mass of cotton sample after drying = 701 mg.

Increase in cotton sample mass after loading and drying = 144 mg.

Mass after sample after submersion in water for 6 h and drying overnight = 0.697 mg.

Burning time = 8 s.

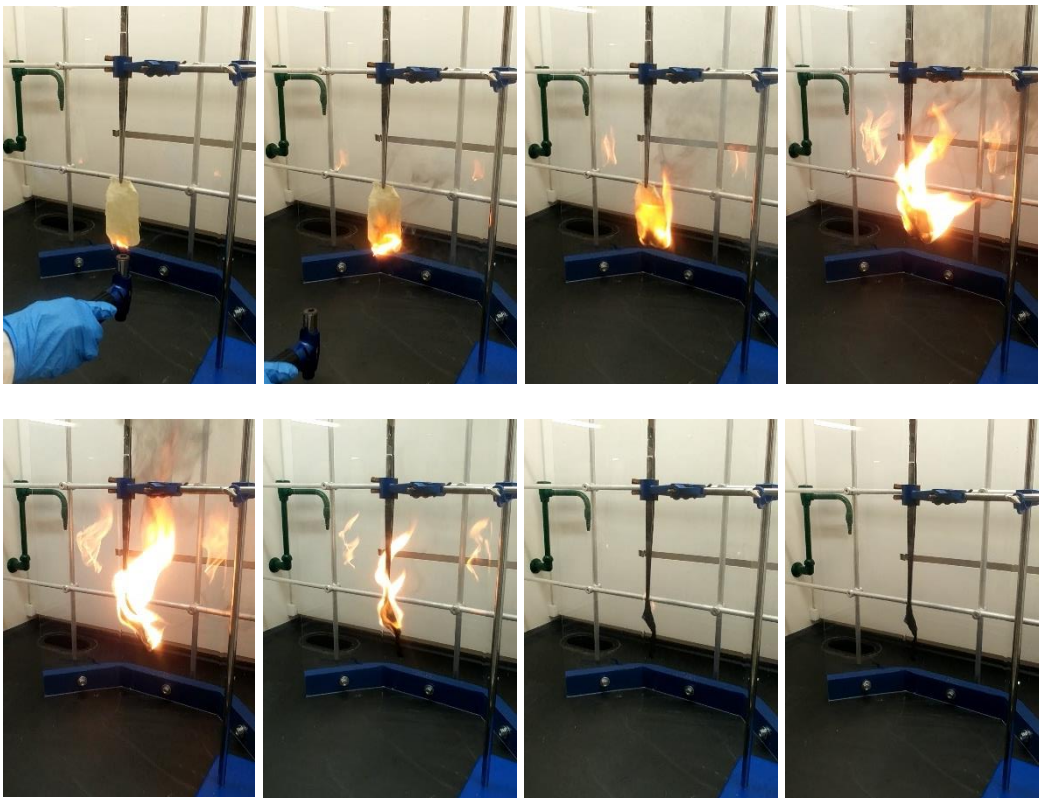

Figure S4.15 Flame test on cotton sample loaded with **4.1a** (152 mg) after submerging in water for 6 h.

4.3 References

1. Buwalda, S. J.; Boere, K. W. M.; Dijkstra, P. J.; Feijen, J.; Vermonden, T.; Hennink, W. E., *J. Control. Release* **2014,** *190*, 254-273.
2. Hennink, W. E.; van Nostrum, C. F., *Adv. Drug Deliv. Rev.* **2012,** *64*, 223-236.
3. Wichterle, O.; Lím, D., *Nature* **1960,** *185*, 117-118.
4. Hoare, T. R.; Kohane, D. S., *Polymer* **2008,** *49*, 1993-2007.
5. Caló, E.; Khutoryanskiy, V. V., *Eur. Polym. J.* **2015,** *65*, 252-267.
6. Peppas, N. A.; Hilt, J. Z.; Khademhosseini, A.; Langer, R., *Adv. Mater.* **2006,** *18*, 1345-1360.
7. Bakaic, E.; Smeets, N. M. B.; Hoare, T., *RSC Adv.* **2015,** *5*, 35469-35486.
8. Lin, C.-C., *RSC Adv.* **2015,** *5*, 39844-39853.

9. Kumar, A.; Han, S. S., *Int. J. Polym. Mater.* **2017,** *66*, 159-182.
10. Ahmadi, F.; Oveisi, Z.; Samani, S. M.; Amoozgar, Z., *Res. Pharm. Sci.* **2015,** *10*, 1-16.
11. Hempenius, M. A.; Cirmi, C.; Savio, F. L.; Song, J.; Vancso, G. J., *Macromol. Rapid Commun.* **2010,** *31*, 772-783.
12. Montheil, T.; Echalier, C.; Martinez, J.; Subra, G.; Mehdi, A., *J. Mater. Chem. B* **2018,** *6*, 3434-3448.
13. Abbasi, F.; Mirzadeh, H.; Katbab, A.-A., *Polym. Int.* **2001,** *50*, 1279-1287.
14. Allcock, H. R., Water-Soluble Polyphosphazenes and Their Hydrogels. In *Hydrophilic Polymers*, American Chemical Society: 1996; Vol. 248, pp 3-29.
15. Allcock, H. R.; Gebura, M.; Kwon, S.; Neenan, T. X., *Biomaterials* **1988,** *9*, 500-508.
16. Allcock, H. E.; Kwon, S.; Riding, G. H.; Fitzpatrick, R. J.; Bennett, J. L., *Biomaterials* **1988,** *9*, 509-513.
17. Bennett, J. L.; Dembek, A. A.; Allcock, H. R.; Heyen, B. J.; Shriver, D. F., *Chem. Mater.* **1989,** *1*, 14-16.
18. Cho, J.-K.; Park, J. W.; Song, S.-C., *J. Pharm. Sci.* **2012,** *101*, 2382-2391.
19. Potta, T.; Chun, C.; Song, S.-C., *Biomaterials* **2009,** *30*, 6178-6192.
20. Potta, T.; Chun, C.; Song, S.-C., *Biomacromolecules* **2010,** *11*, 1741-1753.
21. Potta, T.; Chun, C.; Song, S.-C., *Biomaterials* **2010,** *31*, 8107-8120.
22. Dorn, H.; Singh, R. A.; Massey, J. A.; Lough, A. J.; Manners, I., *Angew. Chem. Int. Ed.* **1999,** *38*, 3321-3323.
23. Dorn, H.; Singh, R. A.; Massey, J. A.; Nelson, J. M.; Jaska, C. A.; Lough, A. J.; Manners, I., *J. Am. Chem. Soc.* **2000,** *122*, 6669-6678.
24. Dorn, H.; Rodezno, J. M.; Brunnhöfer, B.; Rivard, E.; Massey, J. A.; Manners, I., *Macromolecules* **2003,** *36*, 291-297.
25. Clark, T. J.; Rodezno, J. M.; Clendenning, S. B.; Aouba, S.; Brodersen, P. M.; Lough, A. J.; Ruda, H. E.; Manners, I., *Chem. Eur. J.* **2005,** *11*, 4526-4534.
26. Jacquemin, D.; Lambert, C.; Perpète, E. A., *Macromolecules* **2004,** *37*, 1009-1015.
27. Nakhmanson, S. M.; Nardelli, M. B.; Bernholc, J., *Phys. Rev. Lett.* **2004,** *92*, 115504.
28. Schäfer, A.; Jurca, T.; Turner, J.; Vance, J. R.; Lee, K.; Du, V. A.; Haddow, M. F.; Whittell, G. R.; Manners, I., *Angew. Chem. Int. Ed.* **2015,** *54*, 4836-41.
29. Paul, U. S. D.; Braunschweig, H.; Radius, U., *Chem. Commun.* **2016,** *52*, 8573-8576.
30. Marquardt, C.; Jurca, T.; Schwan, K.-C.; Stauber, A.; Virovets, A. V.; Whittell, G. R.; Manners, I.; Scheer, M., *Angew. Chem. Int. Ed.* **2015,** *54*, 13782-13786.
31. Pandey, S.; Lönnecke, P.; Hey-Hawkins, E., *Eur. J. Inorg. Chem.* **2014**, 2456-2465.
32. Hooper, T. N.; Weller, A. S.; Beattie, N. A.; Macgregor, S. A., *Chem. Sci.* **2016,** *7*, 2414-2426.
33. Denis, J.-M.; Forintos, H.; Szelke, H.; Toupet, L.; Pham, T.-N.; Madec, P.-J.; Gaumont, A.-C., *Chem. Commun.* **2003**, 54-55.
34. Cavaye, H.; Clegg, F.; Gould, P. J.; Ladyman, M. K.; Temple, T.; Dossi, E., *Macromolecules* **2017,** *50*, 9239-9248.
35. Turner, J. R.; Resendiz-Lara, D. A.; Jurca, T.; Schäfer, A.; Vance, J. R.; Beckett, L.; Whittell, G. R.; Musgrave, R. A.; Sparkes, H. A.; Manners, I., *Macromol. Chem. Phys.* **2017,** *218*, 1700120.
36. Thoms, C.; Marquardt, C.; Timoshkin, A. Y.; Bodensteiner, M.; Scheer, M., *Angew. Chem.* **2013,** *125*, 5254-5259.
37. Thoms, C.; Marquardt, C.; Timoshkin, A. Y.; Bodensteiner, M.; Scheer, M., *Angew. Chem. Int. Ed.* **2013,** *52*, 5150-5154.
38. Stauber, A.; Jurca, T.; Marquardt, C.; Fleischmann, M.; Seidl, M.; Whittell, G. R.; Manners, I.; Scheer, M., *Eur. J. Inorg. Chem.* **2016**, 2684-2687.
39. Oldroyd, N. L.; Chitnis, S. S.; Annibale, V. T.; Arz, M. I.; Sparkes, H. A.; Manners, I., *Nat. Commun.* **2019,** *10*, 1370.
40. Resendiz-Lara, D.; Annibale, V. T.; Knights, A. W.; Chitnis, S. S.; Manners, I., *Manuscript submitted* **2019**.
41. Arz, M. I.; Knights, A. W.; Manners, I., *Macromol. Rapid Commun.* **2019**, 1900468.
42. Knights, A. W.; Chitnis, S. S.; Manners, I., *Chem. Sci.* **2019,** *10*, 7281-7289.
43. Levchik, S.; Weil, E., *J. Fire Sci.* **2006,** *24*, 345-364.

44. Bourbigot, S.; Duquesne, S., *J. Mater. Chem.* **2007,** *17*, 2283-2300.
45. Morgan, A. B., *Polym. Rev.* **2019,** *59*, 25-54.
46. Lu, S.-Y.; Hamerton, I., *Prog. Polym. Sci.* **2002,** *27*, 1661-1712.
47. Laoutid, F.; Bonnaud, L.; Alexandre, M.; Lopez-Cuesta, J. M.; Dubois, P., *Mater. Sci. Eng. R Rep.* **2009,** *63*, 100-125.
48. Levchik, S. V.; Camino, G.; Luda, M. P.; Costa, L.; Muller, G.; Costes, B., *Polym. Degrad. Stab.* **1998,** *60*, 169-183.
49. van der Veen, I.; de Boer, J., *Chemosphere* **2012,** *88*, 1119-1153.
50. Lewin, M., *Polym. Degrad. Stab.* **2005,** *88*, 13-19.
51. Allen, C., *J. Fire Sci.* **1993,** *11*, 320-328.
52. Fei, S.-T.; Allcock, H., *J. Power Sources* **2010,** *195*, 2082-2088.
53. Potin, P.; De Jaeger, R., *Eur. Polym. J.* **1991,** *27*, 341-348.
54. Ranganathan, T.; Zilberman, J.; Farris, R. J.; Coughlin, E. B.; Emrick, T., *Macromolecules* **2006,** *39*, 5974-5975.
55. Liu, X.; Zhang, C.; Gao, S.; Cai, S.; Wang, Q.; Liu, J.; Liu, Z., *Mater. Chem. Phys.* **2020,** *239*, 122014.
56. Arz, M. I.; Annibale, V. T.; Kelly, N. L.; Hanna, J. V.; Manners, I., *J. Am. Chem. Soc.* **2019,** *141*, 2894-2899.
57. Priegert, A. M.; Siu, P. W.; Hu, T. Q.; Gates, D. P., *Fire Mater.* **2015,** *39*, 647-657.
58. Priegert, A. M.; Rawe, B. W.; Serin, S. C.; Gates, D. P., *Chem. Soc. Rev.* **2016,** *45*, 922-53.
59. Jäkle, F.; Vidal, F., *Angew. Chem. Int. Ed.* **2019,** *58*, 5846-5870.
60. De Chirico, A.; Audisio, G.; Provasoli, F.; Armanini, M.; Franzese, R., *Makromol. Chem., Macromol. Symp.* **1993,** *74*, 343-348.
61. Armitage, P.; Ebdon, J. R.; Hunt, B. J.; Jones, M. S.; Thorpe, F. G., *Polym. Degrad. Stab.* **1996,** *54*, 387-393.
62. Myers, R. E.; Dickens, E. D.; Licursi, E.; Evans, R. E., *J. Fire Sci.* **1985,** *3*, 432-449.
63. Staubitz, A.; Robertson, A. P. M.; Sloan, M. E.; Manners, I., *Chem. Rev.* **2010,** *110*, 4023-4078.
64. Burg, A. B., *J. Inorg. Nucl. Chem.* **1959,** *11*, 258.
65. Wagner, R. I.; Caserio, F. F., *J. Inorg. Nucl. Chem.* **1959,** *11*, 259.
66. Burg, A. B.; Wagner, R. I. Phosphinoborine compounds and their preparation. Patent, U. S., 3071553, 1963.
67. Burg, A. B.; Wagner, R. I. Phosphinoborine compounds and their preparation. Patent, U. S., 2948689, 1960.
68. Muetterties, E. L., The Chemistry of Boron and its Compounds. Wiley: New York, 1967; pp 617-617.
69. Lewin, M., *J. Fire Sci.* **1997,** *15*, 263-276.
70. Harris, R. K.; Becker, E. D.; Cabral de Menezes, S. M.; Goodfellow, R.; Granger, P., *Solid State Nucl. Magn. Reson.* **2002,** *22*, 458-483.
71. Green, J., *J. Fire Sci.* **1994,** *12*, 388-408.

Chapter 5

B-OSi bond formation via a modified Piers-Rubinsztajn reaction

5.1 Abstract

Herein we report a modified Piers-Rubinsztajn reaction for the synthesis of molecular and polymeric borosiloxane species under mild and metal-free conditions using tris(pentafluorophenyl)borane ($B(C_6F_5)_3$) as a catalyst. While the attempted dehydrocoupling of phenylboronic acid ($PhB(OH)_2$) with secondary and tertiary silanes (R_2SiH_2 and R_3SiH; R = Et, Ph) in the presence of 5 mol% $B(C_6F_5)_3$ resulted in the formation of siloxane and boroxine by-products alongside the desired borosiloxane, the $B(C_6F_5)_3$-catalysed reaction of dimethyl phenylboronate ($PhB(OMe)_2$) with Et_3SiH led to the selective formation of $PhB(OSiEt_3)_2$. We also report the formation of linear polymers $[R_2SiO\text{-}B(Ph)O]_n$ featuring alternating boron and siloxane units in the main chain via the reaction of $PhB(OMe)_2$ with Et_2SiH_2. The presence of single peaks in the $^{11}B\{H\}$ and $^{29}Si\{H\}$ NMR spectra supports the alternating nature of this polymer. The extension to analogues via reaction of $PhB(OMe)_2$ with Ph_2SiH_2 or a hybrid organic/inorganic polymer via reaction with bis(dimethylsilylbenzene) resulted in the formation of some siloxane linkages in the polymer chain. These polymers were found to contain high molar mass material by gel permeation chromatography, although, multimodal mass distributions were observed (M = 2,200 – 126,000 g mol^{-1}).

5.2 Introduction

Materials featuring p-block elements are of increasing academic and industrial interest due to advantageous properties that complement those available with all carbon analogues.[1-3] Of particular note are polysiloxanes $[RR'SiO]_n$ which have been widely studied and are commonplace in modern society owing to their thermal stability, low glass transition temperatures, and chemical and biological inertness.[4] The backbone of polysiloxanes can be altered through intensive heating in the presence of a

boron containing compound, commonly boric acid or boric oxide,[5-8] forming materials commonly known as 'bouncing putty' which have found commercial applications owing to their interesting viscoelastic properties.[9, 10] The presence of $B(OH)_2$ end groups allows for hydrogen- and dative-bonding between polymer chains forming an elastomeric material;[11, 12] however, their structures are often ill-defined and the percentage incorporation of boron into the polymer is low.

Borosiloxanes have high chemical and thermal stabilities,[13, 14] and have been shown to have promise in applications such as flame retardants,[15] electrolyte additives,[16, 17] ceramic precursors,[18, 19] and chemical sensors for amines[20] and fluoride anions.[21] Owing to the potential applications of borosiloxanes, research into the formation of these bonds has been of significant interest. Cyclic and cage structures,[22-25] as well as gels and network polymers have all been reported.[13, 18, 26-29] There are, however, limited examples of well-defined linear polymers consisting of alternating borane and siloxane moieties.[21, 30]

Conventional syntheses of borosiloxanes have involved the reaction of hydroxyborane with chlorosilanes[18, 25, 31-34] or the reaction of a silanol with borane derivatives.[35-40] These routes, commonly suffer from laborious experimental set up and work up, and involve formation of undesirable side products, for example, corrosive HCl. The synthesis of linear polyborosiloxanes has been reported by a condensation reaction between $PhB(OH)_2$ and Ph_2SiCl_2, followed by subsequent end group capping using in situ generated phenylacetylide.[30] This polymer showed high thermal and oxidative stability; however, the molecular weight of the material obtained was low (M_w <6,000 g mol^{-1}) and a high polydispersity index (PDI) was found (PDI = 2.7). HCl was also produced as a by-product of polymerisation.

Recently, methods have been developed for the synthesis of borosiloxanes via transition metal catalysed dehydrocoupling[41-43] The formation of linear borosiloxane polymers has been reported via the dehydrocoupling of $Ph_2Si(OH)_2$ with mesitylborane in the presence of $[PdCl_2(PPh_3)_2]$ (20 °C, toluene, 12 h).[21] A single peak was observed in both the ^{11}B and ^{29}Si NMR spectra of this material and the polymer was found to be high molar mass (M_n = 42,500 g mol^{-1}, PDI of 1.2). One limitation, however, was that this required in situ generation of the mesityl borane species and has not been extended to formation of other borosiloxane polymers. Despite these important steps forward in Si-O-B bond

formation chemistry, it is of significant scientific interest to find a method for the formation of both molecular and polymeric borosiloxanes under mild conditions, preferably without the need for expensive and toxic transition metal catalysts or formation of corrosive side products.

The Piers-Rubinsztajn (PR) reaction is a recently developed catalytic route to Si-O bond formation.[44-53] This makes use of tris(pentafluorophenyl)borane ($B(C_6F_5)_3$) as a catalyst for a demethanative condensation reaction between a silane and an alkoxysilane under ambient conditions, liberating methane in the process (Scheme 5.1a). This methodology is tolerant of a range of substrates and has been an area of significant interest for the formation of polysiloxane materials,[53] in particular due to the use of a cheap, non-metal catalyst, and avoiding the formation of toxic by-products.

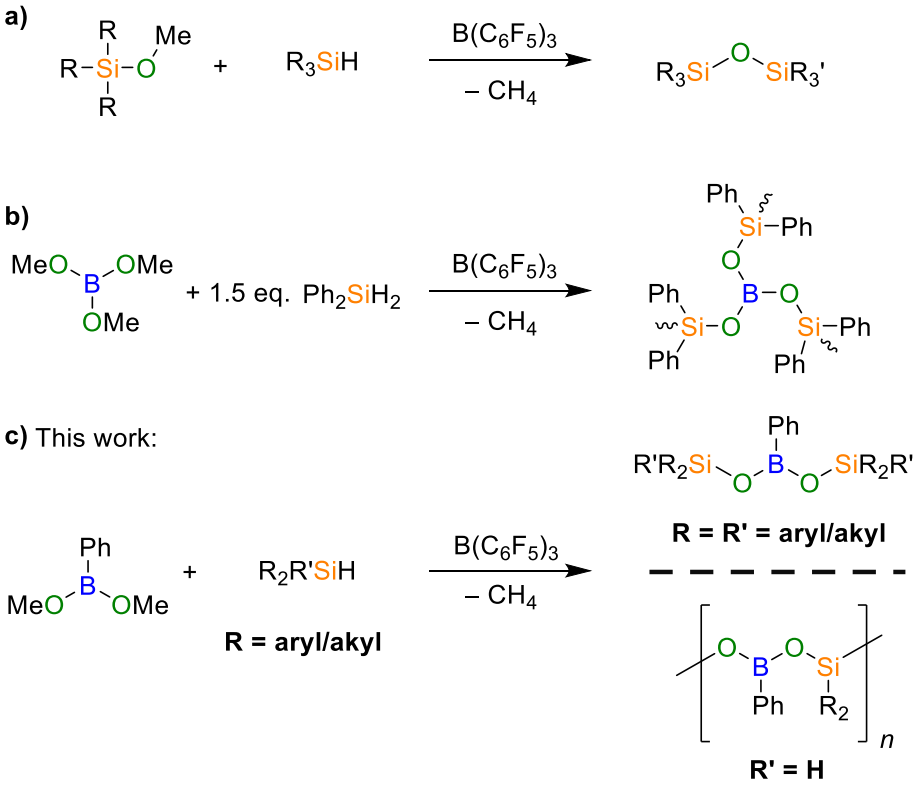

Scheme 5.1 a) The Piers-Rubinsztajn (PR) demethanative condensation between a silane and alkoxysilane in the presence of catalytic amounts of $B(C_6F_5)_3$ yielding siloxane linkages; b) the synthesis of borosiloxane resins using PR type methodology; c) the synthesis of molecular borosiloxanes and linear polymeric species using a PR type reaction.

PR type systems have already shown promise in the formation of borosiloxane materials. In 2014, Rubinsztajn demonstrated the synthesis of borosiloxane resins from the $B(C_6F_5)_3$ reaction of $B(OMe)_3$ and Ph_2SiH_2 (Scheme 5.1b).[26] A patent by Li et al. reported the formation of a linear borosiloxane from reaction of equimolar amounts of $(MeO)_2SiMe_2$ and Me_3Si-O-$SiMe_3$, and a small amount of $PhB(OH)_2$

(5 mol%) in the presence of $B(C_6F_5)_3$ (5 mol%).[54] The resultant material was only characterised by ^1H NMR spectroscopy and gel permeation chromatography (GPC), with no definitive evidence of boron incorporation into the backbone of the polymer. Given that alkoxysilanes and hydrosilanes are known to react very efficiently and are present in vast excess, it is conceivable that a polysiloxane is formed instead. Nevertheless, these reports suggest that this methodology has the potential as a general route to borosiloxane species. Herein, we disclose a protocol for the synthesis of molecular and linear polymeric borosiloxanes from readily available precursors via a modified Piers-Rubinsztajn reaction (Scheme 5.1c).

5.3 Results and Discussion

5.3.1 Dehydrocoupling reactions using phenylboronic acid

5.3.1.1 Reaction of phenylboronic acid with secondary silanes

In an attempt to synthesise linear polymers featuring alternating boron and siloxane units, we first probed the reactivity of commercially available phenylboronic acid ($PhB(OH)_2$) with secondary silanes in the presence of a $B(C_6F_5)_3$ catalyst. Reaction of stoichiometric amounts of $PhB(OH)_2$ and Et_2SiH_2 in DCM in the presence of $B(C_6F_5)_3$ (5 mol%) resulted in immediate rapid gas evolution. After stirring at 20 °C for 5 min under a flow of nitrogen, the reaction was heated to 40 °C. As the reaction progressed, a white crystalline solid precipitated from the solution. After 22 h, ^1H NMR spectroscopy showed a complex mixture of products and incomplete consumption of Et_2SiH_2. A single broad peak was observed in the $^{11}B\{H\}$ NMR spectrum centred at 29.2 ppm. At this point, the white solid was isolated and recrystallised from a DCM/hexane mixture. The $^{11}B\{H\}$ NMR spectrum of this solid revealed a singlet at 28.6 ppm and in the ^1H NMR spectrum, a doublet at 8.26 ppm (J = 6.7 Hz) and overlapping multiplets in the range 7.39 – 7.77 ppm of relative intensity 1:2 were observed. These data are consistent with the formation of triphenyl boroxine (**5.1**) (Scheme 5.2).[55]

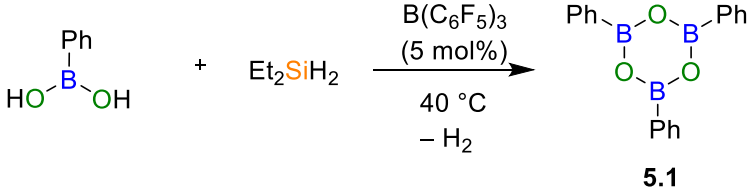

5.1

Scheme 5.2 Reaction of $PhB(OH)_2$ with Et_2SiH_2 in the presence of $B(C_6F_5)_3$.

The addition of three equivalents of Et_2SiH_2 to **5.1** and use of more forcing condition (110 °C, 8 h, toluene) was tested to probe whether this would facilitate the ring opening of the boroxine to yield borosiloxane polymer **5.2a**; however, only **5.1** was isolated from the reaction mixture (Scheme 5.3).

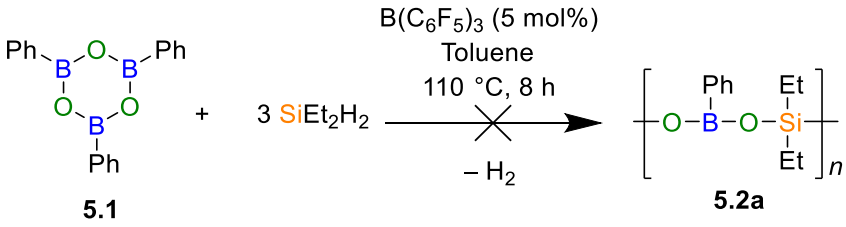

Scheme 5.3 Attempted reaction of **5.1** with Et_2SiH_2 in the presence of $B(C_6F_5)_3$.

Reaction of $PhB(OH)_2$ with Ph_2SiH_2 in the presence of $B(C_6F_5)_3$ (5 mol%) in $CDCl_3$ resulted in incomplete consumption of starting materials after heating at 40 °C for 22 h according to ^{1}H NMR spectroscopy. The emergence of several overlapping signals in the aromatic region was also observed. A single broad peak was found in the ^{11}B{H} NMR spectrum, centred at 30.9 ppm. In the ^{29}Si{H} NMR spectrum, a signal was observed with a chemical shift of −33.4 ppm corresponding to Ph_2SiH_2 as well as signals at −19.4, −20.4, and −20.9 ppm. These match closely with the chemical shift reported for $[Ph_2SiO\text{-}B(Mes)O]_n$ (δ = −22.0 ppm) suggesting some formation of $[Ph_2SiO\text{-}B(Ph)O]_n$;[21] however, the lack of selectivity together with incomplete monomer consumption meant that this reaction was not pursued further.

5.3.1.2 Reaction of phenylboronic acid with tertiary silanes

We also sought to investigate $B(C_6F_5)_3$-catalysed dehydrocoupling of $PhB(OH)_2$ with tertiary silanes (Scheme 5.4). The reaction between $PhB(OH)_2$ and two equivalents of Et_3SiH (5 mol% $B(C_6F_5)_3$, $CDCl_3$, 40 °C) took 18 h for complete consumption of Et_3SiH, as determined by ^{1}H NMR spectroscopy. ^{11}B{H} NMR analysis showed a broad signal with a chemical shift of 24.2 ppm. It is noteworthy that a signal for $B(C_6F_5)_3$ at 40 – 50 ppm was absent and instead a broad peak was centred at 2 ppm, in the range commonly associated with 4-coordinate boron species. This suggests that the $B(C_6F_5)_3$ catalyst is deactivated during the course of the reaction, which may explain the sluggish reaction time.

Two prominent triplets at 1.01 and 0.96 ppm and quartet signals (0.74 and 0.55 ppm) were observed in the alkyl region of the ^{1}H NMR spectrum. We ascribe these to the ethyl groups of the desired $PhB(OSiEt_3)_2$ product (**5.3a**; signals at 1.01 and 0.74 ppm) and to a hexaethyldisiloxane ($Et_3SiOSiEt_3$)

by-product (**5.4a**; signals at 0.96 and 0.55 ppm) (Figure 5.1). Generation of siloxane by-products has previously been reported in the synthesis of borosiloxane resins using PR type methodology.[26] Integration of the CH_2 peaks in the ^{1}H NMR spectrum give a **5.3a**:**5.4a** ratio of 1:0.88. There is therefore low selectivity for the desired product. Two resonances were also observed in the ^{29}Si{H} NMR spectrum at 8.9 and 12.2 ppm: the former matches that reported for **5.4a**,[56] and we assign the latter to **5.3a**.

Signals in the ^{1}H NMR were also observed that corresponded to the formation of **5.1**. Formation of **5.1** liberates water which could explain the apparent deactivation of $B(C_6F_5)_3$, forming the $B(C_6F_5)_3$ hydrate. The effect of trace water on the synthesis of silicones using PR methodology has recently been reported.[57] Water liberated from triphenyl boroxine formation can also generate silanols from silanes which can subsequently form siloxanes providing additional explanation for the formation of **5.4a**. Reaction of silanes with water to give siloxane linkages is well-documented using transition metal catalysis.[56] To test if the addition of water to Et_3SiH would lead to siloxane formation under PR conditions, Et_3SiH (0.1 mmol) and $B(C_6F_5)_3$ (5 mol%) were dissolved in $CDCl_3$ in a J-Young NMR tube. To this mixture a drop of water was added, and the reaction mixture heated to 40 °C for 24 h. Subsequent analysis by ^{1}H, and ^{29}Si{H} NMR showed the complete consumption of Et_3SiH and the selective formation of two silicon-containing species. The NMR data for these species closely matches literature spectra for Et_3SiOH and $Et_3Si\text{-}O\text{-}SiEt_3$.[58] These products are formed in a ratio of ca. 3:1 (determined by integration of the CH_2 signals in the ^{1}H NMR spectrum). This supports our hypothesis that liberation of water from the reaction of $PhB(OH)_2$ and Et_2SiH_2 can lead to a siloxane side product.

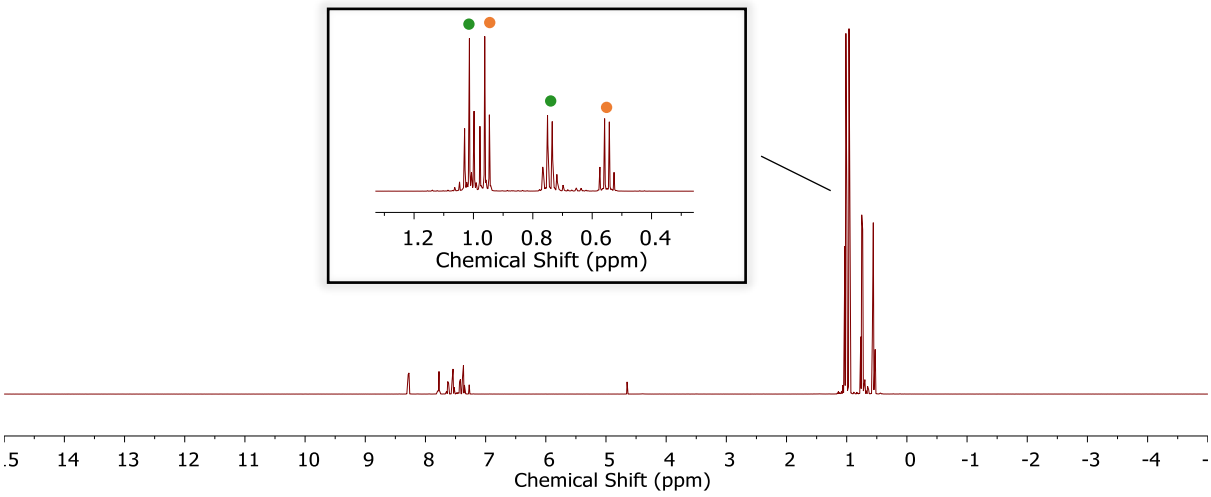

Figure 5.1 ^{1}H NMR (500 MHz, 25 °C, $CDCl_3$) of the reaction between $PhB(OH)_2$ and Et_3SiH in the presence of $B(C_6F_5)_3$ after heating at 40 °C for 18 h. Alkyl signals denoted with ● are assigned to **5.3a** and those with ● to **5.4a**

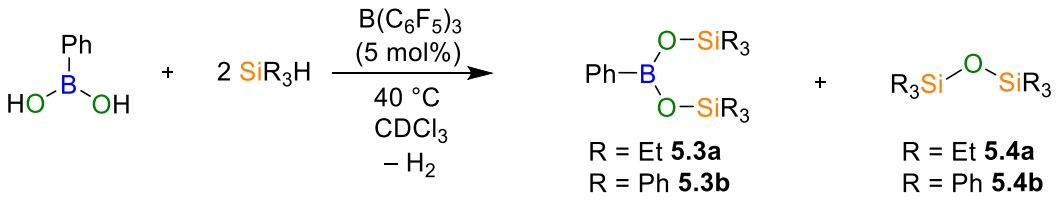

Scheme 5.4 $B(C_6F_5)_3$-catalysed dehydrocoupling of $PhB(OH)_2$ and tertiary silanes.

An analogous reaction was attempted between $PhB(OH)_2$ and Ph_3SiH; however, this was also found to exhibit poor selectivity with the formation of significant amounts of hexaphenyldisiloxane, $Ph_3SiOSiPh_3$ by-product (**5.4b**) alongside the desired $PhB(OSiPh_3)_2$ (**5.3b**). Incomplete reaction was observed after heating to 40 °C for 22 h. In this case we could not quantify the ratio of **5.3b** to **5.4b** because of overlap of signals in the ^{1}H NMR spectrum; however, two signals of roughly equal intensity were observed in the ^{29}Si{H} NMR spectrum which we assigned to **5.3b** (−19.5 ppm) and **5.4b** (−18.6 ppm), together with a minor resonance at −18.1 ppm which corresponds to Ph_3SiH starting material. Overall, while the desired dehydrocoupling between $PhB(OH)_2$ and secondary and tertiary silanes in the presence of catalytic amounts of $B(C_6F_5)_3$ was found to facilitate the formation of B-O-Si linkages, a lack of selectivity over the formation of siloxane bonds suggests that this is not a viable route to borosiloxane products.

5.3.2 Demethanative condensation route to borosiloxane bond formation

In order to avoid the formation of siloxane side products, we investigated a $B(C_6F_5)_3$-catalysed demethanative condensation route to form borosiloxane species. It was anticipated that the absence of water liberation would prevent catalyst poisoning and circumvent silanol formation leading to by-products. To this end we synthesised dimethyl phenylboronate ($PhB(OMe)_2$, **5.5**) as the boron-containing agent using a variation of a previously reported literature procedure,[59] and we then investigated the reactivity of **5.5** with secondary and tertiary silanes in the presence of $B(C_6F_5)_3$ (Scheme 5.5).

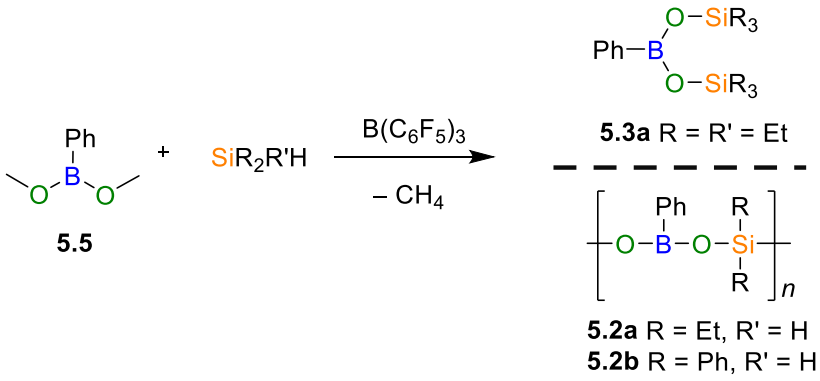

Scheme 5.5 General demethanative condensation route to borosiloxane bond formation.

5.3.2.1 $B(C_6F_5)_3$-catalysed demethanative condensation of 5.5 with Et_3SiH

Slow addition of Et_3SiH (1 eq.) to a solution of **5.5** with $B(C_6F_5)_3$ (5 mol%) in DCM resulted in the observation of immediate effervescence due to the liberation of CH_4. This mixture was stirred for 5 min and then sealed and transferred to a Schlenk line and heated at 40 °C under a slow flow of nitrogen. Complete consumption of **5.5** was observed within 6 h by ^1H NMR spectroscopy. After removal of volatiles under vacuum and washing the residue with pentane, a white solid was isolated. The resultant material was then analysed by NMR spectroscopy. From the ^1H NMR spectrum, complete consumption of **5.5** was determined. We hypothesise that the absence of water liberation prevents $B(C_6F_5)_3$ deactivation resulting in a faster reaction than the analogous dehydrocoupling reaction between $PhB(OH)_2$ and Et_3SiH. A clear improvement in the ratio of borosiloxane to disiloxane by-product was observed, with a ratio of 1:0.04 (**5.3a**:**5.4a**) calculated from the integration of CH_2 signals in the ^1H NMR spectrum (Figure 5.2). This was also reflected in the observation of only one product peak in the $^{29}Si\{H\}$ NMR spectrum at 12.2 ppm indicating selective formation of bis(triethylsilyl) phenylboronate

(**5.3a**). A single broad peak was observed in the $^{11}B\{H\}$ NMR spectrum at 25.3 ppm. The material was also analysed by FTIR spectroscopy. Si-O-Si stretches have been reported to come at around 1100 cm^{-1}.[60] In the FTIR spectrum of **5.3a**, no peaks were observed at this wavenumber, suggesting minimal formation of **5.4a** (Figure S5.16).

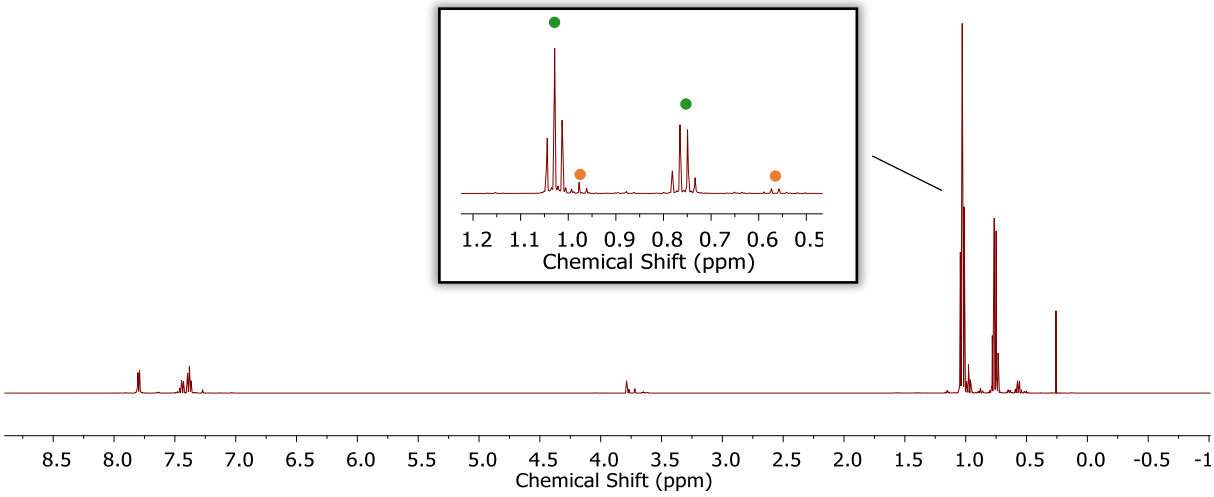

Figure 5.2 ^{1}H NMR (500 MHz, 25 °C, $CDCl_3$) of the reaction between **5.5** and Et_3SiH in the presence of $B(C_6F_5)_3$. Alkyl signals denoted with ● correspond to **5.3a** and signals denoted with ● correspond to **5.4a**.

In order to gain further insight into the $B(C_6F_5)_3$-catalysed demethanative condensation of **5.5** and Et_3SiH, the reaction progress was monitored at 20 °C using ^{1}H NMR spectroscopy. The reaction was found to proceed without heating resulting in complete consumption of **5.5** within 6 h. Integration of resonances for both **5.3a** and **5.4a** with respect to Et_3SiH revealed that the majority of disiloxane by-product, **5.4a** was formed within the first 30 min of the reaction (Figure 5.3). There was a minimal induction period before effervescence was observed, with slow addition of Et_3SiH to avoid pressure build-up. There was no heating of the reaction mixture, which may have an influence on the levels of by-product formation; however, the ratio of products after complete conversion of starting materials (1:0.05 for **5.3a:5.4a**) was found to be similar to the reaction at 40 °C (1:0.04) suggesting that the heating does not significantly influence the distribution of products.

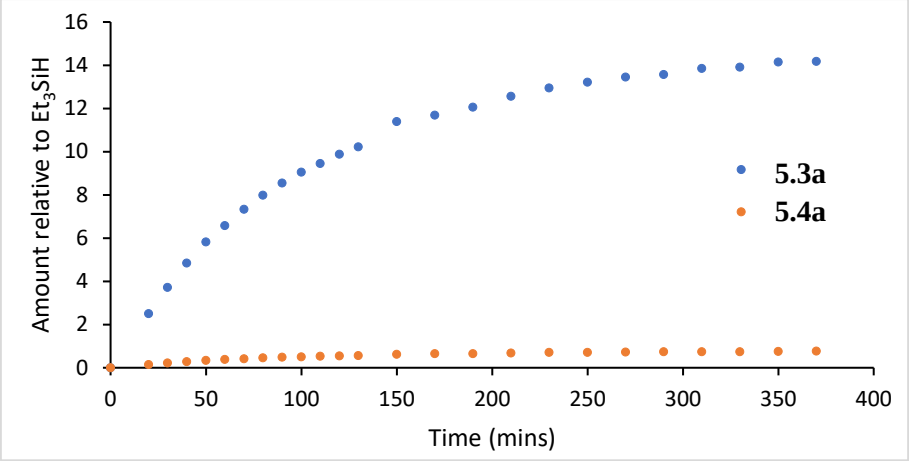

Figure 5.3 Relative amounts of **5.3a** and **5.4a** to the amount of Et_3SiH in the $B(C_6F_5)_3$-catalysed reaction of **5.5** and Et_3SiH at 20 °C.

We also sought to determine if there is any effect of catalyst loading on the reaction. To this end a series of reactions were set up for the reaction of **5.5** with Et_3SiH in $CDCl_3$ in the presence of varying amounts of $B(C_6F_5)_3$ (2, 5, and 10 mol%). After heating at 40 °C for 6 h, the reaction was complete in each case as determined by absence of peaks in the ^1H NMR spectrum corresponding to methoxy protons of **5.5** (δ = 3.72 ppm). There was little difference in the ratio of **5.3a**:**5.4a** formed for different amounts of catalyst (ratios between 1:0.05 and 1:0.07) demonstrating that the amount of catalyst has little impact on the distribution of products.

5.3.2.2 $B(C_6F_5)_3$-catalysed demethanative condensation route to polyborosiloxanes

Following the successful formation of **5.3a** using this demethanative condensation system, with minimal conversion to siloxane by-products, investigations were carried out into forming linear polyborosiloxanes, $[R_2SiO\text{-}B(Ph)O]_n$ (Scheme 5.4).

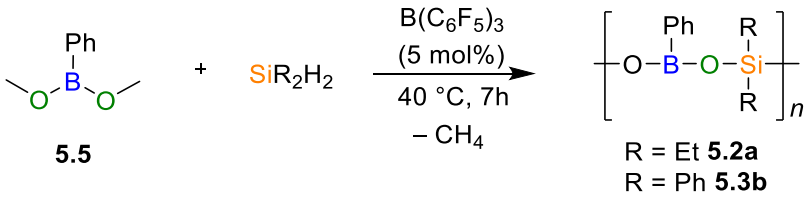

Figure 5.4 Reaction of **5.5** with secondary silanes in the presence of $B(C_6F_5)_3$. to formed linear borosiloxane polymers

Reaction of an equimolar amount of **5.5** and Et_2SiH_2 in the presence of $B(C_6F_5)_3$ in DCM resulted in complete reaction after stirring at 40°C for 7 h. After removal of volatiles under vacuum, **5.2a** was isolated as a white solid. $^{29}Si\{H\}$ NMR spectroscopy show only one peak at −3.6 ppm, suggesting

selective formation of B-O-Si bonds (Figure S5.21). No Si-O-Si units were found to be present in the polymer backbone based on comparison of the ^{29}Si{H} NMR spectrum of **5.2a** with that of poly(diethylsiloxane) (^{29}Si{H} NMR $\delta = -22.3$ ppm).[61] The ^{11}B{H} NMR spectrum revealed the presence of a single, broad peak centred at 25.8 ppm, accompanied by a second low intensity very broad peak at 40 – 50 ppm corresponding to $B(C_6F_5)_3$ catalyst (Figure S5.20). Evidence for the alternating boron/siloxane nature of the polyborosiloxane main chain was reinforced by IR spectroscopy (Figure S5.22), where peaks at 745 and 693 cm^{-1} were observed, closely matching those reported for previous examples of polyborosiloxanes which were assigned to stretching and bending modes of Si-O-B bonds.[21, 26, 30] Further evidence for the formation of borosiloxane linkages is the peak in the IR spectrum at 1310 cm^{-1} which is assigned to the B-O bond stretch which again closely matches the IR data for previously reported polyborosiloxanes.[21, 26, 30] The molar mass of **5.2a** was determined by gel permeation chromatography (GPC) (Figure S5.23). This revealed a multimodal molar mass distribution with *M* ranging from 2,800 – 112,000 g mol^{-1} relative to polystyrene standards. Dynamic light scattering (DLS) studies were undertaken in DCM (1 mg mL^{-1}) in an attempt to further elucidate the presence of high molar mass material. Material with a molar mass around 10,000 g mol^{-1} would be expected to have a hydrodynamic diameter between 1 – 10 nm; however, no peak in this range was observed by DLS. Instead, a hydrodynamic diameter of 140 nm was observed, which suggests the formation of aggregates under these conditions (Figure S5.24).

In an attempt to remove the $B(C_6F_5)_3$ catalyst from **5.2a**, the reaction residue was dissolved in DCM and precipitated into pentane. A white powder was formed; however, when analysed by NMR spectroscopy, this was found to correspond to triphenyl boroxine (**5.1**) suggesting polymer breakdown under these conditions. Analysis of the supernatant by ^{1}H NMR spectroscopy revealed that the polymer is soluble in pentane; however, some peaks associated with **5.1** were also observed. Dissolving **5.2a** in pentane and leaving for 20 h under nitrogen resulted in the precipitation of **5.1** suggesting that the polymer is not stable in solution. Efforts to purify **5.2a** by passing through an alumina or silica plug were unsuccessful as the polymer was found to adhere to the solid phase and was not recovered. Attempts to remove the $B(C_6F_5)_3$ by sublimation at 80 °C under vacuum were also found to lead to polymer breakdown, with evidence of **5.1** formation when the resultant material was analysed by ^{1}H

NMR spectroscopy. We lastly attempted the addition of a few drops of pyridine to a solution of the **5.2a** residue; however, pyridine was found to react with the polymer leading to a number of unassigned chemical shifts emerging in the ^{29}Si{H} NMR spectrum (Figure S5.34).

PR-type condensation of an equimolar mixture of **5.5** and Ph_2SiH_2 in the presence of $B(C_6F_5)_3$ (5 mol%) was also explored under analogous conditions (DCM, 40 °C). After heating at 40 °C for 7 h and removal of volatiles under vacuum, a white solid was isolated. Two singlets were found in the ^{29}Si{H} NMR spectrum of this material (Figure S5.27). The first peak at −20.2 ppm is consistent with the value previously reported for the polyborosiloxane $[Ph_2SiO\text{-}B(Mes)O]_n$ formed from the Pd-catalysed dehydrocoupling of diphenylsilanediol with mesitylborane,[21] confirming formation of borosiloxane linkages in the polymer backbone. A second smaller peak was observed at −46.5 ppm which can be attributed to the formation of siloxane units within the polymer. This is akin to the borosiloxane resin recently reported by Rubinsztajn, where after reaction of $B(OMe)_3$ with Ph_2SiH_2, a number of resonances were observed in the ^{29}Si{H} NMR spectrum of the resultant network with chemical shifts below −45 ppm which were assigned to siloxane linkages.[26] As for **5.2a**, only one broad resonance was observed in the ^{11}B{H} NMR spectrum of **5.2b** as well as a signal for residual $B(C_6F_5)_3$ at around 45 ppm (Figure S5.26). Again, attempts to remove the $B(C_6F_5)_3$ from the polymer sample by washing with pentane were unsuccessful, leading to polymer degradation.

IR spectroscopy of **5.3b** provided evidence for the presence of polyborosiloxane linkages (Figure S5.28),with peaks at 822 and 693 cm^{-1} (stretching and bending modes of Si-O-B bonds) and at 1310 cm^{-1} (B-O bond stretch).[21, 26, 30] Additional peaks between 1000 and 1120 cm^{-1} were assigned to Si-O-Si bond stretching based on the similarity to Si-O-Si bond stretches reported for PDMS (1020 – 1074 cm^{-1}).[60] The polymer was analysed by GPC and an multimodal mass distribution was determined with M = 3,200 – 126,000 g mol^{-1} (Figure S5.29). No evidence of high molar mass material was detectable by DLS studies on **5.2b** in THF, DCM, or chlorobenzene.

We then attempted to extend this methodology to a *tert*-butyl substituted polymer. An equimolar mixture of **5.5** with tBu$_2$SiH$_2$ was heated at 40 °C in $CDCl_3$ in the presence of $B(C_6F_5)_3$ (5 mol%); however, after heating at 40 °C for 3 d, no reaction was observed. Given that the first step of PR reaction

mechanisms is the activation of the silane by $B(C_6F_5)_3$,[45] we anticipated that the increased steric bulk of di-*tert*-butylsilane is sufficient to prevent this initial activation step from occurring.

Owing to the potential of polyborosiloxanes in high temperature applications, thermal analysis was carried out on **5.2a** and **5.2b** to assess their stabilities. Unfortunately, when thermogravimetric analysis (TGA) was carried out, low $T_{5\%}$ (temperature at which 5% mass loss had occurred) of ca. 90 °C were observed for both polymers. Analysis by differential scanning calorimetry (DSC) did not allow for the determination of a glass transition temperature (T_g), possibly because of ongoing degradation pathways at temperatures below the T_g. This low thermal stability was ascribed to the presence of residual $B(C_6F_5)_3$ (attempts to remove this were unsuccessful) which may facilitate the depolymerisation of the polymers.

In order to overcome issues with degradation, we envisaged that the addition of a rigid aromatic group to the polymer backbone may improve the polymer stability. To this end we attempted the reaction of **5.5** with 1,4-bis(dimethylsilyl)benzene in the presence of $B(C_6F_5)_3$ (Scheme 5.6). After heating at 40 °C for 20 h in $CDCl_3$ and removal of volatiles under vacuum, material was obtained which was determined by GPC to be multimodal with a molar mass range of M = 2,200 – 56,000 g mol^{-1} (Figure S5.33). The material was analysed by ^{1}H NMR spectroscopy which revealed the presence of a multitude of peaks in the range 0.37 – 0.59 ppm and aromatic protons in the range 7.10–7.91 ppm (Figure S5.30). In the ^{11}B{H} NMR spectrum, a broad singlet was found at 25.9 ppm (Figure S5.31). In the ^{29}Si{H} NMR spectrum, signals at 2.5, 0.1, −0.4, −1.2 ppm were observed (Figure S5.32). Reaction of **5.5** with 1,4,-bis(dimethylsilyl)benzene was reported to yield a polymer with a signal in the ^{29}Si{H} at −2.3 ppm corresponding to O*Si*Me_2Ar units.[44] The similarity of this to the ^{29}Si{H} NMR spectrum that we observe suggests at least some siloxane linkages are present in the material.

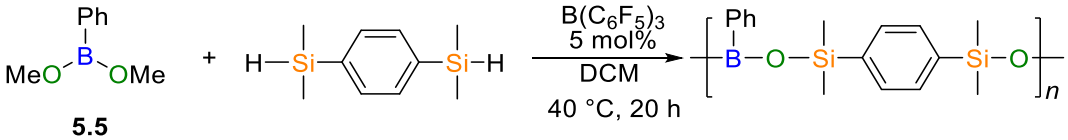

Scheme 5.6 Reaction of **5.5** with 1,4,-bis(dimethylsilyl)benzene

5.4 Conclusions

We report the synthesis of novel borosiloxane molecules and polymers using dehydrocoupling and demethanative condensation routes catalysed by $B(C_6F_5)_3$ under mild conditions. Whereas dehydrocoupling attempts between phenylboronic acid and silane resulted in slow reactions and the formation of boroxine and disiloxane by-products, dehydrocarbonative condensation reactions between dimethyl phenylboronate and the corresponding silane were successful for the formation of both molecular and polymer species. The polymeric nature of these materials was confirmed by gel permeation chromatography. The thermal properties of these borosiloxane polymers were also investigated using TGA and DSC; however, issues with polymer stability, removal of residual $B(C_6F_5)_3$ and reaction selectivity remain. The mild conditions of this methodology for the formation of borosiloxane species bodes well for the development of these materials for more widespread usage.

5.5 Experimental

5.5.1 Synthesis of dimethyl phenylboronate (5.5)

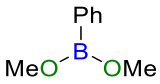

Trimethyl borate (12 mL, 11.18 g, 108 mmol) was added via syringe to a 250 mL Schlenk flask at −78 °C under a nitrogen atmosphere. THF (75 mL) was added and a dropping funnel fitted. A 2.0 M solution of PhMgCl in THF (37 mL, 74 mmol) was transferred to the dropping funnel and added across 2 h with constant stirring. Stirring was continued for 20 h, while allowing the solution to slowly warm to 20 °C. During this time, formation of a white precipitate was observed. A solution of H_2SO_4 (2.2 mL) in MeOH (4 mL) was slowly added and the resulting suspension was stirred for 20 minutes. The reaction mixture was diluted with hexanes (40 mL) before separation of the Mg salts through a frit. The filtrate was dried under vacuum on a rotary evaporator and the remaining liquid distilled at 80 °C/0.01 mbar to give dimethyl phenylboronate (**5.5**) as a colourless liquid (yield: 6.1 g, 55%). The NMR data matches reported literature values.[59]

Spectroscopic data:

^{1}H NMR (400 MHz, 25 °C, $CDCl_3$) δ 7.63 (dd, *J* = 1.79 Hz, 7.69 Hz, 2H), 7.36-7.44 (m, 3H), 3.77 (s, 6H).

$^{11}B\{^1H\}$ NMR (128 MHz, 25 °C, $CDCl_3$) δ 27.8 (s).

5.5.2 Attempted dehydrocoupling route to polyborosiloxanes

5.5.2.1 Reaction of phenylboronic acid with diethylsilane

In a glovebox, a Schlenk flask was charged with phenylboronic acid (150 mg, 1.2 mmol), $B(C_6F_5)_3$ (31 mg, 0.06 mmol) and DCM (5 mL). Diethylsilane (162 μL, 1.2 mmol) was added slowly and immediate effervescence was observed. The flask was then sealed, removed from the glovebox and transferred to a vacuum manifold and placed in an oil bath at 40 °C under a flow of N_2 for 22 h. During this time, formation was a white precipitate was observed. An aliquot of the reaction mixture was analysed by NMR spectroscopy. The white solid was isolated by filtration, recrystallised from DCM/hexane and determined to be triphenyl boroxine **5.1** by ^{1}H and $^{11}B\{H\}$ NMR spectroscopy.

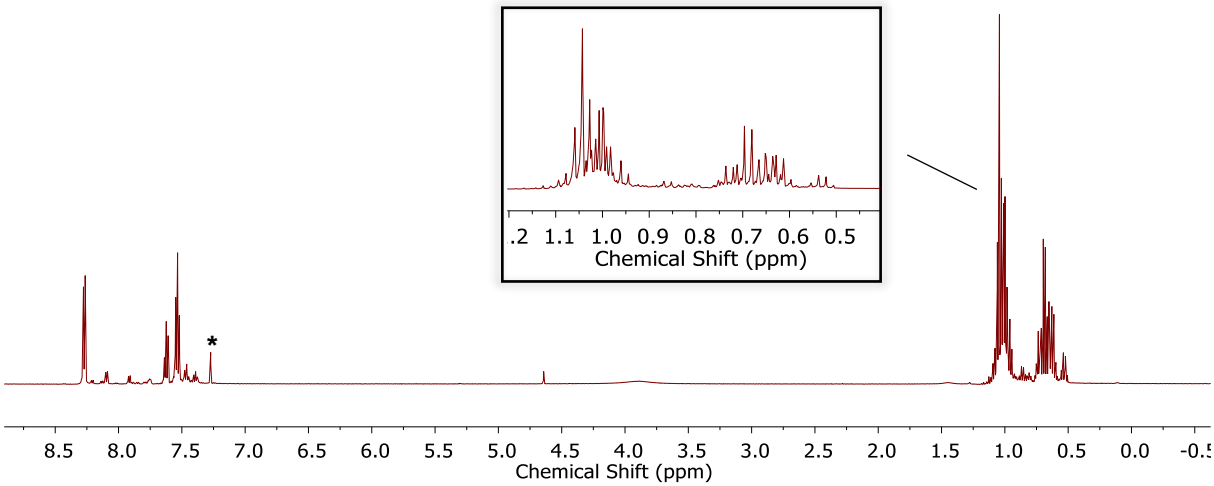

Figure S5.1 ^{1}H NMR spectrum (500 MHz, 25 °C, $CDCl_3$) of the reaction between phenylboronic acid and diethylsilane in the presence of $B(C_6F_5)_3$ after heating at 40 °C for 22 h. Deuterated chloroform residual signal denoted by *.

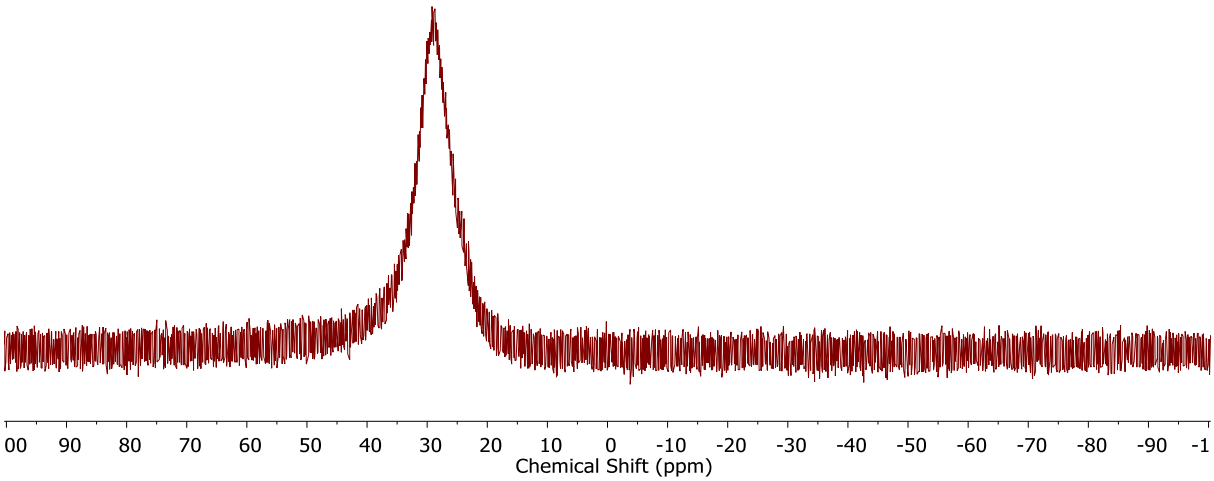

Figure S5.2 ^{11}B{H} NMR (128 MHz, 25 °C, $CDCl_3$) of the reaction between phenylboronic acid and diethylsilane in the presence of $B(C_6F_5)_3$ after heating at 40 °C for 22 h.

5.5.2.2 Reaction of phenylboronic acid with diphenyl silane

In a glovebox, a vial was charged with phenylboronic acid (12 mg, 0.1 mmol). To this was added a $B(C_6F_5)_3$ in $CDCl_3$ (0.01 M, 0.5 mL). Diphenylsilane (18.6 µL, 0.1 mmol) in $CDCl_3$ (0.2 mL) was then added slowly to the vial resulting in a colourless solution. The contents of the vial were transferred to a J-Young NMR tube and heated at 40°C for 22 h, during which a white precipitate was formed. At this point, the reaction mixture was analysed by NMR spectroscopy.

Spectroscopic data:

^{11}B{H} NMR (96 MHz, 25 °C, $CDCl_3$) δ 30.9 (s).

^{29}Si{H} NMR (99 MHz, 25 °C, $CDCl_3$) δ −19.4 (s), −20.4 (s), and −20.9 (s), −33.4 (s, Ph_3SiH).

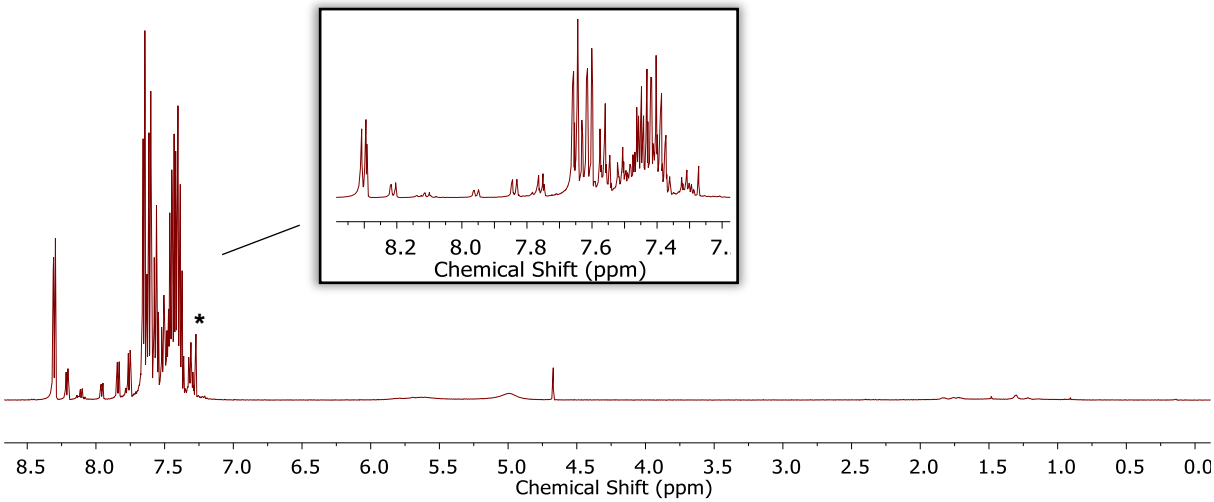

Figure S5.3 ^{1}H NMR spectrum (500 MHz, 25 °C, $CDCl_3$) of the reaction between phenylboronic acid and diphenylsilane in the presence of $B(C_6F_5)_3$ after heating at 40 °C for 22 h. Deuterated chloroform residual signal denoted by *.

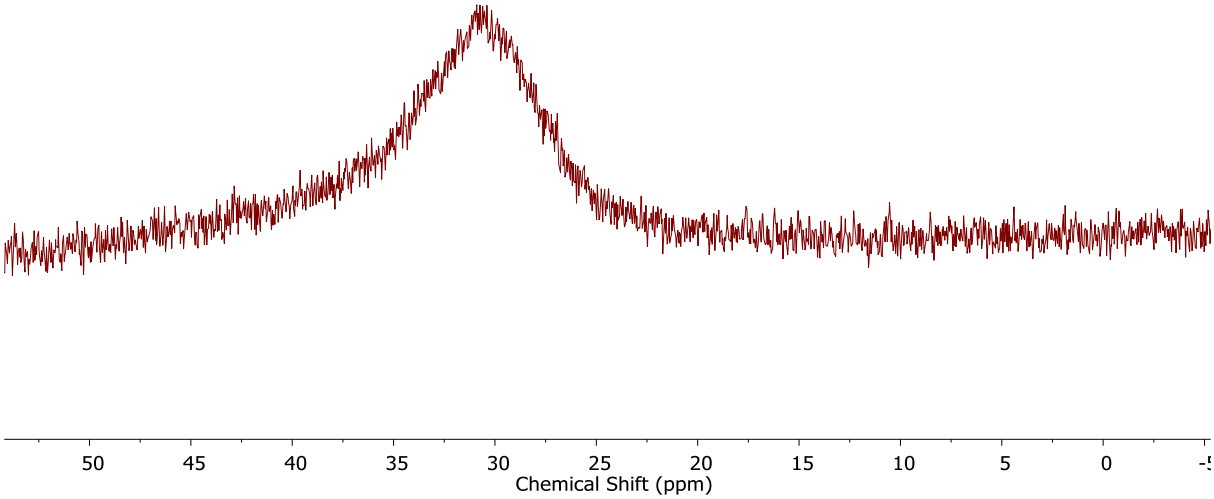

Figure S5.4 ^{11}B{H} NMR (128 MHz, 25 °C, $CDCl_3$) of the reaction between phenylboronic acid and diphenylsilane in the presence of $B(C_6F_5)_3$ after heating at 40 °C for 22 h.

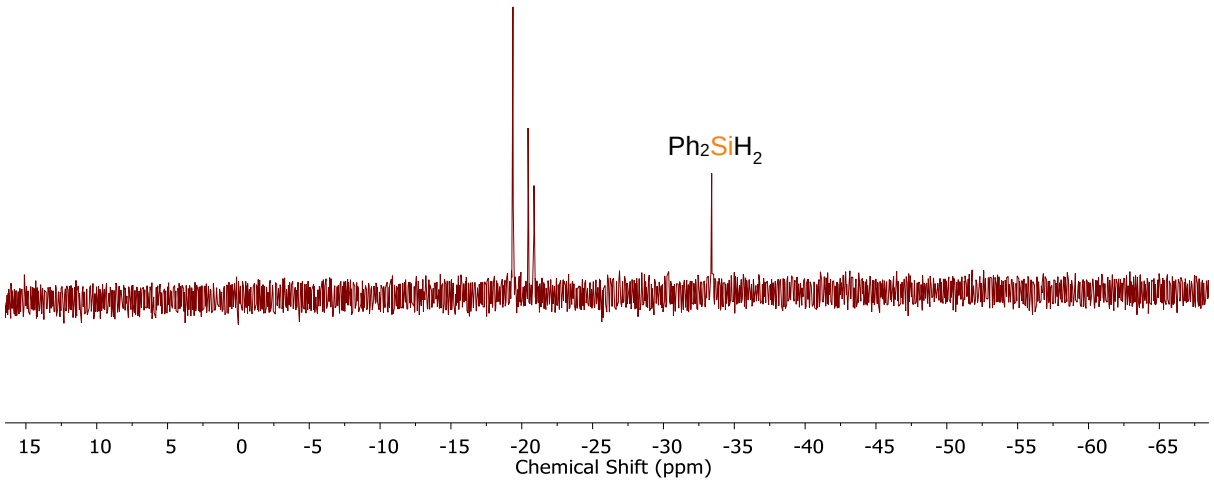

Figure S5.5 ^{29}Si{H} NMR spectrum (99 MHz, 25 °C, $CDCl_3$) of the reaction between phenylboronic acid in the presence of $B(C_6F_5)_3$ and diphenylsilane after heating at 40 °C for 22 h.

5.5.3 $B(C_6F_5)_3$-catalysed dehydrocoupling route to molecular borosiloxanes

5.5.3.1 Reaction of phenylboronic acid and triethylsilane

In a glovebox, $B(C_6F_5)_3$ in $CDCl_3$ (0.01 M, 0.5 mL) was added to phenylboronic acid (12 mg, 0.1 mmol) in a vial. Triethylsilane (32.0 µL, 0.2 mmol) in $CDCl_3$ (0.2 mL) was then added gradually. Effervescence was observed upon addition. The colourless solution was transferred to a J-young quartz NMR tube, the tube was sealed, removed from the glovebox, and placed in an oil bath at 40 °C for 18 hours. At this point the reaction mixture was analysed by ^{1}H, ^{11}B{H}, and ^{29}Si{H} NMR spectroscopy. A ratio of products **5.3a:5.4a** of 1:0.88 was determined by integration of CH_2 signals in the ^{1}H NMR spectrum.

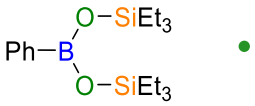

Bis(triethylsilyl) phenylboronate 5.3a:

^{1}H NMR (500 MHz, 25 °C, $CDCl_3$) δ 7.32–7.81 (m, 5H, Ph-*H*), 1.01 (t, *J*=7.9 Hz, 18H, $SiCH_2CH_3$), 0.74 (q, *J*=7.9 Hz, 12H, $SiCH_2CH_3$).

^{11}B{^{1}H} NMR (96 MHz, 25 °C, $CDCl_3$) δ 24.2 (br s).

^{29}Si{^{1}H} NMR (99 MHz, 25 °C, $CDCl_3$) δ 12.2 (s).

Hexaethyldisiloxane 5.4a:

^{1}H NMR (500 MHz, 25 °C, $CDCl_3$) δ 0.96 (t, *J*=7.9 Hz, 18H, $SiCH_2CH_3$), 0.55 (q, *J*=7.9 Hz, 12H, $SiCH_2CH_3$).

^{29}Si{^{1}H} NMR (99 MHz, 25 °C, $CDCl_3$) δ 8.9 (s)

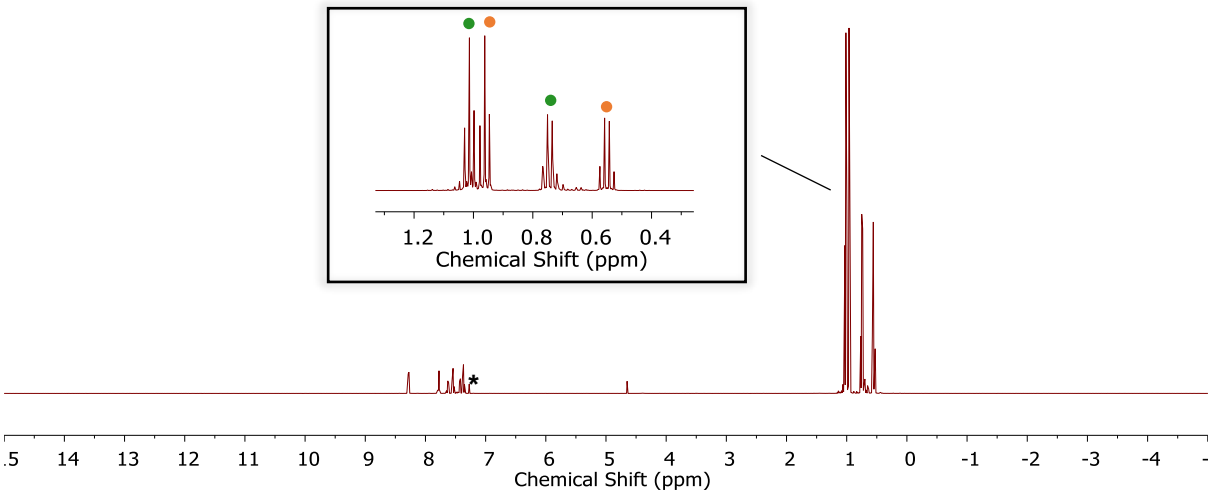

Figure S5.6 ^{1}H NMR (500 MHz, 25 °C, $CDCl_3$) of the reaction between phenylboronic acid and triethylsilane in the presence of $B(C_6F_5)_3$ after heating at 40 °C for 18 h. Deuterated chloroform residual signal denoted by *.

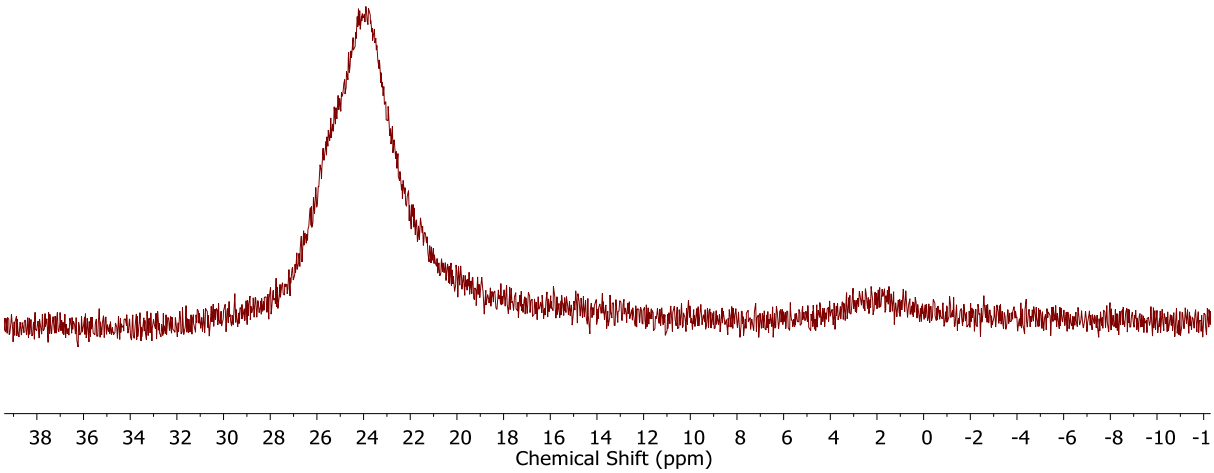

Figure S5.7 ^{11}B{H} (96 MHz, 25 °C, $CDCl_3$) of the reaction between phenylboronic acid and triethylsilane in the presence of $B(C_6F_5)_3$ after heating at 40 °C for 18 h.

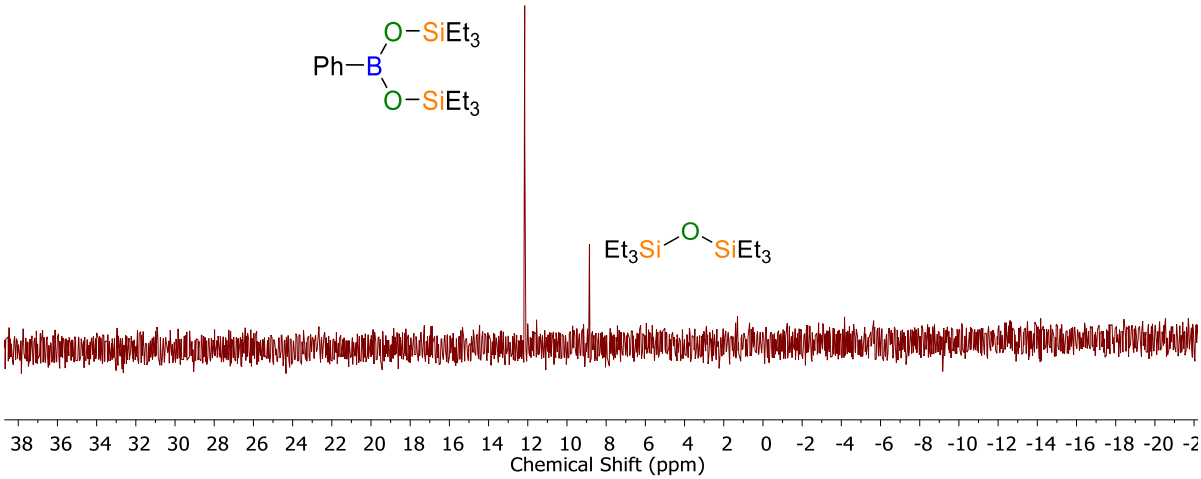

Figure S5.8 ^{29}Si{H} (99 MHz, 25 °C, $CDCl_3$) of the reaction between phenylboronic acid and triethylsilane in the presence of $B(C_6F_5)_3$ after heating at 40 °C for 18 h.

5.5.3.2 Dehydrocoupling of phenylboronic acid and triphenylsilane

In a glovebox, a stock solution of $B(C_6F_5)_3$ in $CDCl_3$ (0.01 M, 0.5 mL) was added to phenylboronic acid (12 mg, 0.1 mmol) in a vial. Triphenylsilane (52 mg, 0.2 mmol) in $CDCl_3$ (0.2 mL) was then added gradually. Effervescence was observed upon addition. The colourless solution was transferred to a J-young quartz NMR tube, the tube was sealed, removed from the glovebox, and placed in an oil bath at 40 °C for 18 hours. At this point the reaction mixture was analysed by ^{1}H, ^{11}B, and ^{29}Si{H} NMR spectroscopy. Overlap of signal corresponding to aromatic protons in the ^{1}H NMR spectrum of **5.3a** and **5.4a** prevented determination of a ratio of products.

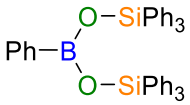

Bis(triphenylsilyl) phenylboronate 5.3b:

^{11}B{^{1}H} NMR (96 MHz, 25 °C, $CDCl_3$) δ ppm 26.9 (br s).

^{29}Si{^{1}H} NMR (99 MHz, 25 °C, $CDCl_3$) δ ppm −19.5 (s).

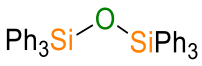

Hexaphenyldisiloxane 5.4b:

^{29}Si{^{1}H} NMR (99 MHz, 25 °C, $CDCl_3$) δ ppm −18.6 (s).

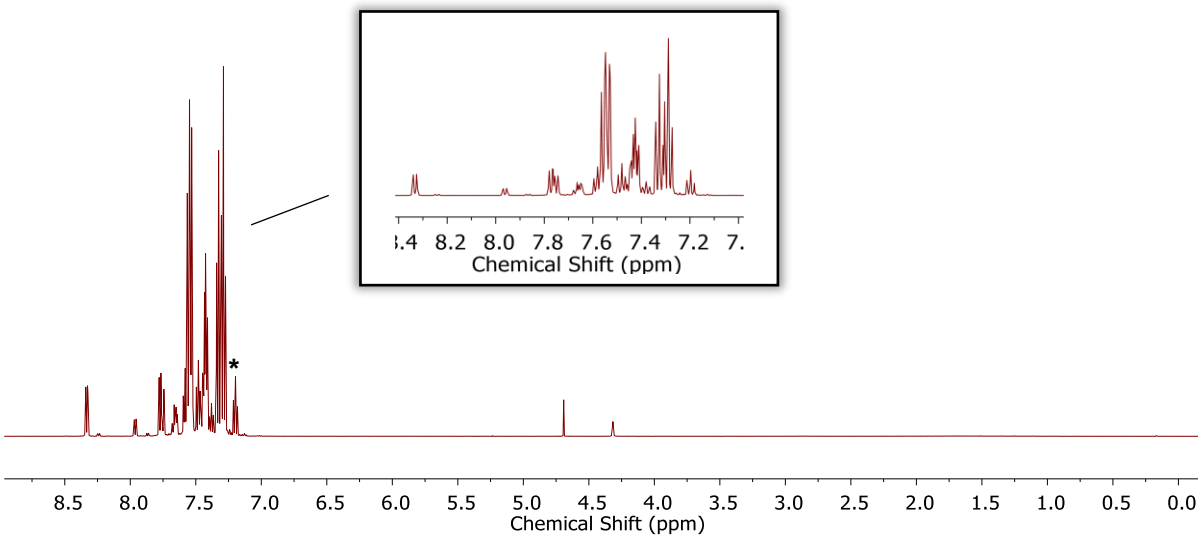

Figure S5.9 ^{1}H NMR spectrum (500 MHz, 25 °C, $CDCl_3$) of the reaction between phenylboronic acid and triphenylsilane in the presence of $B(C_6F_5)_3$ after heating at 40 °C for 18 h. Deuterated chloroform residual signal denoted by *.

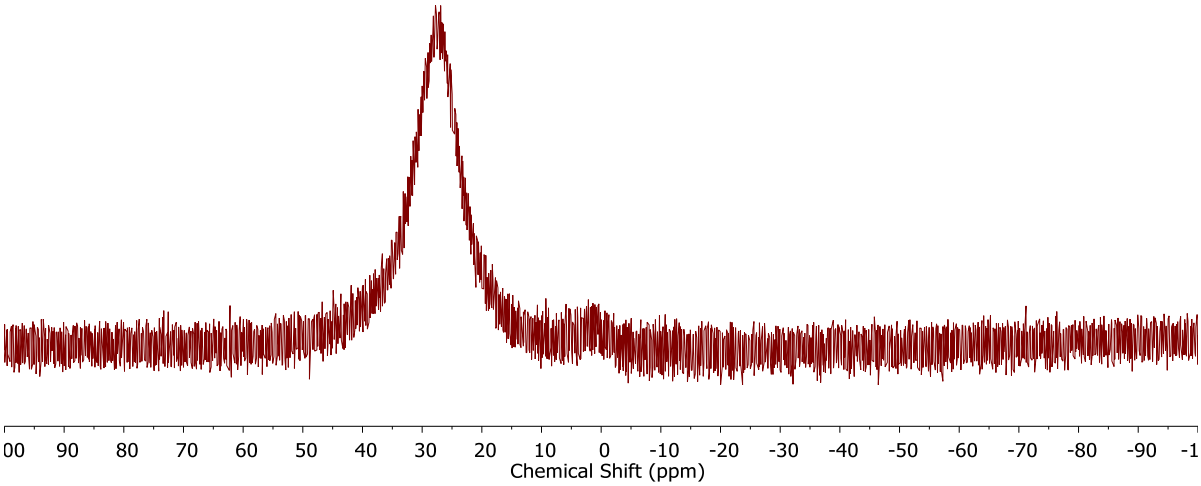

Figure S5.10 ^{11}B{H} NMR (96 MHz, 25 °C, $CDCl_3$) of the reaction between phenylboronic acid and triphenylsilane in the presence of $B(C_6F_5)_3$ after heating at 40 °C for 18 h.

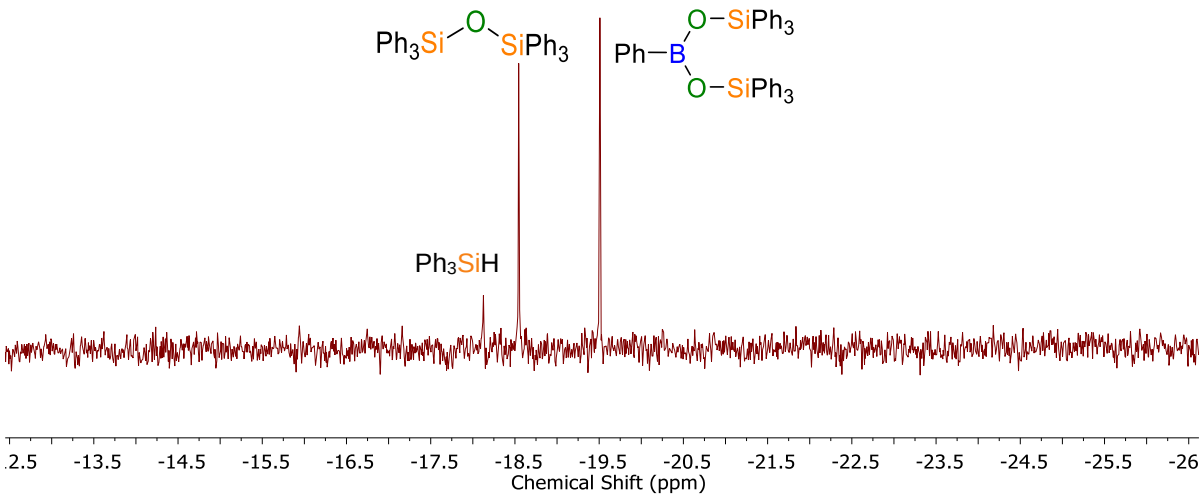

Figure S5.11 ^{29}Si{H} NMR Spectrum (99 MHz, 25 °C, $CDCl_3$) of the reaction between phenylboronic acid and triphenylsilane in the presence of $B(C_6F_5)_3$ after heating at 40 °C for 18 h.

5.5.4 $B(C_6F_5)_3$-catalysed demethanative condensation route to molecular borosiloxanes

5.5.4.1 Synthesis of bis(triethylsilyl) phenylboronate (5.3a)

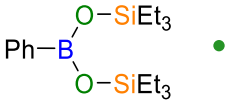

In a glovebox, a Schlenk flask was charged with **5.5** (0.90 g, 6 mmol), $B(C_6F_5)_3$ (0.15 g, 0.3 mmol) and DCM (5 mL). Triethylsilane (1.96 mL, 12 mmol) was slowly added. Effervescence was observed upon addition. The flask was sealed, removed from the glovebox and stirred at 40 °C in an oil bath under an atmosphere of nitrogen. After 6 hours, the flask was removed from the oil bath and volatiles removed under vacuum. The residue was then washed 3 times with pentane and dried under vacuum to yield **5.3a** as a white powder (yield = 1.49 g, 71%).

Spectroscopic data:

^{1}H NMR (500 MHz, 25 °C, $CDCl_3$) δ 7.80 (dd, *J* = 8.1, 1.5 Hz, 2H, Ph-H), 7.48–7.35 (m, 3H, Ph-H), 1.03 (t, *J* = 7.9 Hz, 17H), 0.76 (q, 12H).

^{11}B{H} NMR (160 MHz, 25 °C, $CDCl_3$) δ 25.3.

^{29}Si{H} NMR (99 MHz, 25 °C, $CDCl_3$) δ 12.2.

^{13}C{H} NMR (126 MHz, 25 °C, $CDCl_3$) δ 134.9, 130.3, 127.4, 6.8, 6.0.

IR: 2952, 2875, 1438, 1330, 1304, 1007, 820, 732, 729 cm^{-1}.

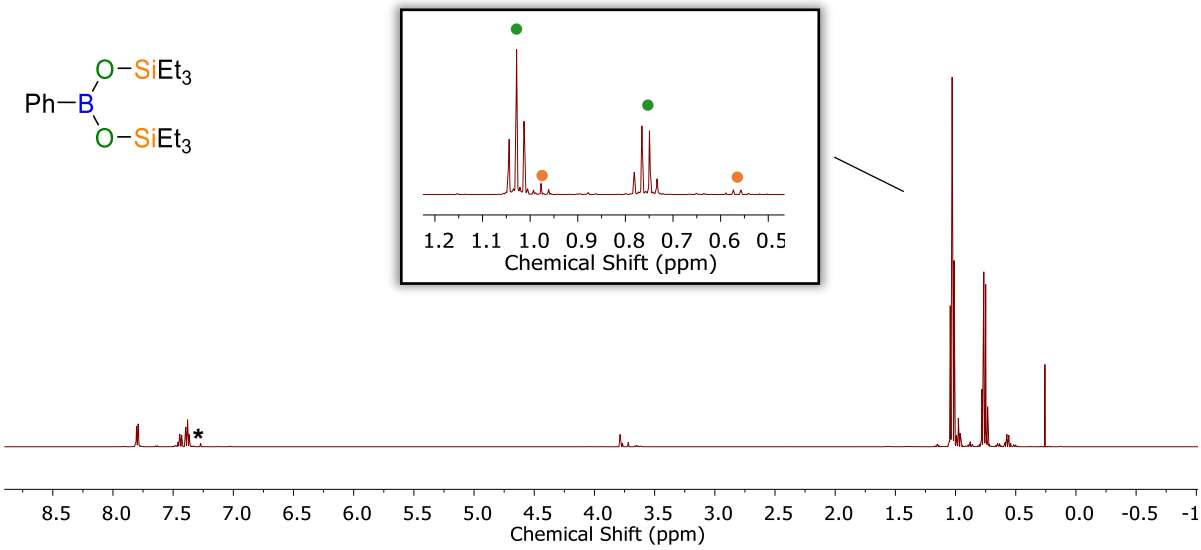

Figure S5.12 ^{1}H NMR spectrum (500 MHz, 25 °C, $CDCl_3$) of isolated **5.3a**. Deuterated chloroform residual signal denoted by *.

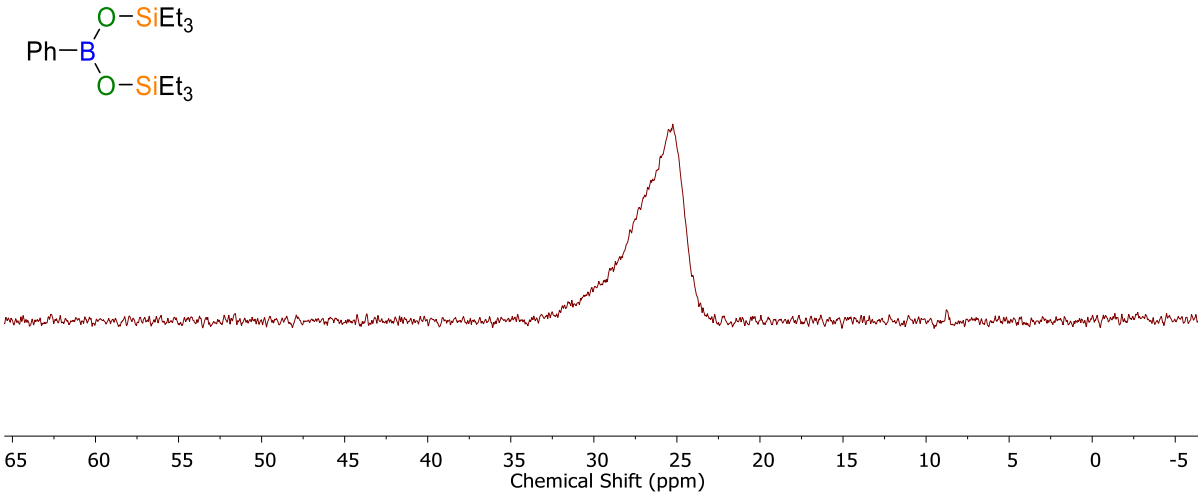

Figure S5.13 ^{11}B{H} NMR spectrum (160 MHz, 25 °C, $CDCl_3$) of isolated **5.3a**.

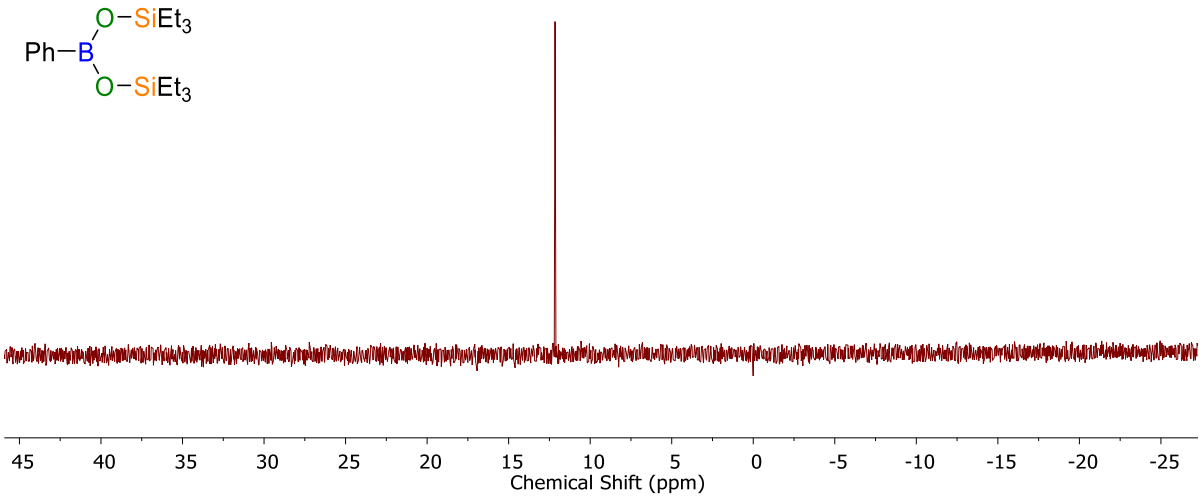

Figure S5.14 ^{29}Si{H} NMR spectrum (99 MHz, 25 °C, $CDCl_3$) of isolated **5.3a**.

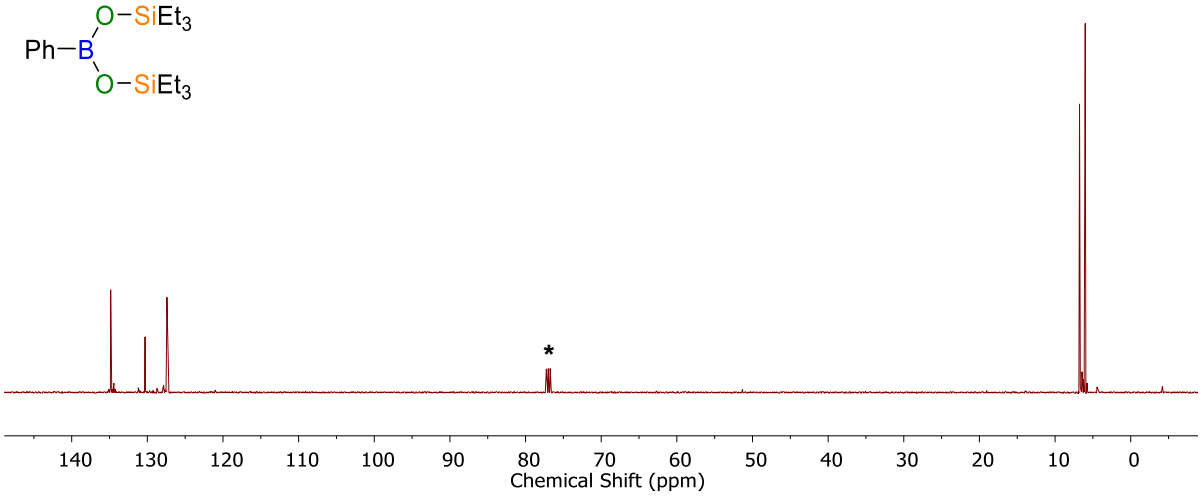

Figure S5.15 ^{13}C{H} NMR (126 MHz, 25 °C, $CDCl_3$) of isolated **5.3a**. Deuterated chloroform residual signal denoted by *.

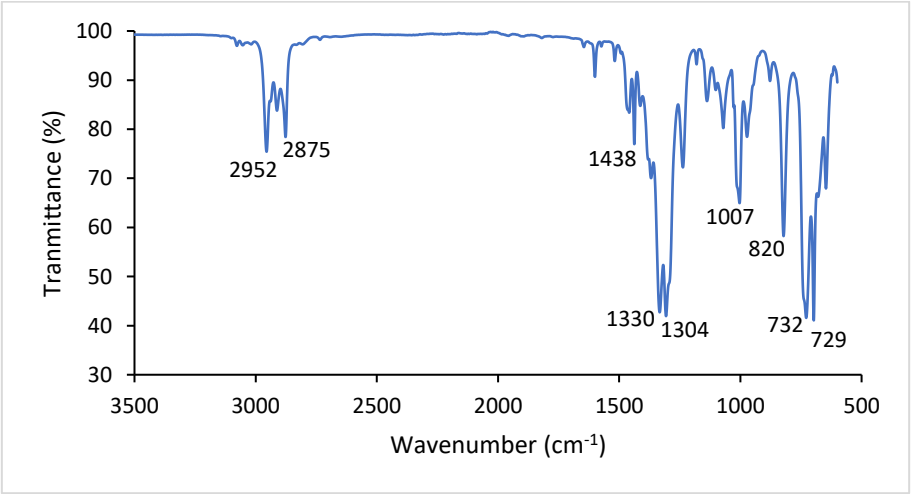

Figure S5.16 Solid state ATR FT-IR spectrum of isolated **5.3a**.

5.5.4.2 Kinetic study on the reaction of triethylsilane with 5.5 in the presence of $B(C_6F_5)_3$

In a glovebox, $B(C_6F_5)_3$ in $CDCl_3$ (0.01 M, 0.5 mL) was added to **5.5** (12 mg, 0.1 mmol) in a vial. To this was added triethylsilane (15.9 μL, 0.1 mmol). The contents of the vial were transferred to a J-Young NMR tube, sealed and heated in an oil bath at 40 °C. The reaction was monitored by ^1H NMR spectroscopy. In order to obtain Figure 5.3, peaks corresponding to CH_2 protons on the ethyl groups of **5.3a** and **5.4a** (δ = 0.76 and 0.55 ppm respectively) were integrated relative to the CH_2 protons of triethylsilane (δ = 0.64 ppm).

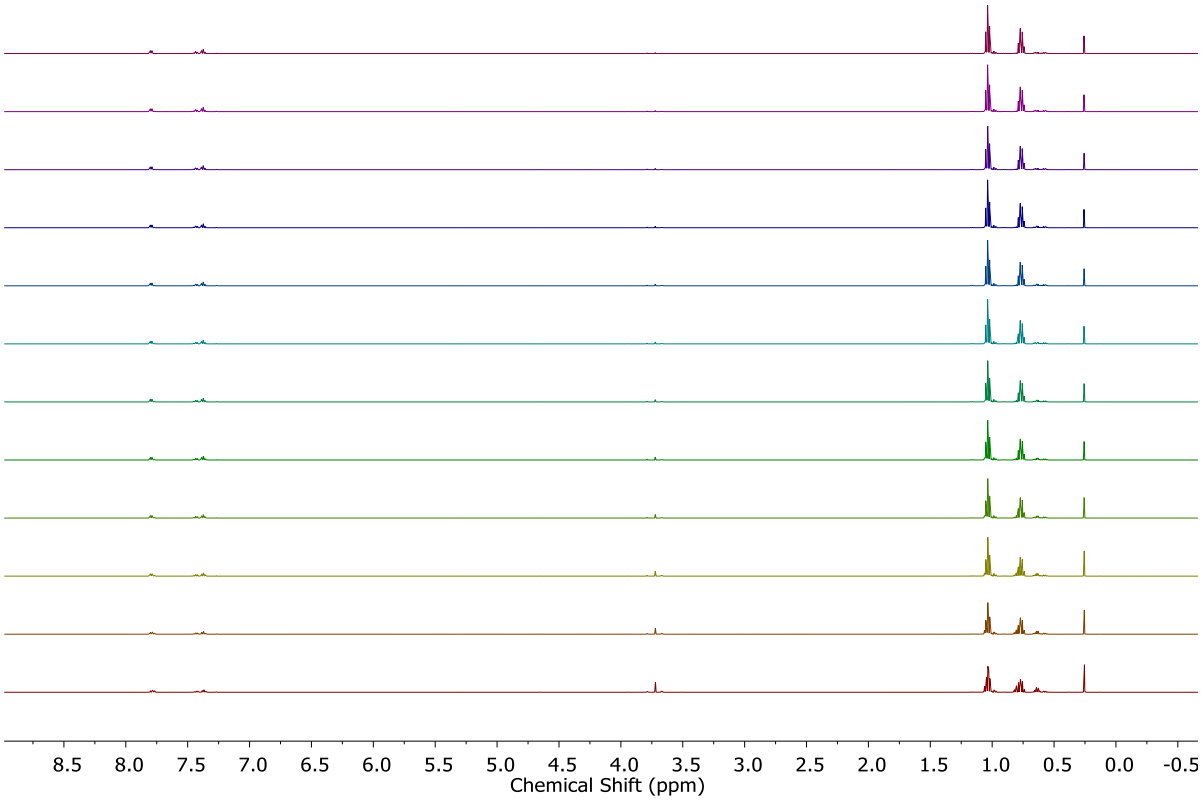

Figure S5.17 ^1H NMR spectra (500 MHz, 25 °C, $CDCl_3$) measured every 10 min from 10 (bottom) to 120 min (top) for the reaction of **5.5** with triethylsilane in the presence of $B(C_6F_5)_3$.

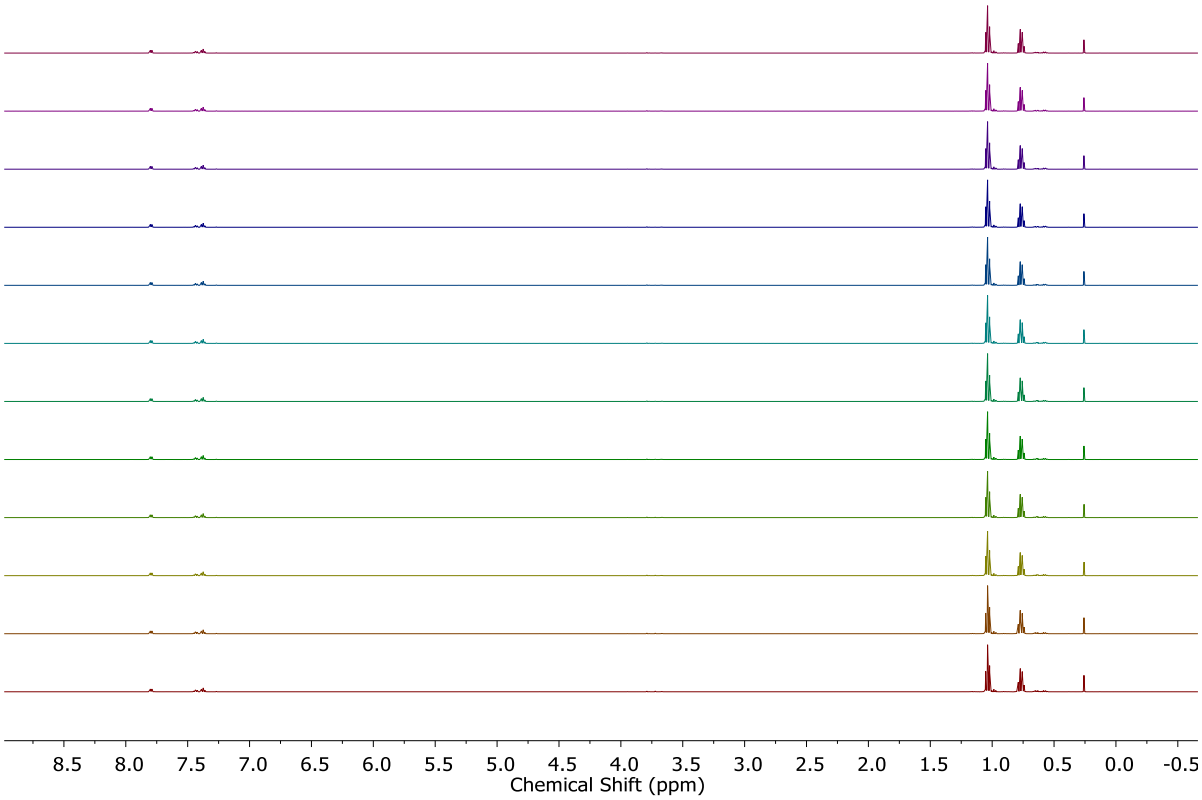

Figure S5.18 ^{1}H NMR spectra (500 MHz, 25 °C, $CDCl_3$) measured every 20 min from 140 (bottom) to 360 min (top) for the reaction of **5.5** with triethylsilane in the presence of $B(C_6F_5)_3$.

5.5.5 $B(C_6F_5)_3$-catalysed demethanative condensation polymerisation reactions

5.5.5.1 $B(C_6F_5)_3$-catalysed demethanative polymerisation of dimethyl phenylboronate and diethylsilane

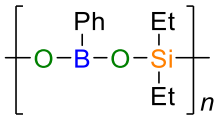

In a glovebox, a Schlenk flask was charged with **5.5** (0.90 g, 6 mmol), $B(C_6F_5)_3$ (0.15 g, 0.3 mmol) and DCM (5 mL). To this diethylsilane (0.78 mL, 6 mmol) was slowly added. Effervescence was observed upon addition. The flask was sealed, removed from the glovebox and stirred at 40 °C in an oil bath under an atmosphere of nitrogen. After 7 h, the flask was removed from the oil bath and volatiles removed under vacuum yielding **5.2a** as a white solid (yield = 0.84 g, 68%). Attempts to remove residual $B(C_6F_5)_3$ from the polymer were unsuccessful. There was no difference between a GPC taken immediately and after remaining dissolved in THF for 1 d which suggests that there is no THF polymerisation caused by residual $B(C_6F_5)_3$ remaining.

Spectroscopic data:

^{1}H NMR (500 MHz, 25 °C, $CDCl_3$) δ 8.30–8.20 (m, Ph-H), 7.65–7.47 (m, Ph-H), 1.13–0.92 (m, $SiCH_2CH_3$), 0.76–0.58 (m, $SiCH_2CH_3$).

^{11}B{H} NMR (128 MHz, 25 °C, $CDCl_3$) δ ppm 25.8 (br s).

^{29}Si{H} NMR (43 MHz, 25 °C, $CDCl_3$) δ ppm −3.6 (s).

IR: 2956, 2884, 1651, 1599, 1495, 1480, 1310, 1008, 971, 745, 693 cm^{-1}.

GPC: Multimodal distribution M = 2,800 – 112,000 g mol^{-1}.

DLS: 140 nm.

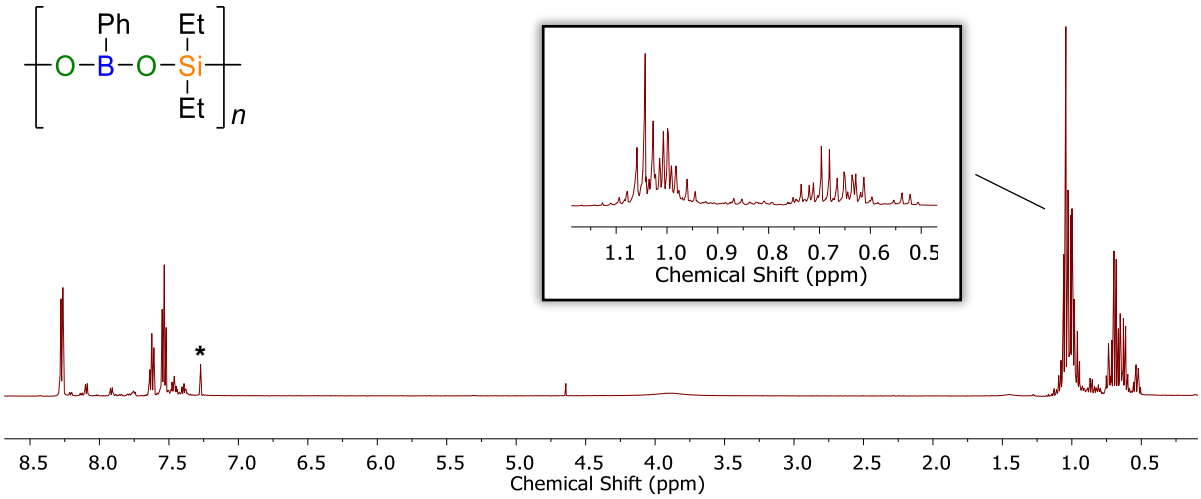

Figure S5.19 ^{1}H NMR (500 MHz, 25 °C, $CDCl_3$) of isolated **5.2a**. Deuterated chloroform residual signal denoted by *.

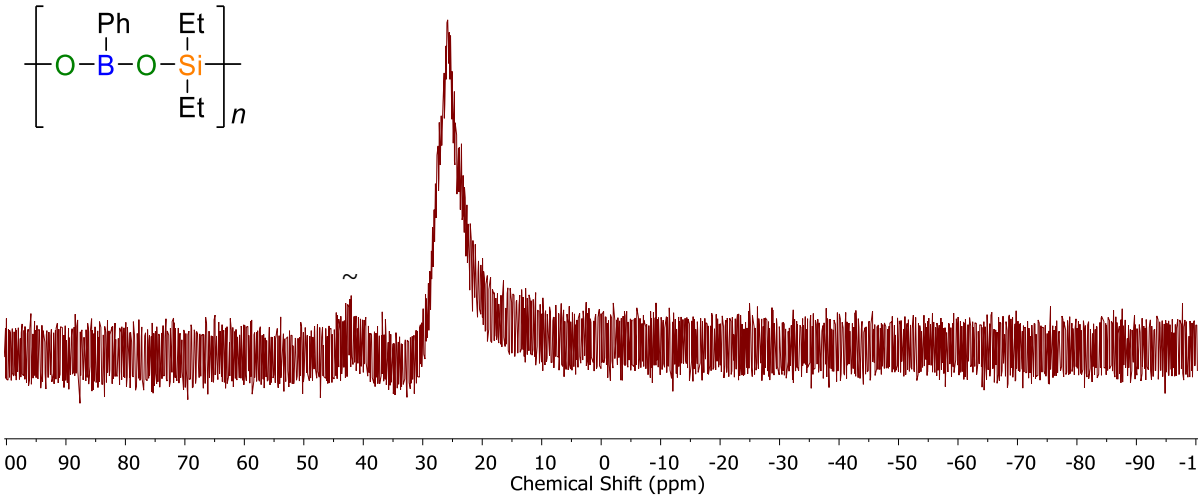

Figure S5.20 ^{11}B{H} NMR (128 MHz, 25 °C, $CDCl_3$) of isolated **5.2a**. Peak corresponding to $B(C_6F_5)_3$ is denoted with ~.

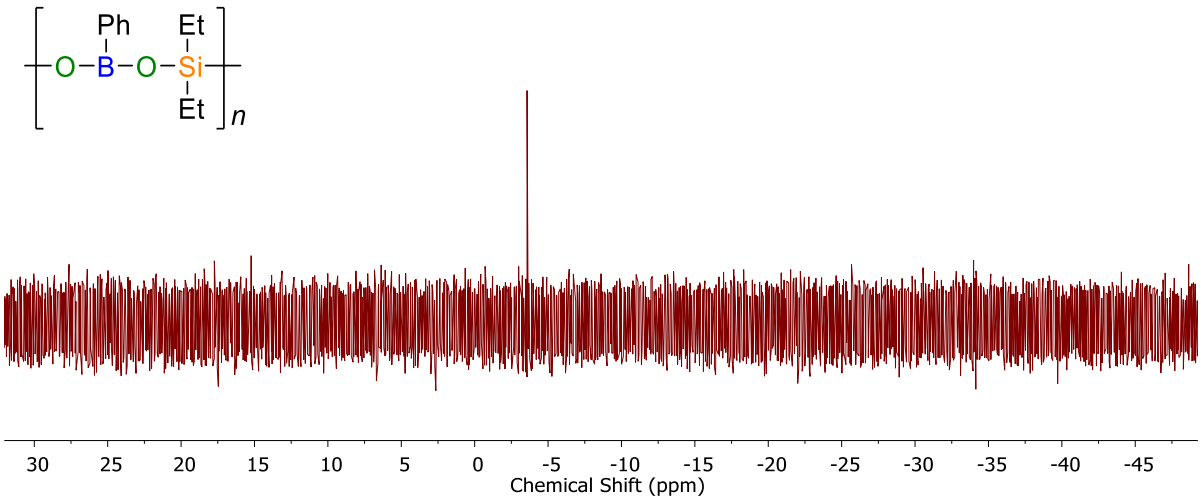

Figure S5.21 ^{29}Si{H} NMR (80 MHz, 25 °C, $CDCl_3$) of isolated **5.2a**.

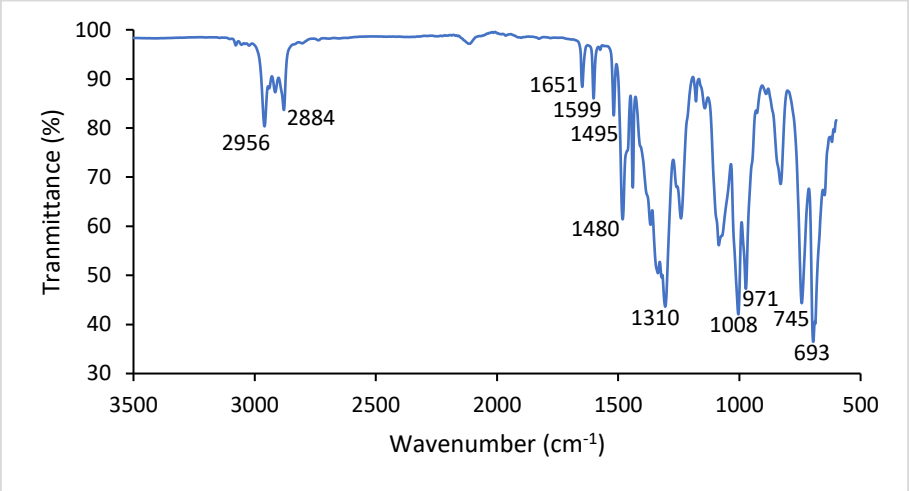

Figure S5.22 Solid state ATR FT-IR spectrum of isolated **5.2a**

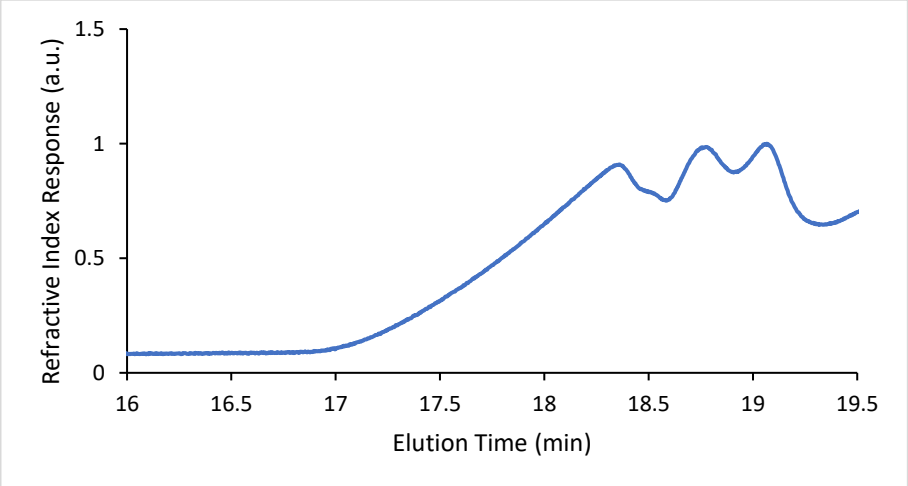

Figure S5.23 GPC chromatogram of isolated **5.2a** (2 mg mL^{-1} in THF, 0.1 w/w % nBu$_4$NBr in the THF eluent).

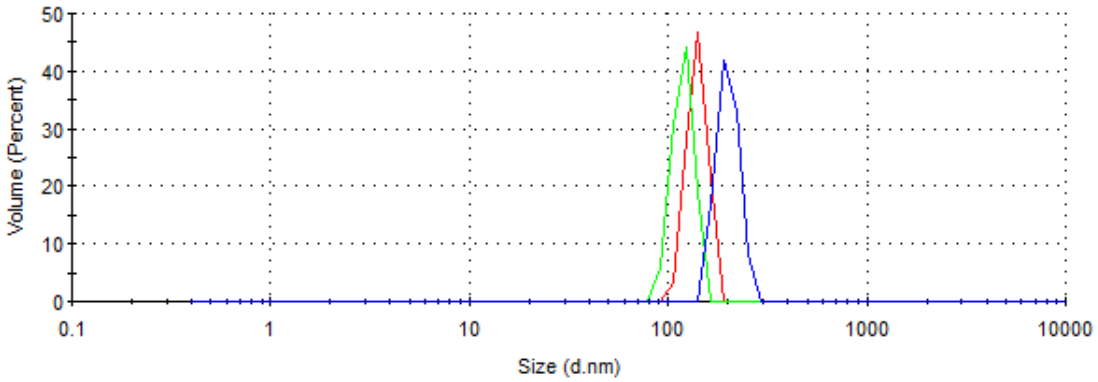

Figure S5.24 DLS size distribution by volume of isolated **5.2a** in DCM (1 mg mL^{-1}).

5.5.5.2 Dehydrocarbonative polymerisation of dimethyl phenylboronate and diphenylsilane

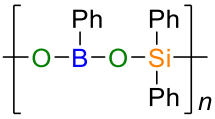

In a glovebox, a Schlenk flask was charged with **5.5** (0.90 g, 6 mmol), $B(C_6F_5)_3$ (0.15 g, 0.3 mmol) and DCM (5 mL). To this, diphenylsilane (1.104 g, 6 mmol) was slowly added. Effervescence was observed upon addition. The flask was sealed, removed from the glovebox and stirred at 40 °C in an oil bath under an atmosphere of nitrogen. After 7 h, the flask was removed from the oil bath and volatiles removed under vacuum yielding **5.2a** as a white solid (yield = 1.34 g, 73%). Attempts to precipitate the polymer into pentane were unsuccessful, resulting in polymer decomposition.

Spectroscopic data:

^{1}H NMR (400 MHz, 25 °C, $CDCl_3$) δ 8.27–8.23 (m), 7.74–7.69 (m), 7.65–7.57 (m), 7.55–7.49 (m), 7.44–7.36 (m), 7.33–7.28 (m).

$^{11}B\{^{1}H\}$ NMR (128 MHz, 25 °C, $CDCl_3$) δ ppm 28.6 (br s).

$^{29}Si\{^{1}H\}$ NMR (79 MHz, 25 °C, $CDCl_3$) δ ppm −20.2 (s), −46.5 ppm (s). The signal at −46.5 ppm is assigned to diphenylsiloxane units within the polyborosiloxane backbone.

IR: 3067, 2144, 1310, 1118, 1010, 822, 693 cm^{-1}.

GPC: Multimodal distribution M = 3,200 – 126,000 g mol^{-1}.

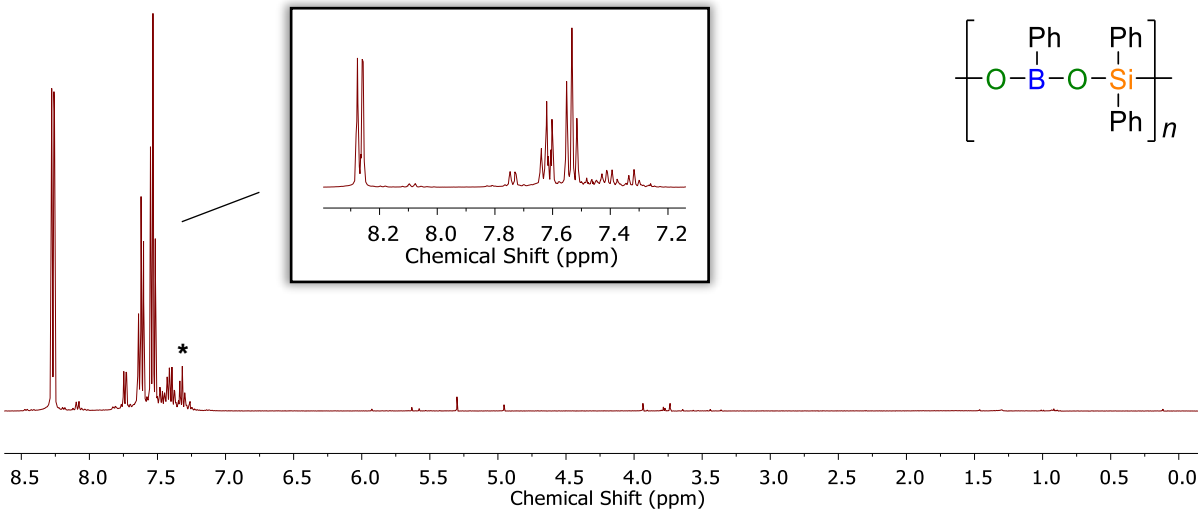

Figure S5.25 ^{1}H NMR (500 MHz, 25 °C, $CDCl_3$) of isolated **5.2b**. Deuterated chloroform residual signal denoted by *.

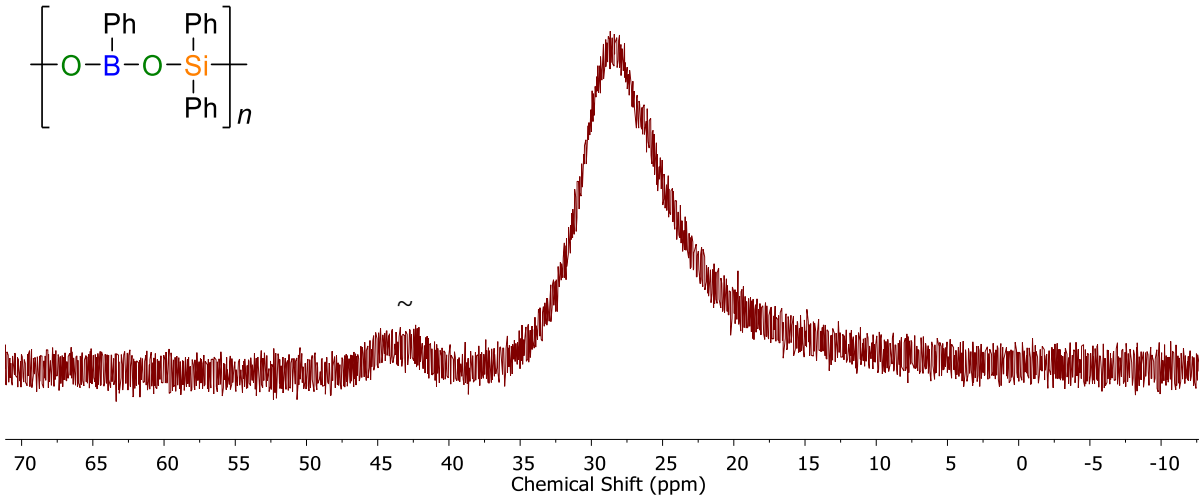

Figure S5.26 ^{11}B{H} NMR (500 MHz, 25 °C, $CDCl_3$) of isolated **5.2b**. Peak corresponding to $B(C_6F_5)_3$ is denoted with ~.

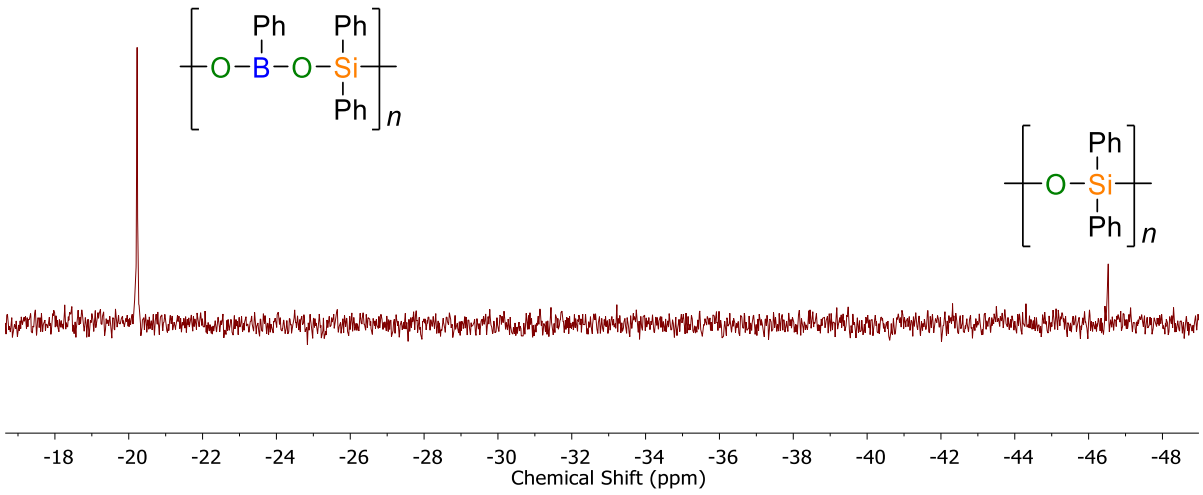

Figure S5.27 ^{29}Si{H} NMR (80MHz, 25 °C, $CDCl_3$) of isolated **5.2b**.

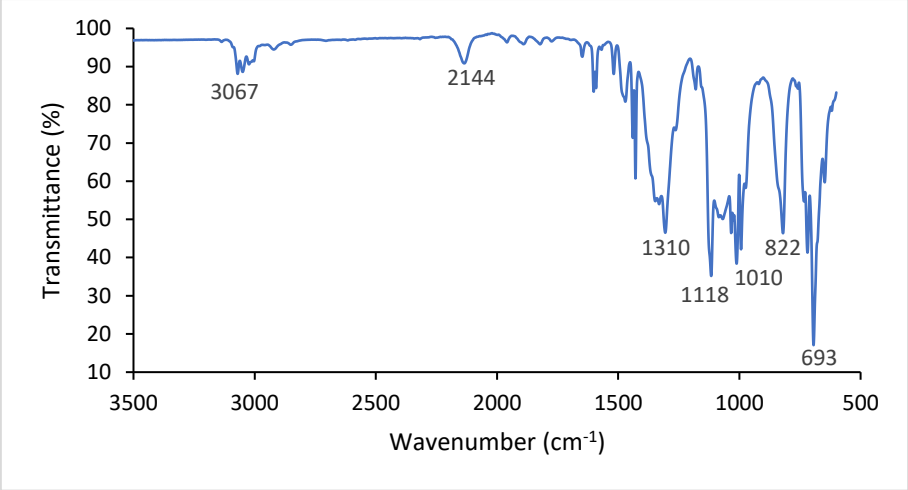

Figure S5.28 Solid state ATR FT-IR spectrum of isolated **5.2b**.

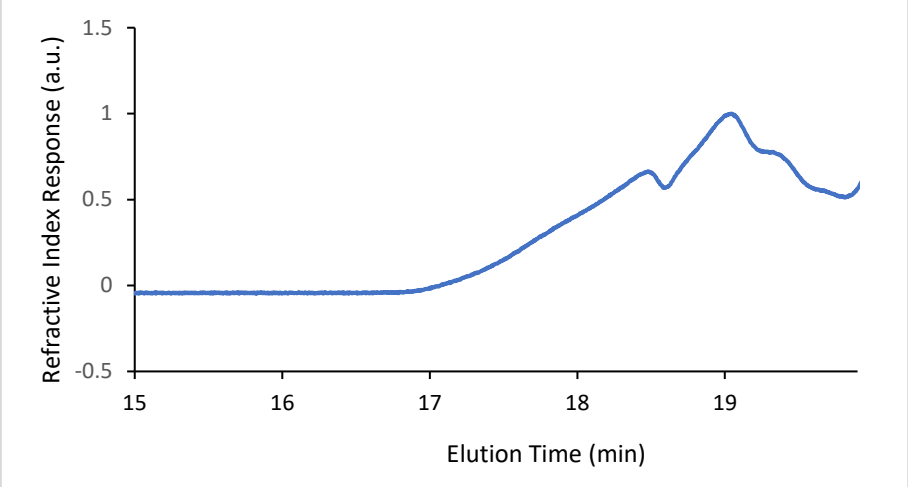

Figure S5.29 GPC chromatogram of ioslated **5.2b** (2 mg mL^{-1} in THF, 0.1 w/w % $n$$Bu_4NBr$ in the THF eluent).

5.5.5.3 Attempted dehydrocarbonative polymerisation of dimethyl phenylboronate and di-tert-butylsilane

In a glovebox, $B(C_6F_5)_3$ in $CDCl_3$ (0.01 M, 0.5 mL) was added to dimethyl phenylboronate (9 mg, 0.06 mmol) in a vial. To this was added di-*tert*-butylsilane (11.9 μL, 0.06 mmol): no effervescence was observed. The contents of the vial were transferred to a J-Young NMR tube, sealed and heated in an oil bath at 40 °C. After 3 d, ^{1}H and $^{11}B\{H\}$ NMR spectroscopy showed that no reaction had occurred.

5.5.5.4 Attempted dehydrocarbonative polymerisation of dimethyl phenylboronate and 1,4-Bis(dimethylsilyl)benzene

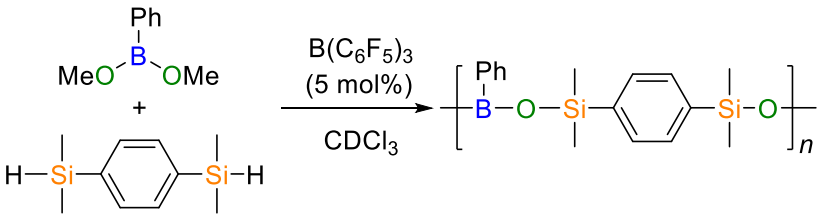

In a glovebox, $B(C_6F_5)_3$ in $CDCl_3$ (0.01 M, 0.5 mL) was added to dimethyl phenylboronate (9 mg, 0.06 mmol) in a vial. To this was added bis(dimethylsilyl)benzene (13.3 μL, 0.06 mmol). Rapid effervescence was observed at this point. The reaction was stirred for 10 min and then the contents of the vial transferred to a J-Young NMR tube, sealed and heated to 40 °C for 20 h. Volatiles were removed from the reaction mixture and the material analysed by NMR spectroscopy and GPC.

Spectroscopic data:

$^{11}B\{H\}$ NMR (161 MHz, 25 °C, $CDCl_3$) δ 25.9.

$^{29}Si\{H\}$ NMR (99 MHz, 25 °C, $CDCl_3$) δ 2.5, 0.1, −0.4, −1.2.

GPC: Multimodal distribution: M = 2,200 – 56,000 g mol^{-1}

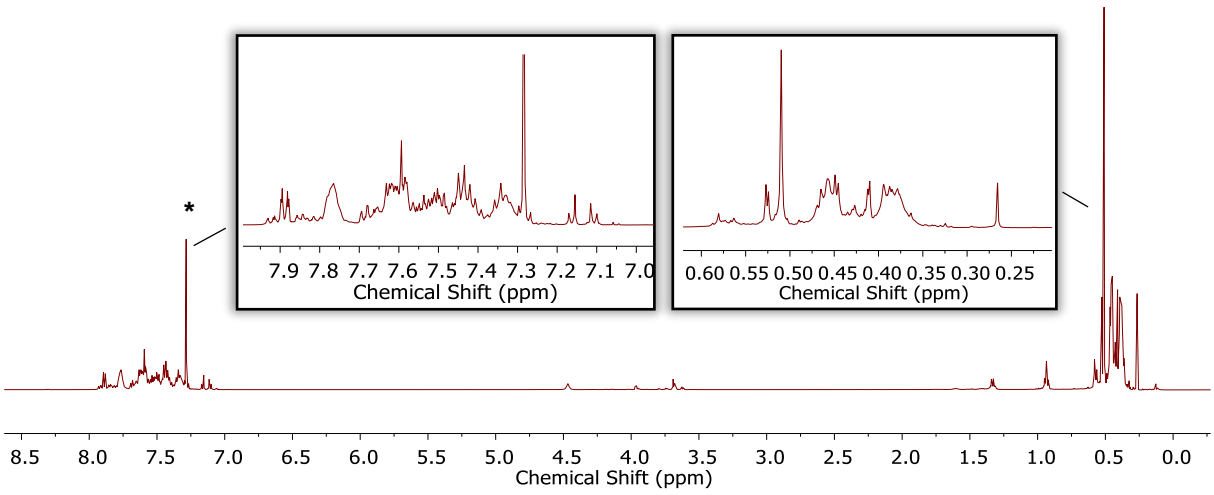

Figure S5.30 ^{1}H NMR (500 MHz, 25 °C, $CDCl_3$) of the isolated residue of the reaction between **5.5** and bis(dimethylsilyl)benzene. Deuterated chloroform residual signal is denoted by *.

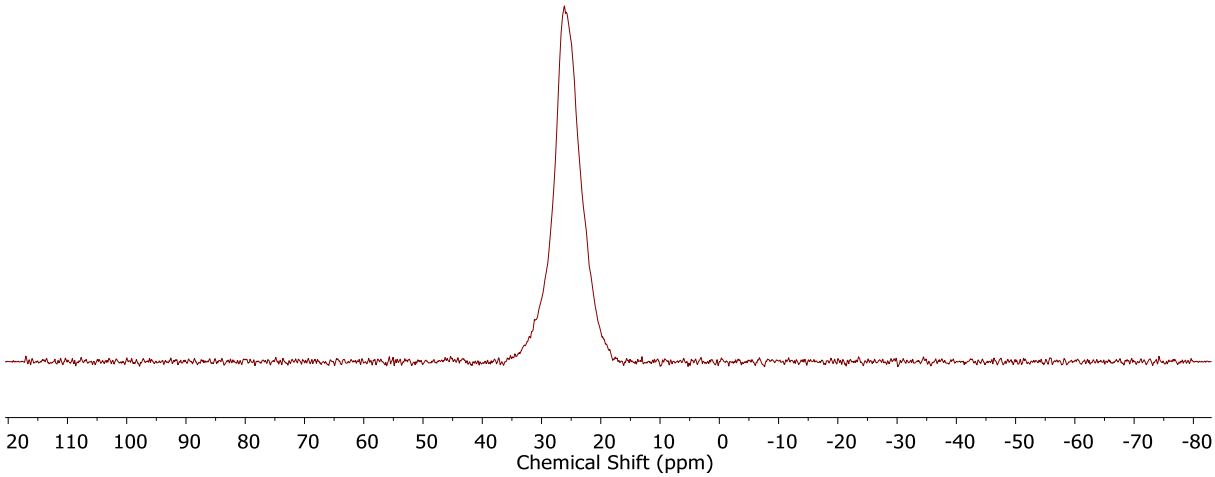

Figure S5.31 $^{11}B\{H\}$ (161 MHz, 25 °C, $CDCl_3$) of the isolated residue of the reaction between **5.5** and bis(dimethylsilyl)benzene.

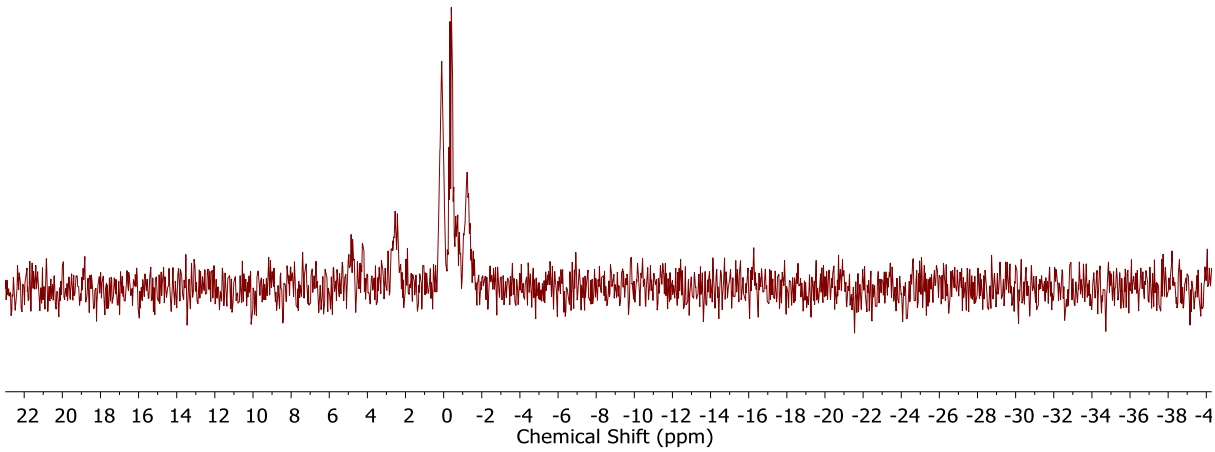

Figure S5.32 $^{29}Si\{H\}$ NMR (99 MHz, 25 °C, $CDCl_3$) of the isolated residue of the reaction between **5.5** and bis(dimethylsilyl)benzene.

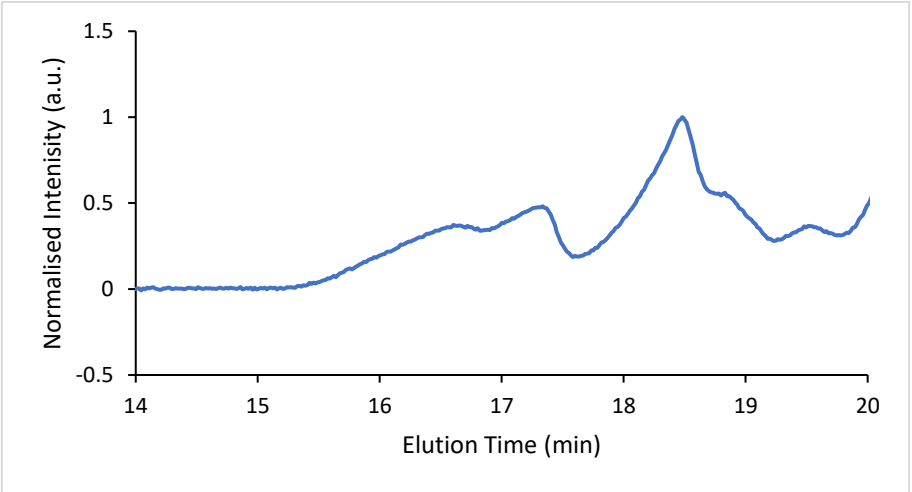

Figure S5.33 GPC chromatogram of isolated residue of the reaction between **5.5** and bis(dimethylsilyl)benzene (2 mg mL^{-1} in THF, 0.1 w/w % nBu$_4$NBr in the THF eluent).

5.5.6 Addition of pyridine to 5.2a

In a glovebox, **5.2a** (10 mg) was dissolved in $CDCl_3$ (0.5 mL) in a vial. A few drops of pyridine were added to this and the reaction mixture was analysed by $^{29}Si\{H\}$ NMR spectroscopy. The formation of a number of unassigned peaks determined that this was not a suitable method to removed $B(C_6F_5)_3$ from the polymer.

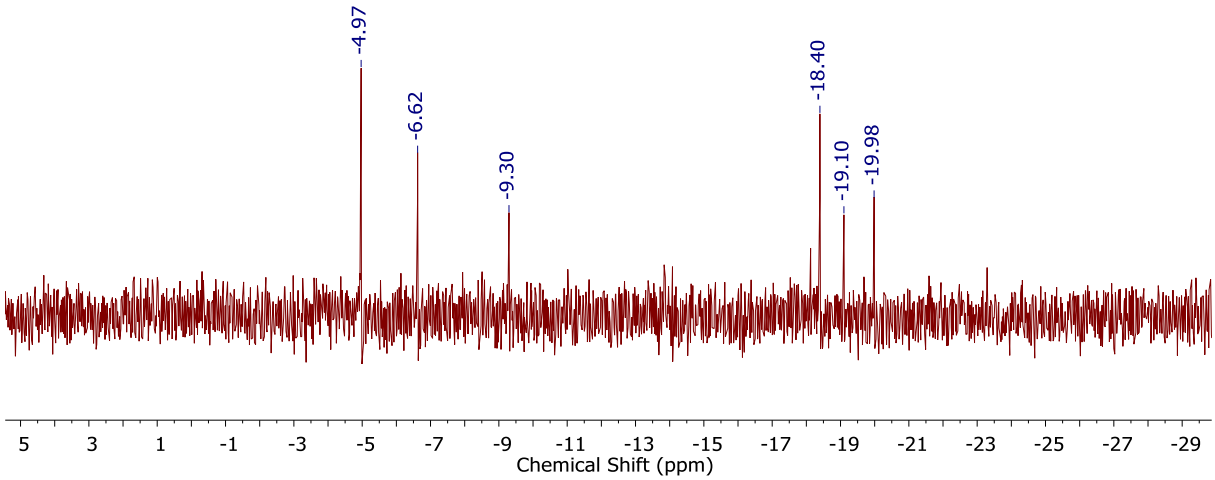

Figure S5.34 $^{29}Si\{H\}$ NMR (99 MHz, 25 °C, $CDCl_3$) after the addition of pyridine to **5.3a**.

5.6 References

1. Priegert, A. M.; Rawe, B. W.; Serin, S. C.; Gates, D. P., *Chem. Soc. Rev.* **2016,** *45*, 922-53.
2. Manners, I., *Angew. Chem. Int. Ed.* **1996,** *35*, 1602-1621.
3. Mark, J. E.; Allcock, H. R.; West, R., *Inorganic Polymers*. Second Edition ed.; Oxford University Press: New York, 2005.
4. Clarson, S. J.; Semlyen, J. A. *Siloxane Polymers*. Prentice Hall: New Jersey, 1993.
5. Rob Roy Mcgregor, W. E. L. Treating dimethyl silicone polymer with boric oxide. Patent, U. S., 1943.
6. Wright, J. G. E. Process for making puttylike elastic plastic, siloxane derivative composition containing zinc hydroxide. Patent, U. S., 2541851A, 1944.
7. Zinchenko, G. A.; Mileshkevich, V. P.; Kozlova, N. V., *Polym. Sci. (USSR)* **1981,** *23*, 1421-1429.
8. Vale, R. L., *J. Chem. Soc.* **1960**, 2252-2257.
9. Goertz, M. P.; Zhu, X. Y.; Houston, J. E., *J. Polym. Sci., Part B: Polym. Phys.* **2009,** *47*, 1285-1290.
10. Kulikov, O.; Hornung, K., *J Vinyl Addit. Technol.* **2006,** *12*, 131-142.
11. Liu, Z.; Picken, S. J.; Besseling, N. A. M., *Macromolecules* **2014,** *47*, 4531-4537.
12. Foran, G. Y.; Harris, K. J.; Brook, M. A.; Macphail, B.; Goward, G. R., *Macromolecules* **2019,** *52*, 1055-1064.
13. Yajima, S.; Hayashi, J.; Okamura, K., *Nature* **1977,** *266*, 521-522.
14. S. N. Borisov, M. G. V., E. Ya. Lukevits, *Organosilicon Heteropolymers and Heterocompounds*. Plenum Press: New York, 1970.
15. Lu, S.-Y.; Hamerton, I., *Prog. Polym. Sci.* **2002,** *27*, 1661-1712.
16. Li, J.; Xing, L.; Zhang, R.; Chen, M.; Wang, Z.; Xu, M.; Li, W., *J. Power Sources* **2015,** *285*, 360-366.
17. Han, Y.-K.; Yoo, J.; Yim, T., *Electrochim. Acta* **2016,** *215*, 455-465.
18. Schiavon, M. A.; Armelin, N. A.; Yoshida, I. V. P., *Mater. Chem. Phys.* **2008,** *112*, 1047-1054.

19. Bai, H. W.; Wen, G.; Huang, X. X.; Han, Z. X.; Zhong, B.; Hu, Z. X.; Zhang, X. D., *J. Eur. Ceram. Soc.* **2011,** *31*, 931-940.
20. Liu, W.; Pink, M.; Lee, D., *J. Am. Chem. Soc.* **2009,** *131*, 8703-8707.
21. Puneet, P.; Vedarajan, R.; Matsumi, N., *ACS Sensors* **2016,** *1*, 1198-1202.
22. Neville, L. A.; Spalding, T. R.; Ferguson, G., *Angew. Chem. Int. Ed.* **2000,** *39*, 3598-3601.
23. Beckett, M. A.; Hibbs, D. E.; Hursthouse, M. B.; Malik, K. M. A.; Owen, P.; Varma, K. S., *J. Organomet. Chem.* **2000,** *595*, 241-247.
24. O'Dowd, A. T.; Spalding, T. R.; Ferguson, G.; Gallagher, J. F.; Reed, D., *J. Chem. Soc., Chem. Commun.* **1993**, 1816-1817.
25. Foucher, D. A.; Lough, A. J.; Manners, I., *Inorg. Chem.* **1992,** *31*, 3034-3043.
26. Rubinsztajn, S., *J. Inorg. Organomet. Polym.* **2014,** *24*, 1092-1095.
27. Wang, Q.; Fu, L.; Hu, X.; Zhang, Z.; Xie, Z., *J. Appl. Polym. Sci.* **2006,** *99*, 719-724.
28. Sorarù, G. D.; Dallabona, N.; Gervais, C.; Babonneau, F., *Chem. Mater.* **1999,** *11*, 910-919.
29. Abel, E. W.; Singh, A., *J. Chem. Soc.* **1959**, 690-693.
30. Cheng, R.; Zhou, Q.; Ni, L.; Chen, Y.; Wang, J., *J. Appl. Polym. Sci.* **2011,** *119*, 47-52.
31. Hong, F. E.; Eigenbrot, C. W.; Fehlner, T. P., *J. Am. Chem. Soc.* **1989,** *111*, 949-956.
32. Mingotaud, A.-F.; Héroguez, V.; Soum, A., *J. Organomet. Chem.* **1998,** *560*, 109-115.
33. Beckett, M. A.; Rugen-Hankey, M. P.; Sukumar Varma, K., *Polyhedron* **2003,** *22*, 3333-3337.
34. Makarova, E. A.; Shimizu, S.; Matsuda, A.; Luk'yanets, E. A.; Kobayashi, N., *Chem. Commun.* **2008**, 2109-2111.
35. Gridina, V. F.; Klebanskii, A. L.; Dorofeyenko, L. P.; Krupnova, L. Y., *Polym. Sci. (USSR)* **1968,** *9*, 2196-2202.
36. Metcalfe, R. A.; Kreller, D. I.; Tian, J.; Kim, H.; Taylor, N. J.; Corrigan, J. F.; Collins, S., *Organometallics* **2002,** *21*, 1719-1726.
37. Thieme, K.; Bourke, S. C.; Zheng, J.; MacLachlan, M. J.; Zamanian, F.; Lough, A. J.; Manners, I., *Can. J. Chem.* **2002,** *80*, 1469-1480.
38. Zhao, Z.; Cammidge, A. N.; Cook, M. J., *Chem. Commun.* **2009**, 7530-7532.
39. Kijima, I.; Yamamoto, T.; Abe, Y., *Bull. Chem. Soc. Jpn.* **1971,** *44*, 3193-3194.
40. Fujdala, K. L.; Oliver, A. G.; Hollander, F. J.; Tilley, T. D., *Inorg. Chem.* **2003,** *42*, 1140-1150.
41. Marciniec, B.; Walkowiak, J., *Chem. Commun.* **2008**, 2695-2697.
42. Ito, M.; Itazaki, M.; Nakazawa, H., *J. Am. Chem. Soc.* **2014,** *136*, 6183-6186.
43. Yoshimura, A.; Yoshinaga, M.; Yamashita, H.; Igarashi, M.; Shimada, S.; Sato, K., *Chem. Commun.* **2017,** *53*, 5822-5825.
44. Rubinsztajn, S.; Cella, J. A., *Macromolecules* **2005,** *38*, 1061-1063.
45. Chojnowski, J.; Rubinsztajn, S.; Cella, J. A.; Fortuniak, W.; Cypryk, M.; Kurjata, J.; Kaźmierski, K., *Organometallics* **2005,** *24*, 6077-6084.
46. Cella, J.; Rubinsztajn, S., *Macromolecules* **2008,** *41*, 6965-6971.
47. Thompson, D. B.; Brook, M. A., *J. Am. Chem. Soc.* **2008,** *130*, 32-33.
48. Kurjata, J.; Fortuniak, W.; Rubinsztajn, S.; Chojnowski, J., *Eur. Polym. J.* **2009,** *45*, 3372-3379.
49. Kamino, B. A.; Grande, J. B.; Brook, M. A.; Bender, T. P., *Org. Lett.* **2011,** *13*, 154-157.
50. Keddie, D. J.; Grande, J. B.; Gonzaga, F.; Brook, M. A.; Dargaville, T. R., *Org. Lett.* **2011,** *13*, 6006-6009.
51. Grande, J. B.; Fawcett, A. S.; McLaughlin, A. J.; Gonzaga, F.; Bender, T. P.; Brook, M. A., *Polymer* **2012,** *53*, 3135-3142.
52. Cella, S.; Rubinsztajn. J. A., Silicone condensation reaction. Patent, U. S., 7064173, 2006.
53. Brook, M. A., *Chem. Eur. J.* **2018,** *24*, 8458-8469.
54. Li, M.; Ge, T.; Ding, H.; Lai, G. Patent, C. 107312175A, 2017.
55. Bomio, C.; Kabeshov, M. A.; Lit, A. R.; Lau, S.-H.; Ehlert, J.; Battilocchio, C.; Ley, S. V., *Chem. Sci.* **2017,** *8*, 6071-6075.
56. Pattanaik, S.; Gunanathan, C., *ACS Catal.* **2019,** *9*, 5552-5561.
57. Schneider, A. F.; Chen, Y.; Brook, M. A., *Dalton Trans.* **2019,** *48*, 13599-13606.
58. Garcés, K.; Fernández-Alvarez, F. J.; Polo, V.; Lalrempuia, R.; Pérez-Torrente, J. J.; Oro, L. A., *ChemCatChem* **2014,** *6*, 1691-1697.

59. Elkin, P. K.; Levin, V. V.; Dilman, A. D.; Struchkova, M. I.; Belyakov, P. A.; Arkhipov, D. E.; Korlyukov, A. A.; Tartakovsky, V. A., *Tetrahedron Lett.* **2011,** *52*, 5259-5263.
60. Johnson, L.; Gao, L.; Shields Iv, C.; Smith, M.; Efimenko, K.; Cushing, K.; Genzer, J.; López, G., *J. Nanotechnol.* **2013,** *11*, 22.
61. Litvinov, V. M.; Whittaker, A. K.; Hagemeyer, A.; Spiess, H. W., *Colloid. Polym. Sci.* **1989,** *267*, 681-686.

Chapter 6

Outlook

The work presented in this thesis focuses on the development of synthetic routes to novel main group element-containing polymers and investigations into potential applications of these materials. Hydrophosphination of olefins was found to be an efficient method to modify polyphosphinoboranes facilitating the formation of P-disubstituted polymers and crosslinked gels. Investigations into the dehydrocoupling of phenylphosphine-borane using $CpFe(CO)_2OTf$ have furthered our understanding of the mechanism of polymerisation and have also resulted in the development of non-metal catalysed routes to polyphosphinoboranes. Applications of polyphosphinoboranes have been developed: these materials have been shown to form hydrogels and act as flame-retardant additives for cotton fabric. A metal-free route to borosiloxane molecules and polymers via demethanative condensation has also been established.

This outlook chapter serves to outline future directions based on the results obtained during the course of the studies described in this thesis.

6.1 Post-polymerisation modification of polyphosphinoboranes

Chapter 2 reports the radical hydrophosphination of olefins using poly(phenylphosphinoborane) giving access to a range of modified polymers. Previously, the hydrophosphination of a variety of unsaturated compounds has been reported using phosphine-borane adducts. For example, Gaumont and co-workers have found that phenylphosphine-borane will react with unsaturated compounds such as alkenes,[1, 2] alkynes,[3] carbonyls,[4] and enones (Scheme 6.1),[5] using either microwave irradiation (MWI) or palladium catalysis. We anticipate that the hydrophosphination of unsaturated compounds other than alkenes using polyphosphinoborane will be possible allowing a wide variety of side groups to be installed onto the polymer chain introducing additional functionality.

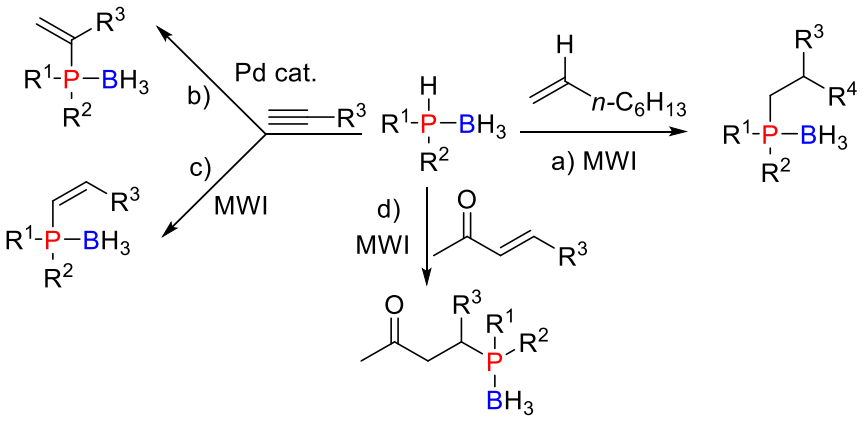

Scheme 6.1 Hydrophosphination of a) alkenes, b) and c) alkynes, d) enones using phosphine-borane adducts.

To this end, preliminary experiments involving the hydrophosphination of 1-pentyne using poly(phenylphosphinoboranes) have been undertaken. Irradiation of $[PhHP\text{-}BH_2]_n$ in the presence of an equimolar amount of 1-pentyne in the presence of 10 mol% DMPA and TEMPO in THF resulted in 85% consumption of starting polymer after 24 h according to integration of the ^{31}P NMR spectrum. Along with a minor signal at −49.0 ppm corresponding to $[PhHP\text{-}BH_2]_n$ units, three prominent peaks emerged in the ^{31}P NMR at –3.8, −11.5, and −25.9 ppm which we assign to the formation of E and Z alkenes, resulting from anti-Markovnikov addition; and to Markovnikov addition (Scheme 6.2). No evidence of crosslinking was observed which suggests that the formed alkene bonds do not react with further polymer chains. High molar mass polymer was retained according analysis by gel permeation chromatography (GPC; M_n = 78,700, PDI = 1.2) and repeat units of 190.1 m/z were identified from the ESI-MS spectrum which correspond to successive loss of $[Ph(C_5H_9)P\text{-}BH_2]$. Efforts will focus on the development of selective methods for the hydrophosphination of alkynes using polyphosphinoboranes, either under radical or metal-mediated conditions.

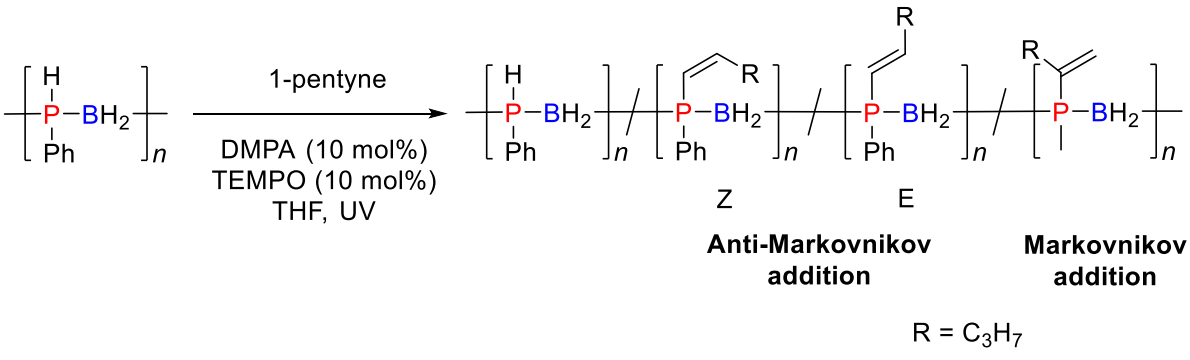

Scheme 6.2 UV irradiation reaction of $[PhHP\text{-}BH_2]_n$ with 1-pentyne in the presence of DMPA and TEMPO.

Furthermore, while extensive work has been carried out on the modification of poly(phenylphosphinoborane), there is scope for the extension of this to other polymer precursors. $CpFe(CO)_2OTf$-catalysed dehydrocoupling has provided access to a range of P-monosubstituted polymers featuring both aryl or alkyl side chain.[6, 7] Preliminary investigations into the modification of $[n\text{HexHP-BH}_2]_n$ using 1-octene have been promising. The P-monosubstituted precursors have vastly different properties, for example, the T_g of $[\text{PhHP-BH}_2]_n$ is 38 °C,[8] whereas that of $[n\text{HexHP-BH}_2]_n$ is much lower (−76 °C).[6] The hydrophosphination of a variety of unsaturated compounds using different starting polymers will allow the formation of a library of polymers, with tailored physical and chemical properties.

6.2 Mechanism of polymerisation of phosphine-boranes using $CpFe(CO)_2OTf$

Chapter 3 describes investigations into the polymerisation of phenylphosphine-borane using $CpFe(CO)_2OTf$. While it is clear that the dehydrocoupling consists of a hybrid mechanism rather than the chain-growth process previously postulated, the exact nature of this mechanism remains unclear. A detailed understanding of the mechanism will aid future catalyst design.

Several studies have been carried out on the dehydrocoupling of secondary phosphine-boranes as model substrates using rhodium precatalysts which have significantly improved the understanding of dehydrocoupling pathways through the isolation of reaction intermediates, labelling studies and computational approaches.[9-11] The isolation of different products $[\text{Rh(dppp)}(\eta^2\text{-H}_3\text{B}\cdot\text{P}t\text{Bu}_2\text{BH}_2\cdot\text{P}t\text{Bu}_2\text{H})][\text{BAr}^\text{F}_4]$ and $[\text{Rh(dppp)H}(\sigma,\eta^2\text{-PPh}_2\cdot\text{BH}_2\text{PPh}_2\cdot\text{BH}_3)][\text{BAr}^\text{F}_4]$ from the stoichiometric reaction of $[\text{Rh}(\eta^6\text{-FC}_6\text{H}_5)(\text{dppp})][\text{BAr}^\text{F}_4]$ with $\text{R}_2\text{HP}\cdot\text{BH}_3$ (R = Ph, *t*Bu; Scheme 6.3),[11] suggests that the mechanism of dehydrocoupling may also be substrate dependent.

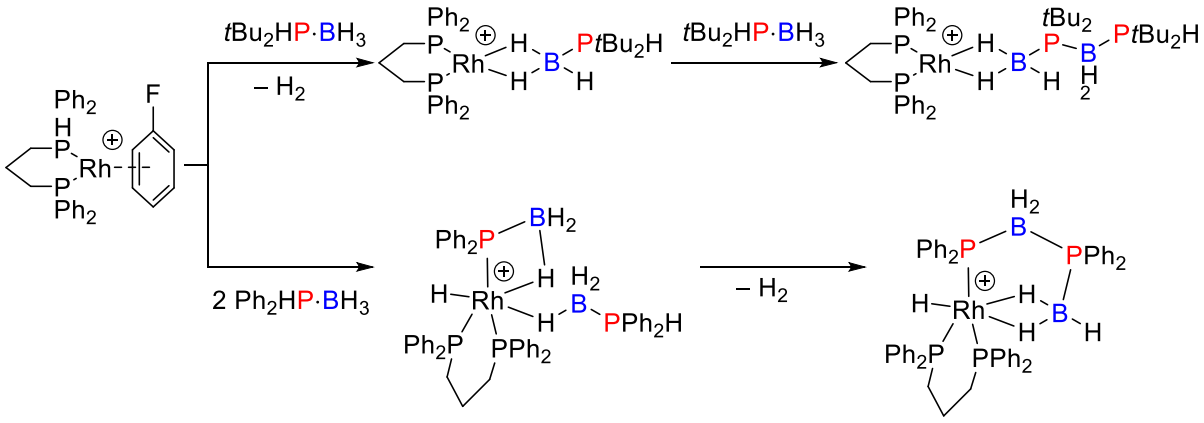

Scheme 6.3 Species isolated from the stoichiometric reaction of $R_2HP{\cdot}BH_3$ (R = *t*Bu or Ph) with $[Rh(\eta^6\text{-}FC_6H_5)(dppp)][BAr^F{}_4]$. $[BAr^F{}_4]$ anions omitted for clarity.

The dehydrocoupling of $Ph_2HP{\cdot}BH_3$ using $CpFe(CO)_2OTf$ was found to occur very slowly; however selective formation of the linear dimer $Ph_2HP{\cdot}BH_2\text{-}PPh_2{\cdot}BH_3$ was observed.[8] We anticipate that reactions using $Ph_2HP{\cdot}BH_3$ and other secondary phosphine-boranes with $CpFe(CO)_2OTf$ will provide insights into the dehydrocoupling of phosphine-boranes using iron precatalysts.

6.3 Polymerisation of polyphosphinoboranes using non-metal catalysts

During our studies in Chapter 3, we also describe the formation of polyphosphinoboranes using non-metal precatalysts, in particular triflic acid. Combined computational and experimental studies will be undertaken to improve our understanding of the reaction mechanism with a particular focus on attempts to isolate reaction intermediates. We will also examine the dehydrocoupling of phosphine-boranes using other acids to determine the effect of pKa and other factors on the dehydropolymerisation.

6.4 Polyphosphinoborane hydrogels

The first part of Chapter 4 describes the formation of swellable hydrogels with polyphosphinoborane backbones. To further these studies, polyphosphinoborane hydrogels will be tested for their biocompatibility via cell culture experiments.

One method that has been investigated for improving the properties of hydrogels is through the synthesis of interpenetrating polymer networks (IPNs) through polymerisation of a second crosslinked polymer within the hydrogel network. This allows access to properties that are hybrid of the component materials. For example a interpenetrating network of poly[bis-((methoxyethoxy)ethoxy)phosphazene] (MEEP) and poly(methylmethacrylate) (PMMA) can be formed via radical polymerisation of methyl

methacrylate and crosslinking agent ethylene glycol dimethacrylate within a swollen crosslinked MEEP polymer matrix.[12] This yielded a composite with glass transition temperatures intermediate of the parent polymers. We envisage that the formation of IPNs featuring polyphosphinoborane units could improve the structural robustness of the hydrogels reported in Chapter 4. To this end, the polymerisation and crosslinking of organic polymers such as PMMA and polystyrene within a swollen poly(phenylphosphinoborane) gel will be investigated.

6.5 Polyphosphinoborane flame-retardants

Following the promising results on the use of polyphosphinoboranes as a flame-retardant additive for cotton described in Chapter 4, future work will focus on testing these materials using industry standard tests such as identifying limiting oxygen indices (LOIs). The LOI of a material is defined as the minimum percentage of oxygen that must be present to support combustion. If the LOI is higher than atmospheric oxygen concentration, then the material is likely to inhibit a fire under standard conditions.

6.6 The synthesis of polyborosiloxanes

Chapter 5 reports the synthesis of borosiloxane molecules and polymers using a modified Piers-Rubinsztajn reaction. The $B(C_6F_5)_3$-catalysed demethanative condensation of dimethyl phenylboronate and secondary siloxanes resulted in the successful formation of polymer; however, there were some issues with selectivity and polymer decomposition. In order to expand the polymerisation substrate scope, other potential routes to polyborosiloxanes will be investigated. It was recently reported that [(Ru(*p*-cymene)Cl_2)$_2$] was a precatalyst for the synthesis of molecular borosiloxanes from boronic acids, tertiary silanes and water (Scheme 6.4).[13] Preliminary investigations into the use of this catalyst for the formation of polyborosiloxanes have been promising. Reaction of phenylboronic acid with diphenylsilane and a drop of degassed water in the presence of [(Ru(*p*-cymene)Cl_2)$_2$] (10 mol%) in C_6D_6 resulted in immediate and rapid gas evolution. After 20 h at 20 °C volatiles were removed from the reaction mixture, resulting in the isolation of a white polymeric material which was subjected to GPC analysis. This revealed a monomodal mass distribution of the polymer with M_n = 56,000 g mol^{-1} and a low PDI of 1.2. Efforts are underway to fully characterise this material and to extend this to other polymers.

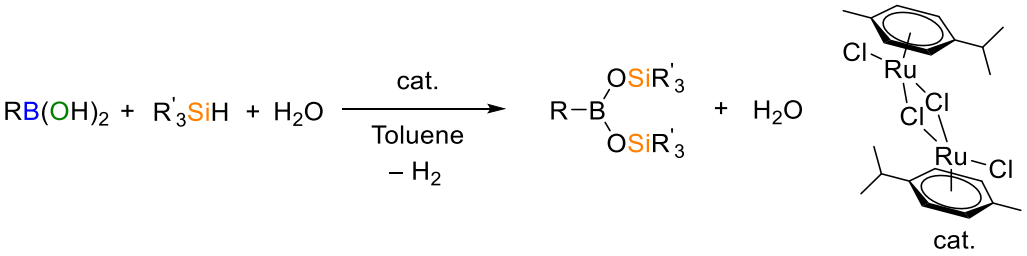

Scheme 6.4 Ruthenium catalysed synthesis of borosiloxanes.

6.7 References

1. Mimeau, D.; Delacroix, O.; Gaumont, A.-C., *Chem. Commun.* **2003**, 2928-2929.
2. Bourumeau, K.; Gaumont, A.-C.; Denis, J.-M., *Tetrahedron Lett.* **1997,** *38*, 1923-1926.
3. Mimeau, D.; Gaumont, A.-C., *J. Org. Chem.* **2003,** *68*, 7016-7022.
4. Bourumeau, K.; Gaumont, A.-C.; Denis, J.-M., *J. Organomet. Chem.* **1997,** *529*, 205-213.
5. Join, B.; Delacroix, O.; Gaumont, A.-C., *Synlett* **2005,** *2005*, 1881-1884.
6. Resendiz-Lara, D.; Annibale, V. T.; Knights, A. W.; Chitnis, S. S.; Manners, I., *Manuscript submitted* **2020**.
7. Turner, J. R.; Resendiz-Lara, D. A.; Jurca, T.; Schäfer, A.; Vance, J. R.; Beckett, L.; Whittell, G. R.; Musgrave, R. A.; Sparkes, H. A.; Manners, I., *Macromol. Chem. Phys.* **2017,** *218*, 1700120.
8. Schäfer, A.; Jurca, T.; Turner, J.; Vance, J. R.; Lee, K.; Du, V. A.; Haddow, M. F.; Whittell, G. R.; Manners, I., *Angew. Chem. Int. Ed.* **2015,** *54*, 4836-41.
9. Hooper, T. N.; Huertos, M. A.; Jurca, T.; Pike, S. D.; Weller, A. S.; Manners, I., *Inorg. Chem.* **2014,** *53*, 3716-3729.
10. Hooper, T. N.; Weller, A. S.; Beattie, N. A.; Macgregor, S. A., *Chem. Sci.* **2016,** *7*, 2414-2426.
11. Huertos, M. A.; Weller, A. S., *Chem. Sci.* **2013,** *4*, 1881-1888.
12. Visscher, K. B.; Manners, I.; Allcock, H. R., *Macromolecules* **1990,** *23*, 4885-4886.
13. Chatterjee, B.; Gunanathan, C., *Chem. Commun.* **2017,** *53*, 2515-2518.